To my parents.

ON DESIGNING ALGORITHMS FOR CONTROLLING pH

W A Badran

St. John's College, Oxford



Thesis submitted for

the degree of Doctor of Philosophy

University of Oxford

Trinity Term 1984

On Designing Algorithms For Controlling pH

W A Badran
St. John's College, Oxford

Thesis submitted for
the degree of Doctor of Philosophy
University of Oxford
Trinity Term 1984

ABSTRACT

This thesis describes an investigation of how techniques of modelling, estimation and control can be used to improve regulation of pH.

A novel mathematical model of neutralization is used which explicitly accounts for two separate sources of non-linearities in pH systems: the inherent non-linearity of the pH measurement and the variable and uncertain non-linearity of the neutralization chemistry.

A detailed interactive simulation package was developed. It has been used to study:

1. The application of a Bayes' non-linear estimator to a noisy pH measurement. The estimator is used in conjunction with an Extended Kalman Filter in order to generate estimates for use in combined feedforward/feedback controllers. A novel version of the Bayes' estimator is developed which successfully estimated jumping and drifting bias on the pH measurement.

2. A novel cautious stochastic control law which uses the generated estimates and allows for their uncertainty. Reduced quality of estimation forces the controller to regulate the pH at an optimally tuned target value where control is easier.

3. Comparisons of a variety of modern and conventional control algorithms. The modern algorithms include three self-tuners, the non-linear estimators and the cautious controller. The conventional algorithms include a PID controller, analytical linearisation of the pH measurement and the use of estimated or measured feedforward signals. Twenty-five pH control laws are simulated.

The quality of regulation which can be achieved depends on what prior information is available about the neutralisation process. A strategy is

proposed which matches controller structure to available information. This strategy provides guidelines to the control configurations that can be implemented as well as their relative limitations.

It is shown that improvement in performance over a PID regulator is possible if one uses more complex controllers. This improvement is investigated by simulation because it varies from one process to another. It is also shown how the resulting simulation package has been used for computer aided design of pH control systems in the chemical industry.

ACKNOWLEDGEMENTS

I would like to thank Dr. O.L.R. Jacobs for his constant assistance and advice, and for his conscientious supervision.

I would also like to thank Chris Proudfoot for useful discussions and for his help in implementing the different selftuners. Thanks are also due to Jerome Kelleher for some of the simulation results for Unilever.

I am also grateful to Cherif Badran for leading the way, and to Tony Khayat for his friendship and encouragements.

Finally, I wish to thank my wife Hanni for her support and understanding during the last three years, and for drawing the diagrams of the thesis during our honeymoon.

ICI and Unilever financial supports are gratefully acknowledged.

Part of the research work was a joint collaborative project between ICI plc Engineering Department and the University of Oxford, supported by UK SERC grant GR/A/90098.

CHAPTER 1 INTRODUCTION

1.1 COLLABORATION WITH INDUSTRY 1-2
1.2 INTRODUCTION TO pH CONTROL 1-4
1.3 OBJECTIVES AND METHODS 1-12
1.4 CONTRIBUTIONS 1-13
1.5 ORGANISATION OF THE THESIS 1-18

CHAPTER 2 pH CONTROL : A SURVEY

2.1 INTRODUCTION 2-2
2.2 SUGGESTIONS AND THEORETICAL STUDIES 2-2
2.3 ANALOG AND DIGITAL SIMULATIONS 2-6
2.4 PILOT PLANT TRIALS 2-8
2.5 INDUSTRIAL-SCALE APPLICATIONS 2-10
2.6 CONCLUSION 2-13

CHAPTER 3 ON MODELLING pH

3.1 INTRODUCTION 3-1
3.2 CHEMICAL ANALYSIS OF NEUTRALIZATION REACTIONS . . 3-2
3.3 THE pH MEASUREMENT 3-20
3.4 MODELLING pH REGULATION IN CSTR 3-20
3.5 MODEL VALIDATION 3-29
3.6 CONCLUSION 3-29

CHAPTER 4 NON-LINEAR ESTIMATION THROUGH THE pH MEASUREMENT

4.1 INTRODUCTION 4-1
4.2 THE BAYES' RULE 4-3
4.3 RECURSIVE ESTIMATION THROUGH A BIAS-FREE pH MEASUREMENT 4-8
4.4 RECURSIVE ESTIMATION THROUGH A BIASED pH MEASUREMENT 4-25
4.5 CONCLUSION 4-47

CHAPTER 5 STATE ESTIMATION OF THE pH MODEL

5.1 INTRODUCTION 5-3
5.2 DEVELOPMENT OF THE EKF EQUATIONS 5-4
5.3 OBSERVABILITY OF THE MODEL 5-9
5.4 ROBUSTNESS OF THE EKF ESTIMATOR 5-11
5.5 SIMULATION RESULTS 5-16
5.6 CONCLUSION 5-21

CHAPTER 6 CONTROL STRATEGIES FOR pH REGULATION

6.1 INTRODUCTION 6-1
6.2 pH COST FUNCTIONS 6-4
6.3 CLASSICAL CONTROLLERS 6-5

6.4 STOCHASTIC CONTROL 6-27
6.5 CONCLUSION 6-48

CHAPTER 7 PHDESIGN: CAD PACKAGE FOR DESIGNING pH CONTROL SYSTEMS

7.1 INTRODUCTION 7-1
7.2 THE MATHEMATICAL MODEL AND THE CONTROL ALGORITHMS 7-3
7.3 STRUCTURE AND INTERACTIVE FEATURES 7-5
7.4 CONCLUSION 7-10

CHAPTER 8 CASE STUDIES IN pH REGULATION

8.1 CASE STUDY 1: ICI 8-1
8.2 CASE STUDY 2: UNILEVER 8-9
8.3 CONCLUSION 8-22

CHAPTER 9 CONCLUSIONS

9.1 REVIEW 9-1
9.2 FUTURE RESEARCH 9-5
9.3 CONCLUSION 9-7

APPENDIX A CALCULATION OF THEORETICAL TITRATION CURVES

APPENDIX B IMPLEMENTATION OF THE pH NON-LINEARITY

APPENDIX C CALCULATION OF MODELLING ERRORS

APPENDIX D PHDESIGN: USERGUIDE

APPENDIX E STABILITY ANALYSIS OF COUPLED SYSTEMS

REFERENCES

CHAPTER 1

INTRODUCTION

This thesis describes work done as part of a collaborative project between the chemical industry and the Department of Engineering Science at Oxford University to investigate applications of modern control technology to the control of pH in industrial processes.

The author developed a CAD package which simulates a general class of pH problems under a variety of control laws. This provided the basis for a design methodology for pH control systems. The work also included development of a generalized mathematical model of pH processes, as well as investigation of control laws based on non-linear estimators and comparisons of many control algorithms.

The objectives of the work carried here are related to the interest of the chemical industry in general and to those of the various sponsors in particular. This chapter summarises their interest and introduces the major contributions of the thesis.

A first section describes collaborative projects with two chemical engineering companies: ICI and Unilever. A second section defines pH and explains the importance and the difficulties in regulating it. Section 3 outlines the objectives of the thesis and the methods used to

achieve them. Section 4 presents the contribution of the author to pH control and the last section describes the organisation of the thesis.

1.1 COLLABORATION WITH INDUSTRY

The collaborative projects described in this section have been jointly supported by SERC, ICI and Unilever. The ICI project is an evaluation of the advantages of modern control to pH regulation of effluent waste. The Unilever project is a design study of pH control in a production process.

1.1.1 ICI/OXFORD pH Project

The author's work is a continuation of that done by Hewkin (1979) and reported by Jacobs et al (1980). The objects of this earlier investigation were to study application of modern methods to pH systems and to produce improved control of a full scale industrial process with the help of a dedicated on-line minicomputer. Hewkin's contribution was to show that an on-line computer programmed in the light of modern control theory could achieve significant improvements in the control of one particular pH process but that further investigations would be necessary in order to apply these techniques on a more general basis.

The present investigation lasted three years and took place on a different full scale industrial process: the neutralisation tank T103A of the Waste Brine Treatment Plant (WBTP) in Runcorn, Cheshire. WBTP is used to treat brine from mercury cell rooms used in chlorine production. Objectives of the investigations were :

1. confirm that modern control can contribute to better pH control;

2. from a design view point find a general methodology to achieve good pH control elswhere;

3. better control of pH on the WBTP to achieve reagent savings.

The investigation began in November 1980 and has employed two research workers: W. Badran (the author) and C. Proudfoot. The author was based at Oxford to investigate a general methodology for pH control and to develop a simulation package for use in the development of control laws based on non-linear estimators. C. Proudfoot, in Runcorn, was mainly concerned with the actual implementation of the digital computer and the development of modern control algorithms on-line; his work is reported elsewhere (Proudfoot 1983).

The objectives of the project were achieved: control of pH in the neutralisation tank had improved considerably under computer control (Proudfoot 1983), hence achieving reagent savings. The investigation also confirmed that modern control technology can contribute to better pH control. The general methodology and the simulation package developed during the project were used to recommend alternative control techniques to other neutralisation processes at ICI.

Case study 1 of chapter 8 describes the simulation results of the neutralisation tank T103A and assesses the success of the collaborative research.

1.1.2 UNILEVER: pH Regulation In A Production Process

A joint project between the Department of Engineering Science and Unilever was initiated in May 1983. It is a design study of pH regulation in a production process using sulphonic acid. Objectives of this project were:

1. study the feasibility and assess the merit of various configuration for pH control schemes: single tank and multitank systems, one-loop and two-loop systems;

2. establish key parameters in plant design: reactor residence time, recycle rate, pipe sizing and control valve sizing;

3. compare the performances of different controllers: PID regulators, Selftuning regulators, with and without feedforward measurements.

The investigation involved simulating the above systems under different controllers using the CAD package. Recommendations based on the simulated quality of control were made to Unilever enabling the company to rule out unpromising configurations and to size new plants. Investigation of the simulated results and recommendations are presented in chapter 8.

1.2 INTRODUCTION TO pH CONTROL

One of the most important properties of aqueous solutions is the concentration (in gm.ions l^{-1}) of dissociated hydrogen or hydroxyl ions, known as acidity or alkalinity. A solution is said to be acid, neutral, or alkaline depending on whether the hydrogen ion concentration $[H^+]$ is greater than, equal to, or less than the hydroxyl ion concentration

$[OH^-]$. The difference between the two ionic concentrations ~~is~~ are defined (Orava and Niemi 1974) as the ionic concentration difference (i.c.d.), X

$$X = [OH^-] - [H^+] \qquad (1.1)$$

The severe nonlinearity of figure 1.1 relates pH to alkalinity/acidity as measured by ionic concentration difference . This is completely determined by the definition of pH (Sørenson 1909a,b, Sørenson and Landerstrøm-Lang 1924)

$$pH = - \log_{10}[H^+] \qquad (1.2)$$

together with the dissociation equation of water

$$[H^+][OH^-] = K \qquad (1.3)$$

where K is the temperature-dependent dissociation constant (10^{-14} at standard temperature).

1.2.1 Importance Of pH Control

The regulation of the acidity of a solution, indicated by its pH value, is a most common task in in the chemical production industry and in waste water treatment. The importance of the pH in production processes of food, medicine or detergents lies in the fact that many physical and chemical operations occur best at some certain pH value which is specific for every process and every product.

In waste water treatment, the pH is important in order to minimize corrosion of sewers and pumps and to protect the life of micro-organisms in water which can survive best within a pH range of 5 - 9. The pH value is also essential in preventing undesirable chemical reactions which might involve ions of heavy metals such as mercury, lead and zinc; a low pH value will keep the ions in solution, thus creating a health hazard for man, while a high pH value will cause them to precipitate thus causing severe problems to aquatic life.

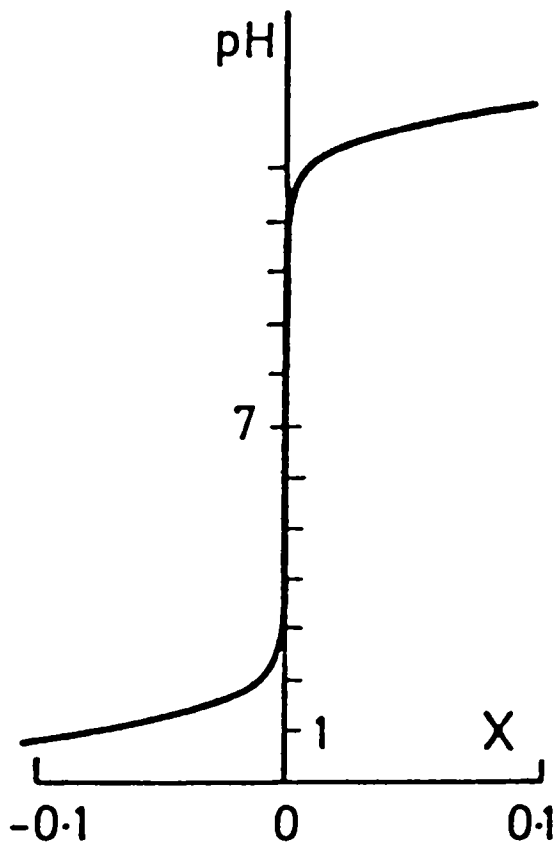


Fig 1.1 Non-linearity of the pH scale

pH regulation in production processes and in waste treatment, though having different objectives and environment, are usually carried out in a Continuous Stirred Tank Reactor (CSTR) having the standard configuration of figure 1.2 where an influent stream of variable acidity and flow rate are neutralised by mixing with concentrated reagents. The pH is measured at the exit of the CSTR that has uniformly dispersed the reagent into the effluent stream. The measurement, a feedback signal, is transmitted to a controller which automatically compares the measured variable to the set point. The controller output is transmitted to an automatic control valve which positions itself to add the proper amount of reagent to the effluent hence bringing the pH to the required set point. Feedforward measurements of disturbances of influent flow rate and pH may be available. The static gain of the controlled process is the titration curve.

1.2.2 · The Titration Curve

The titration curve characterizes the relationship between reagent flow rate and measured pH. It is usually determined on volumetric basis, which can be translated to flow rate basis for control purposes. Knoweledge of it is essential for designing good pH control systems.

Titration curves are normally determined experimentally. In principle they could be found theoretically, for known reagents, by solving simultaneously, and usually numerically, equations of reaction chemistry in the form of dissociation equations together with equations of mass conservation and of electroneutrality. However, most effluents have so many components that the titration curve computation would be very complex with ionization coefficients which are difficult to obtain for some chemicals. Furthermore, most waste effluents have unidentified

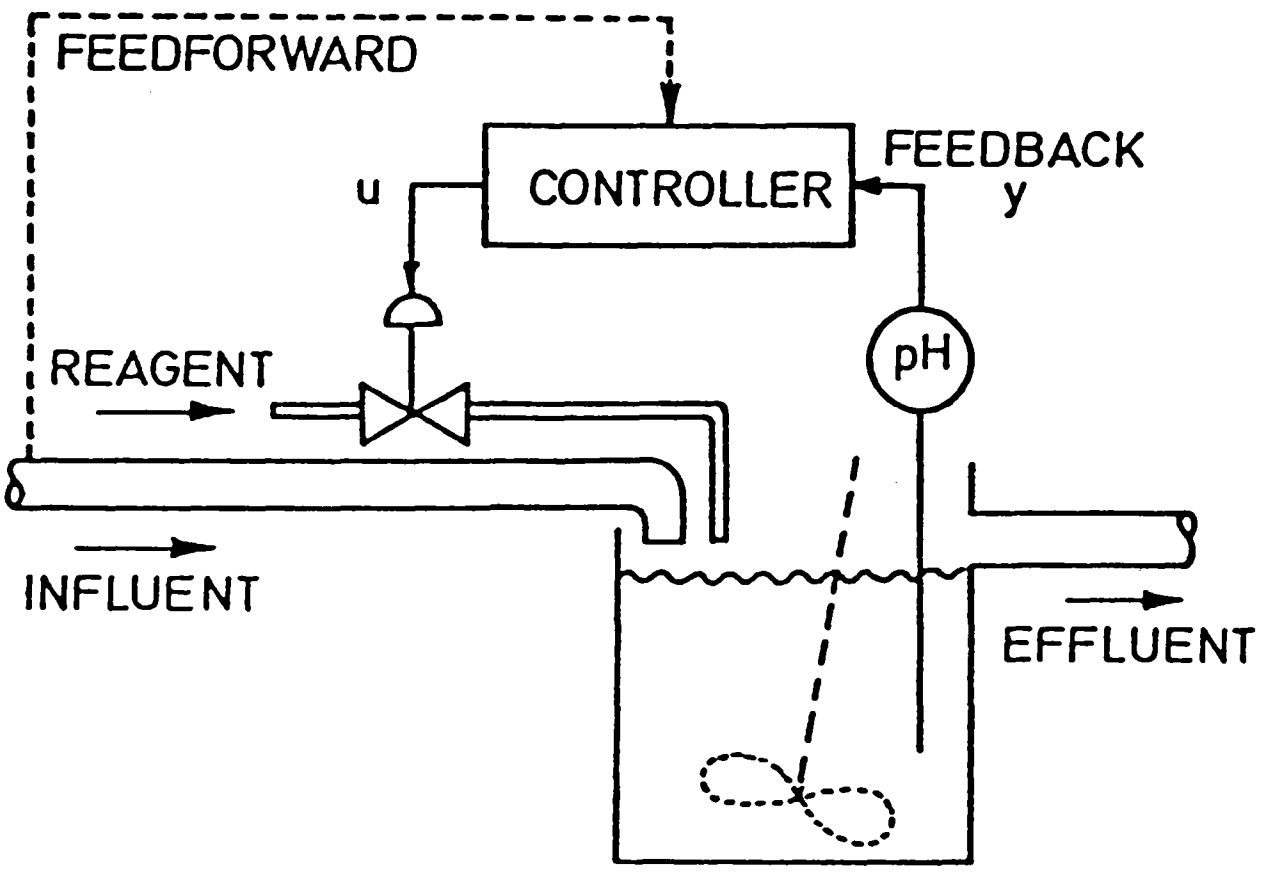


Fig 1.2 pH regulation in a CSTR

components, so the experimental titration curve is by far the most reliable design information. Examples illustrating the calculation of theoretical titration curves are shown in appendix A. Figure 1.3 shows a typical laboratory titration curve of a waste effluent.

Waste effluents usually contain " weak " components as well as " strong " components. The distinction between strong and weak reagent describes the way in which that reagent dissociates. A strong reagent is one which, when dissolved in water, dissociates completely into its ionic species; weak reagents, or buffered solutions, dissociate only partially and the concentrations of their species is governed by their dissociation constants. The chemistry of the titration curve is discussed in chapter 3.

1.2.3 Characteristics Of pH Control

pH regulation in CSTR using feedback control is regarded in the process industries as a notoriously difficult control system. This is because the severe non-linearity which is associated with pH makes it difficult for conventional feedback control to cope with common imperfections of the system. They are:

1. High process gain at the operating point: often the setpoint in pH regulation is in the steepest part of the titration curve, near the neutral point. Here, a very small change in reagent flow rate, or in influent stream flow rate or in influent composition will cause a large change in effluent pH. Shinskey (1973) reported process gains at the neutral point ranging from 10^6 for titration of strong reagents to 10 for titration of buffered reagents.

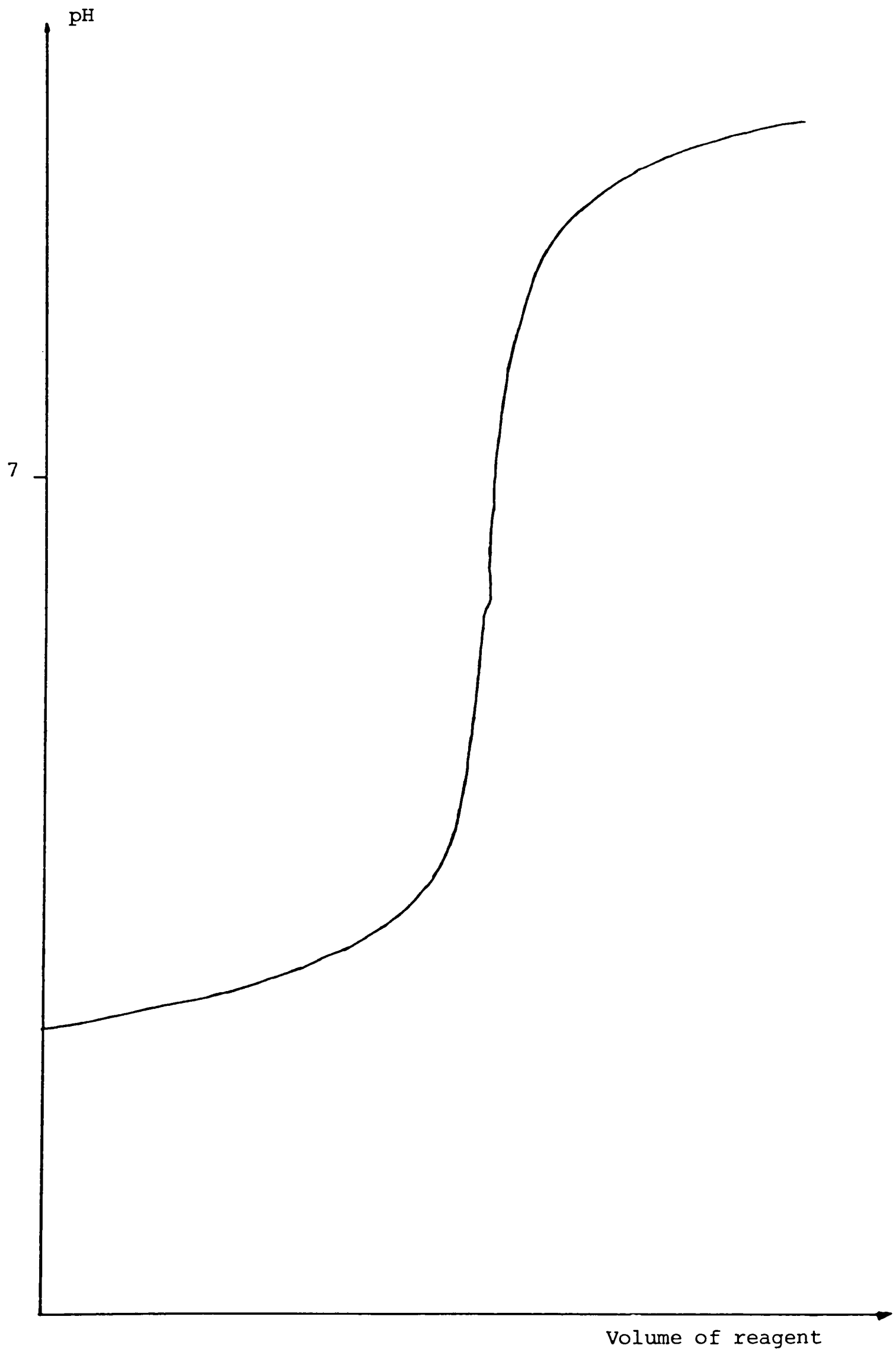


Fig. 1.3 Typical waste effluent titration curve

2. Non-linear gain: the slope of the titration curve and hence the open-loop steady state gain of the pH process can vary by as much as a factor of 10 for one unit change in setpoint pH. For such high variation of gain, the closed-loop system can become unstable when the operating point changes and the output pH may oscillate in a limit cycle.

3. Composition of the influent stream: concentration and flow of the influent stream in waste treatment may change rapidly causing large disturbances and poor control. Variable composition or variable buffering of the influent stream is very difficult to control because the titration curve changes causing variations of process gain at a given operating point.

4. Rangeability of reagent valve: rangeability is the ratio of the maximum to the minimum reagent flows required. Extreme valve rangeability of up to several thousand may be needed to handle large variation of inflow in some pH regulation processes. This can require the use of two or more control valves of different sizes in parallel (Trevathan 1972). It is usually difficult to tune these valves to achieve constant open-loop gain of the process.

5. pH measurement: measurement difficulties such as fouling or reactions at the pH sensor may lead to unreliable and inaccurate pH measurements causing many problems in pH control. Reduction in response speed of the pH electrode can occur because of electrode fouling, blockage, calibration drift and noise. Some measurement lag might also be introduced if the electrode is placed in a sample pipe.

The concatenation of these common features with the severe non-linearity of the pH scale makes pH regulation difficult.

1.3 OBJECTIVES AND METHODS

pH regulation was seen as a field to which modern control technology could make a contribution. One objective was to arrive to a generalised mathematical model of pH regulation in a CSTR. This model can be used as a basis for a better understanding of neutralisation reactions in process industries. It can also be used for designing improved feedback and feedforward controllers. Another objective was to help designing well-controlled pH plants because of more stringent legislation on pollution control and of financial gains as a result in increased efficiency.

A necessary introduction to the current investigation was a survey of publications on existing pH control schemes. The survey is part of the author's contribution to a better understanding of the difficulties encountered in industrial pH regulation. In the past twenty years there have been well over one hundred articles and two books (Moore 1978, Shinskey 1973) on pH control; many books on process control contain large sections on pH regulation (Lajoy 1954, Harriot 1964, Shinskey 1979, Leigh 1982). In chapter 2 an attempt is made to classify different control techniques applied to pH, to assess their importance in relation to this investigation and their application to industrial pH control.

A model based on pH neutralisation in a CSTR was also developed. It provided an essential part for a generalised approach to pH control. Two principal dynamic effects of the CSTR are modelled: the exponential time constant of flow through a holding tank and a variable distance-velocity lag which accounts for dead-time in the reagent flow and in the mixing. The model of the CSTR consists of three essential state variables: the ionic concentration differences of the effluent and influent pH, and the influent flow rate. Poor quality of the pH measurement is represented by

additive noise and additive bias. External disturbances and modelling inaccuracies are also represented by including stochastic terms in a manner suitable for inclusion in a state estimator.

The main novel feature of the model is the application of a separation of the chemical analysis of the neutralisation reaction from the tank dynamics and from the pH measurement. The logarithmic non-linearity of the pH measurement (figure 1.1) is by definition well specified and very severe. On the other hand, the chemical analysis introduces a less severe but more uncertain non-linearity due to the presence of various components in the effluent streams. The novel representation of the chemistry of titration curves is based on dimensional analysis.

The separated model also led to the development of a CAD package for pH systems. The package simulates pH regulation in a common class of unit process. A selection of conventional and novel algorithms for classical control, adaptive control and on-line estimation is included so that their performances can be compared and the likely return on their implementation costs can be assessed. The simulation is accurate in detail, sensitive to uncertainty and well provided with interactive features.

1.4 CONTRIBUTIONS

In addition to the pH survey, the CAD package and the general methodology, this thesis presents four more specific novel contributions to pH control.

1. Application of a novel approach to modelling pH. This uses a mathematical model which explicitly accounts for two separate sources of non-linearity in titration curve: the non-linear chemical analysis of buffered neutralisation reactions and the non-linear pH measurement of figure 1.1.

2. Application of a novel non-linear Bayes' estimator (Jacobs 1983) to the measurement non-linearity. The estimator extracts the ionic concentration difference X from a noisy pH measurement. It is extended here to account for bias on the pH measurement.

3. A cautious stochastic control law which uses estimates of influent flow and acidity generated by a Kalman filter and allows for their uncertainty.

4. Comparisons of a variety of classical, adaptive and stochatic control algorithms.

1.4.1 Mathematical Modelling Of pH Systems

A new general model of neutralisation reaction in a CSTR based on dimensional analysis is developed. The separation of the two non-linearities, the chemical analysis and the pH measurement, provides a basis for the model. Separation of these non-linearities is helpful in understanding the different pH control problems.

The model led to the development of a control methodology using a general classification of pH control configuration on a CSTR. The classification is made according to the absence or presence of buffering which in its turn maybe unknown and changing. A priori information, such as measurements, of flow and pH of influent can be used in different

feedforward configurations. If no measurements are available, an extended Kalman filter state estimator, based on the model, may provide estimates which can be used as synthetic feedforward signals or to drive suboptimal control laws.

1.4.2 The Non-linear Bayes' Estimator

A novel non-linear estimator based on Bayes' rule estimates the ionic concentration difference of the effluent from a noisy non-linear pH measurement by generating numerically a complete probability distribution of the concentration. The mean and variance of the distribution provide respectively an estimate of the i.c.d. and a confidence in the estimate. The Bayes' estimator is used recursively for succesive pH measurements. Propagation of the distribution from one measurement to the next is carried out in two stages: first by linearising the estimate and then by considering the resulting approximate a posteriori distribution after one measurement as the a priori distribution for the next.

The linearised estimate of the i.c.d. is used as a pseudo-measurement to drive an extended Kalman filter which estimates the three essential states of the CSTR. These estimates can be sufficiently accurate to provide synthetic feedforward information of the disturbances when no feedforward measurements are available, or to drive a suboptimal stochastic control law.

A two-dimensional implementation of the Bayes' estimator is investigated. As well as the concentration of effluent, an unpredictable and jumping bias or a slowly varying bias on the pH measurement is successfully estimated provided that the feedforward measurements of disturbance variables are available. The estimation of the measurement bias is necessary in pH regulation because the bias modifies the

effective set point at which a feedback controller operates; also a biased measurement affects the estimation and prediction of the model-based state estimator leading to poor estimation of the states. The bias estimation uses two tests in the case of jumping bias: the first, based on the size of the innovation is for whether the bias seems to have jumped; the second, which is is believed to be novel, is for whether both the concentration of the effluent and the bias can be estimated separately from one measurement.

1.4.3 The Stochastic Cautious Controller

A separated stochastic controller has been developed. It uses estimates of the disturbances generated by the Kalman filter to minimize a cost function which can be defined in terms of ionic concentration difference or of pH. The pH cost function is used because pH is the measured variable and the quality of control is quantified in terms of deviation from pH setpoint. Furthermore, a pH control law would take into account the asymmetry of the pH non-linearity about the operating point.

Caution arises in the controller when the pH cost function is minimized: numerical calculations of an optimal operating point lead to an effective setpoint which is directly influenced by the confidence in the estimates. The effect of this interaction is that reduced quality of estimation results in the optimal operating point moving to a region of lesser slope on the pH non-linearity where control is easier. The caution reproduces what a plant operator would do when he readjusts the operating point if control is not satisfactory.

1.4.4 Comparisons Of pH Control Algorithms

About two dozen different control algorithms are simulated in the CAD package. Most use error-actuated feedback, with feedforward signals as additional options. The error signal driving the feedback controller can be generated either as an error in pH or as an error in ionic concentration difference X.

Simulated feedback controllers include:-

(i) Standard three-term (PID) control with integral desaturation

(ii) Self-tuning three-term (PID) control (Proudfoot 1983)

(iii) Generalised k-incremental minimal variance self-tuning control (Clarke et al 1983)

(iv) Pole placement self-tuning control (Wellstead et al 1979, Clarke 1982, Proudfoot 1983)

Some of the self-tuners include a self-tuning feedforward controller. All feedforward controllers, whether self-tuning or classical, can be driven either by measurements of load flow and acidity or, if the necessary instrumentation is assumed to be unavailable, by online estimates of these load variables.

One simulated algorithm does not have the structure of feedback, feedforward controller. It is the suboptimal stochastic controller of section 1.3.3, in which online estimates of the state variables characterising both plant and load drive an optimal control law.

To provide quantitative comparisons for the different controllers, statistical results in the form of root mean square error in pH, average excess acidity below set point and average reagent flow are calculated.

1.5 ORGANISATION OF THE THESIS

Chapter 2 is a survey of existing pH control schemes. The publications are classified under four sections: theoretical studies, simulations, pilot plant trials and industrial scale applications. The survey shows that few applications of modern control theory have yet been used on-line in full scale processes.

A state space model of a neutralisation reaction in a CSTR is derived in chapter 3. The model uses the separation of the chemistry from the measurement. Process elements are modelled in detail and selected approximations lead to a simplified model.

Chapters 4 & 5 report on application of the novel non-linear estimator, matched to the mathematical model of chapter 3 and to the pH non-linearity, which provides on-line estimates of influent flow rate and acidity. The estimator includes a numerical implementation of Bayes' rule driving an extended Kalman filter estimating the three essential states of the CSTR. An alternative version of the estimator is presented which can estimate the value of bias on the pH measurement provided that measurements of influent flow and pH are available. Observability of the non-linear model and robustness of the estimator are also discussed.

Chapter 6 discusses how different control strategies can be matched to features of a controlled pH process such as chemical analysis of the titration curve, a priori information of flow and acidity of the influent and a priori information of the quality of pH measurement. The control algorithms discussed in this chapter mostly use error-actuated feedback, with feedforward signals as additional options. The error signal is either an error in pH or an error in concentration. The feedback controllers outlined include a standard three-term (PID) regulator with

integral desaturation and a brief summary of different self-tuning regulators. The novel cautious stochastic controller driven by the estimates of the non-linear estimator is also derived in this chapter; the controller takes into account the uncertainty of the estimates.

The simulation package PHDESIGN, written in FORTRAN on the VAX 11/780 at the Department of Engineering Science at Oxford, is described in chapter 7. The chapter outlines the mathematical model and the control algorithms used in the simulation and presents the structure and the interactive features of the package.

The generalised mathematical model of chapter 3 is used for development of controllers in existing processes and for design of new processes. Chapter 8 presents simulation results in the form of case studies of two such processes which were specified in collaboration with the chemical industry. The first process is the neutralisation tank T103A of WBTP; it has been used in the development and design of controllers. It is shown that the simulation results are comparable with those of the full scale plant thus validating the simulation and the model. Performances of modern controllers were better than that of the existing analog controller; this meant reagent savings and confirmed that pH control could benefit from modern control technology. The second process is an example of design of pH regulation in a production process. Here, simulation results establish some key parameters in plant design such as residence time and recycle rate. Also are investigated other aspects of control such as the use of multi-loop systems, feedforward signals and comparison of different controller configurations.

Finally, chapter 9 concludes the thesis with a discussion of the success and the reliability of the algorithms and of their results, and outlines further development of the work initiated in the thesis.

CHAPTER 2

pH CONTROL : A SURVEY

This chapter surveys existing pH control schemes over the last twenty years. An attempt is made to classify over eighty publications, and to outline major ideas applied for regulating pH specially in industrial applications.

Two surveys (Moore 1978, Trevathan 1978) on pH control have been published recently. They summarise different control techniques in the chemical industry until 1975. The present survey is needed because in the last few years there has been much resarch and interest in applying modern control technology, such as digital, adaptive and self-tuning control, to regulating pH. The interest is due to stricter legislation on pollution control, to a need for an increase in efficiency from the industry and to low cost of computing power. The survey classifies the application of control technology to pH regulation and assesses the extent and the success of implementing this technology on an industrial scale.

The chapter is arranged as follows: section 2.1 introduces the classification of pH control in the form of tables, section 2.2 summarise a large number of theoretical studies applied to pH control; section 2.3

surveys different analogue and digital simulation of pH regulation and section 2.4 investigates the merits of pilot plant trials. Section 2.5 discusses in details seven full-scale industrial applications of modern control techniques to pH regulation. Section 2.6 concludes the chapter.

2.1 INTRODUCTION

The pH survey carried out in this chapter is summarised in two tables. Table 2.1 groups all the research papers under four different headings: suggestions and theoretical studies, analog and digital simulations, pilot plant trials, and industrial scale applications. Each study appears only once in any one group. The table shows that few of the suggestions were applied on industrial scale and that all but two of the full-scale applications were carried out in the last ten years. Table 2.2 classifies the more important publications according to their control techniques: linearization of the pH measurement, feedback control, feedforward control and adaptive control; batch, on-off control and data sampling are grouped under other techniques. The table shows that the four major control techniques have been suggested or used equally often to improve regulation and that most of the publications reported on two or more techniques usually in the form of comparison of performance.

2.2 SUGGESTIONS AND THEORETICAL STUDIES

Theoretical analysis of the pH titration curve was carried out by Creason (1978), Findley (1961), Hoffman (1979), Hoyle (1975), Shinskey (1973, 1979), and Trevathan (1974). It included investigations of the effects of the presence of buffer solutions in waste streams on the pH process gain. Their analysis concluded that buffering facilitates

SUGGESTIONS	SIMULATIONS	PILOT PLANTS	INDUSTRIAL SCALE
Best(1978)	Ersü, Mao(1983)	Bergman, Lachman(1980)	Belletrutti et al(1976)
Bown(1983a,b)	Field(1959)	Buchholt, Kümmel(1979)	Hewkin(1979)
Creason(1978)	Galetti, Friedmann(1972)	Fraade(1978)	Iverson, Ochai(1977)
Findley(1961)	Goodwin et al(1982)	Gupta, Coughanowr(1978)	Jacobs et al(1980)
Grässel(1974a,b)	Gupta, Coughanowr(1974)	Kaesser(1980)	Jutila(1983)
Gray(1980)	Jacobs et al(1984)	Kirlin, Marshall(1975)	Proudfoot(1983)
Greer(1966)	Jutila, Orava(1981)	McAvoy(1972)	Rowton(1968)
Harriot(1964)	Jutila et al(1981)	McAvoy et al(1972)	Shinskey(1974)
Hoffmann(1979)	Kuhn, Bender(1981)	Morris et al(1981)	Stansbury et al(1980)
Hoyle(1975)	Marra(1974)	Niemi, Jutila(1977)	Wilson, Wylupeck(1969)
Hoyle(1976)	Mellichamp et al(1966)	Peters(1970)	
Jacobs(1983)	Niemi, Jutila(1978b)		
Jungk, Woytowicz(1971)	Nihtilä, Jutila(1982)		
McAvoy(1974)	Richter et al(1974a)		
McCormack(1962)	Richter et al(1974b)		
Moore(1978)	Roberts(1971)		
Myron, Shinskey(1974)	Wolfunder et al(1978a,b)		
Niemi(1978)			
Niemi, Jutila(1978a)			
Orava, Niemi(1974)			
Pluhar(1983)			
Rang(1975)			
Rang(1977)			
Shinskey(1968)			
Shinskey(1973)			
Shinskey(1979)			
Sommer(1981)			
Trevathan(1972)			
Trevathan(1974)			
Trevathan(1978)			
Walter, Wilke(1973)			
Williams(1971)			

TABLE 2.1 pH control publications

PUBLICATIONS	LINEAR	F.BACK	F.FORWRD	ADAPTIVE	OTHERS
Belletrutti et al(1976)	X				
Bergman, Lachman(1980)				X	
Best(1978)	X	X			
Buchholt, Kümmel(1979)	X			X	
Ersü, Mao(1983)				X	
Field(1959)	X	X			
Fraade(1978)					X
Galetti, Friedmann(1972)	X	X	X		
Goodwin et al(1982)	X			X	
Gray(1980)	X	X	X		
Gupta, Coughanowr(1974)				X	
Gupta, Coughanowr(1978)				X	
Harriot(1964)		X			
Hewkin(1979)	X	X	X	X	X
Hoyle(1976)			X		
Iverson, Ochai(1977)	X	X			
Jacobs(1983)	X				
Jacobs et al(1980)	X	X	X	X	
Jacobs et al(1984)	X	X	X	X	
Jungk, Woytowicz(1971)					X
Jutila(1983)	X	X	X	X	
Jutila, Orava(1981)	X	X	X	X	
Jutila et al(1981)	X	X	X	X	
Kaesser(1980)				X	
Kirlin, Marshall(1975)					X
McAvoy(1972)		X			
McAvoy(1974)					X
McCormack(1962)	X				
Mellichamp et al(1966)				X	
Moore(1978)	X	X	X	X	X
Morris et al(1981)				X	
Myron, Shinskey(1974)				X	X
Niemi(1978)	X	X	X		
Niemi, Jutila(1977)	X	X	X		
Niemi, Jutila(1978a)	X	X	X		
Niemi, Jutila(1978b)	X	X	X		
Nihtilä, Jutila(1982)	X	X	X	X	
Peters(1970)		X			
Pluhar(1983)	X	X	X		
Proudfoot(1983)		X	X	X	
Richter et al(1974a)				X	
Roberts(1971)	X	X			
Rowton(1968)					X
Shinskey(1968)			X		
Shinskey(1973)	X	X	X	X	X
Shinskey(1974)				X	
Shinskey(1979)	X	X	X	X	X
Sommer(1981)	X				
Stansbury et al(1980)	X	X	X	X	
Trevathan(1972)				X	
Trevathan(1978)	X	X	X	X	X
Walter, Wilke(1973)	X				
Williams(1971)			X		
Wilson, Wylupeck(1969)	X		X		
Wolfunder et al(1978a,b)				X	

TABLE 2.2 pH control techniques

control of pH around the neutral point but that variable composition of the influent stream makes the pH response to large load changes of flow rate very poor. No remedies were proposed except for Shinskey's adaptive controller which is discussed in section 2.4.

Effects of the high and non-linear process gain of the titration curve on valve rangeability and on pH control are discussed by Moore (1978), by Myron and Shinskey (1974) and by Trevathan (1972). They suggest keeping the gain product of the valve and the titration curve constant by using split range valves as mentioned in section 1.2.3 (4).

Various schemes have been proposed which attempt to linearize the forward pH control loop by compensating for the non-linear measurement. Best (1978) inverts the titration curve, hence his scheme is curve-dependent. Gray (1980) and Pluhar (1983) describe two similar industrial pH controllers developed by Leeds & Northrup Instruments. They are microprocessor-based controllers which generate a model of the process titration curve based on laboratory data taken from representative process samples. The microprocessor inverts the model to linearize the pH process allowing standard linear controller tuning methods to be used. Provisions for the inclusion of feedforward signals of effluent flow are provided. No comparisons of performance of the controllers were published.

Another possibility is to introduce an ionic concentration variable which is a difference between concentration of hydrogen ions and concentration of hydroxyl ions in a solution. Greer (1966) named the variable acidity; the term ionic concentration difference (i.c.d.) was introduced by Orava and Niemi (1974). The relationship between i.c.d. and pH, figure 1.1, is symmetric about the neutral point of pH 7. Jacobs

(1983) developed a non-linear Bayes' estimator which extracts the ionic concentration difference from a noisy pH measurement. Application of the Bayes' estimator to the pH non-linearity are discussed in detail in chapter 4.

In other developments McAvoy (1974) models pH regulation in a CSTR using material balances on some chemical species. The modelled reaction consists of neutralisation of a strong reagent by a weak one of known dissociation constant; the model cannot be generalised to more complex situations. Stability analysis of the pH control system using Lyapunov's second method and Popov's criteria is reported by Orava and Niemi (1974) and by Rang (1975, 1977) who derives an equation for the concentration of hydrogen ions in terms of hyperbolic trigonometric functions. Few of these ideas have been tested beyond simulations trials because they are usually specific to the process under study and are difficult to implement. Analysis of pH control systems using frequency response methods is reported by McCormack (1962) and by Marra (1974); the frequency analysis method was time-consumming and failed to yield any meaningful controller settings for all the pH span.

The author developed a general model of pH regulation in CSTR. It separates the non-linear measurement of figure 1.1 from the non-linear chemistry of buffered reagents; it is derived in chapter 3.

2.3 ANALOG AND DIGITAL SIMULATIONS

As early as 1959, Field (1959) pioneered the use of computer simulation for design and for analysis of pH control systems. He reported an analog simulation of stirred tank reactors for designing a waste disposal treatment system. Optimum performance in simulation was achieved by high speed mixing in the tanks, by a linearised pH

measurement using an anti-log converter, and by the use of three-stage neutralisation vessels. No results of the industrial system were published.

Roberts (1971) used a digital simulation of a CSTR to study the application of a non-linear controller to the regulation of pH. The controller comprised an inversion of the process titration curve coupled to a proportional regulator. Results were only shown for one strong reagent titration curve which is symmetrical about the operating point.

In a simulation of a feedforward and adaptive pH control system, Richter et al (1974a) used an identifier consisting of a plug flow system tuned to sustain limit cycles. Reagent flow rate and average gain of the titration curve were calculated from measurements of incoming flow rate and incoming pH. Accuracy of the identifier was severely limited when unsymmetric titration curves were analysed.

Adaptive control was also tested in simulation by Jutila and Orava (1981) and by Jutila et al (1981). Their study included modelling a pH process using basic physico-chemical laws. The model was characterized by the presence of hypothetical chemical species which can be chosen by static fitting of the titration curve. The non-linear curve fitting algorithm needs considerable computing power and is carried out off-line. A Kalman filter algorithm estimates concentrations of the chemical species from linearized measurements of influent and effluent pH and from a measurement of influent flow rate. The simulation results were backed by on-line tests (Jutila 1983) which are discussed in section 2.5.

Jacobs and Badran (1984a,b) reports on a CAD package for pH systems developed by the author in which the user specifies process dynamics and the process titration curve. The package was introduced in chapter 1 and

is described in detail in chapter 7.

2.4 PILOT PLANT TRIALS

In a specific case of neutralising sodium hydroxide with acetic acid, McAvoy et al (1972) derived a theoretical model for pH control in a CSTR. The model is based on electroneutrality and mass balance equations. McAvoy (1972) then applied Pontryagin's principle to derive an optimal control law. A pilot plant is used to test the model and to compare the time-optimal control law with a Ziegler-Nichols tuned PD controller which achieved the best performance. In his experimental work, McAvoy kept the concentration of the acid and the concentration of the base, and the flow rate of the base constant; thus the results shown are very specific to this particular example and cannot be generalised.

Niemi and Jutila (1977) studied a combination of linearization and proportional control with feedforward signals in simulation and on a laboratory-scale experiment controlled by a mini-computer. Their results showed good performance for effluent streams containing known weak acids and/or weak bases at known concentrations.

In a pilot plant, Gupta and Coughanowr (1978) used a square wave input to an identifier tank (test cell) to calculate the gain of a pH process in which changing concentrations and variable buffering were present in the influent. The feedback controller gain in the main tank could be modified to compensate for the process changes. Disadvantages of this adaptive scheme are: the period of the identifying signal is critical to the performance of the gain estimator, a large identification lag between the true process gain and the estimated gain may lead to oscillatory response, and the cost of implementing the hardware is high.

In the last few years the introduction of mini and microcomputers enabled researchers to investigate adaptive controllers in which the identification procedure is carried out in software and on-line. Kaesser (1980) and Bergman and Lachman (1980) used a Recursive Least Square (RLS) identifier to estimate the pH process gain. Kaesser used lime and sulfuric acid to neutralise waste water in a pilot plant reactor. The RLS estimator identified the time-varying gain of the titration curve and adjusted parameters of a PI regulator. A two-chambers reactor was used to allow for the lime to react completely. The performance of the controller was good and could be improved if the feedforward signals were incorporated in the estimator. Bergman and Lachman described the application of two controllers for the neutralisation of acid with base in a pilot plant process for which the titration curve is held constant. Although the authors claim that the acid and the base are strong, the published titration curve is buffered probably due to the presence of carbonate ions in the water. The two controllers were: an Extended Minimal Variance controller for load disturbances and a Dead Beat controller for set point changes. Improvments in performance of the two controllers over an analog PI regulator do not justify in the view of the author this 'adaptive' scheme.

Self-tuning controllers for pH systems were investigated on pilot plants by Buchholt and Kümmel (1979) and by Morris et al (1981). Neutralization of a strong acid with a strong base was carried out in both experiments. The first experimental apparatus consisted of a packed column modelling a time delay coupled to a CSTR while Morris and co-workers used an electrochemical cell interfaced to a microprocessor. Performances of the self-tuning controllers were better than those of digital PID regulators for runs of few hundred samples. Experimental investigations of the adaptive controllers for buffered titration curves

would have been necessary to complete the study.

2.5 INDUSTRIAL-SCALE APPLICATIONS

Most of the industrial-scale applications of pH control were carried out in the last ten years probably due to tightning of legislation governing waste stream qualities. Improvements in the quality of control in the publications surveyed were essentially due to the application of better engineering design rather than to modern control.

Shinskey (1974) reports on an early investigation of application of pH control on a full-scale process for waste neutralization in which the process effluent concentration and composition were variable. Shinskey's pH controller is a non-linear adaptive controller. The adaptive part can distinguish between oscillatory response of pH and a drifting response. The detector is made of parallel low-pass and high-pass filter circuits. High frequency oscillation of the pH would be blocked by the low-pass filter but would pass through the high-pass circuit and reduce the controller gain. The low frequency drifting would have the opposite effect. The non-linear part of the controller consists of a dead band function in which the dead-band width and the gain within it are both adjustable and the gain outside it is equal to unity. The output of the filter circuits widens or narrows the dead-band of the controller. Performance of the controller for load changes justified its cost within twelve days but the adjustment of dead-band width and gain, and the high and low band pass widths would require sophisticated tuning techniques. The controller will perform well only if the operating point is symmetrical about the titration curve.

Shinskey's adaptive controller was also used on two other full-scale neutralizations of waste stream as reported by Iverson and Ochai (1977) and by Stansbury et al (1980). In both applications, good control was achieved by better engineering and by using the adaptive controller when variable buffering was present. In the first process, neutralization of a heavily buffered carbonated effluent stream with sulfuric acid was carried out in a canal system. Improvment in pH control was due to better mixing of the effluent with the acid by incorporating in the canal a narrowing junction to increase the stream velocity. Positioning the pH probe nearer to the junction reduced the measurement lag considerably. In order to linearize the reagent flow loop, the output of the non-linear controller was cascaded as an input to the flow controller. The overall control system was effective and the resulting controlled pH output was successfully held within the required limits of pH 6 - 9.

Stansbury et al (1980) describe a process of pH control for mercury elimination from waste water. A triple-stage CSTR design is used with a combination of feedback, feedforward, and non-linear adaptive control. The adaptive control is needed because of changes in the slope of the neutralization curve in the control region due to variable buffering. The primary tank system takes out major variations in acid requirements; the non-linear adaptive feedback system is used to control the reagent addition in the second reaction tank and the third tank attenuates pH swings from the second tank. The design of the three tanks, the sizing of control valves and good tuning of the feedback controller helped to stabilize pH within 0.1 pH unit.

Recently, Jutila (1983) applied an adaptive controller developed and tested on simulation and on a pilot plant (see section 2.3) to a municipal waste water treatment plant. The pH of the incoming waste

varied between pH 6 and pH 10 and the flow rate varied by a factor of 4. The required operating point was pH 5.5. Estimates of concentration generated by a Kalman-type filter would drive a linearized PI regulator. The developed algorithm gave better control response then the original plant controller for large acid changes in the load . The process neutralization curve was well buffered and the process was " somewhat too easy too control with this adaptive algorithm. " (Jutila 1983, section 7).

As part of the current collaborative university/industry project introduced in chapter 1, Hewkin (1979) tested some modern control algoritms on a full scale neutralization process of waste stream. A summary of his results is reported by Jacobs et al (1980). The control algorithms included a digital PID controller, a self-tuning controller and an "optimal" adaptive controller. A linearized pH measurement, processed feedforward signals of effluent flow and a cascaded flow controller on the reagent valve combined with the PID regulator to achieve good pH control. Proudfoot's (1983) work is a continuation to that of Hewkin's. Proudfoot developed and applied different self-tuning regulators on an industrial neutralization reactor. The CSTR is used to treat acidic effluent from mercury cell rooms used in chlorine production. The controllers performed well over long periods of time achieving significant reagent savings. An extensive simulation of this pH process is carried out in chapter 8.

Measurement difficulties resulting from pH probe fouling have affected some of the industrial applications. Shinskey (1974) used an electrosonic cleaner to increase the response speed of the electrode. Jutila (1983) suggested stopping estimation while the measuring instrument was cleaned. Hewkin (1979) include a bias term in the

estimator to account for drift on the probe and Proudfoot (1983) used a newly developed cleaning mechanism to prevent blockage of the pH measurement. Section 4 of chapter 4 of the thesis deals at length with biased pH measurements and reports on a new method to solve this difficulty in some circumstances.

2.6 CONCLUSION

Existing pH control schemes have been surveyed; the reported successful applications of modern control theory to industrial scale pH processes are few and specific to particular plants. In most of these applications, good pH control was achieved when good engineering design was implemented: correct control configuration, tank design and valve sizing, linearization of reagent flow loop using cascaded control and usage of feedforward signals when available. Modern control techniques such as adaptive control were necessary only when variable buffering was present in the influent stream. The CAD package presented in the thesis facilitates a large number of these design procedures and gives the user an insight in the quality of control which can be achieved.

CHAPTER 3

ON MODELLING pH

This chapter contains a generalised approach to modelling pH in a common class of unit process. The model is based on a separation of the chemistry of process neutralization and the pH measurement. Based on dimensional analysis, a novel theoretical representation of titration curves for known reagents is derived. Selected approximations are made in the case of unknown reagents and the representation is used to derive a general state space model of the process.

The general approach to modelling pH regulation is introduced in section 3.1. Titration curve chemistry and the pH measurement are investigated in sections 3.2 and 3.3; the state space model of the process, in the form of stochastic equations, is derived in section 3.4 and validated in section 3.5. Section 3.6 concludes the chapter.

3.1 INTRODUCTION

An initial step in developing a suitable process control system is the construction of a process model. As introduced in chapter 1, the process is a pH neutralization system in a Continuous Stirred Tank Reactor (CSTR) and is shown in figure 1.2. The steady-state process gain, the ratio of effluent pH to reagent flow, is the highly non-linear

titration curve (figure 3.1a).

Two separate features which contribute to the non-linearity of titration curves are shown in figure 3.1b. They are: the known logarithmic non-linearity of the pH measurement, equation 1.1, and the less known but often more uncertain effect of reaction chemistry which determines how $[H^+]$ depends on volumes and compositions of reagents. The chemical reaction between the influent and the reagent starts usually in pipes prior to entering the tank and is completed in the tank. The steady-state concentration of the regulated effluent stream is a complex non-linear function of concentration and flow rate of the reagent and of the influent; this function is derived in section 3.2. It provides the basis for analytical modelling of the chemistry of pH regulation in a CSTR. The model of the CSTR is derived in state-space form in section 3.3 and comprises two major dynamics: a first order lag which accounts for the effluent flow through the holding tank, and a variable dead time which models delays in the mixing. The process model is then used in the next chapters for estimation and control.

3.2 CHEMICAL ANALYSIS OF NEUTRALIZATION REACTIONS

3.2.1 Introduction To The Chemistry Of Neutralization

In this section, a general chemical analysis of titration curves is derived from basic principles for 'strong' (section 3.2.2) and for 'weak' (section 3.2.3) reagents as defined in chapter 1. The analysis relates in a novel way the concentration of the effluent to the flow rate and concentration of the influent and the reagent. This relationship, in order to be used in a model of pH regulation, is reduced to a three-dimensional surface using dimensional analysis. The relationship

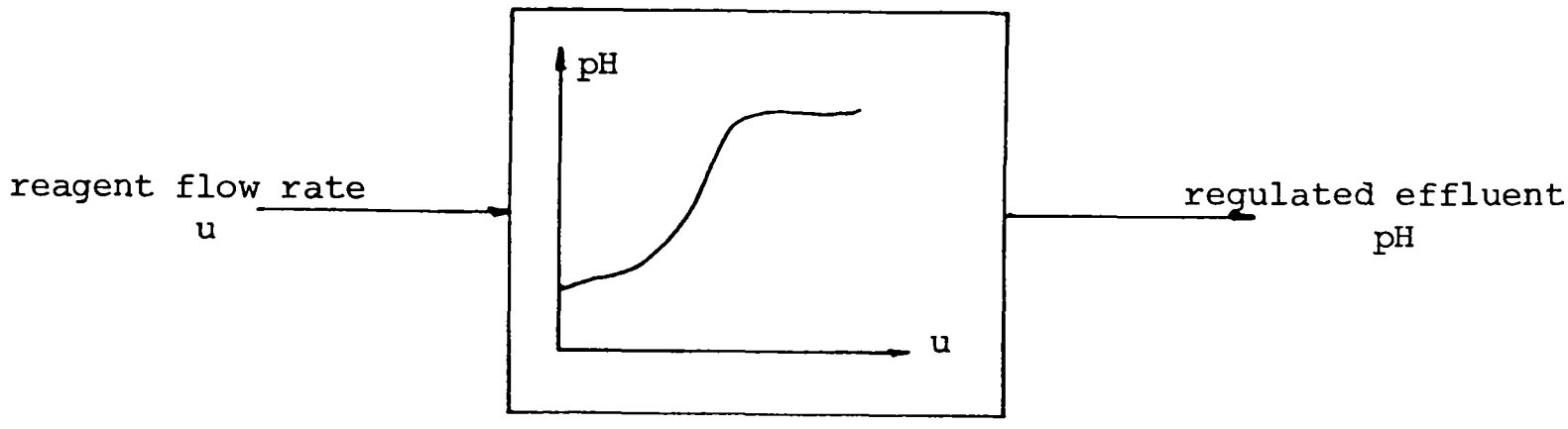


Fig 3.1a The steady-state process gain

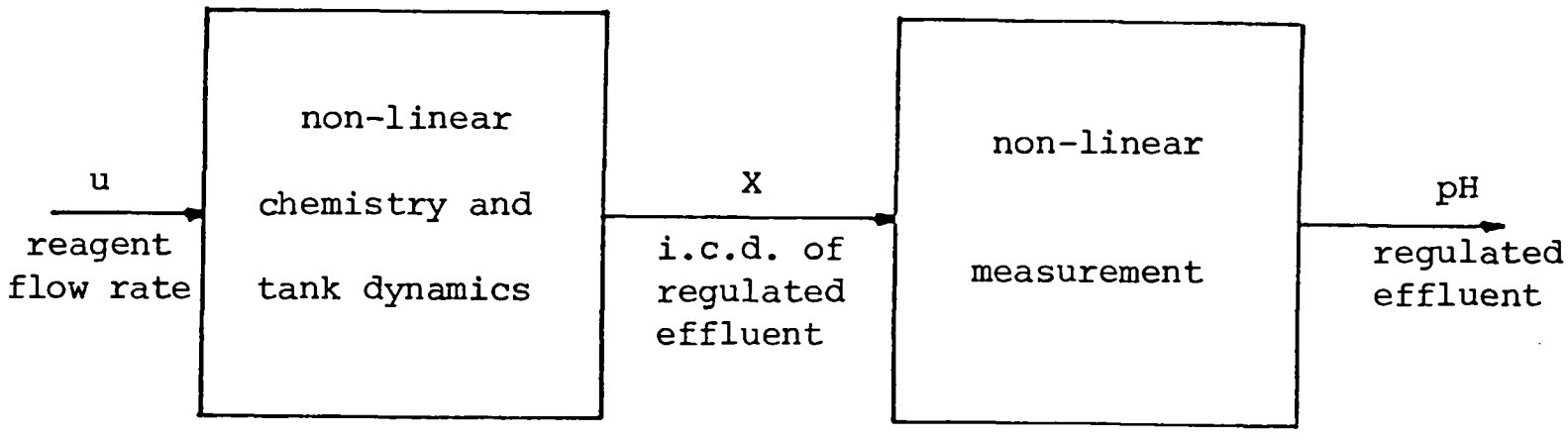


Fig 3.1b The separation of the pH model

provides a basis for modelling the chemical reaction of the state space model of pH regulation in a CSTR in section 3.4.

A distinction between 'strong' and 'weak' reagents simplifies the analysis of titration curves for neutralization reactions. This distinction describes the way that reagents dissociate, it has nothing to do with concentration. A strong reagent is one which, when dissolved in water, dissociates completely into its ionic species; weak reagents and water itself dissociate only partially and the concentration of their ionic species are governed by a dissociation equation similar to equation 1.3.

The acidity and the basicity of a aqueous solution is related to the concentration of hydrogen ions H^+ and hydroxyl ions OH^- as introduced in section 1.2. The concentration $[H^+]$ and $[OH^-]$ always satisfy the dissociation equation:

$$[H^+][OH^-] = K_w \qquad (1.3)$$

It is convenient to represent acidity and basicity not by $[H^+]$ but by the ionic concentration difference (i.c.d.) X defined by

$$X = [OH^-] - [H^+] \qquad (1.1)$$

which combined with equation 1.3 gives:

$$[H^+] = -\frac{X}{2}\left(1+\sqrt{(1+4K_w/X^2)}\right) \quad \text{if } X < 0 \qquad (3.1a)$$

$$[H^+] = -\frac{X}{2}\left(1-\sqrt{(1+4K_w/X^2)}\right) \quad \text{if } X > 0 \qquad (3.1b)$$

The representation in i.c.d. is chosen because it leads to a symmetric relationship between pH and X as in figure 1.1; X is negative for an acid solution, positive for a basic one and zero for pure water.

The relationships between the i.c.d. of a mixture and the concentrations of its components are derived in the following sections for strong and weak solutions of known and unknown reagents.

3.2.2 Strong Reagents

Chemical neutralization reactions in aqueous solution of strong reagents are well defined in virtue of the complete ionic dissociation of the reagents. These reactions seldom occur in real life because carbonate and other ions, which are usually dissolved in the water, act as buffer agents.

Consider the reaction between a sample of strong acid HCl, and a strong base reagent NaOH. Both are completely ionized in their solutions:

$$HCl + NaOH + H_2O \rightarrow H^+ + OH^- + Na^+ + Cl^- \qquad (3.2)$$

The ionic concentrations satisfy the principle of electroneutrality:

$$[H^+] + [Na^+] = [OH^-] + [Cl^-] \qquad (3.3)$$

Combining with equation 1.1, we have

$$X = [Na^+] - [Cl^-] \qquad (3.4)$$

where $[Na^+]$ & $[Cl^-]$ are the concentration of the base ion and the acid ion. They are given by:

$$[Na^+] = \frac{V_r X_r}{V_r+V_s} \qquad [Cl^-] = -\frac{V_s X_s}{V_r+V_s} \qquad (3.5)$$

where V_r, X_r and V_s, X_s are volumes and i.c.d.'s (in gm.ions l^{-1}) of samples and reagents respectively. X_r and V_s are kept constant during titration.

Usually, the reagent is highly concentrated so that $V_r << V_s$ and:

$$[Na^+] \simeq V_r X_r / V_s \qquad [Cl^-] \simeq -X_s \tag{3.6}$$

Replacing in equation 3.4, we have:

$$X = X_s + V_r X_r / V_s \tag{3.7}$$

The relationships between the i.c.d. X & X_s and between X & $V_r X_r / V_s$ are linear with unity slope.

Other strong acids include HBr, HI, $HClO_4$ and HNO_3. Although H_2SO_4 may sometimes be considered as a strong acid, it is not completely dissociated below pH 2 and its relationship of X vs. $V_r X_r / V_s$ will deviate from the strong reagent one (section 3.2.3). Strong bases include LiOH and KOH. Here again lime, $Ca(OH)_2$, is not completely ionized above pH 12 and is considered a weak base.

3.2.3 Weak Reagents

Weak reagents, unlike strong ones, do not dissociate completely. The relationship governing their concentrations is well defined only in the case of known reagents and known dissociation constants. Two cases are analysed: one for which all the reagents are known; the other, the more common, for which a titration curve is the only available information.

CASE 1: Known weak reagents:-

Consider a neutralization of a sample of acetic acid, HAc, by the strong base reagent sodium hydroxide, NaOH (Shinskey 1973):

$$HAc + NaOH + H_2O \rightarrow H^+ + OH^- + Na^+ + Ac^- \tag{3.8}$$

Satisfying the principle of electroneutrality:

$$[H^+] + [Na^+] = [OH^-] + [Ac^-] \quad (3.9)$$

Here, only NaOH is completely ionized; the concentration of its base ion $[Na^+]$ is given by equation 3.6:

$$[Na^+] = V_r X_r / V_s \quad (3.10)$$

Only a fraction of the weak acid will ionize, the remainder [HAc] being in equilibrium with the product of its ions, obeying the relationship:

$$K_c = [H^+][Ac^-]/[HAc] \quad (3.11)$$

where K_c is the dissociation constant of acetic acid ($= 10^{-4.75}$ at STP).

The total concentration of the acetic group [Ac] is the sum of the dissociated acetic ions $[Ac^-]$ and the non-dissociated acid [HAc]:

$$[HAc] = [Ac] - [Ac^-] \quad (3.12)$$

Substituting equation 3.12 in equation 3.11 and rearranging, we have:

$$[Ac^-] = \frac{[Ac]}{1+[H^+]/K_c} \quad (3.13)$$

Replacing $[Ac^-]$ in equation 3.1 we have:

$$[OH^-] - [H^+] = [Na^+] - \frac{[Ac]}{1+[H^+]/K_c} \quad (3.14)$$

Substituting $[OH^-] - [H^+]$ and $[Na^+]$ from equations 1.1 and 3.10:

$$X = V_r X_r / V_s - \frac{[Ac]}{1+[H^+]/K_c} \quad (3.15)$$

This same result was also derived by Niemi and Jutila (1977).

The following discussion is believed to be original: an equation governing the relationship between i.c.d.'s and volumes of the different chemical components is derived from equation 3.15 and from geometric representation. This relationship is then reduced by dimensional analysis and discussions of relevant approximations are made.

Let X_s be the value of i.c.d. X when no reagent is added (V_r=0):

$$X_s = - \frac{[Ac]}{1+[H^+]/K_c} \qquad (3.16a)$$

Substituting for X_s in equation 3.15 which combines with equation 3.1a to give:

$$X_s = - K_c[Ac]/(K_c - \frac{X_s}{2}(1+\sqrt{(1+4K_w/X_s^2)})) \qquad (3.16b)$$

or:

$$X_s = - K_c[Ac]/g(X_s) \qquad (3.17)$$

where the function g(x) is defined by:

$$g(x) = K_c - \frac{x}{2}(1\pm\sqrt{(1+4K_w/x^2)}) \qquad (3.18)$$

Replacing [Ac] in equation 3.15 and rearranging:

$$Xg(X) = X_s g(X_s) + \frac{V_r X_r}{V_s} g(X) \qquad (3.19)$$

Equation 3.19 defines the non-linear relationship between X & X_s and between X & $V_r X_r/V_s$. This relationship is complex but well defined provided that the dissociation constant of the acid K_c is known. In the case of strong reagents g(X) equals $g(X_s)$ and equations 3.7 and 3.19 are the same.

The functional relationship $X(X_s,X_r,V_s,V_r)$ of equation 3.19 determines the i.c.d. X in a mixture of two specific components. From Buckingham's Π theorem, the five dimensional relationship can be reduced by the number of fundamental dimensions used, which is two here (volume and molecular mass). So a three-dimensional surface should completely describe the chemistry of a given pair of components. The choice of dimensionless groupings has been influenced by the values of the variables and by the known equation for strong reagents (equation 3.7). The three dimensionless groups are: X/X_r, X_s/X_r and V_r/V_s. X_r and V_s will not take the value of zero, and the groups are well defined for other values of X_r and V_s and for all values of X, X_s and V_r.

For strong reagents, equation 3.7 can be written as

$$X/X_r = X_s/X_r + V_r/V_s \qquad (3.20)$$

On a three-dimensional axis labelled by the dimensionless groups X/X_r, X_s/X_r and V_r/V_s (for x,y and z) the chemistry of strong reagents is defined by a plane passing through the points (0,0,0), (1,0,1) and (0,1,1).

For known weak reagents, the relationship

$$X/X_r = h_1(X_s/X_r,V_r/V_s) \qquad (3.21)$$

may be calculated numerically over some range of the variables such as

i) $X_s/X_r \leqslant 0$ limiting the titration process to the neutralization of acid with base or vice versa (but not addition of base to base or acid to acid);

ii) $0 \leqslant V_r/V_s \leqslant 1$ which is true in most cases where the reagent is more concentrated than the sample.

Figure 3.2 shows the three-dimensional solution of equation 3.21 for the

neutralization of acetic acid with sodium hydroxide, when varying X_s/X_r from -0.01 to -0.005 and V_r/V_s from 0.0 to 0.5. For a fixed X_s (figure 3.2a), X/X_r levels off at around zero as V_r/V_s increases creating a plateau typical of buffering solutions, until the effect of the buffering becomes negligible and the relationship reverts to the linear relationship of strong reagents. The figure is a titration curve in which the vertical axes of pH is transformed into ionic concentration difference X. For a fixed V_r (figure 3.2b), X/X_r vs. X_s/X_r is highly non-linear: as X_s/X_r increases, X/X_r is held constant until the buffering effect of the weak acid is predominant and X/X_r increases gradually and levels off as the buffering effect decreases.

The objective of this analysis is to provide an approximate relationship which governs the chemistry of unknown weak reagents. This approximation may either be in terms of i.c.d., figure 3.2, or in terms of pH as in figure 3.3 which is obtained by transforming the i.c.d. X of equation 3.21 into pH:

$$pH = h_2(X_s/X_r, V_r/V_s) \qquad (3.22)$$

Here, the effect of the buffering of the acetic acid is concealed because the strong non-linearity of figure 1.1 prevails. Equation 3.22 describes the relationship of the mixture pH for variation in sample pH and in reagent volume but it cannot be used for approximation in the case of unknown weak reagents. Equation 3.21 (or figure 3.2) is a better candidate because the effect of buffering is more readily apparent.

In the next sections, titration curve data is used to approximate equation 3.22 from a three-dimensional surface to a two-dimensional function. The function is used to calculate the i.c.d. X of the mixture and provides a basis for the development of the state space model.

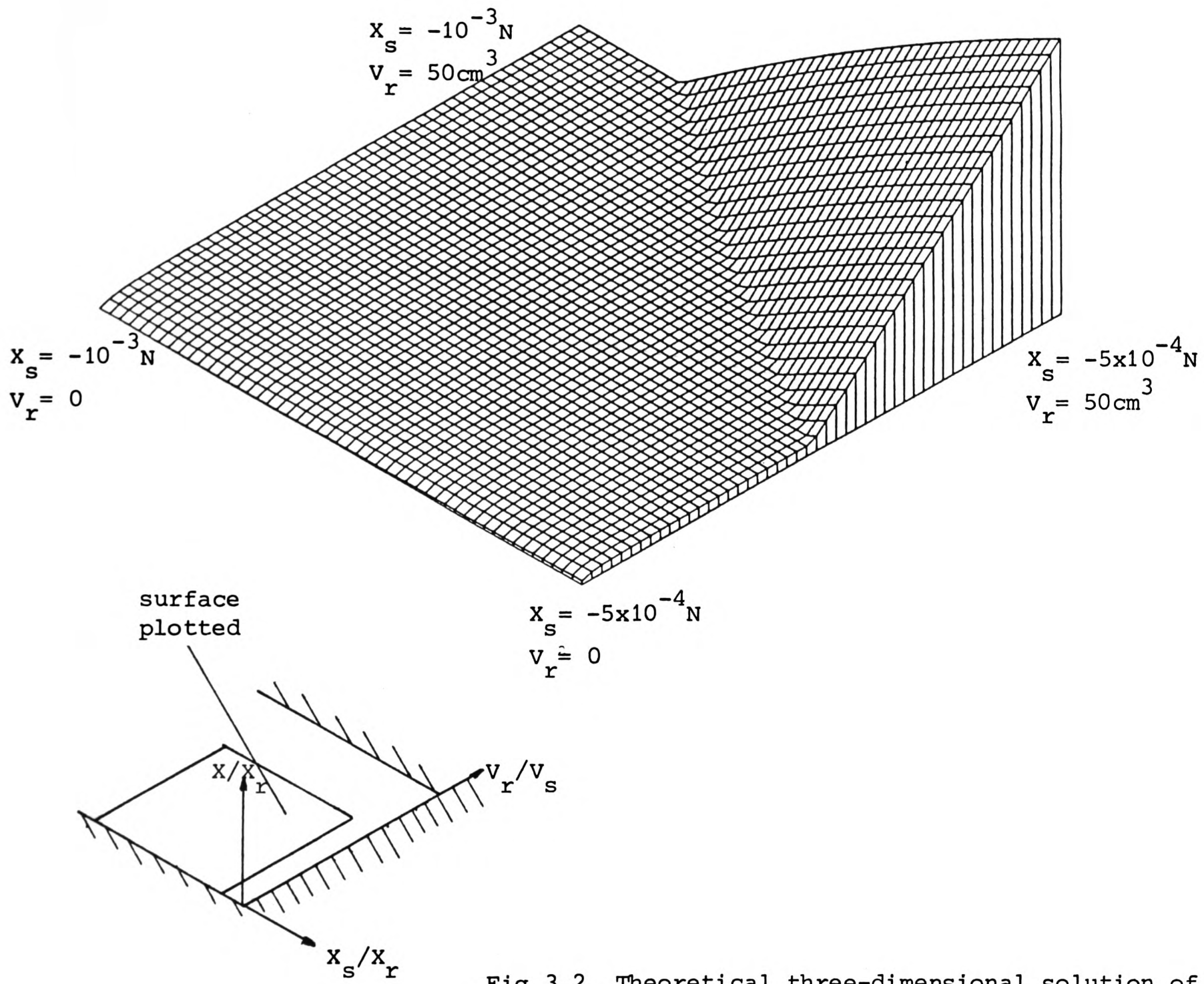


Fig 3.2 Theoretical three-dimensional solution of

$$X/X_r = h_1(X_s/X_r, V_r/V_s)$$

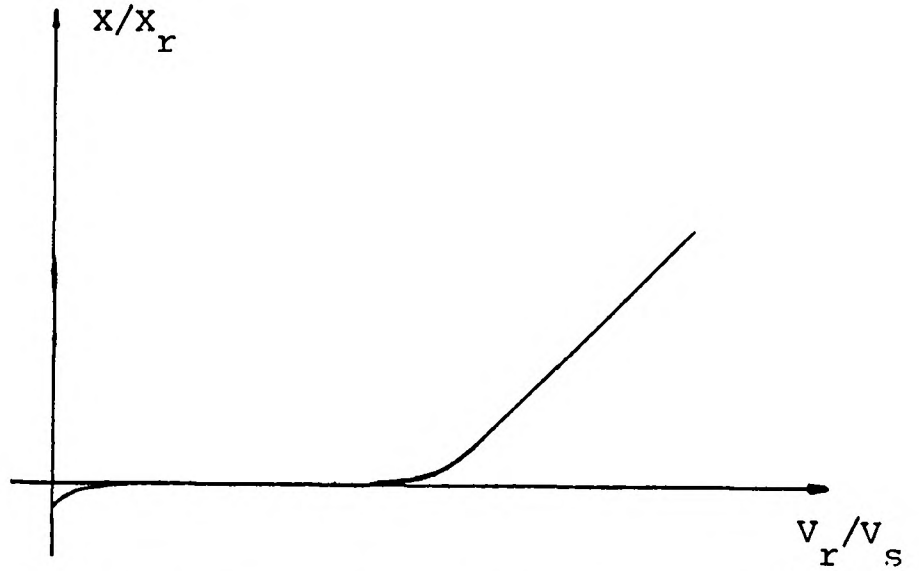


Fig 3.2a For constant X_s (= $-5x10^{-4}$N.)

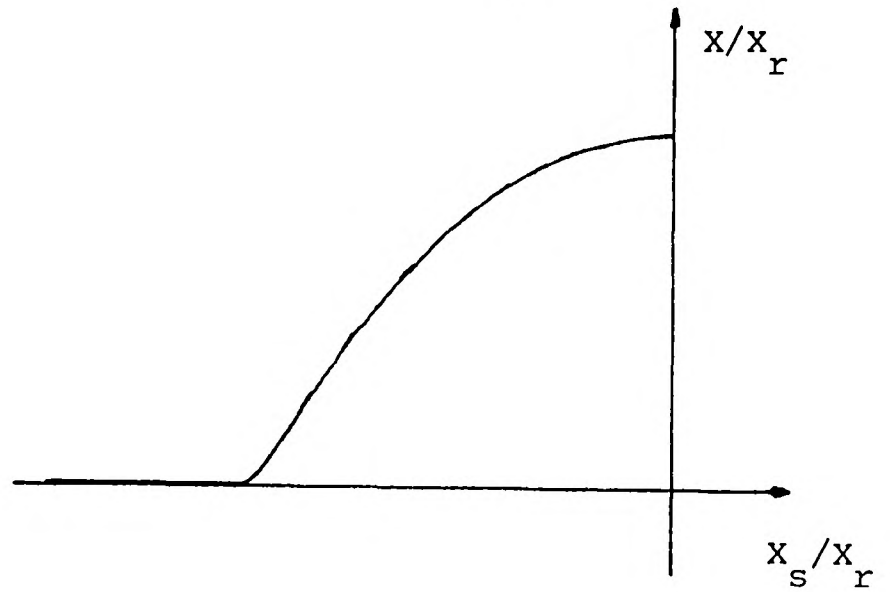


Fig 3.2b For constant V_r (= $50cm^3$)

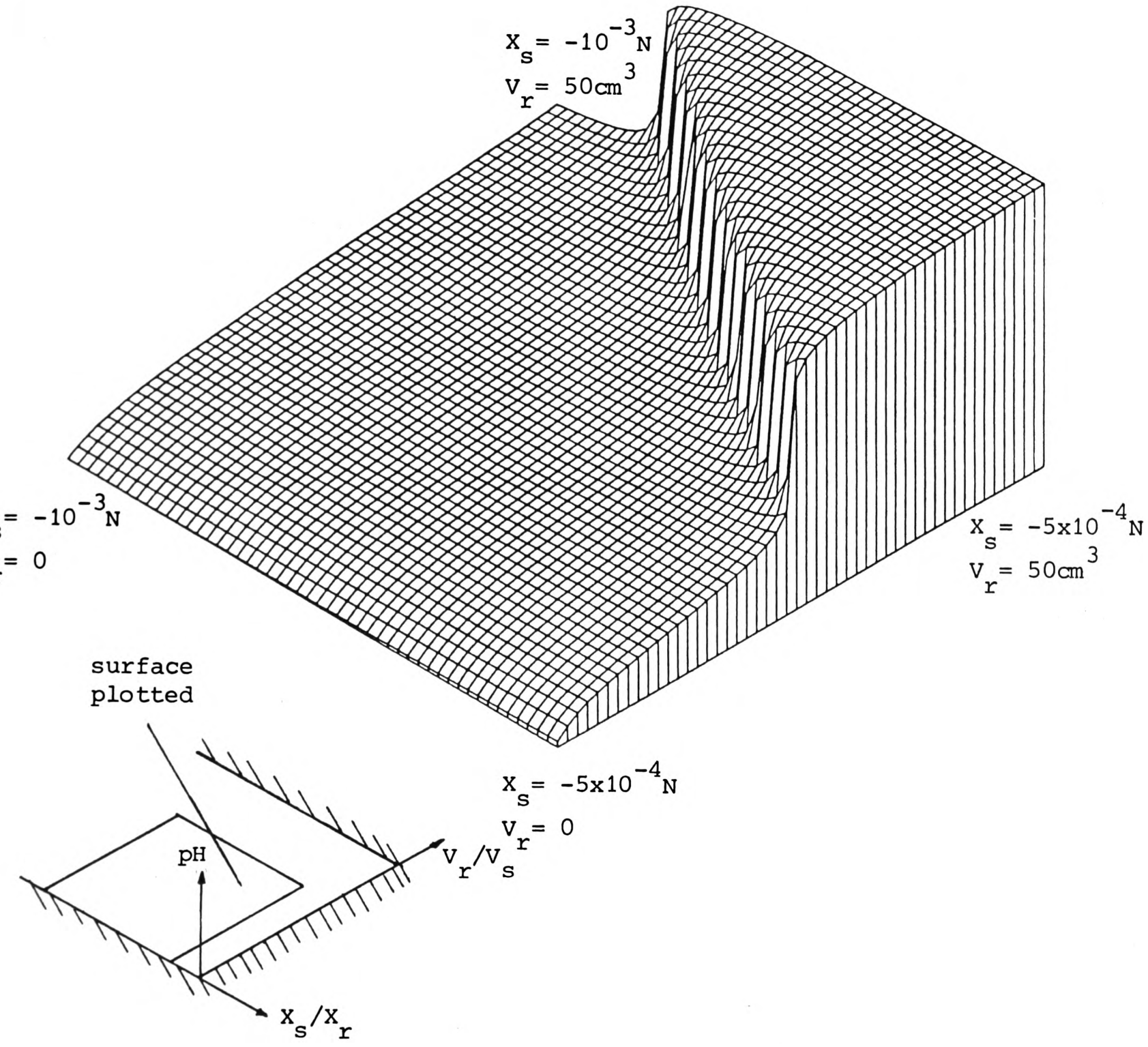


Fig 3.3 Theoretical three-dimensional solution of

$$pH \doteq h_2(X_s/X_r, V_r/V_s)$$



Fig 3.3a For constant X_s (= $-5x10^{-4}N$.)

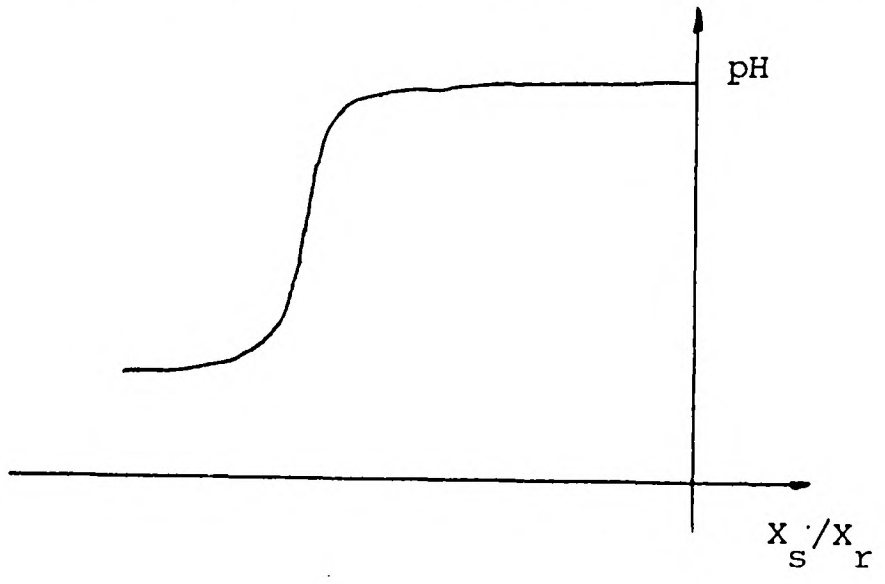


Fig 3.3b For constant V_r (= $50cm^3$)

CASE 2: Unknown weak reagents:-

In most practical neutralization cases, there is more than one weak reagent, and in the case of effluent treatment these reagents are not identified and their dissociation constants are unknown or difficult to obtain. The only chemical information available is usually a titration of an effluent sample carried out in the laboratory. The titration curve data is in the form of pH vs. reagent volume V_r for a given sample volume V_s and reagent concentration X_r as shown in figure 1.3.

From equation 3.19 and from figure 3.2, it is apparent that the i.c.d. of a mixture X is a function of V_r and X_s. The relationship between X and V_r is given by the titration curve data which is a section through the three-dimensional surface of figure 3.2 for a given sample concentration X_s; but the relationship between X and X_s is determined mostly by the dissociation constants of the components which are usually unavailable.

Consider equation 3.19; we define a function G(x) as:

$$G(x) = xg(x) \tag{3.23}$$

Substituting in equation 3.19:

$$G(X) = G(X_s) + \frac{V_r X_r}{V_s} G(X)/X \tag{3.24}$$

We can reduce the three-dimensional surface of equation 3.24 into a two-dimentional function and facilitate the calculation of X numerically by assuming that the relationship between G(X) & $G(X_s)$ is independent of X: $G(X)/X \simeq 1$ for all values of X. This assumption is validated (cf. figure 3.7) by a geometric interpretation of the relation between X and X_s/X_r & V_r/V_s. Substituting the approximation in equation 3.24:

$$G(X) \simeq G(X_s) + \frac{V_r X_r}{V_s} \qquad (3.25)$$

By inverting equation 3.25, we have:

$$X \simeq G^{-1}(G(X_s) + V_r X_r / V_s) \qquad (3.26)$$

where $G^{-1}(.)$ is the inverse of $G(.)$. Replacing $G^{-1}(.)$ by $f(.)$ and $G(.)$ by $f^{-1}(.)$, we have:

$$X \simeq f(f^{-1}(X_s) + V_r X_r / V_s) \qquad (3.27)$$

which is the required approximation relating the i.c.d. of the mixture X to the volumes V_s and V_r, and the i.c.d. X_s and X_r, of the sample and the reagent. Knowledge of the sample composition and dissociation constant is not required when using equation 3.27.

Figure 3.4 shows the titration curve of the waste effluent of figure 1.3 on different axis using equation 3.27: pH is inverted into i.c.d. X and V_r is scaled by X_r/V_s. The non-linear function $f(.)$ represents the chemistry of the waste neutralization reaction. The chemistry of strong reagents with the same concentrations X_s and X_r of the waste effluent is represented as a straight line with unity slope because $f(.)$ is linear. Equation 3.27 is used to represent the chemistry of neutralization reaction in modelling pH regulation in section 3.4.

A laboratory titration curve data of neutralization of acetic acid with sodium hydroxide, figure 3.5, is transformed into a relationship between X and $V_r X_r / V_s$ in figure 3.6. Using equation 3.27, the i.c.d. X_s of the sample equals the i.c.d. X when no reagent is added. As V_r increases, X levels off creating a plateau typical of buffering solutions in the same manner as in figure 3.2a. Changing the i.c.d. X_s of the sample

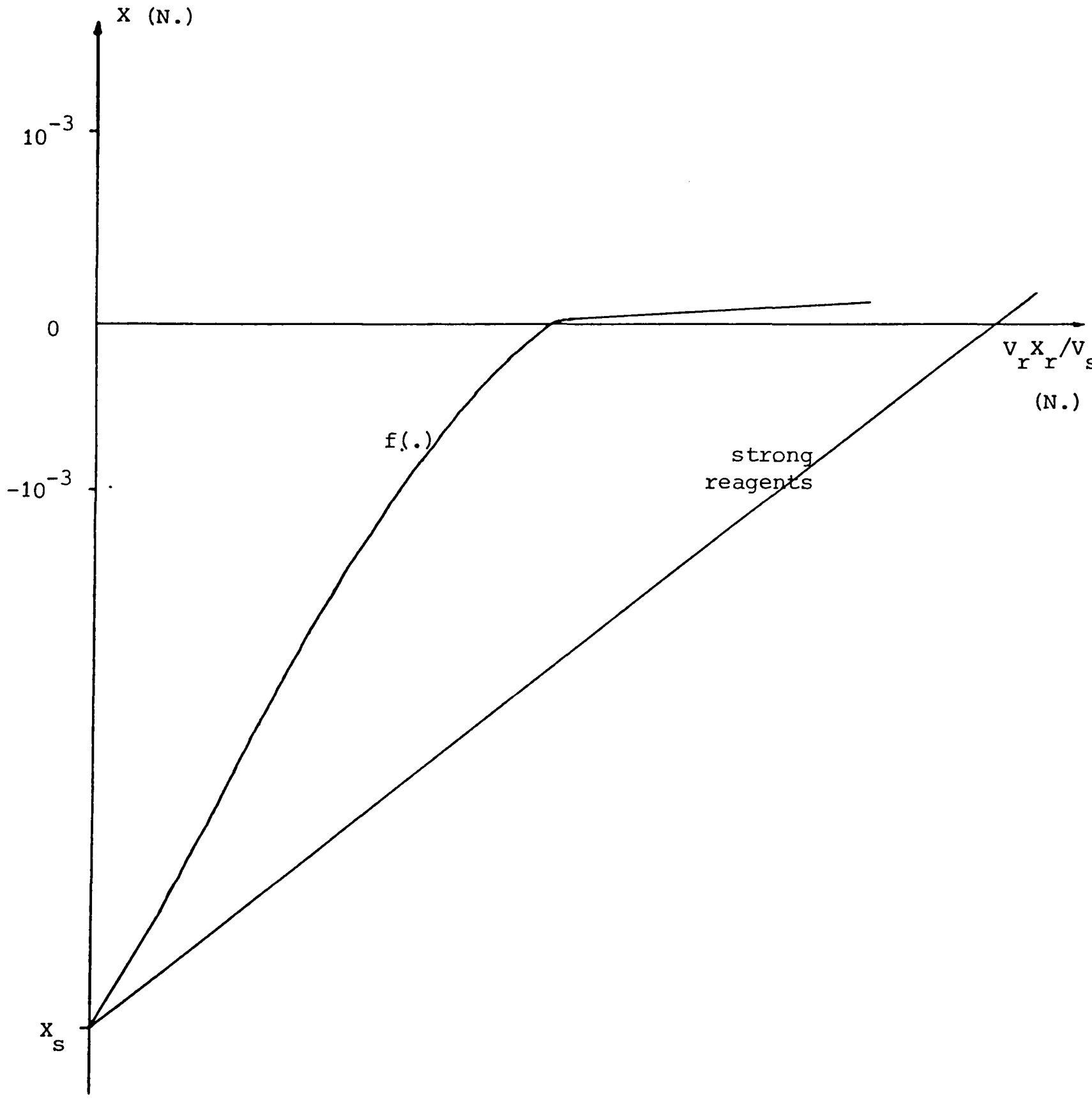


Fig 3.4 Chemistry of neutralisation of waste effluent

(from fig 1.3)

generates a family of curves parallel to that of the original X_s. Figure 3.7 shows the three-dimensional solution of the approximate equation 3.27 for the titration curve data of figure 3.5. The solution is comparable to that of equation 3.19, figure 3.2, because the ranges of X_s/X_r & V_r/V_s are the same. For a fixed X_s, the projections of the two solutions onto the plane X/X_r V_r/V_s are similar. But for a fixed V_r, the relationship between X/X_r & X_s/X_r is independent of X_s for the approximation while it is non-linearly dependent on X_s for the true solution.

Based on the dimensional analysis and the approximation, another novel way of representing titration curves is shown in figure 3.8. Here, the dimensionless groups are $(X-X_s)/X_r$ and V_r/V_s. The inclusion of X_s in the vertical axis forces the chemistry of strong reagents represented by equation 3.7 to appear as a main diagonal through the origin. From titration curves generated in a laboratory, other mixtures have their non-linear chemistry represented as lines above or below the diagonal depending on whether they are buffered toward alkalinity or acidity. A particularly interesting sample is H_2SO_4 as discussed in section 3.2.1. It is clear that the acid is buffered for small X_s (< pH 2); as V_r increases, the chemistry of the acid reverts to the linear relationship of strong reagents. The advantage of such representation is the grouping on the same axis of varied titration curves which may not be compared on more conventional axis and a better appreciation of the effect of buffering.

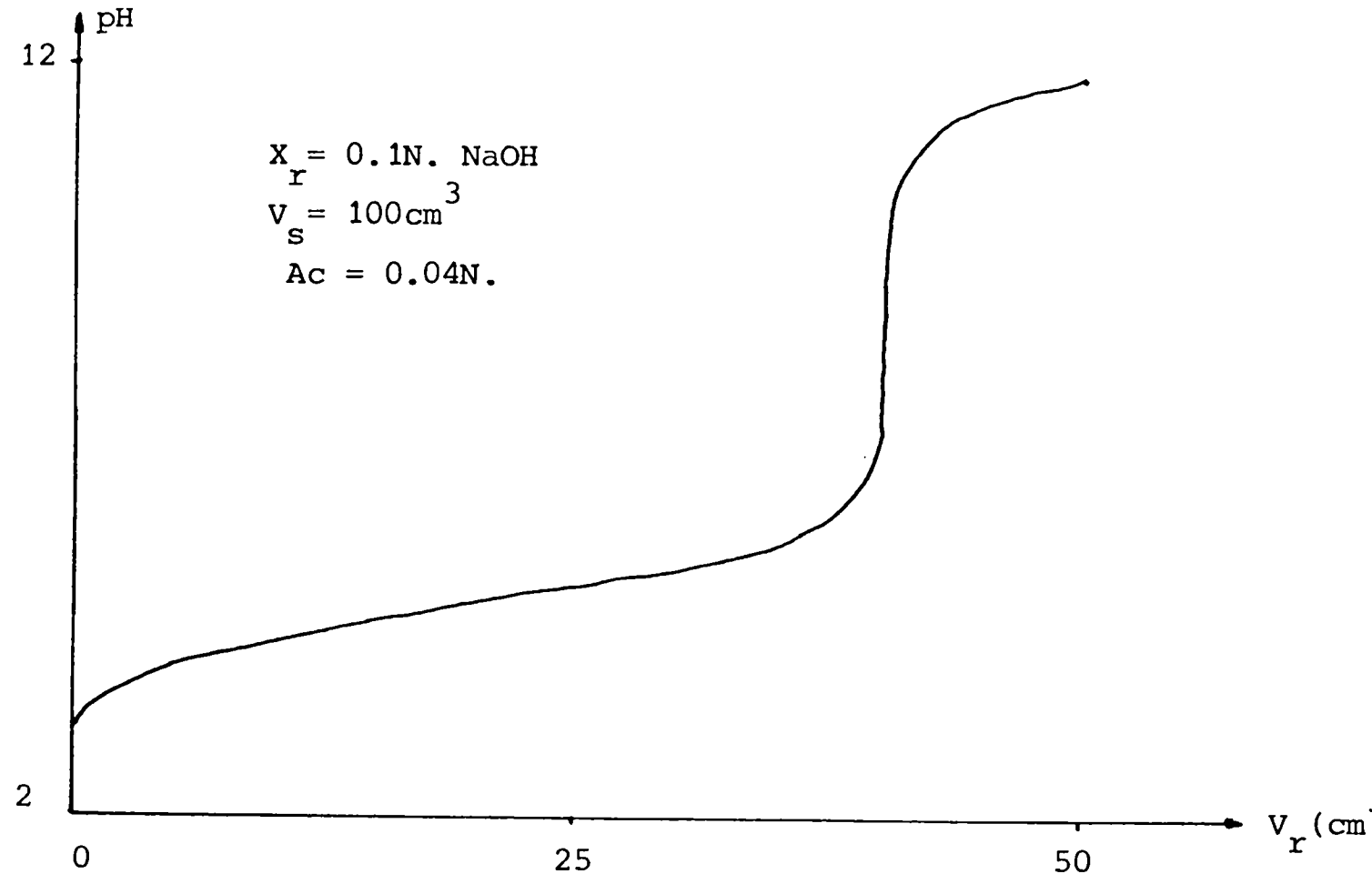


Fig 3.5 Laboratory titration curve of HAc with NaOH

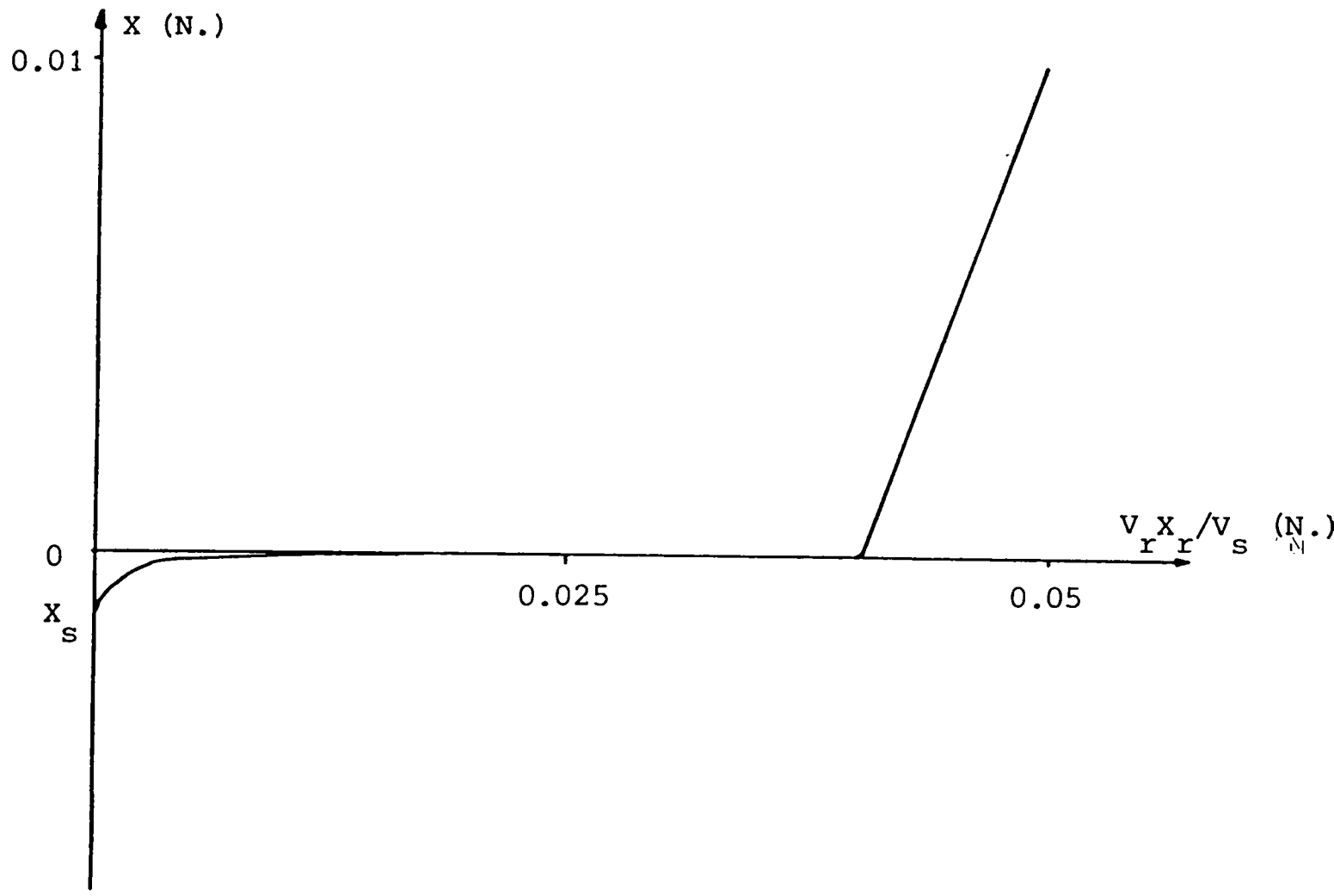


Fig 3.6 Chemistry of titration of HAc with NaOH

(from fig 3.5)

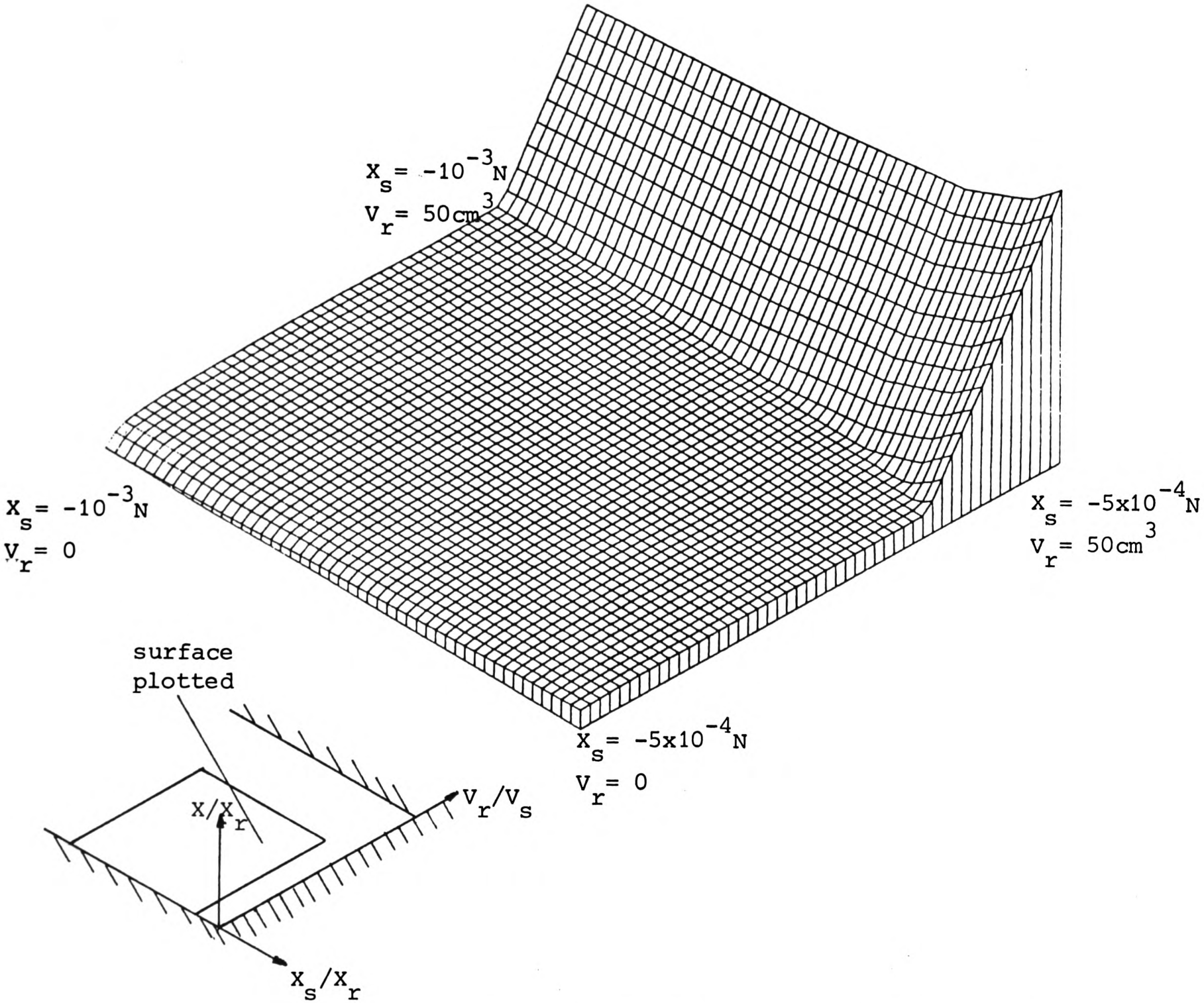


Fig 3.7 Approximate three-dimensional solution of

$$X/X_r = h_1(X_s/X_r, V_r/V_s)$$

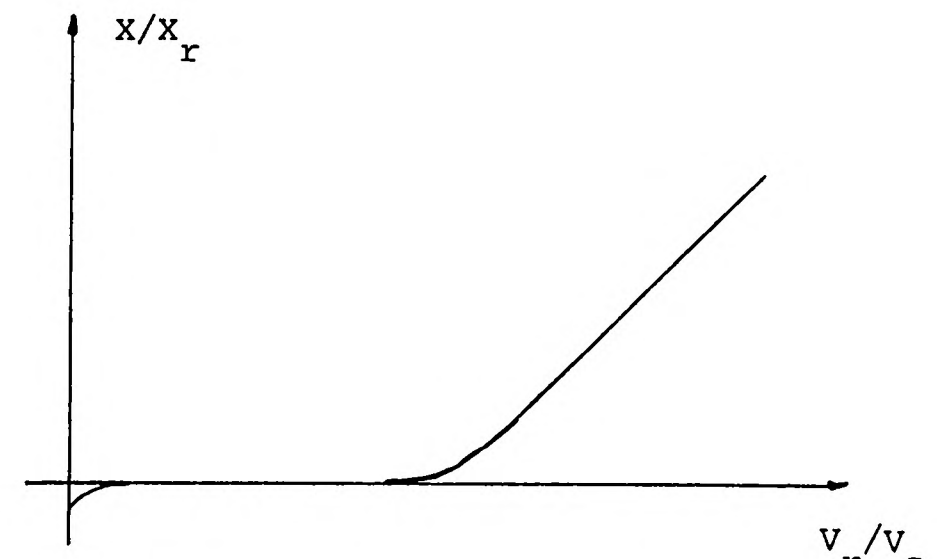


Fig 3.7a For constant X_s (= $-5x10^{-4}$N.)

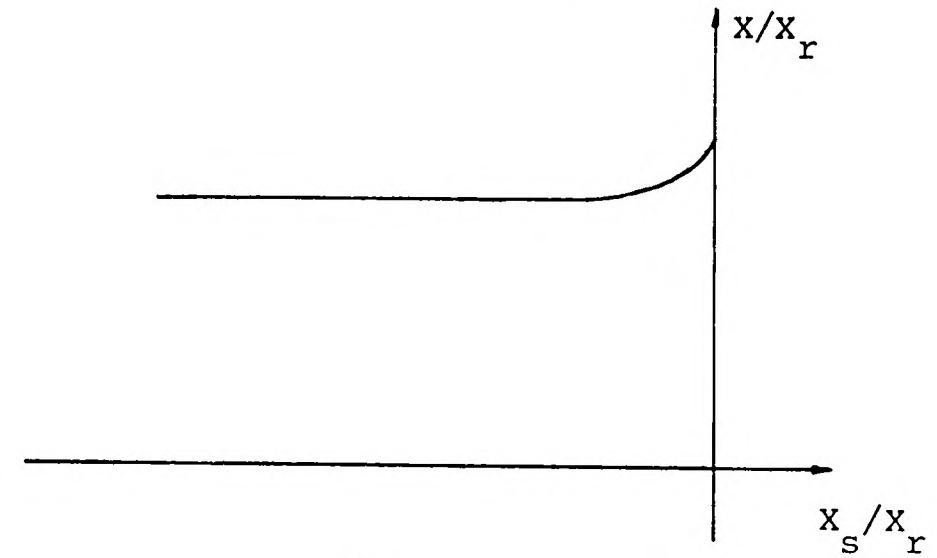


Fig 3.7b For constant V_r (= $50cm^3$)

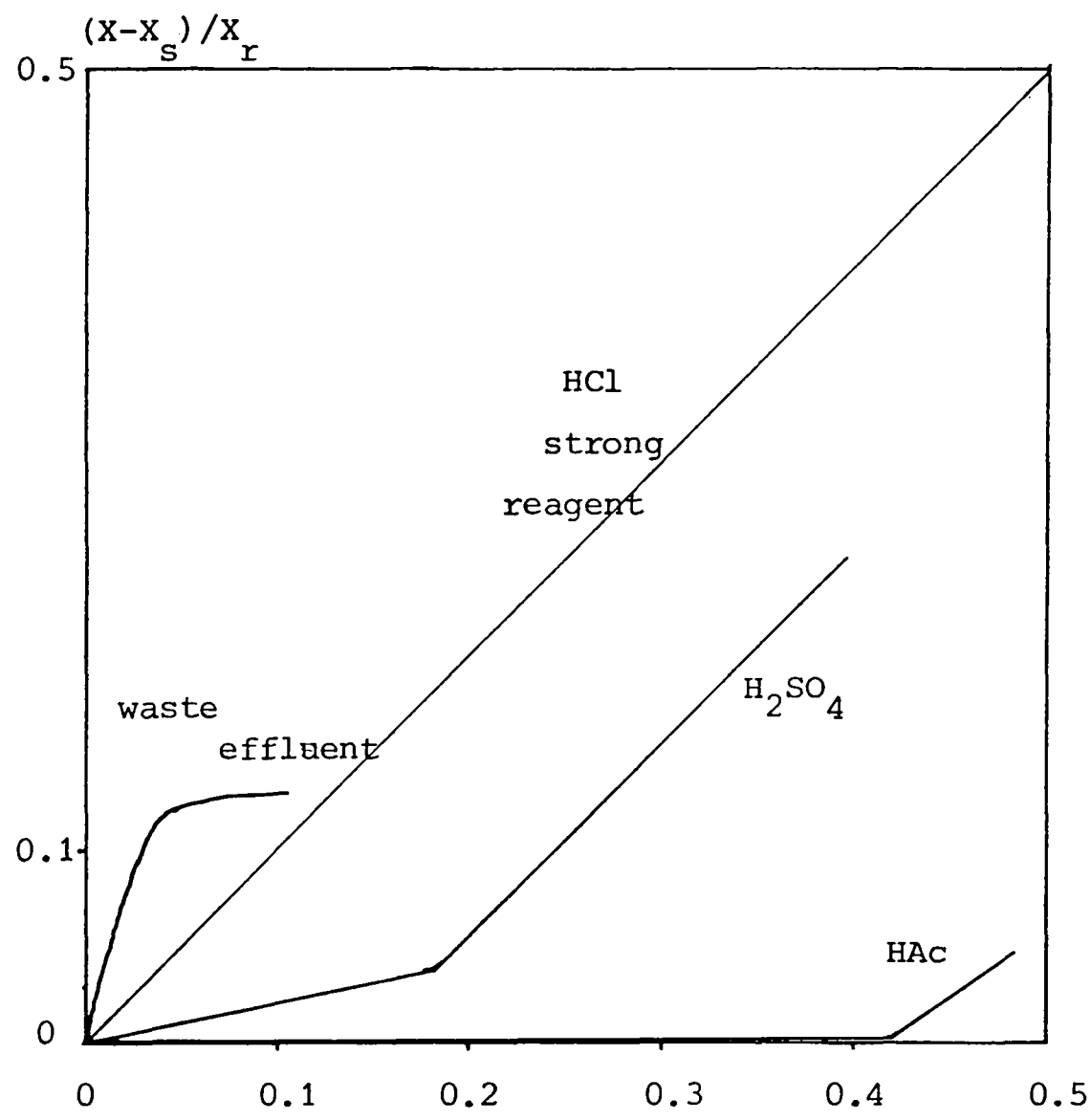


Fig 3.8 Chemistry of neutralisation of acids with NaOH

3.2.4 Conclusion To Neutralization Chemistry

In this section, a chemical analysis of titration curve for strong and for weak reagents has been presented. A non-linear relationship between the concentration of the titration mixture and the concentrations and volumes of the sample and the reagent has been derived using dimensional analysis. This relationship is approximated to provide a model for the chemistry of titration curves which is incorporated, in section 3.4, into a general model of pH systems.

3.3 THE pH MEASUREMENT

pH is related to the ionic concentration difference X as in figure 1.1 by combining equation 1.2 with equation 3.1:

$$pH(X) = -\log_{10}\left(-\frac{X}{2}\left(1+\sqrt{(1+4K_w/X^2)}\right)\right) \qquad \text{if } X < 0 \qquad (3.28a)$$

$$pH(X) = -\log_{10}\left(-\frac{X}{2}\left(1-\sqrt{(1+4K_w/X^2)}\right)\right) \qquad \text{if } X > 0 \qquad (3.28b)$$

This known severe non-linearity is present in all pH systems. The relationship is temperature-dependent because K_w varies with temperature from about $1.2\text{x}10^{-13}$ at 0°C to $1.01\text{x}10^{-14}$ at 25°C, and $9.61\text{x}10^{-14}$ at 60°C (Considine 1957). At 25°C, the slope of the pH function varies from 0.343 at pH 0 & pH 14 to $2.17\text{x}10^{6}$ at pH 7. The numerical implementation of equations 3.28 is discussed in appendix II.

3.4 MODELLING pH REGULATION IN CSTR

In this section, a mathematical model for neutralization reactions in a CSTR, which was described in section 1.2, is presented. The chemistry of neutralization reactions, the essential dynamics of the CSTR

and associated measurements are represented by a set of stochastic equations of the form:

$$\underline{x}(i+1) = G_1(\underline{x}(i),\underline{u}(i),\underline{\xi}(i),i) \qquad (3.29a)$$

$$\underline{y}(i) = G_2(\underline{x}(i),\underline{\eta}(i),i) \qquad (3.29b)$$

where $\underline{x}$ is a vector of states which fully describe the process, $\underline{u}$ is a vector of known inputs to the process, $\underline{\xi}$ and $\underline{\eta}$ are vectors of zero-mean noise terms, $\underline{y}$ is a vector of measured process outputs and i is the discrete-time index. The model will be employed in chapter 5 in the development of an Extended Kalman Filter used for state estimation and control.

3.4.1 Introduction

In order to simplify the handling of the mathematical equations describing the pH system and to relate these equations to the appropriate physical variables we consider a state space approach to modelling pH neutralization in a CSTR. The dynamic modelling of mixing in a CSTR is derived in this section. The dynamics of the mixing process can be represented (Roberts 1971, Jacobs et al 1980) by a first order lag and a time delay proprtional to this lag. Figure 3.9 is the block diagram of a mathematical model of neutralization by mixing influent with concentrated strong reagents in continuous stirred tank reactor shown in figure 1.2. The input u is the flow rate of neutralising reagent of i.c.d. X_r, the output y_1 is the measured pH. There are three essential state variables: x_1 the i.c.d. of the regulated effluent, x_2 the flow rate of the influent and x_3 the i.c.d. of the influent. Stochastic disturbances affect the states x_2 and x_3 and the measurement of y_1 of x_1 is corrupted by additive noise and bias.

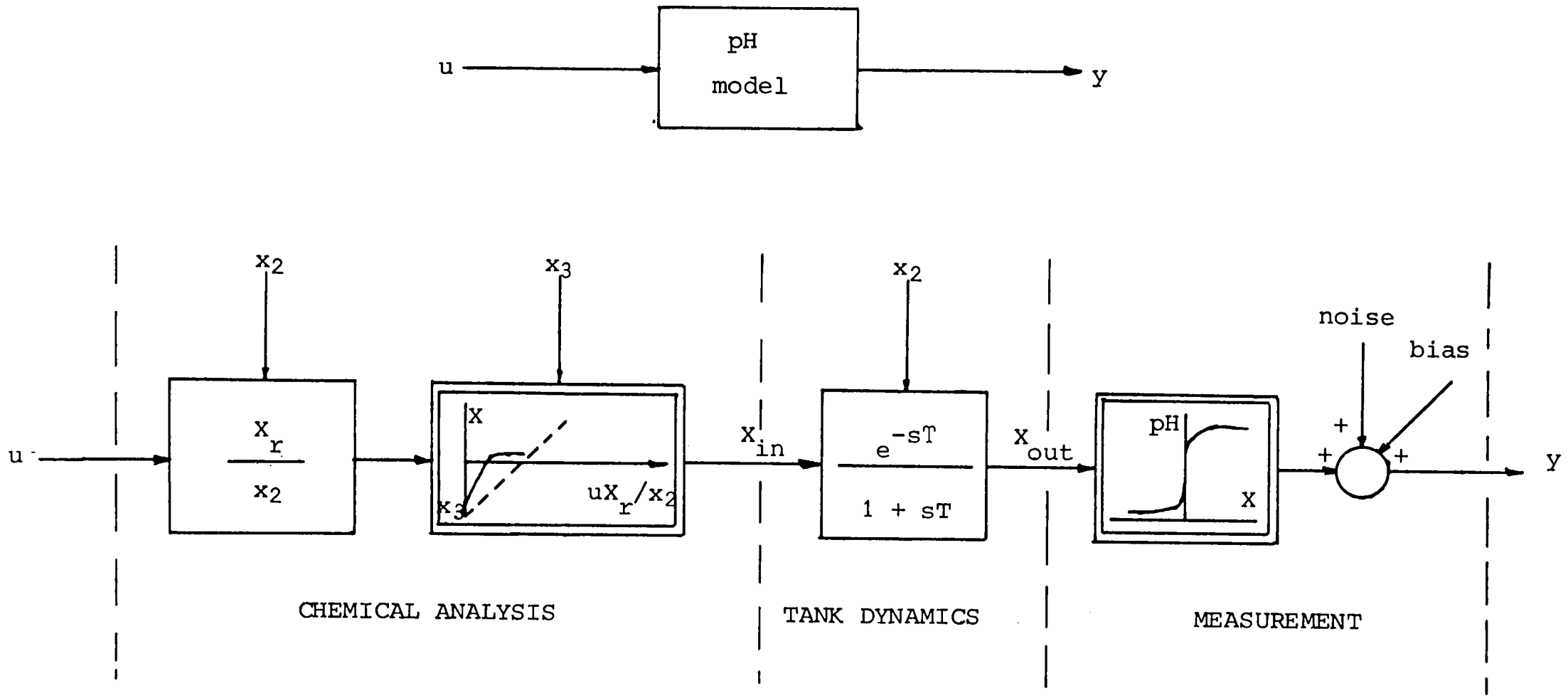


Fig 3.9 Mathematical model of pH neutralisation in a CSTR

From the chemical analysis of neutralization reactions which was in section 3.2, the i.c.d. X_{in} and the flow rate F_{in} of the incoming mixture of influent and reagent are given by equation 3.27:

$$X_{in} = x_3 + uX_r/x_2 \qquad \text{for strong reagents} \qquad (3.30a)$$

$$X_{in} \simeq f(f^{-1}(x_3) + uX_r/x_2) + \delta X \qquad \text{for weak reagents} \qquad (3.30b)$$

$$F_{in} = x_2 + u \qquad (3.30c)$$

As discussed in section 3.2, equation 3.30a for strong reagents is well defined. For buffered reagents, equation 3.30b is an approximation and a random variable δX is added to account for uncertainty in the chemistry of the titration curve (section 3.2.3).

The equations of the model are derived first in continuous time (section 3.4.2) and the model is discretized in section 3.4.3 in order to be implemented digitally.

3.4.2 Continuous Time State-space Representation

The dynamics of a CSTR of volume V are modelled in continuous time by:

$$V \frac{dX_{out}}{dt} = F_{in}X_{in} - F_{out}X_{out} \qquad (3.31)$$

where X_{out} and F_{out} are the i.c.d. and the flow rate of the regulated effluent. X_{out} is x_1 and $F_{out} = F_{in} \simeq x_2$; the equality is because there is no holdup of flow in the tank and the approximation is due to $F_{in} >> u$ because of the concentrated reagent. Replacing in equation 3.31, we have:

$$T \frac{dx_1}{dt} = X_{in} - x_1 \qquad (3.32)$$

where $T = V/x_2$ is the time constant of the tank and X_{in} is defined by equations 3.30.

A more accurate description of CSTR dynamics is given by introducing a dead time τ to account for mixing delays and a random term μ_1 which may account for non-uniform mixing. The random variable μ_1 can also accounts for the uncertainty δX of the chemistry; μ_1 is assumed to be zero-mean with a Gaussian distribution. Equation 3.32 then becomes:

$$x_1(t+\tau) + T \frac{dx_1(t+\tau)}{dt} = X_{in} + \mu_1 \qquad (3.33)$$

Taking the Laplace transform of equation 3.33:

$$\frac{x_1}{X_{in}}(s) = \frac{e^{-s\tau}}{1+sT} \qquad (3.34)$$

Equation 3.34 represents a first order dynamic system of time constant T and time delay τ which is proportional to the time constant T: $\tau = f_t T$. The factor of proportionality f_t was found to have values ranging from 0.1 (Roberts 1971) to 0.05 (Jacobs et al 1980) for a CSTR.

The stochastic disturbances which affect the influent flow x_2 and the influent i.c.d. x_3 may be modelled as slowly varying random parameters. A convenient way of representing the models is in terms of a stochastic Wiener processes (Papoulis 1965). These processes are not introduced to represent an accurate description of flow and incoming concentration. They can however be used as a means of obtaining estimates of those quantities. Although the random variable of a Wiener process has zero mean, we can represent variables of non-zero mean by adding a constant offset value to the model. The gaussian distribution of the random variable of the process will ensure that its inclusion in a Kalman filter estimator will produce a robust filter (cf. chapter 5). In

continuous time, the flow x_2 and the i.c.d. x_3 are modelled by:

$$T_j \frac{dx_j}{dt} = \bar{x}_j + \mu_j - x_j \qquad j = 2,3 \qquad (3.35)$$

where T_j is the time constant of the model, $\bar{x}_j$ is the mean value and μ_j is a gaussian random variable with distribution: $N(0.;var(x_j))$.

The model may have three measurements: y_1 the regulated effluent pH, y_2 the influent flow rate and y_3 the influent pH. y_1 is essential for feedback control while y_2 and y_3 may provide feedforward information. They relate to their corresponding states as follow:

$$\begin{aligned} y_1(t) &= pH(x_1(t)) + z(t) + \eta_1 \\ y_2(t) &= x_2(t) + \eta_2 \\ y_3(t) &= pH(x_3(t)) + \eta_3 \end{aligned} \qquad (3.36)$$

where pH(.) is defined by equation 3.28, z(t) is a bias term which may corrupt the effluent pH and η_i (i = 1 to 3) are random measurement noise assumed to be zero mean white gaussian sequences.

Measurement drift z(t) on the pH measurement may be modelled as a slowly varying bias due to pH probe fouling and poor calibration or as a constant random variable which may exhibit sudden jumps when a probe is recalibrated or when switching from one probe to another. The varying bias is represented by a Wiener process in continuous time:

$$T_z \frac{dz}{dt} = \bar{z} + \mu_z - z \qquad (3.37)$$

Alternatively, the jumping bias is modelled as a random variable which remains constant but makes occasional jumps at random time.

3.4.3 Discrete Time State-space Representation

In order to implement the state-space model derived in the previous section on a digital computer, a discrete-time state space representation is required. Let i be the discrete-time index at time t and Δ be the discrete sample interval. We can express the CSTR dynamics of equation 3.33 by taking the first term of the Taylor's series expansion of the derivative:

$$x_1(i+k+1) = x_1(i+k) + \frac{\Delta}{T}(X_{in}(i) - x_1(i+k)) + \xi_1 \qquad (3.38)$$

where $k = \frac{\tau}{\Delta}$ is the discrete time delay assumed to be integer, and ξ_1 ($N(0.;var(\xi_1))$ is the discrete representation of the random variable μ_1 which accounts for the uncertainty in the weak reagent chemistry and in the CSTR mixing. Substituting for T ($= V/x_2(i)$) in equation 3.38, we have:

$$x_1(i+k+1) = x_1(i+k) + \frac{\Delta}{V} x_2(i)(X_{in}(i) - x_1(i+k)) + \xi_1 \qquad (3.39)$$

At time i, equation 3.39 predicts the value of x_1 at time (i+k+1) from $x_1(i+k)$. For the system to be fully defined, it is necessary to introduce state variables $x_1(i+k-1)$, $x_1(i+k-2)$, .., $x_1(i)$ to account for the time delay augmenting the state vector by k states. They are represented by:

$$x_4(i) = x_1(i+k-1)$$
$$x_5(i) = x_1(i+k-2) \qquad (3.40)$$

$$x_{k+3}(i) = x_1(i)$$

The disturbances dynamics of the Wiener processes can be expressed in discrete time from equation 3.35 as follow:

$$x_j(i+1) = g_j x_j(i) + \alpha_j + \xi_j \qquad j=2,3 \qquad (3.41)$$

where g_j is the rate constant of the model, α_j is its offset and $var(\xi_j)$ is the variance of its white noise ξ_j:

$$g_j = (1-\Delta/T_j) \qquad \alpha_j = \bar{x}_j(1-g_j) \qquad var(\xi_j) = var(\mu_j)(1-g_j^2) \qquad (3.42)$$

Discretizing the measurements of equation 3.36, we have:

$$\begin{aligned} y_1(i) &= pH(x_1(i)) + z(i) + \eta_1 \\ y_2(i) &= x_2(i) + \eta_2 \\ y_3(i) &= pH(x_3(i)) + \eta_3 \end{aligned} \qquad (3.43)$$

In the case of the bias being modelled as a Wiener process, z(i) is calculated from equation 3.37:

$$z(i+1) = g_z z(i) + \alpha_z + \xi_z \qquad (3.44)$$

where:

$$g_z = (1-\Delta/T_z) \qquad \alpha_z = \bar{z}(1-g_z) \qquad var(\xi_z) = var(\mu_z)(1-g_z^2) \qquad (3.45)$$

3.4.4 the CSTR Model Of pH Neutralization

The state-space model derived in section 3.4 will be used in the following chapters for estimation and control. The dynamics of the model are summarised by:

$$x_1(i+k+1) = x_1(i+k) + \frac{\Delta}{V} x_2(i)(X_{in}(i) - x_1(i+k)) + \xi_1$$

$$x_j(i+1) = g_j x_j(i) + \alpha_j + \xi_j \qquad j=2,3$$

$$x_4(i+1) = x_1(i+k)$$

$$x_5(i+1) = x_1(i+k-1) \qquad (3.46a)$$

.

.

$$x_{k+3}(i+1) = x_1(i+1)$$

$$z(i+1) = g_z z(i) + \alpha_z + \xi_z$$

and the measurements by:

$$y_1(i) = pH(x_1(i)) + z(i) + \eta_1$$

$$y_2(i) = x_2(i) + \eta_2 \qquad (3.46b)$$

$$y_3(i) = pH(x_3(i)) + \eta_3$$

From equations 3.46, there can be up to three non-linear elements in the model: the first is present only in the modelling of the chemistry X_{in} for buffered reagents (equation 3.30b); the second element is due to the multiplication of $x_2(X_{in} - x_1)$, and the last element is the non-linear measurement function pH(.) (equations 3.28) of the effluent pH. In chapter 4, a Bayes' rule estimator reduces the non-linear pH function to a pseudo-linear measurement of i.c.d. of the effluent, and in chapter 5 an EKF approximates and resolves the non-linearities of the dynamic state equations.

It is seen that equations 3.46 are of the same form of equations 3.29. The dynamics of the neutralization vessel and the measurements have been represented by a set of of stochastic equations. This model will be used in chapter 5 for the development of an Extended Kalman Filter.

3.5 MODEL VALIDATION

In the model developed in the previous sections, two areas may need some validation: the reduction of the three-dimensional function of the chemical analysis to a two-dimensional one, and the representation of the disturbance dynamics in terms of Wiener processes.

The chemical approximation is validated partially by the comparison of figures 3.2 & 3.7 and also partially by the similarity between simulated time histories of regulated pH using the approximate model and actual time histories of a real plant (Proudfoot 1983) as described in chapter 8. The addition of a system noise term ξ_1 in equation 3.38 may account for part of the approximation.

The stochastic modelling of the influent disturbances (equation 3.34) are not intended to describe accurately the inflow and the incoming i.c.d. However, when patterns of time-histories of plant data are available from recording measurements, simulated records can be generated and the estimator may provide estimates of the disturbance variables. Chapter 5 reports on good estimation and tracking of actual time-histories of flow using a Wiener model provided that the effluent pH measurement is bias-free.

3.6 CONCLUSION

In this chapter, a general non-linear model of pH regulation in a CSTR has been derived. It is based on a novel separation of the chemical analysis form the pH measurement in which chemical models for strong and weak reagents have been presented in three-dimensionnal space. Reduction of the model using dimensional analysis and selective approximations has led to a pH process model which can be used in the development of

non-linear estimators (chapter 4 & 5) and classical and stochastic controllers (chapter 6). The general model also has provided the basis of the simulation package which is described in chapter 7.

CHAPTER 4

NON-LINEAR ESTIMATION THROUGH THE pH MEASUREMENT

This chapter reports on the application of a novel non-linear estimator (Jacobs 1983) based on Bayes' rule to the pH model developed in the previous chapter. The estimator estimates the ionic concentration difference from the non-linear pH measurement. The estimator is extended to account for bias on the measurement.

The chapter is arranged as follows: section 4.1 introduces the non-linear Bayes' estimation algorithms for bias-free and biased pH measurements. Bayes' rule equations are outlined in section 4.2 and applied to the pH non-linearity in single-stage estimation (Jacobs and Briggs 1984). These equations are then used to derive recursive estimators for bias-free and for biased measurements in section 4.3 and 4.4 respectively. Section 4.5 concludes the chapter.

4.1 INTRODUCTION

A non-linear estimator, tailored to the model of chapter 3, and based on Bayes' rule estimates the ionic concentration difference of the effluent from a noisy non-linear pH measurement by generating numerically a complete probability distribution of the concentration. The mean and

variance of the distribution provide respectively an estimate of the i.c.d. and a confidence in the estimate. The Bayes' estimator is used recursively for succesive pH measurements. Propagation of the distribution from one measurement to the next is carried out in two stages: first by linearising the estimate and then by considering the resulting approximate a posteriori distribution after one measurement as the a priori distribution for the next.

The linearised estimate provides a pseudo-measurement of i.c.d. to drive an Extended Kalman Filter (EKF). The EKF estimates the three essential states of the model: i.c.d. of effluent mixture in the CSTR, flow rate, and i.c.d. of the influent provided that the titration curve of the process is known. These estimated states can be sufficiently accurate to provide feedforward information about the influent disturbance or to drive suboptimal control laws. With the help of an example, the performance of the linearised estimator is compared with that of an optimal Bayes' estimator and an EKF for the pH non-linearity in section 4.3. When the noise on the pH measurement is small, an analytical linearisation of the pH non-linearity may be used (Proudfoot 1983) instead of the Bayes' estimator to provide a linearised measurement of effluent i.c.d. which drives the EKF. The EKF and the control strategies are discussed in chapter 5 & 6.

A two-dimensional implementation of the Bayes' estimator is also investigated in section 4.4. As well as the concentration of the effluent, the measurement bias, modelled in section 3.4 either as a slowly varying process or as a jumping random variable, is estimated. As introduced in chapter 1, the estimation of ionic concentration difference through a biased pH measurement is motivated by the fact that in frequent occasions pH probes are subject to fouling, poor calibration, dirt

clogging and random switching from one probe to another. The effect of measurement bias on pH regulation is to change the effective set point at which the feedback controller is operating by an amount equal to the value of the bias. The biased measurement also affects the estimation and prediction of the model-based EKF leading to poor estimation of the states. Hence, either the feedforward information provided by the estimates will be unreliable or the performance of the suboptimal control laws driven by the estimated states will be unacceptable. Simulation results in chapter 5 discusses the effect of biased measurement on the state estimation and chapter 6 investigates the effect of the bias on the feedback controllers. Because of observability considerations, the bias estimation will be possible only if the feedforward measurements of the disturbance variables and the neutralisation titration curve are available.

4.2 THE BAYES' RULE

In this section, Bayes' rule equations are derived for the pH non-linearity of figure 1.1 in single-stage estimation (Jacobs and Briggs 1984). The equations and some of their results provide a useful introduction and a validation for necessary approximations of recursive estimators (section 4.3) through the non-linearity.

Let consider that a state x and a measurement y are related in a linear or non-linear fashion; the problem is: given the measurement y, what is the best estimate of x ? The Bayes' rule (Aoki 1967, Jazwinski 1970) approach to solve this problem is to determine the a posteriori conditional density function of x since by definition it contains all the information about the state x provided by the available measurement data y. From Bayes' rule, the conditional density function p(x|y) can be

evaluated as follows:

$$p(x|y) = \frac{p(x)p(y|x)}{\int_x p(x)p(y|x)dx} \qquad (4.1)$$

where p(x) is the a priori density function of x before a measurement y, p(y|x) is the likelihood of the measured value y as a function of possible values of x and the integral is a normalisation constant.

Consider a scalar linear measurement:

$$y = Hx + \eta \qquad (4.2)$$

The state x and the measurement noise η are independent with Normal prior distribution

$$p(x) = N(m_0; v_0) \qquad (4.3a)$$

$$p(\eta) = N(0.; v_\eta) \qquad (4.3b)$$

The conditional distribution of x is calculated from Bayes' rule. It is Normal with mean m and variance v:

$$p(x|y) = N(m; v) \qquad (4.4)$$

The mean and variance of the estimate x are given by the single-stage Kalman filter equations (Lee 1964):

$$m = m_0 + (y - Hm_0)Hv/v_\eta \qquad (4.5a)$$

$$v = v_0 v_\eta / (H^2 v_0 + v_\eta) \qquad (4.5b)$$

Now consider the estimation of x from the non-linear pH function defined by equations 3.28:

$$pH(X) = -\log_{10}\left(-\frac{X}{2}\left(1+\sqrt{(1+4K_w/X^2)}\right)\right) \quad \text{if } X < 0 \qquad (3.28a)$$

$$pH(X) = -\log_{10}\left(-\frac{X}{2}\left(1-\sqrt{(1+4K_w/X^2)}\right)\right) \quad \text{if } X > 0 \qquad (3.28b)$$

As introduced in equation 3.36, the scalar measurement y relates to the state x through the pH function. The measurement is corrupted by additive random measurement noise η assumed to be zero mean white Gaussian sequence:

$$y = pH(x) + \eta \qquad (4.6)$$

x and η are independent with Normal prior distribution given by equations 4.3.

Single-stage non-linear estimators through the pH non-linearity were investigated by Jacobs and Briggs (1984). The estimators are: direct inversion of the non-linearity, Bayes' rule and extended Kalman filter (EKF). The performance of the estimators were compared using Monte-Carlo simulations. They found that the estimates of Bayes' rule are in many cases significantly better than the other estimates. Their results are not unexpected: Bayes' rule is an optimal estimator to which the EKF is a linear approximation (Jazwinski 1970) and the inversion will give near optimal estimates only in the case of small variance of the measurement noise. Proudfoot (1983) reports on the use of the analytical inversion in a full-scale industrial process; because the inversion does not give any indication of the accuracy of the i.c.d. estimate, the calculation of artificial variance of the estimate is needed. Some of their discussions are reproduced here because the Bayes' rule equation are needed for the development of recursive estimators of bias-free and biased pH measurements. Parts of their results, in the form of two examples, provide some validation for a necessary approximation of the conditional distribution p(x|y) in the recursive estimation.

From the Bayes' rule (equation 4.1), we can evaluate the conditional density function p(x|y) of x given the prior distributions p(x) and $p(\eta)$. p(x) is given by:

$$p(x) = \frac{1}{\sqrt{2\pi v_0}} \exp\left\{ - \frac{(x-m_0)^2}{2v_0} \right\} \qquad (4.7)$$

and the likelihood function p(y|x) is calculated from $p(\eta)$:

$$p(y|x) = p(\eta = y-pH(x)) = \frac{1}{\sqrt{2\pi v_\eta}} \exp\left\{ - \frac{(y-pH(x))^2}{2v_\eta} \right\} \qquad (4.8)$$

Replacing in equation 4.1, we have the posteriori distribution:

$$p(x|y) = C \exp\left\{ - \frac{(x-m_0)^2}{2v_0} - \frac{(y-pH(x))^2}{2v_\eta} \right\} \qquad (4.9)$$

where C is a normalisation constant independent of x.

Knowing the density p(x|y), we can readily determine the mean and variance of the distribution: the conditional mean provides the estimate m_{Bay} of x:

$$m_{Bay} = \int_x xp(x|y)dx \qquad (4.10)$$

The variance v_{Bay} provides the spread of the distribution and the confidence in the estimate:

$$v_{Bay} = \int_x (x-m_{Bay})^2 p(x|y)dx \qquad (4.11)$$

The Bayes' rule single-stage estimator derived leads to an optimal estimate of x because there are no approximations.

Two examples show the prior, likelihood and conditional distribution of the Bayes' estimator together with its estimate m_{Bay}. Also displayed are two other estimates: The analytical inversion of the pH non-linearity m_{inv} and the EKF estimate m_{EKF} (Jacobs and Briggs 1984). The estimation algorithm prior information is: mean m_0 and variance v_0 of the Normal prior distribution p(x), and the variance v_η of the Normal zero mean distribution $p(\eta)$.

The conditional distribution p(x|y) and its statistics were evaluated using Simpson's rule over a minimum range R. R is defined with reference to the mean and variance of the prior distribution p(x) and the likelihood p(y|x):

$$R = \min \{h_1, h_2\} - \max \{l_1, l_2\}$$

where
$$l_1 = m_0 - 4\sqrt{v_0}$$
$$l_2 = pH^{-1}(y - 4\sqrt{v_\eta})$$
$$h_1 = m_0 + 4\sqrt{v_0}$$
$$h_2 = pH^{-1}(y + 4\sqrt{v_\eta})$$

The number of subintervals for Simpson's rule into which this range was discretized was 50; this was assumed adequate because similar results were obtained when using 100 subintervals.

Example 1 shows, figure 4.1, the probability distributions and the different estimates of x. For this particular example, the prior information was: $p(x) = N(10^{-4}; 10^{-6})$ and $p(\eta) = N(0.; 0.04)$; x is best estimated by m_{Bay} and is within two standard deviations, $\sqrt{v_{Bay}}$, of the estimate. The inversion is less accurate and does not give any information of its accuracy. The EKF estimator is the worst because $\sqrt{v_0} > m_0$ making the extent of v_0 include a large non-linear section of pH

function; it is grossly overconfident in estimating x (its standard deviation $\sqrt{v_{EKF}}$ is very small) and its estimate is well at the edge of the conditional distribution.

Example 2 shows different results (figure 4.2) for different prior information: $p(x) = N(10^{-3};10^{-8})$ and $p(\eta) = N(0.;0.04)$. The Bayes' and the EKF estimates are almost identical and very accurate while the inversion estimate is grossly inaccurate. The shape of the conditional distribution is nearly Gaussian but the estimation has not significantly reduced the uncertainty about x: $\sqrt{v_0} \cong \sqrt{v_{Bay}}$.

The examples illustrates the performance of the Bayes' rule estimator and show that the shape of the conditional distribution p(x|y) may be in some cases be nearly Gaussian and in other cases maybe approximated by a Gaussian distribution. This approximation provides a basis for the derivation of the recursive estimators in the next section.

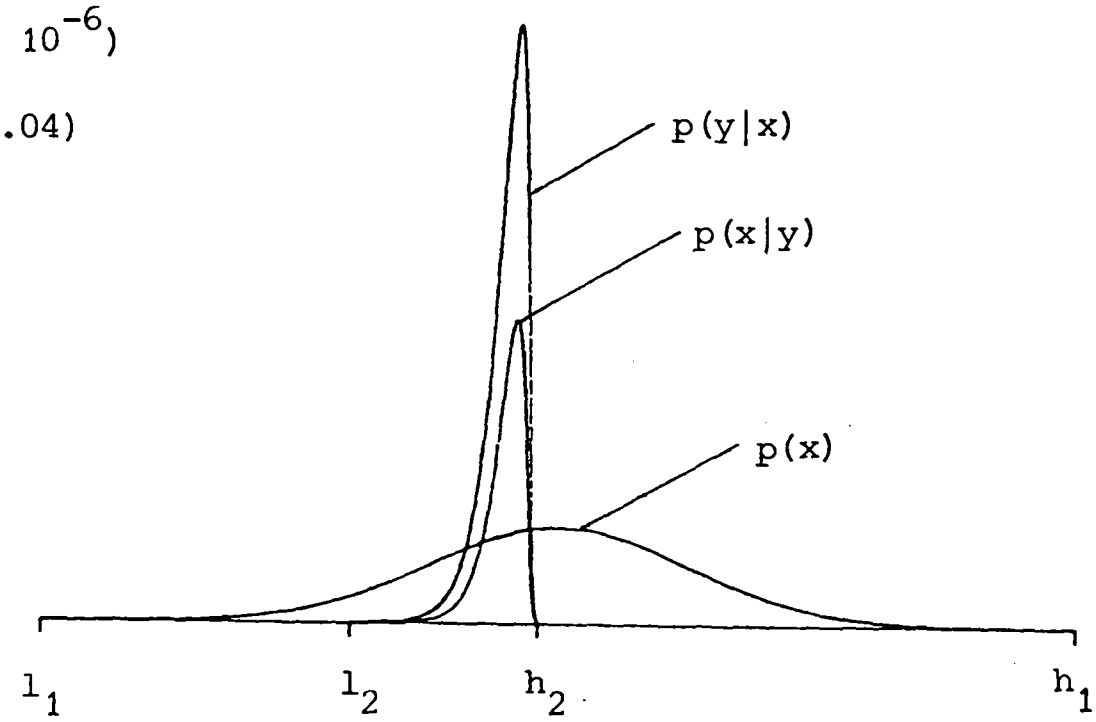
4.3 RECURSIVE ESTIMATION THROUGH A BIAS-FREE pH MEASUREMENT

Recursive data processing in which measurements are utilised sequentially as they become available is used because there is no need to store past measurements for the purpose of computing present state estimates. The estimated states can either provide a feedback controller with additional feedforward information or drive an optimal stochastic controller; these techniques are investigated in chapter 6.

In this section, an estimator is developed which extracts the i.c.d. of the effluent from a bias-free pH measurement. The section is arranged as follows: section 4.3.1 explains the difficulties in recursive non-linear estimation and introduces estimators which attempt to solve these

$p(x) = N(10^{-4}, 10^{-6})$

$p(\tilde{\eta}) = N(0., 0.04)$



$x \cong -4.742 \times 10^{-4}$

$m_{inv} = -2.409 \times 10^{-4}$

$m_{Bay} = -3.183 \times 10^{-4}$ $\quad \sqrt{v_{Bay}} = 1.478 \times 10^{-4}$

$m_{EKF} = -1.366 \times 10^{-3}$ $\quad \sqrt{v_{EKF}} = 4.600 \times 10^{-5}$

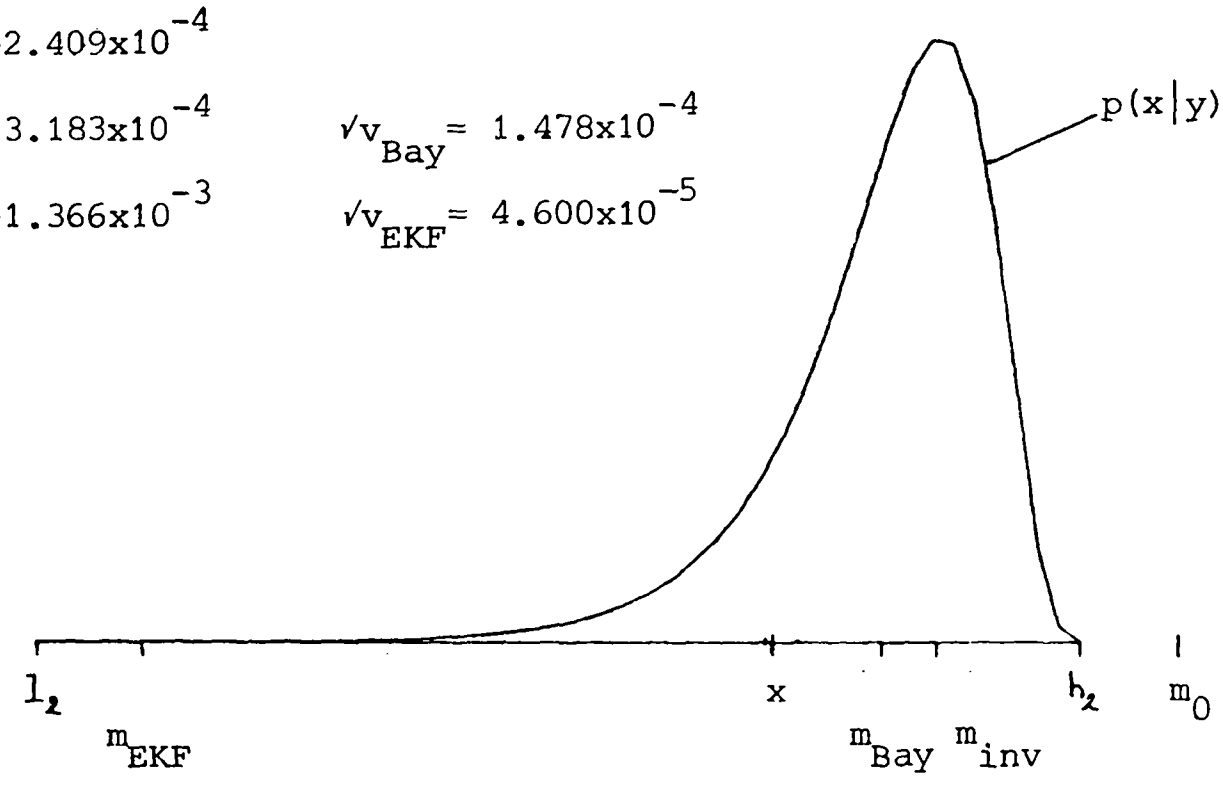


Fig 4.1 Single-stage estimation: example 1.

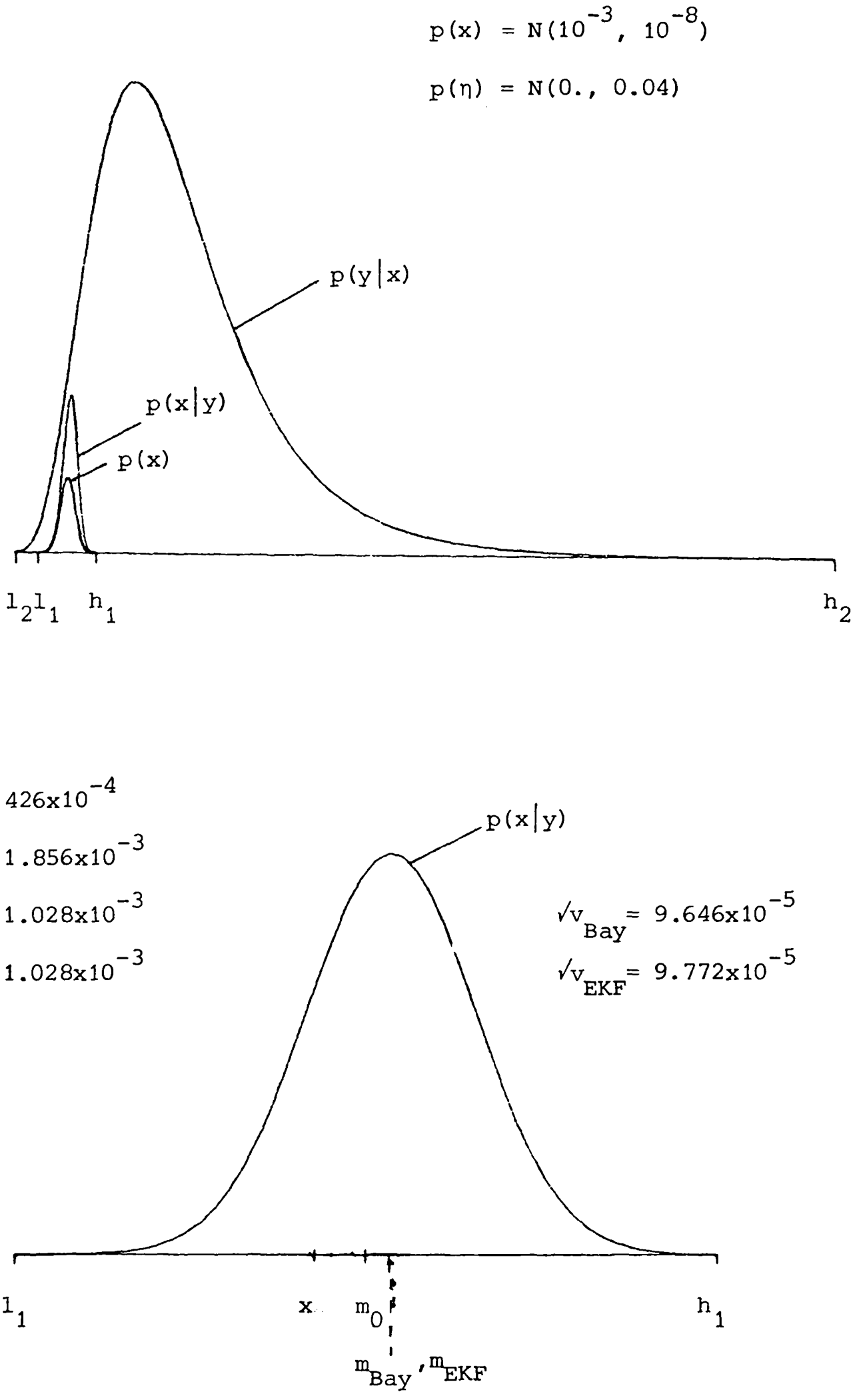


Fig 4.2 Single-stage estimation: example 2.

difficulties with reference to the pH non-linearity. The estimators are: the optimal recursive Bayes' estimator (section 4.3.2), the Extended Kalman Filter (section 4.3.3),and the Gaussian Approximation and the Linearised Estimator (section 4.3.4). Their performances are compared with respect to a generic example. Section 4.3.5 concludes section 4.3 by discussing the implementation and the results of the Linearised Estimator when estimating the i.c.d. of the effluent of the multi-state model of chapter 3.

4.3.1 Introduction To Recursive Non-linear Estimation

Recursive estimation of dynamic states through measurement non-linearities such as the pH function are generally difficult. the difficulty is in the need to propagate the conditional distribution of every state after one measurement as prior distribution before the next. This problem does not arise when the measurement is linear: consider a discrete linear first-order Wiener process with dynamic state equation specified by

$$x(i+1) = gx(i) + \alpha + \xi \qquad (4.12)$$

Initially, x is drawn from a Normal distribution; g is the rate constant of the process, α its offset and ξ is white Gaussian noise of variance v_{ξ}. When the measurement is linear, the conditional distribution is Normal and is propagated through its sufficient statistics of mean m and variance v by the prediction equations of the Kalman filter:

$$m_0(i+1) = gm(i) + \alpha \qquad (4.13a)$$

$$v_0(i+1) = g^2 v(i) + v_{\xi} \qquad (4.13b)$$

For a linear system, when more than one dynamic state is estimated, the

propagation of the conditional distribution of the states is carried out in the same way as for a scalar state through its vector mean $\underline{m}$ and matrix covariance $\underline{\Sigma}$ by the prediction equations of the Kalman Filter (Jazwinski 1970). This technique is used in the next chapter for the prediction of the dynamic states modelled in chapter 3.

If the measurement is non-linear, the posteriori distribution is not Normal and its propagation is complicated. A number of approximate solutions to this non-linear filtering problem were suggested and are surveyed by Sorenson (1974). The solutions are based on either an approximation of the distribution by a finite series, (Alspasch and Sorenson 1970), or an approximation of the non-linear function over a previously defined floating grid (Bucy and Senne 1970). The approximate filter the author proposes is one in which the posteriori distribution is approximated by a Gaussian distribution. This may seem a coarse approximation but results presented here show that although the filter performance is not optimal it is better than the widely used Extended Kalman filter and that the approximation works well in practice for the pH non-linearity.

In order to compare the performance and robustness of the Gaussian approximation, three recursive filters are considered in the next sections for the non-linear scalar pH measurement. The first filter is the optimal recursive Bayes' estimator (Lee 1964). The second filter is the approximate recursive Extended Kalman Filter (Jazwinski 1970) which assumes that both the likelihood and the conditional density functions of the scalar state x are Normal; the EKF can be generalised to account for a vector state $\underline{x}$. The third filter is the recursive Gaussian approximation in which only the conditional distribution for the scalar state x is assumed Normal; this is extended by the Linearisation

Estimator (Jacobs 1983) to account for the estimation of the vector state $\underline{x}$.

4.3.2 The Recursive Bayes' Estimator

Bayes' rule (equation 4.1) specifies an expression for updating the conditional probability density p(x(i)|y(i)) of the current state x(i):

$$p(x(i)|y(i)) = C\ p(x(i)|y(i-1))\ p(y(i)|x(i)) \qquad (4.14)$$

where C is a constant, p(x(i)|y(i-1)) is the prior distribution at time i and p(y(i)|x(i)) is the likelihood function. At time i = 1, equation 4.14 reverts to equation 4.9 because the initial prior distribution of x, p(x(1)), is Normal. For i > 1, the prior probability is calculated from the preceeding conditional distribution by the convolution integral:

$$p(x(i)|y(i-1)) = \int_{x(i-1)} p(x(i)|x(i-1))\ p(x(i-1)|y(i-1))dx(i-1) \qquad (4.15)$$

From equation 4.12 and the Gaussian white noise assumption for ξ, it follows that the density p(x(i)|x(i-1)) is given by:

$$p(x(i)|x(i-1)) = \frac{1}{\sqrt{2\pi v_\xi}} \exp\left\{ - \frac{(x(i)-gx(i-1)-\alpha)^2}{2v_\xi} \right\} \qquad (4.16)$$

The moments of the conditional distribution p(x(i)|y(i)) give the mean m_{Bay} and the standard deviation $\sqrt{v_{Bay}}$ of the optimal estimate. The Bayes' estimator is optimal because all the conditional distribution p(x|y) and not its approximation whether in terms of series or in terms of its moments is propagated as a prior distribution. The price of the optimality is in the heavy computational burden in calculating the convolution integral.

The performance of the estimator is better illustrated with reference to a generic example: consider the first order system of equation 4.12 with the dynamic state x seen through the pH measurement of equation 4.6. The parameters of these two equations for a simulation run of 50 samples are:

$g = 0.9$ $\alpha = 1.0$

$p(x(1) = N(0.1;0.01)$ $p(\xi) = N(0.;0.05)$ $p(\eta) = N(0.;0.01)$

Figure 4.3a shows the measured pH. Time-histories of the simulated state x, its Bayes' rule estimate, m_{Bay}, and its standard deviation $\sqrt{v_{Bay}}$ are shown in figure 4.3b. Because the estimate almost coincides with the simulated state, for clarity purposes, the error $x(i) - m_{Bay}(i)$ and $\sqrt{v_{Bay}(i)}$ are plotted on a larger scale in figure 4.3c. Note that the estimate m_{Bay} is not identical to the state x because of necessary approximation in calculating the convolution integral.

When x is a vector of dimension $n > 2$, the problems of storing the probability distributions and computing the convolution integrals are formidable and for all practical purposes prohibitive. These limitations have led to the development of approximate solutions such as the Extended Kalman Filter.

4.3.3 The Recursive Extended Kalman Filter

The Kalman filter equations (equation 4.5) of the linear system are extended (Jazwinski 1970) to the non-linear measurement of equation 4.6 which is generated by the linear dynamic state of equation 4.12. The extension is in assuming that the non-linear function pH(x) can be linearized about the prior mean m_0 of the state x to give the coefficient H_{EKF} instead of H in equations 4.5:

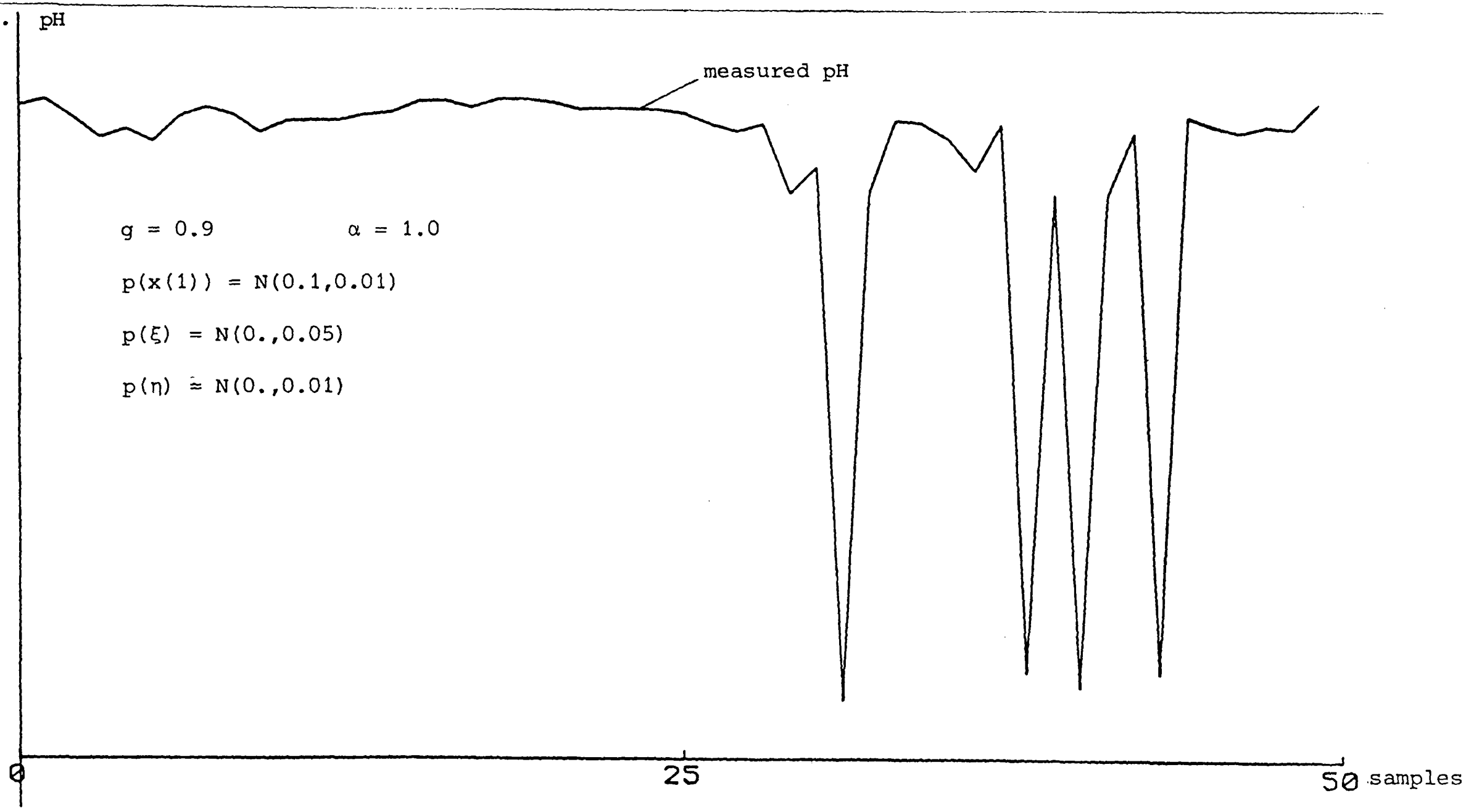


Fig 4.3a Recursive estimation: measured pH

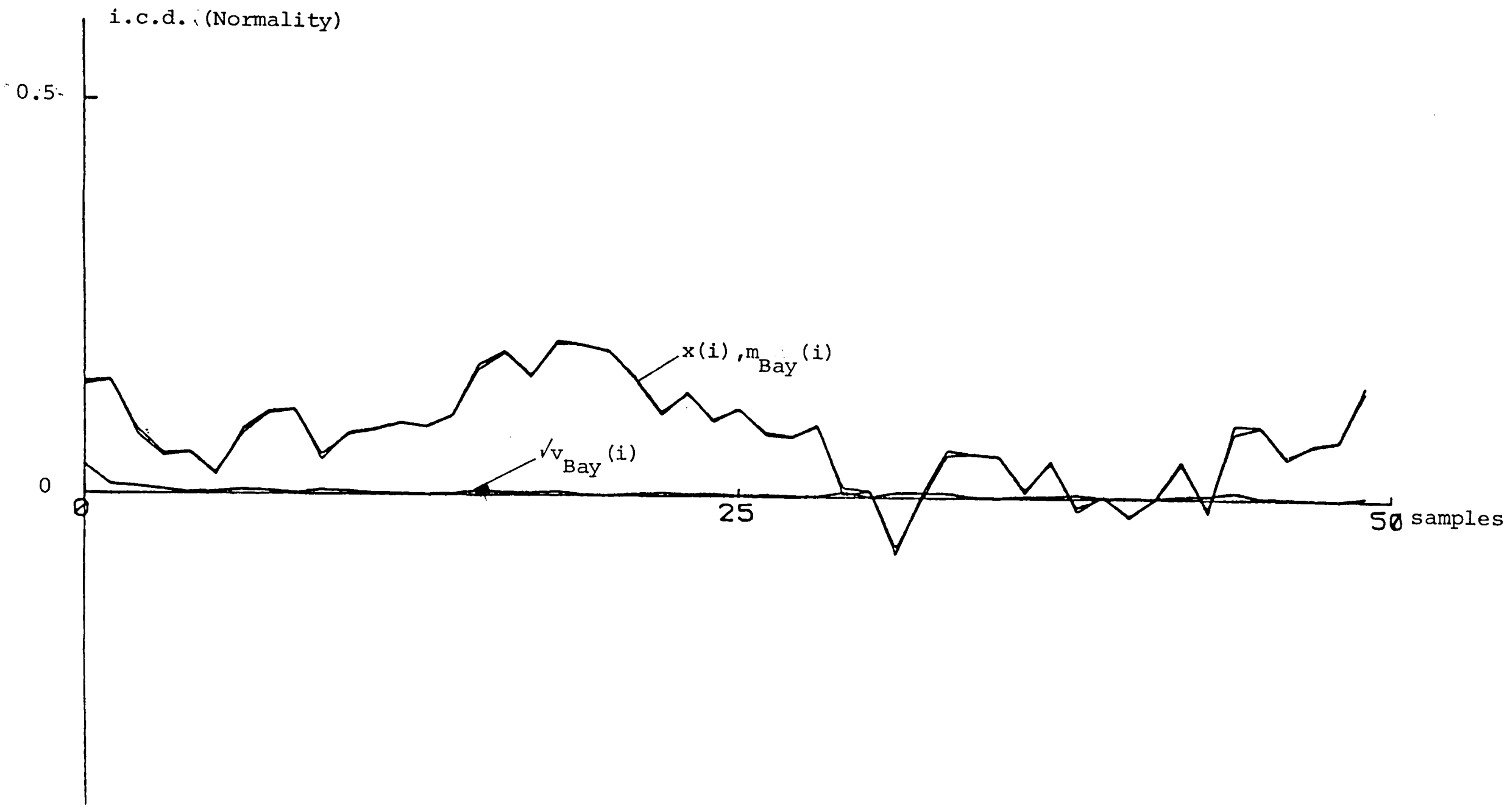


Fig 4.3b Recursive estimation: the Bayes' estimator

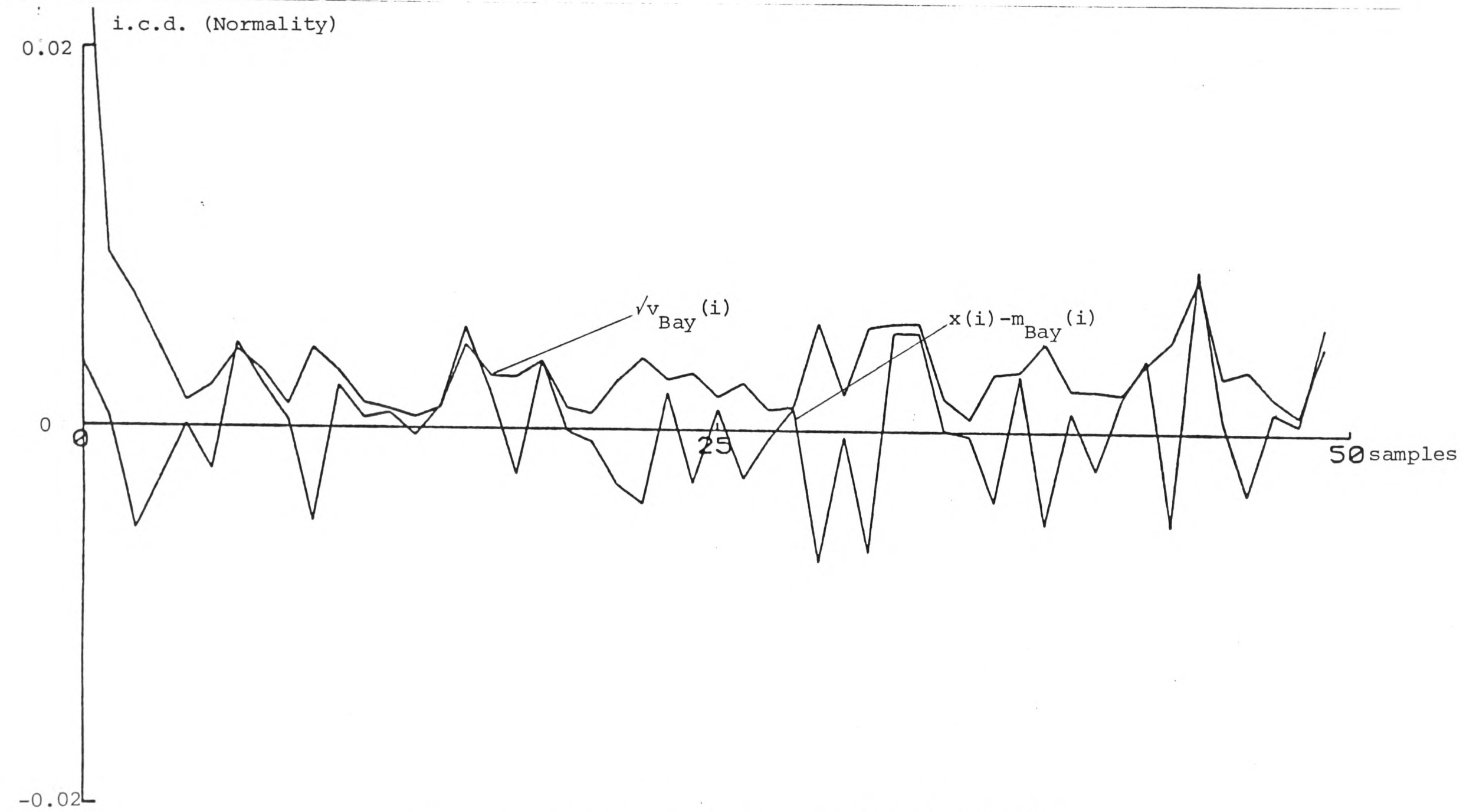


Fig 4.3c Recursive estimation: the Bayes' estimator

$$H_{EKF} = \left.\frac{dpH(x)}{dx}\right|_{x=m_0} \qquad (4.17)$$

The linearisation is equivalent to assuming that the likelihood function of equation 4.8 is Normal: $N(pH(m_0);v_\eta)$. Hence, $p(x,y)$ is equal to the product of two Normal distributions and is also Normal with mean m_{EKF} and variance v_{EKF} given by the Extended Kalman Filter:

$$m_{EKF} = m_0 + (y-pH(m_0))H_{EKF}v/v_\eta \qquad (4.18a)$$

$$v_{EKF} = v_0 v_\eta/(H_{EKF}^2 v_0 + v_\eta) \qquad (4.18b)$$

The EKF leads to a Gaussian conditional distribution and therefore, the propagation equations are the same as equations 4.13. In a large number of cases, this approximation is valid provided that the non-linearity is not severe; chapter 5 will discuss such a case in which additionally the number of estimated states is larger than one. But in case of the pH measurement, the EKF cannot cope with the non-linearity as can be seen in the time-histories of figure 4.4 with statistics and random sequences identical to those of the optimal Bayes' estimator of figure 4.3. The EKF estimate follows the state closely as long as the measured pH is in a region of lesser slope (pH ≃ 13), but when the pH dips in a region of high slope (after 30 samples), the estimate diverges; the estimator recovers after the pH returns to pH 13.

The numerical implementation of the derivative of equation 4.17 is outlined in appendix II.

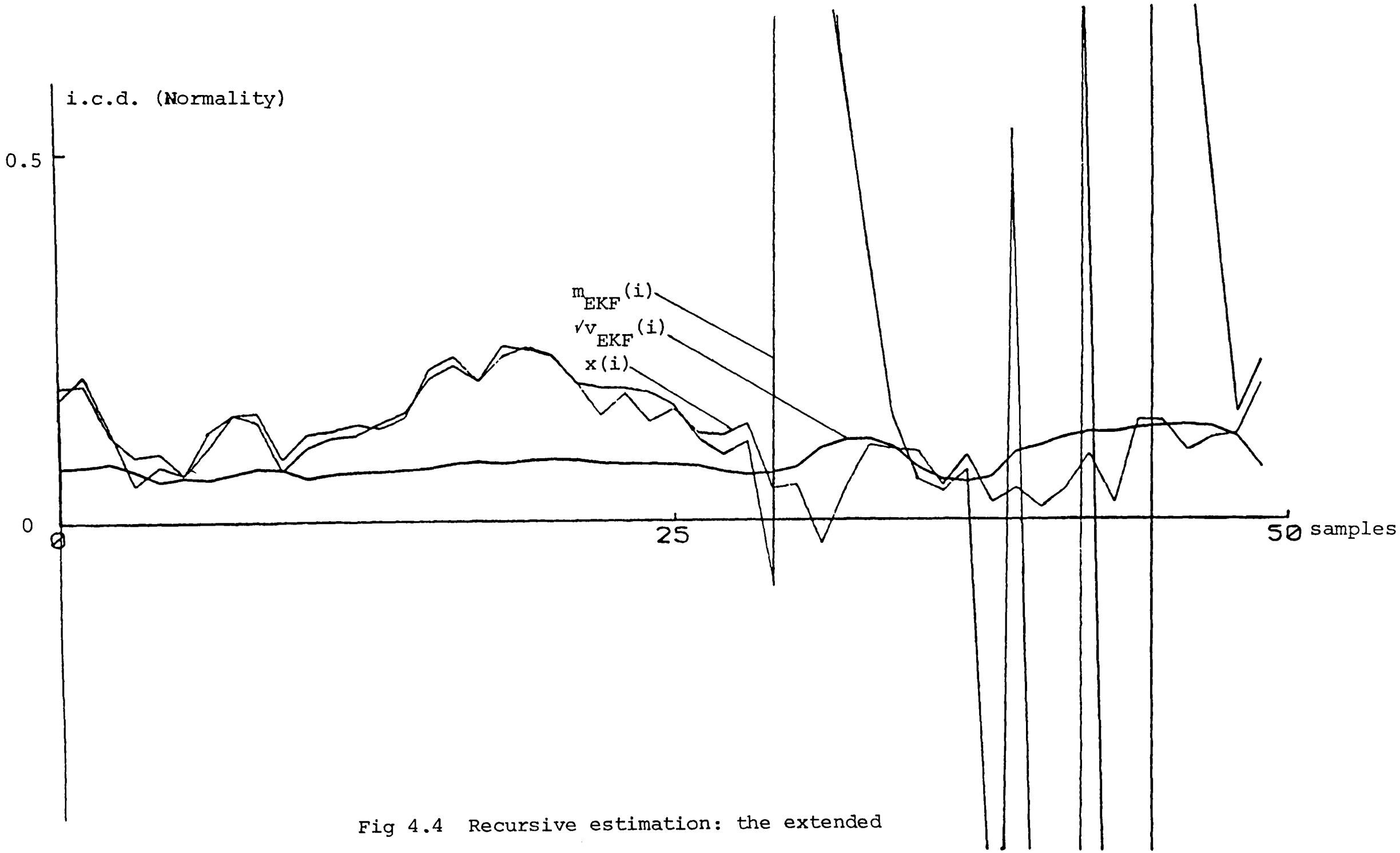


Fig 4.4 Recursive estimation: the extended

Fig 4.4 Recursive estimation: the extended Kalman filter

4.3.4 Gaussian Approximation And The Linearisation Estimator

The Gaussian Approximation can be considered as a compromise between the optimal Bayes' estimator of section 4.2.1 and the Extended Kalman Filter of section 4.2.2. It is based on the assumption that the posteriori distribution is Gaussian and can be sufficiently specified by its mean and variance. This assumption may be validated by the Central Limit Theorem (Papoulis 1965) and by some cases such as in figure 4.2 which shows an almost Normal conditional distribution. The assumption does then provide the same way of propagating the conditional distribution to a prior distribution for the next stage estimation as in the EKF. Hence, the approximation has reduced the numerically cumbersome convolution integral of the Bayes' estimator to the much simpler prediction equation of the Kalman filter. But unlike the EKF, the likelihood function is not assumed to be Normal and is calculated for all possible values of the state x for the non-linear measurement function.

For the dynamic system represented by equation 4.12 and the measurement of equation 4.6, we assume that at any time i, the prior distribution p(x(i)) is Normal $N(m_0(i),v_0(i))$; this is true for i = 1. Then, Bayes' rule is used to compute the conditional distribution p(x(i)|y(i)) from the prior distribution and the likelihood function as in equation 4.14. According to the Gaussian approximation, the posteriori distribution is specified by the conditional mean m(i) and the conditional variance v(i) which are given by the moments of the distribution as described in the introduction. m(i) and v(i) are used in the linear prediction equations 4.13 to propagate the information for the next Normal priori distribution.

Figure 4.5 shows time-histories of the simulated state x(i), the Gaussian

estimate $m_{Gaus}(i)$ and the standard deviation $\sqrt{v_{Gaus}(i)}$ of the estimate. Comparing figure 4.5 with figure 4.3 & 4.4, it can be seen that the Approximate Gaussian estimator is not as good as the optimal Bayes', but is significantly more robust than the EKF. The cost of improvement in performance over that of the EKF is in the numerical calculation of the likelihood function p(y|x). The extension of the Gaussian Approximation for the estimation of the state vector $\underline{x}$ is not straight forward because of difficulties in calculating and storing the likelihood function and the conditional distribution of all the states. The Linearisation Estimator (Jacobs 1983) restricts this numerical calculation to a one-dimensional distribution by linearising the combination of the non-linear pH measurement followed by Bayes' rule, to provide a linear pseudo-measurement.

The Linearisation Estimator (Jacobs 1983) is used for the estimation of the dynamic model derived in chapter 3. The dynamic equations 3.46 are condensed as follows:

$$\underline{x}(i+1) = \underline{G}(\underline{x}(i),u(i),\underline{\xi}) \qquad (4.19)$$

where $\underline{x}$ is the state vector, $\underline{G}$ is the non-linear vector function, u(i) is the current control action and $\underline{\xi}$ is the system white noise. The scalar pH measurement, when no bias is present, is given by:

$$y(i) = pH(x_1(i)) + \eta \qquad (4.20)$$

The Linearisation estimator, shown in figure 4.6, is based on the linearisation of the combination of the non-linear measurement followed by Bayes' rule to provide a linear pseudo-measurement y' of the state x_1 plus independent pseudo noise η':

$$y'(i) = x_1(i) + \eta'(i) \qquad (4.21)$$

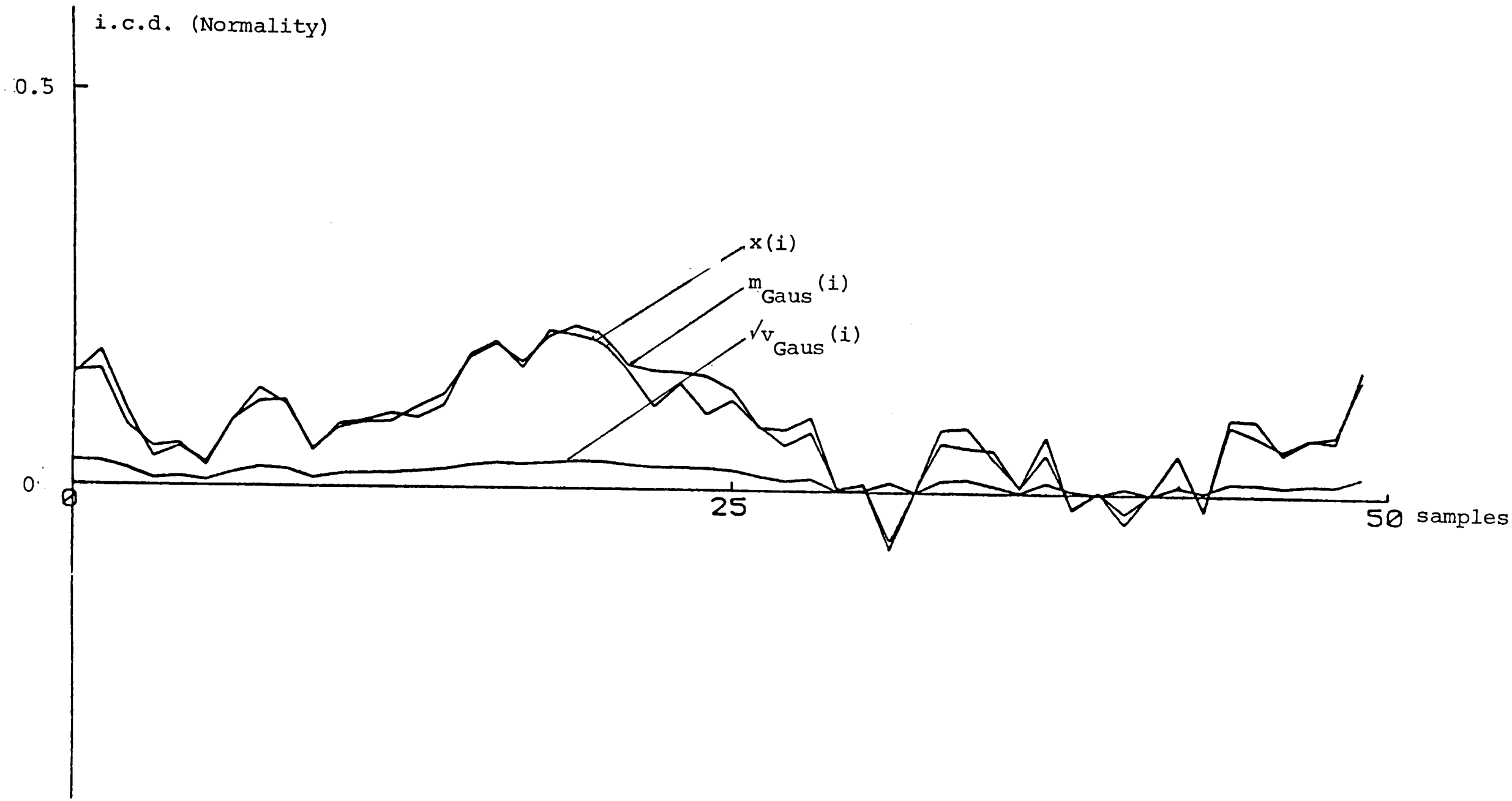


Fig 4.5 Recursive estimation: the Gaussian Approximation

y' and v'_η are given by (Jacobs 1983):

$$y' = m + (m-m_0)v'_\eta/v_0 \qquad (4.22a)$$

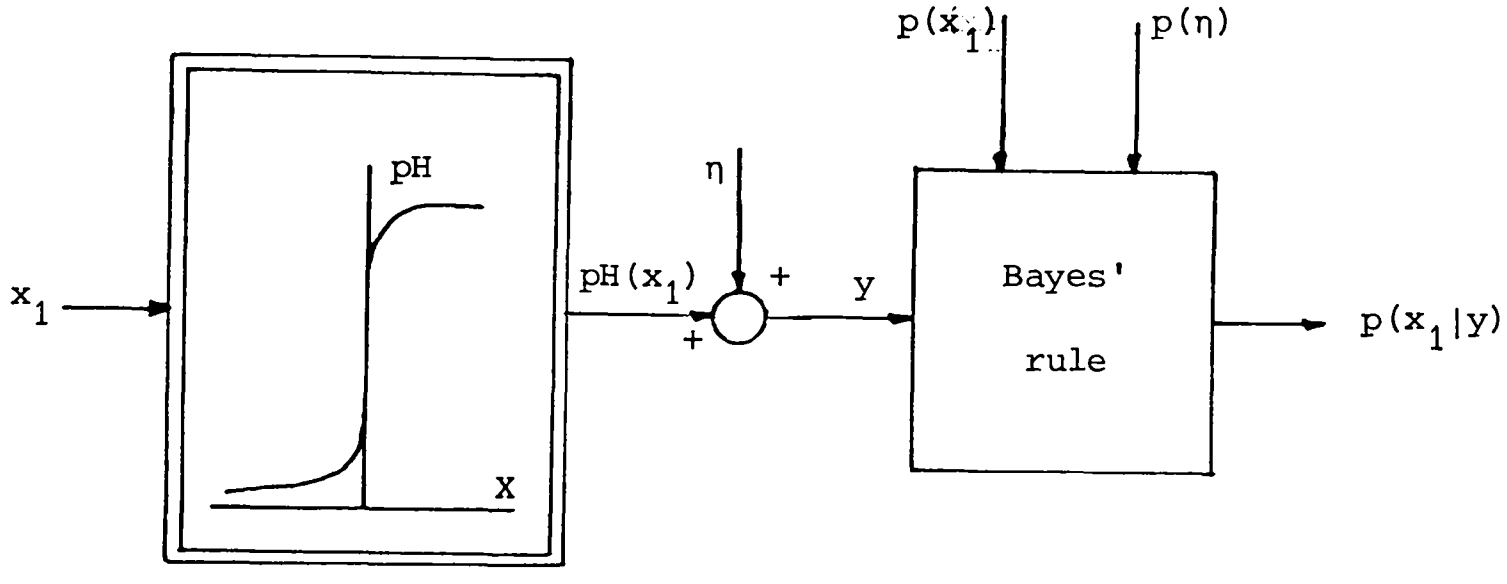
$$v'_\eta = v_0 v/(v_0-v) \qquad (4.22b)$$

where m_0 & v_0 are the prior statistics of x_1 and m & v are the conditional statistics of x_1 given by the Gaussian approximation.

The pseudo-measurement and pseudo noise variance are then used to drive an EKF for the estimation of the non-linear state equations 4.19; the EKF produces estimate $\hat{\underline{x}}(i)$ of $\underline{x}(i)$ and covariance estimate $\underline{\Sigma}(i)$. The state estimation and prediction are discussed in chapter 5.

4.3.5 Application Of The Linearised Estimator To The pH Model

The Linearised Estimator algorithm has been implemented in the CAD simulation package, introduced in chapter 1 and described in detail in chapter 7, which simulates and estimates the general multi-state model of chapter 3. The estimator has shown to be robust and reliable over a large number of samples (> 3000). Figures 4.7 and 4.8 show time-histories of the simulated i.c.d. $x_1(i)$ of equation 3.46, its EKF estimate $\hat{x}_1(i)$ and the standard deviation of its estimate $\sqrt{\sigma_{11}(i)}$ (from $\underline{\Sigma}$) over 360 samples only for clarity, for two setpoints (pH 8.5 & 12) and for two different measurement noise standard deviation (s_η = 0.05, 0.1 pH units). The estimate was generated by the Linearised Estimator coupled to the EKF under feedback control. At a lower setpoint (figures 4.7a,b) the effect of the pH non-linearity is more severe making the estimation of the state $x_1(i)$ worse than for the higher setpoint (figures 4.8a,b). At a setpoint of pH 12, the estimator is more robust because the slope of the pH non-linearity does not change significantly for small changes of



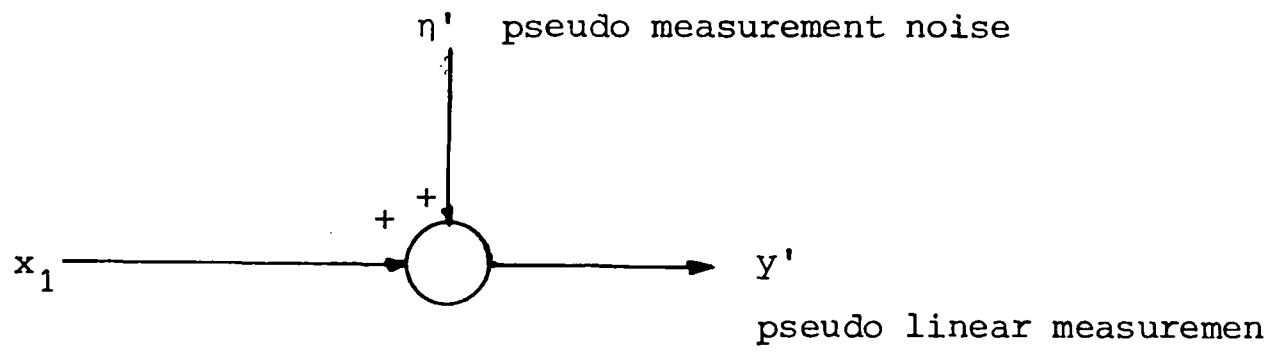


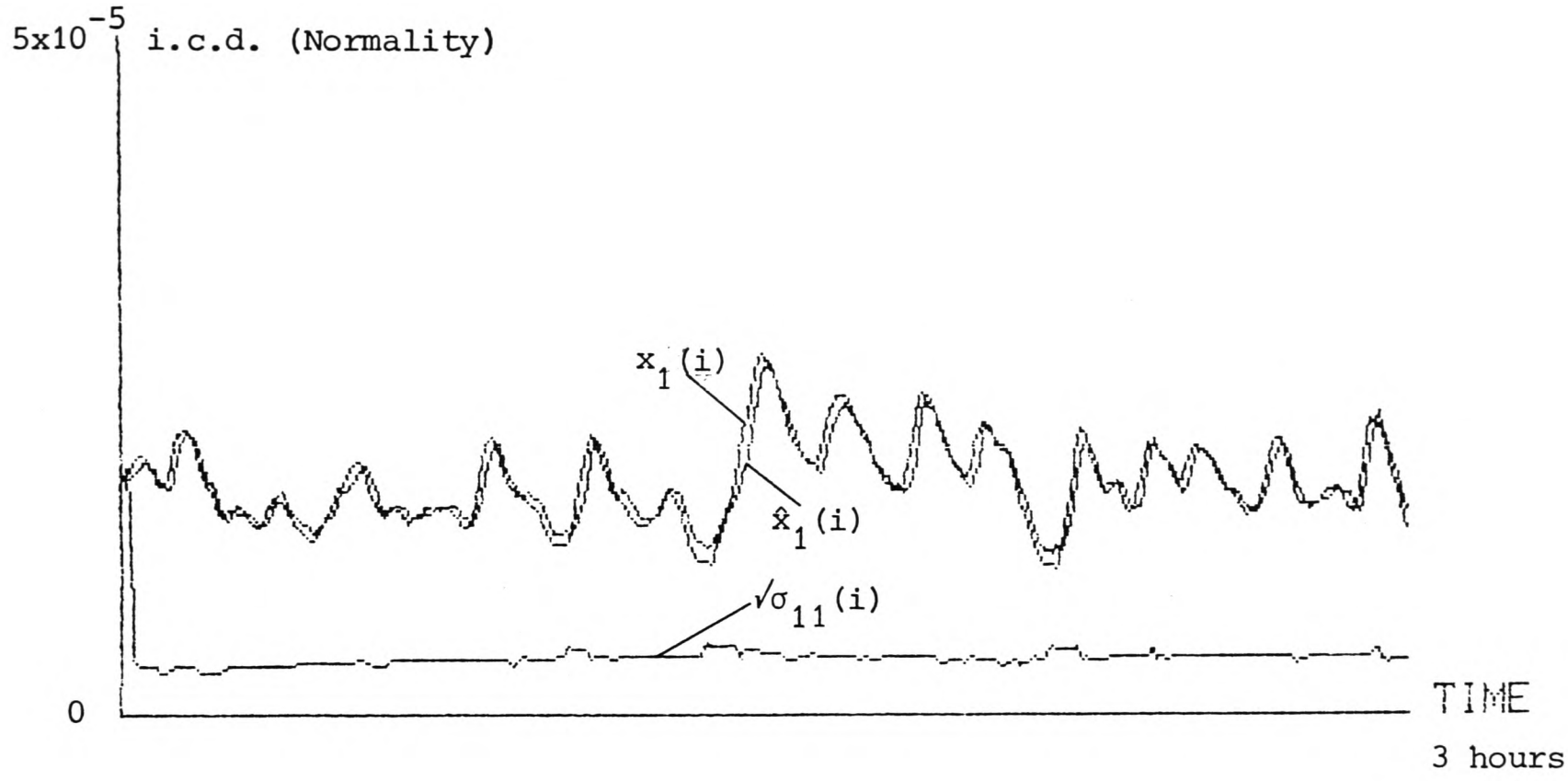
Fig 4.6 The Linearised Estimator

i.c.d. (figure 1.1); hence, the estimate follows closely the actual state. As the measurement noise increases, the performance of the estimator deteriorates the more so at the lower setpoint because the estimator is at its most sensitive near the neutral point. The standard deviation $\sqrt{\sigma_{11}(i)}$ is a fair indication of the confidence in the estimate. $\sqrt{\sigma_{11}(i)}$ is large in figures 4.7a,b because it reflects the uncertainty in the buffered titration curve of this particular process (section 3.4). For the process of figure 4.8, the titration curve is the strong reagent one, and $\sqrt{\sigma_{11}(i)}$ is relatively small because the chemistry is well defined.

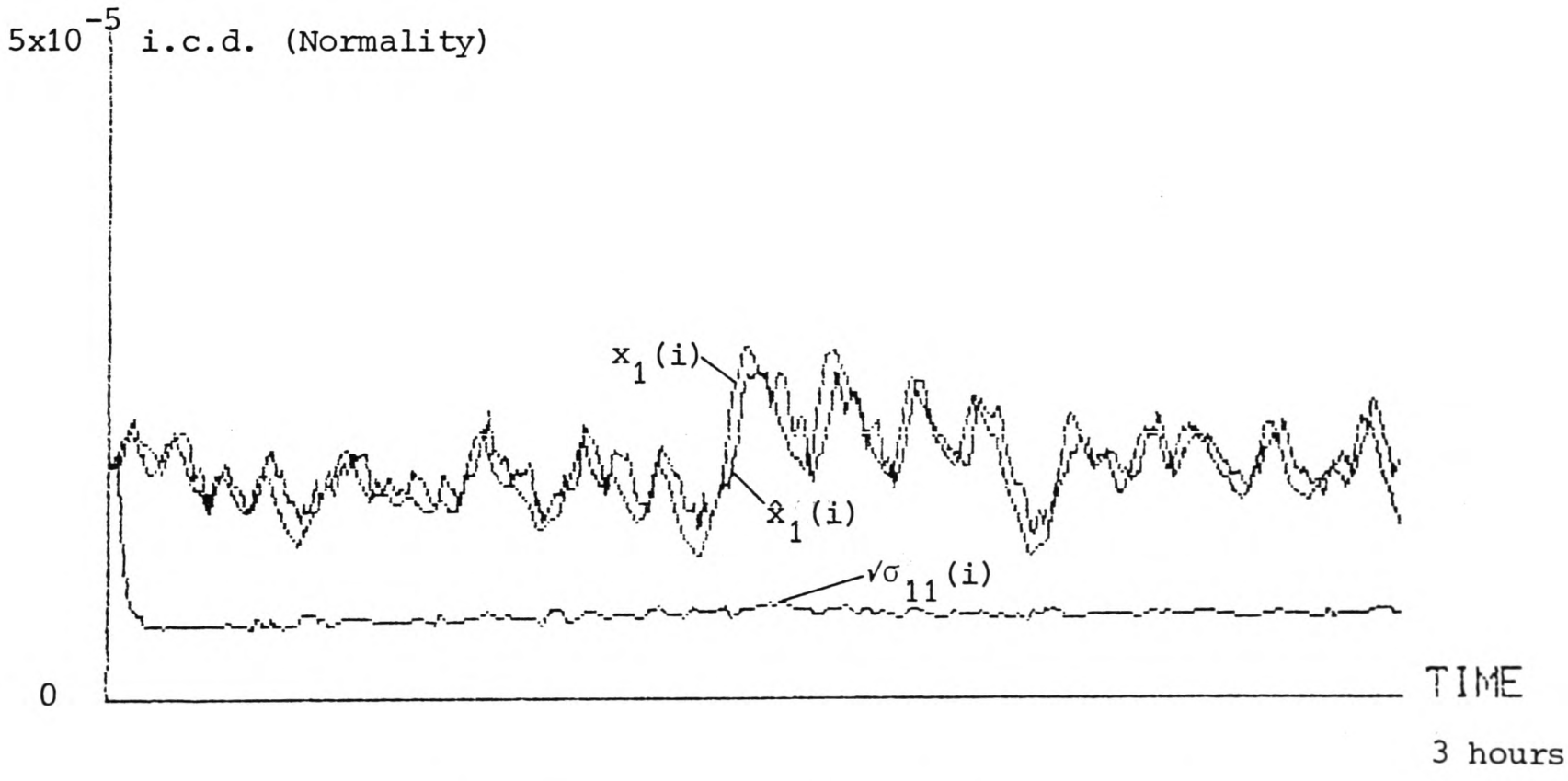
In section 4.3, different recursive estimation techiques of scalar and vector states through the pH non-linearity were discussed. The difficulties involved in the mathematical implementation of the optimal Bayes' estimator was found to be formidable. The extended Kalman filter failed to estimate the i.c.d. because of the severity of the non-linearity. The Gaussian Approximation and by extension the Linearised Estimator estimated succesfully the i.c.d. even though analysis convergence of the algorithm was not available; it has been implemented in the CAD pakage PHDESIGN for the state estimation of the model of chapter 3.

4.4 RECURSIVE ESTIMATION THROUGH A BIASED pH MEASUREMENT

In this section, a novel non-linear estimator based on Bayes' rule successfully estimates bias on the effluent pH measurement. The estimator has the basic structure of the Linearised Estimator (Jacobs 1983) of section 4.3.4. It is implemented to the pH model of section 3.4.

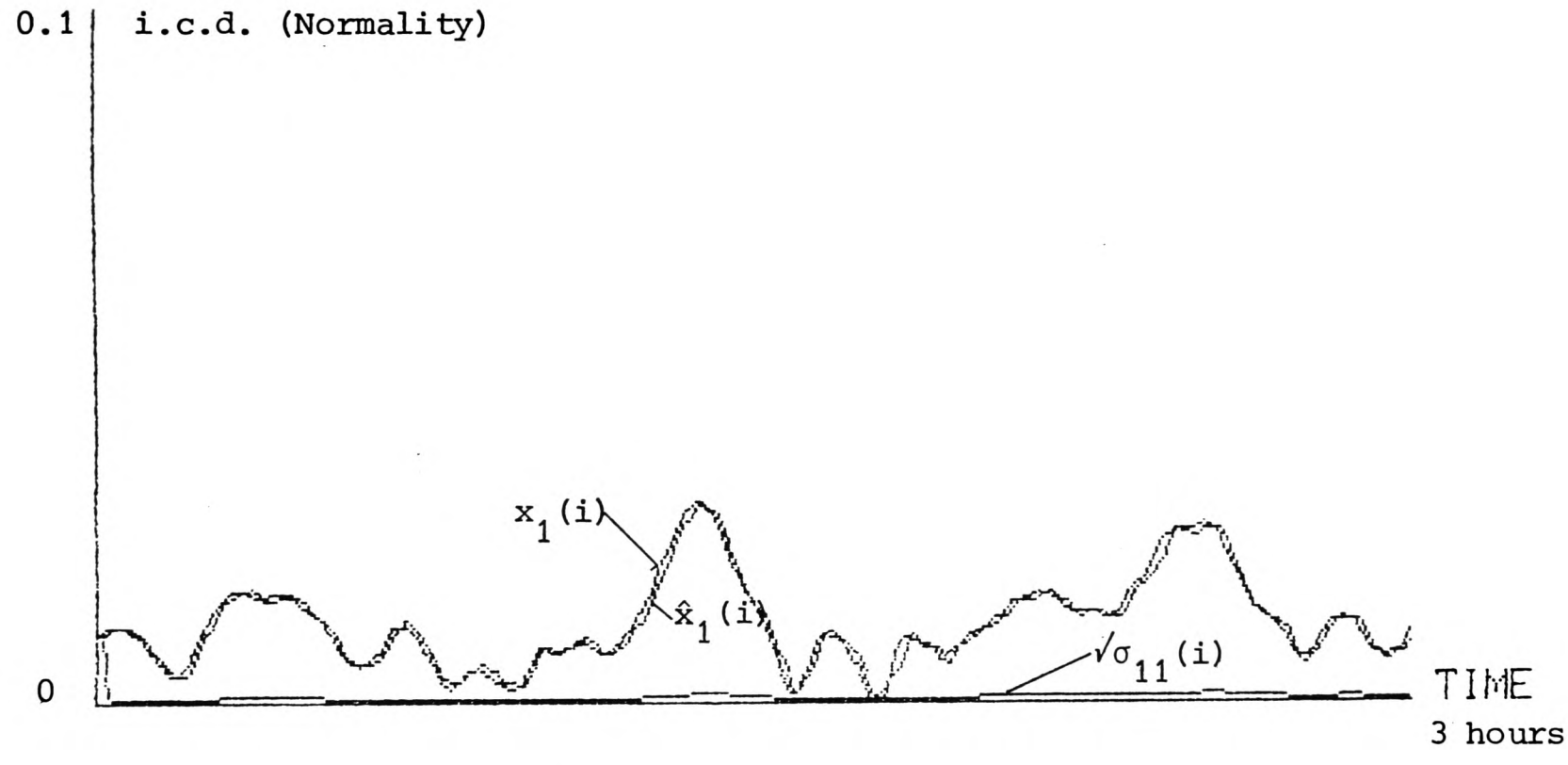


a. Measurement noise s_η = 0.05 pH units

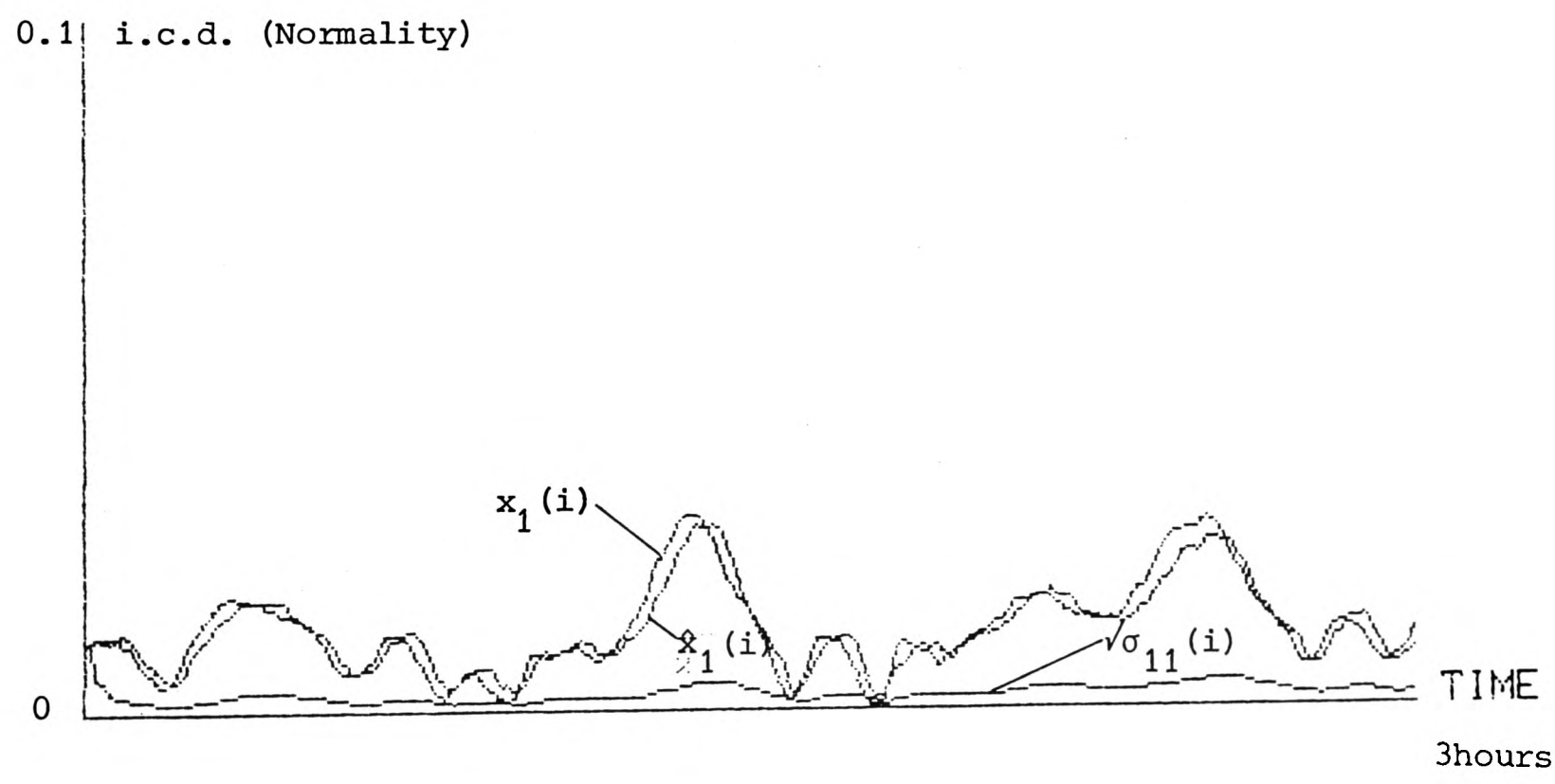


b. Measurement noise s_η = 0.1 pH units

Fig 4.7 The Linearised Estimator: pH setpoint= 8.5 pH



a. Measurement noise s_η = 0.05 pH units



b. Measurement noise s_η = 0.1 pH units

Fig 4.8 The Linearised Estimator: pH setpoint= 12.0 pH

Estimators of constant bias in linear systems have been investigated previously either as unreliable instrumentation (Friedland 1969) or as fault detection systems (Mendel and Washburn 1978). The estimators are based on separating the estimation of the bias from the dynamic state variables by augmenting the state vectors. In some cases (Friedland 1978), a slower estimation rate for the bias when infrequent estimates are needed has been implemented successfully. Estimation of sudden changes of bias in linear systems (Friedland 1982) has been based on well founded techniques (Basseville and Benveniste 1983, Willsky and Jones 1976, Mehra and Peschon 1971) for jump detection based on the examination of the innovation sequence of the estimators. No estimation of bias for non-linear systems has been reported.

This section reports on a bias estimator to the pH non-linearity. The estimator estimates the bias on the pH measurement and the effluent i.c.d. which is used to provide a linearised pseudo-measurement to drive a model-based EKF.

4.4.1 Introduction To Bias Estimation

The modelling of the bias discussed in section 3.4 is summarised in section 4.4.1; this is followed by a discussion of observability considerations which limit the bias estimation to cases when only feedforward measurements of the disturbances of influent flow and concentration are available. In order to estimate the i.c.d. of the effluent x_1 and the bias z the Linearised Estimator is extended to a two-dimensional Bayes' rule in section 4.4.2. The estimator uses two tests which are discussed in section 4.4.3: the first test based on the size of the innovation is for whether the bias seemed to have jumped;

the second is an observability test to determine whether both x_1 and z can be estimated simultaneously from one measurement y (equation 3.46b). Finally, section 4.4.4 concludes the bias estimation by summarising the estimation algorithm and discussing its implementation and its results.

As discussed in the previous chapter, the pH measurement, y(i) at time i, may be modelled as the actual pH of the effluent, $pH(x_1(i))$, corrupted by additive bias, z(i), and white measurement noise η:

$$y(i) = pH(x_1(i)) + z(i) + \eta \qquad (3.46b)$$

The bias z is modelled as a jumping random variable which remains constant but makes occasional jumps at random time, for example because of probe switching; for a constant z:

$$z(i+1) = z(i) = z \qquad (4.23)$$

Alternatively, the bias may be modelled as a slowly varying Wiener process drift to account for probe fouling (section 3.4):

$$z(i+1) = g_z z(i) + \alpha_z + \xi_z \qquad (3.42)$$

where g_z is the rate of change of the model, α_z is the mean value of the process and the standard deviation of ξ_z is a measure of the extent of the change of bias; values of g_z, α_z and ξ_z are given in the implementation of the bias estimation algorithm in section 4.3.3.

In the multi-state model of chapter 3, the bias may be estimated only if the titration curve and the feedforward measurements of the influent flow and concentration are available. Observability considerations prevent the simultaneous estimation of the influent disturbances, the effluent i.c.d. and the bias from the pH measurement. Poor observability occurs because the disturbance models x_2 & x_3 have large variances to allow for tracking of large variations; this

uncertainty in x_2 and x_3 and the uncertainty in z affect the effluent i.c.d. x_1 in the same way. Hence, the model cannot differentiate between the effect of the two uncertainties on x_1, and by extension (equation 3.46b) on the measurement y so that accurate estimation of the states x_1, x_2 and x_3, and of the bias z from the measurement y of equation 3.46b becomes impossible.

4.4.2 Two-dimensional Bayes' Rule Estimator

As discussed earlier (section 4.2), difficulties arise in recursive state estimation of non-linear systems when propagating the information about the states between each measurement. In the two-dimensional Bayes' rule estimator, the information is passed from one measurement to another on a floating grid in the form of a two-dimensional distribution. It is evaluated at each grid point in standardised coordinates μ_x and μ_z which are defined by:

$$\mu_x = (x_1 - \tilde{m}_x)/\tilde{s}_x \qquad (4.24a)$$

$$\mu_z = (z - \tilde{m}_z)/\tilde{s}_z \qquad (4.24b)$$

where $\tilde{m}_x$, $\tilde{m}_z$ and $\tilde{s}_x$, $\tilde{s}_z$ are the means and the standard deviations of the prior distribution of x_1 and z. $\tilde{v}_x$ and $\tilde{v}_z$ are their variances.

The bias z is assumed to be independent of the i.c.d. x_1. In the case of jumping bias, it is uniformly distributed over a prespecified range and the prior two-dimensional distribution $p(x_1,z)$ is initialised as uniform in z and Normal in x_1 as shown in figure 4.9a. In standard coordinates, $p(x_1,z)$ is written as:

$$p(x_1,z) = \text{constant exp } (-\mu_x^2/2) \qquad (4.25)$$

Alternatively if the bias is drifting slowly, z is Normal and $p(x_1,z)$ is

initialised as a bivariate Normal distribution (figure 4.9b):

$$p(x_1,z) = \text{constant exp } (-(\mu_x^2 - 2\tilde{r}\mu_x\mu_z + \mu_z^2)/2(1 - \tilde{r}^2)) \qquad (4.26)$$

where $\tilde{r}$ (initially set to zero) is the correlation coefficient of the prior distribution defined by:

$$\tilde{r} = E[(x_1 - \tilde{m}_x)(z - \tilde{m}_z)]/\tilde{s}_x\tilde{s}_z \qquad (4.27)$$

where E[.] denotes the expected value.

The two estimation tests introduced earlier are made sequentially after the effluent pH is measured; they are explained in detail in section 4.3.2. The first test to determine changes in bias value is made immediately after each measurement. The second test provides a measure of whether both the i.c.d. of the effluent x_1 and the bias z can be estimated concurrently using the measurement y. The second test is needed because poor observability of x_1 and z may lead to numerical problems. Provided that neither of the tests indicate a need for special action, the estimation algorithm proceeds to combine the two-dimensional prior distribution $p(x_1,z)$ with a two-dimensional likelihood function $p(y|x_1,z)$ to yield a two-dimensional conditional distribution $p(x_1,z|y)$ according to Bayes' rule. The likelihood function, shown in figure 4.10, is calculated from the measurement noise distribution $p(\eta)$ for all possible values of x and z:

$$p(y|x_1,z) = p(\eta = y-pH(x_1)-z) = c \exp\left\{ - \frac{(y-pH(x_1)-z)^2}{2v_\eta} \right\} \qquad (4.28)$$

The conditional distribution which results when the likelihood intersects the initial prior distribution of figure 4.9a is shown in figure 4.11:

$$p(x_1,z|y) = C\ p(x_1,z)\ p(y|x_1,z) \qquad (4.29)$$

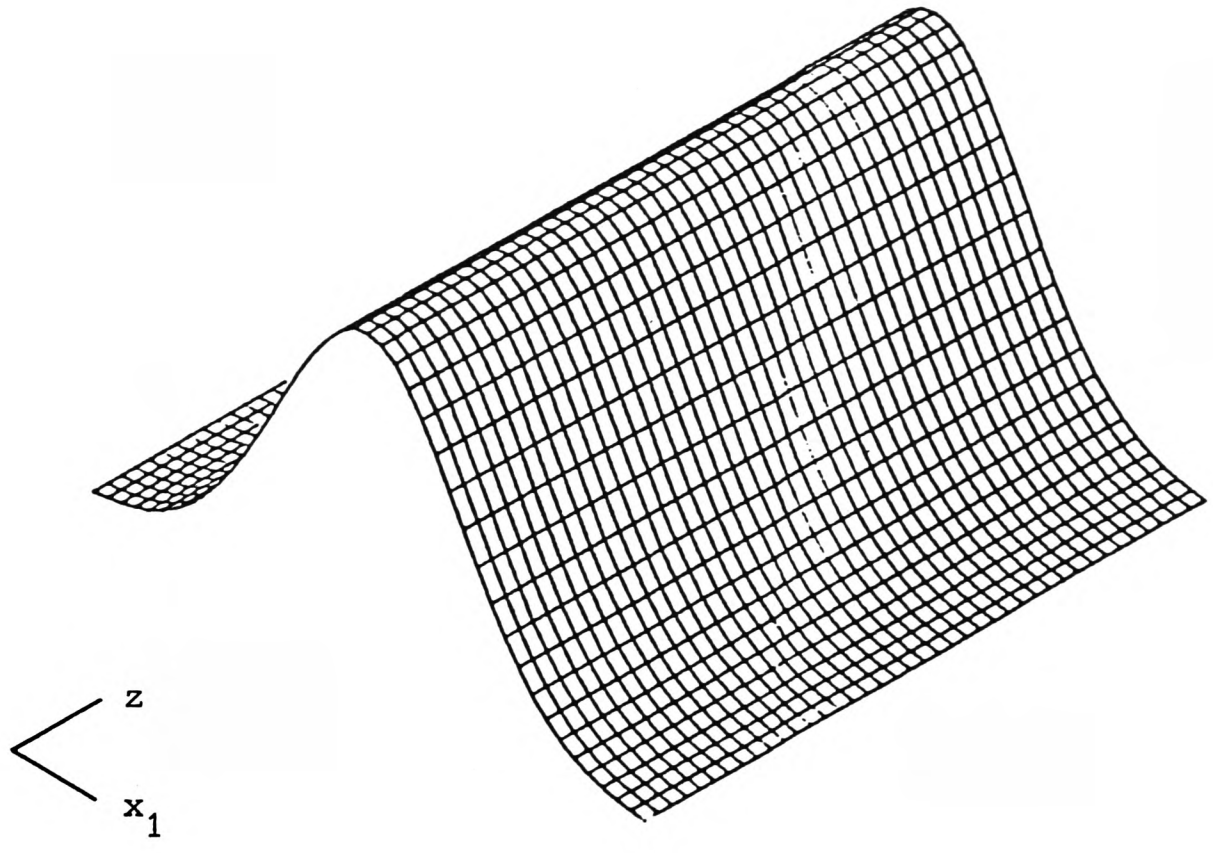


Fig 4.9a Prismatic prior probability $p(x_1,z)$ for jumping bias

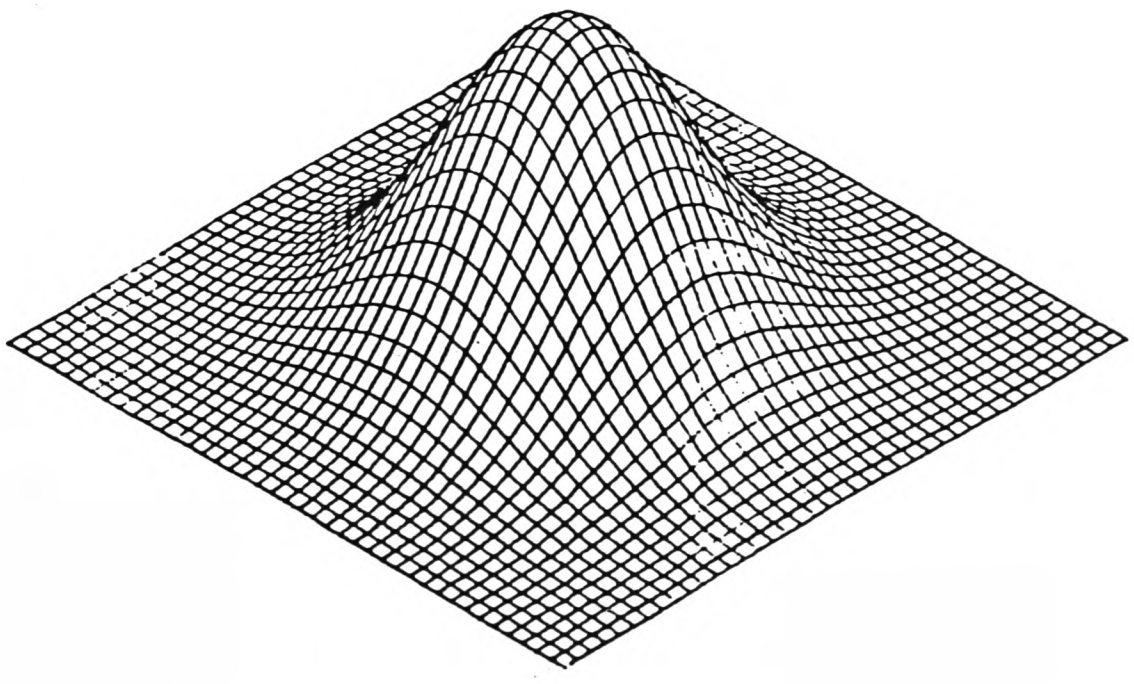


Fig 4.9b Normal prior probability $p(x_1,z)$ for slowly varying bias

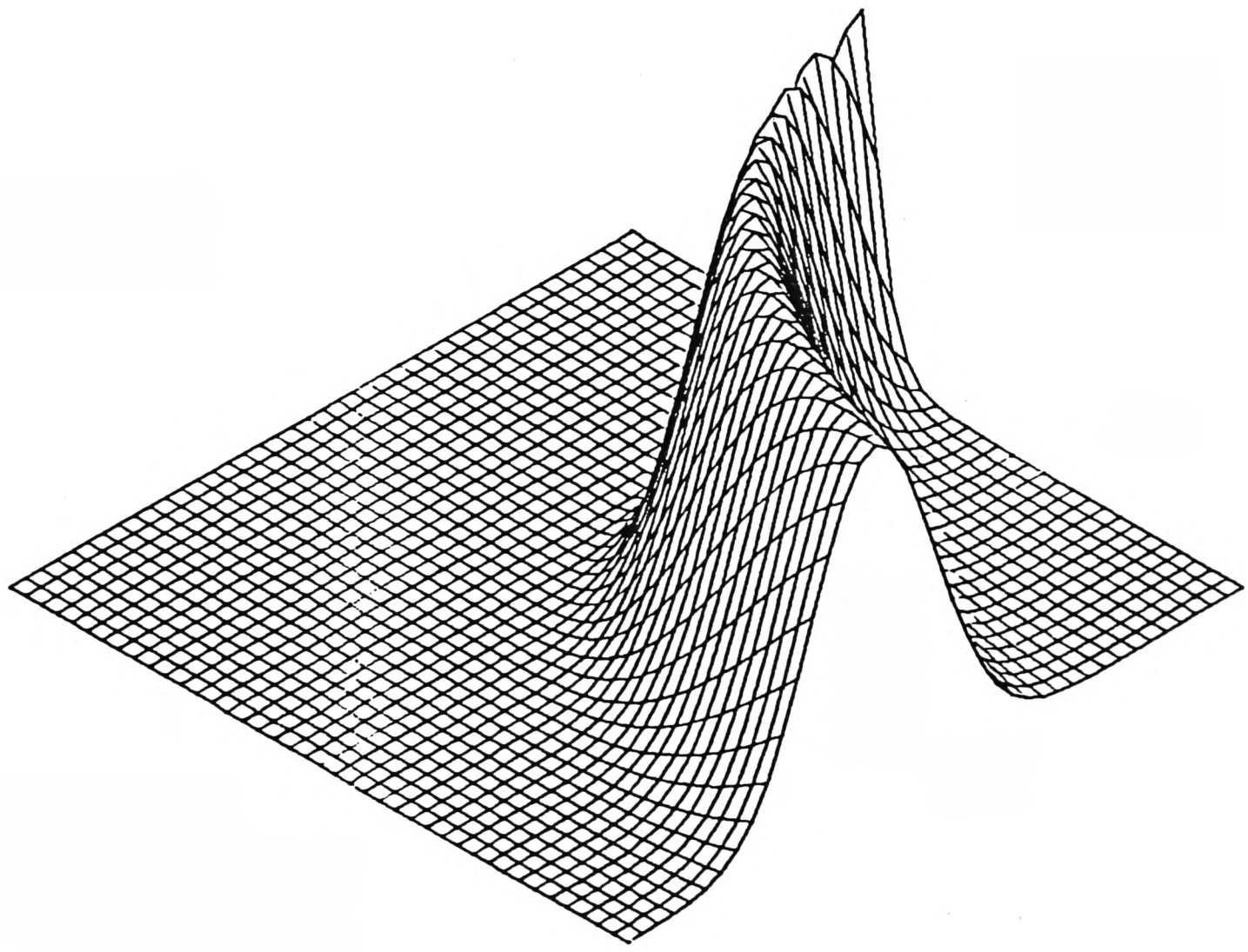


Fig 4.10 Likelihood function $p(y|x_1,z)$

where C is the normalisation constant given by:

$$C = \left\{ \int_{x_1} \int_{z} p(x_1,z)p(y|x_1,z)dzdx_1 \right\}^{-1} \qquad (4.30)$$

Statistics of the conditional distribution can be computed numericallly to provide conditional estimates of the random variables x_1 and z:

$$\text{mean of } x_1: \quad m_x = \int_{x_1} \int_{z} x_1 p(x_1,z|y)dzdx_1 \qquad (4.31a)$$

$$\text{mean of } z: \quad m_z = \int_{x_1} \int_{z} z\, p(x_1,z|y)dzdx_1 \qquad (4.31b)$$

$$\text{var. of } x_1: \quad v_x = \int_{x_1} \int_{z} (x_1-m_x)^2 p(x_1,z|y)dzdx_1 \qquad (4.31c)$$

$$\text{var. of } z: \quad v_z = \int_{x_1} \int_{z} (z-m_z)^2 p(x_1,z|y)dzdx_1 \qquad (4.31d)$$

$$\text{cov. of } x_1 \text{ \& } z: \quad v_{xz} = E[(x_1 - m_x)(z - m_z)] \qquad (4.31e)$$

$$= \int_{x_1} \int_{z} (x_1-m_x)(z-m_z)p(x_1,z|y)dzdx_1$$

$$\text{correlation coeff.}: \quad r = v_{xz}/s_x s_z \qquad (4.31f)$$

where s_x and s_z are the standard deviation of the estimates.

The conditional statistics $m_x(i)$ and $v_x(i)$ at time i combine with the prior statistics $\tilde{m}_x(i)$ and $\tilde{v}_x(i)$ as in equations 4.22 to provide a linearised pseudo-measurement y'(i) and a pseudo-measurement noise $v'_\eta(i)$ needed in the recursive scheme of the Linearised Estimator (section 4.2.3). y'(i) and $v'_\eta(i)$ are then used to drive an E.K.F. for the estimation of the multi-state model of chapter 3:

$$\underline{x}(i+1) = \underline{G}(\underline{x}(i),u(i),\underline{\xi})$$

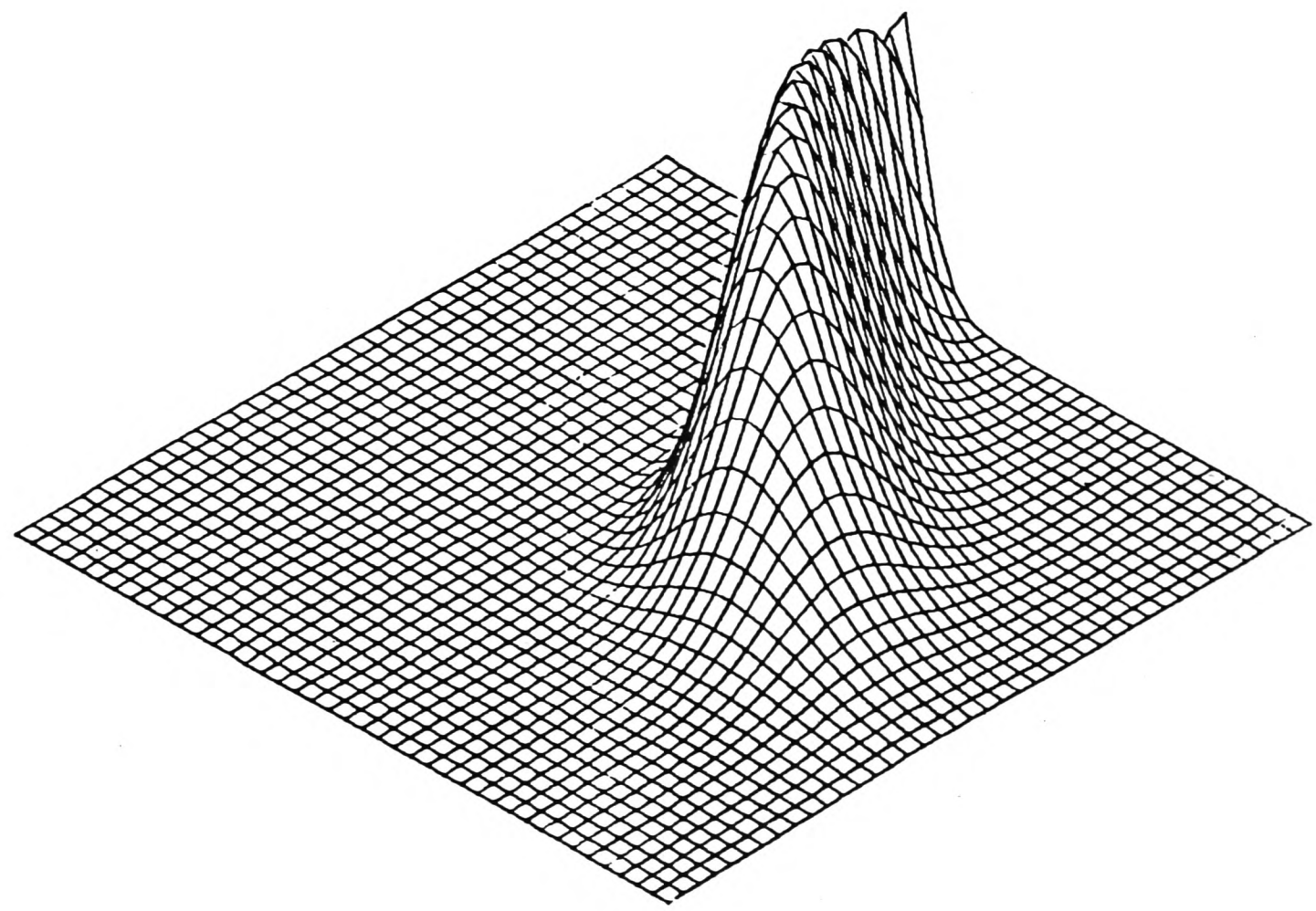


Fig 4.11 Conditional distribution $p(x_1,z|y)$

$$y'(i) = x_1(i) + \eta'$$

which produces estimates $\hat{\underline{x}}(i)$ of $\underline{x}(i)$ and covariance estimate $\underline{\Sigma}(i)$. The control action u(i+1) is then used to predict the state vector $\tilde{\underline{x}}(i+1)$ and the covariance $\tilde{\underline{\Sigma}}(i+1)$:

$$\tilde{\underline{x}}(i+1) = \underline{G}(\hat{\underline{x}}(i), u(i+1), \underline{0}) = \underline{A}(i)\hat{\underline{x}}(i) \qquad (4.32a)$$

$$\tilde{\underline{\Sigma}}(i+1) = \underline{A}(i)\underline{\Sigma}(i)\underline{A}^T(i) + \underline{\xi} \qquad (4.32b)$$

where $\underline{A}(i)$ is the transition matrix which is computed in chapter 5.

Propagation of the information between each measurement is made in terms of the approximated two-dimensional Normal prior distribution of equation 4.26. The scaling of μ_x and μ_z propagates the information and the prior distribution is calculated from the predicted states x_1 and z. the prior statistics of x_1 are:

$$\tilde{m}_x(i+1) = \tilde{x}_1(i+1) = g_1(\hat{\underline{x}}(i), u(i+1), \underline{0}) \qquad (4.33a)$$

$$\tilde{v}_x(i+1) = \tilde{\sigma}_{11}(i+1) \qquad (4.33b)$$

$$\tilde{s}_x(i+1) = \sqrt{\tilde{v}_x(i+1)} \qquad (4.33c)$$

where $\tilde{x}_1$ and $\tilde{\sigma}_{11}$ are the appropriate terms of the prediction $\tilde{\underline{x}}$ and $\tilde{\underline{\Sigma}}$, and $g_1(\hat{\underline{x}}(i), u(i+1), \underline{0})$ is defined by:

$$g_1(\hat{\underline{x}}(i), u(i+1), \underline{0}) = \sum A_{1,j}(i)\hat{x}_j(i) \qquad j = 1,2,\ldots n \qquad (4.34)$$

where n is the dimension of the square matrix $\underline{A}$.

The prediction of the bias z may take one of two forms depending whether z is constant or slowly varying:

for constant z:

$$\tilde{m}_z(i+1) = m_z(i) \qquad (4.35a)$$

$$\tilde{v}_z(i+1) = v_z(i) \qquad (4.35b)$$

for slowly varying z:

$$\tilde{m}_z(i+1) = g_z m_z(i) + \alpha_z \qquad (4.36a)$$

$$\tilde{v}_z(i+1) = g_z^2 v_z(i) + \xi_z \qquad (4.36b)$$

for constant and slowly varying z:

$$\tilde{s}_z(i+1) = \sqrt{\tilde{v}_z(i+1)} \qquad (4.37)$$

The propagation of the correlation coefficient $\tilde{r}$ accounts for the correlation between the prediction $\tilde{m}_x$ and $\tilde{m}_z$. From equation 4.27

$$\tilde{r}(i+1) = g_1 g_z \, E[(x_1 - m_x)(z - m_z)]/\tilde{s}_x \tilde{s}_z \qquad (4.38)$$

Substituting for the covariance term $E[(x_1 - m_x)(z - m_z)]$ from equation 4.31f, we have:

$$\tilde{r}(i+1) = g_1 g_z \, r(i) \, s_x s_z / \tilde{s}_x \tilde{s}_z \qquad (4.39)$$

Figure 4.12 shows the resulting prior Normal distribution using the statistics of the conditional distribution of figure 4.11. It can be seen that the approximation is reasonable even though figure 4.11 results from intersecting two such non-Normal distribution of figure 4.9a and 4.10; this may be attributed to the central limit theorem.

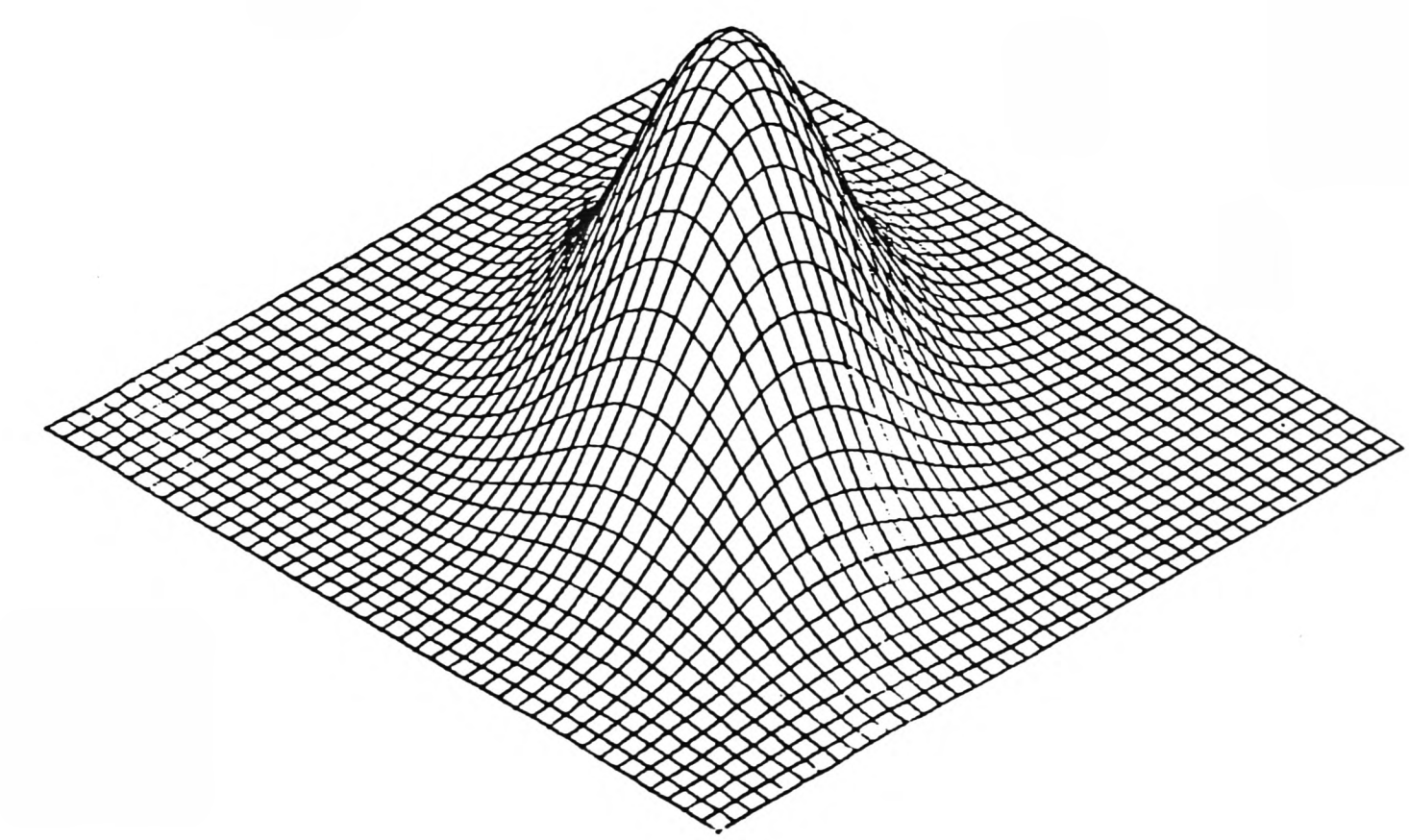


Fig 4.12 Normal approximation to the conditional distribution of fig 4.11

4.4.3 Tests For Bias Observability

The two tests for the estimation of random jumping bias introduced earlier are discussed here. The first, for jump detection, is based on the size of the innovation sequence of the estimator; the second is for the detection of conditions of poor observability when the bias is constant. It is associated with the alignement of the ridge of the two-dimensional likelihood function of figure 4.10 with an axis of the two-dimensional Normal prior distribution of equation 4.26. Both tests are unnecessary when the bias is varying slowly: no jump detection is required and the ridge of the likelihood function changes enough as to ensure that its alignement with an axis with the prior distribution does not occur. The effluent pH is sufficiently excited because of the additive variable bias (equation 3.46b) making the effluent i.c.d. and the bias observable simultaneously.

After a measurement y(i) is taken, the two tests are made only if jumps in the bias are expected. The jumping bias test is made to determine whether the bias z(i) appears to have jumped. The test (Mehra and Peschon 1971) is based on a diagnostic d in the form of normalised prediction error of y(i):

$$d(i) = (y(i) - \tilde{y}(i))/\sqrt{\tilde{v}(i)} \qquad (4.40)$$

where $\tilde{y}(i)$ and $\tilde{v}(i)$ are the predicted mean and variance of the measurement y(i). they are computed from the pH non-linearity using the a priori Normal distribution $p(x_1, z)$:

$$\tilde{y}(i) = \tilde{m}_{pH}(i) + \tilde{m}_z(i) \qquad (4.41a)$$

$$\tilde{v}(i) = \tilde{v}_{pH}(i) + \tilde{v}_z(i) + v_\eta \qquad (4.41b)$$

where $\tilde{m}_{pH}$ & $\tilde{v}_{pH}$ are the pH prediction and $\tilde{m}_z$ & $\tilde{v}_z$ are the prediction of

the bias z (equations 4.35) and v_η is the variance measurement noise η. The statistics of the pH prediction are calculated from the prior marginal distribution of x_1 ($p(x_1) = N(\tilde{m}_x;\tilde{v}_x)$):

$$\tilde{m}_{pH} = \int_{x_1} pH(x_1)p(x_1)dx_1 \qquad (4.42a)$$

$$\tilde{v}_{pH} = \int_{x_1} (pH(x_1) - \tilde{m}_{pH})^2 p(x_1)dx_1 \qquad (4.42b)$$

The test is whether the absolute magnitude of the sum of d exceeds a threshold value D:

$$\left| \sum d(i) \right| > D \qquad (4.43)$$

If the result of the test is positive, the prior distribution for Bayes' rule $p(x_1,z)$ is reinitialised to the prismatic shape of figure 4.9a and $\sum d(i)$ is reset to zero. If the test indicates no jump, the Normal prior distribution $p(x_1,z)$ is retained and used for Bayes' rule in equation 4.29. A typical useful value for D was found to be four.

The second test was devised to detect conditions of poor observability which were found to lead to numerical problems. They are associated with alignement of the ridge of the two-dimensional likelihood distribution $p(y|x_1,z)$ with an axis of the two-dimensional Normal prior distribution $p(x_1,z)$. According to Bayes' rule, the intersection of the two distributions yields new information about the sum $pH(x_1) + z$. It cannot be used to estimate both x_1 and z separately if the two distributions are aligned. The unobservability is because the measurement y is not always linearly independent in x_1 and z. The question the observability test tries to answer is whether there is a useful intersection between $p(x_1,z)$ and $p(y|x_1,z)$.

The test is based on the alignement between the likelihood ridge and possible shapes of the contours of the standardised distribution $p(x_1,z)$ of equation 4.26. These shapes are ellipses (figure 4.13) characterised by axes having slopes ± 1 and lengths in a ratio which depends on the correlation coefficient $\tilde{r}$. When the absolute magnitude of $\tilde{r}$ is less than some threshold T ($0 < T < 1$), the contours are so nearly circular and the prior distribution is so well spread on the grid that its intersection with the likelihood will lead to new useful information about x_1 and z; hence, there is no need to test further for observability. Otherwise ($|r| > T$) the test continues by determining the orientation of the ridge of the likelihood function in terms of the normalised variables μ_x and μ_z. Considering the likelihood ridge on the x_1 and z plane, we have:

$$z = y - pH(x_1) \qquad (4.44)$$

which can be mapped (as shown in figure 4.14a) onto the standardised grid by substituting for x_1 and z from equations 4.24:

$$\mu_z = (y - pH(\tilde{s}_x\mu_x + \tilde{m}_x) - \tilde{m}_z)/\tilde{s}_z \qquad (4.45)$$

The ridge can be approximated as in figure 4.14b by a straight line using a numerical least square fit :

$$\mu_z = a\mu_x + b \qquad (4.46)$$

The fitting parameter a is taken to indicate the slope of this ridge. The condition for non-alignement is that the magnitude of a be not close to the slope (unity) of the axes of $p(x_1,z)$. This is tested with respect to a threshold magnitude A in the form of an inequality:

$$A^{-1} < |a| < A \qquad (4.47)$$

which indicates when linear dependence and the resulting numerical

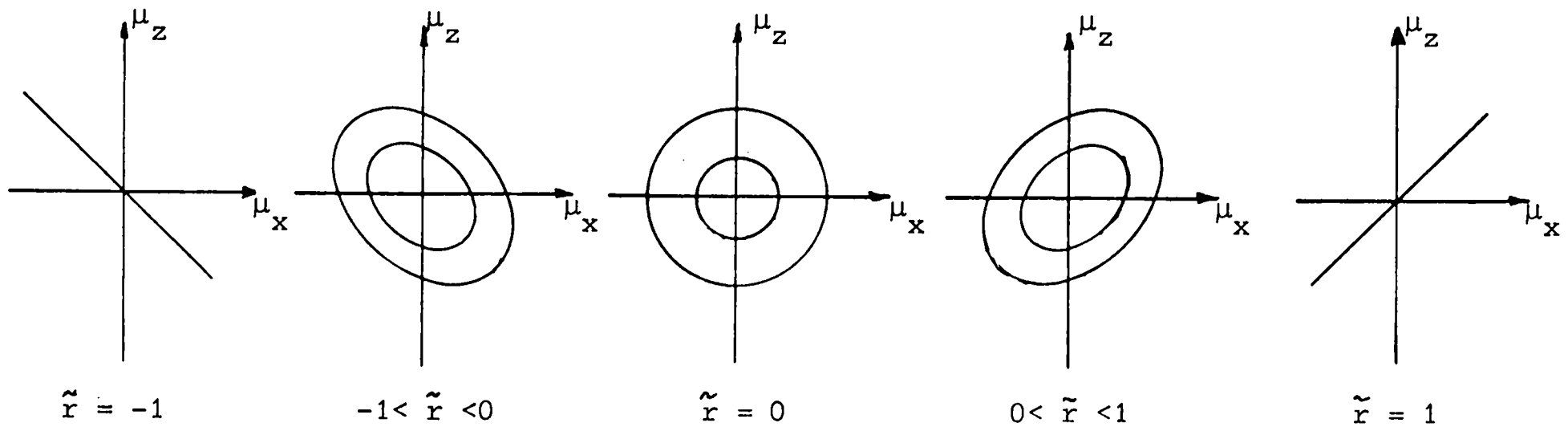


Fig 4.13 Contours of the standardised Normal distribution $p(x_1, z)$

problems are to be anticipated. A typical value of A was found to be two.

The numerical implementation of the above test represents only a small increase in the computational load for recursive estimation. It is performed after every measurement except those where the first test has already indicated a jump in bias z so that the prior distribution $p(x_1,z)$ has been reinitialised to the prismatic shape of figure 4.9a. When inequality 4.47 indicates that x_1 and z cannot both be estimated the algorithm reverts to one-dimensional estimation of x_1 only and assumes that the current estimate of z is valid. This is achieved as in section 4.2.3 but using a corrected measured value y_c of bias-free pH:

$$y_c(i) = y(i) - \tilde{m}_z(i) \qquad (4.48)$$

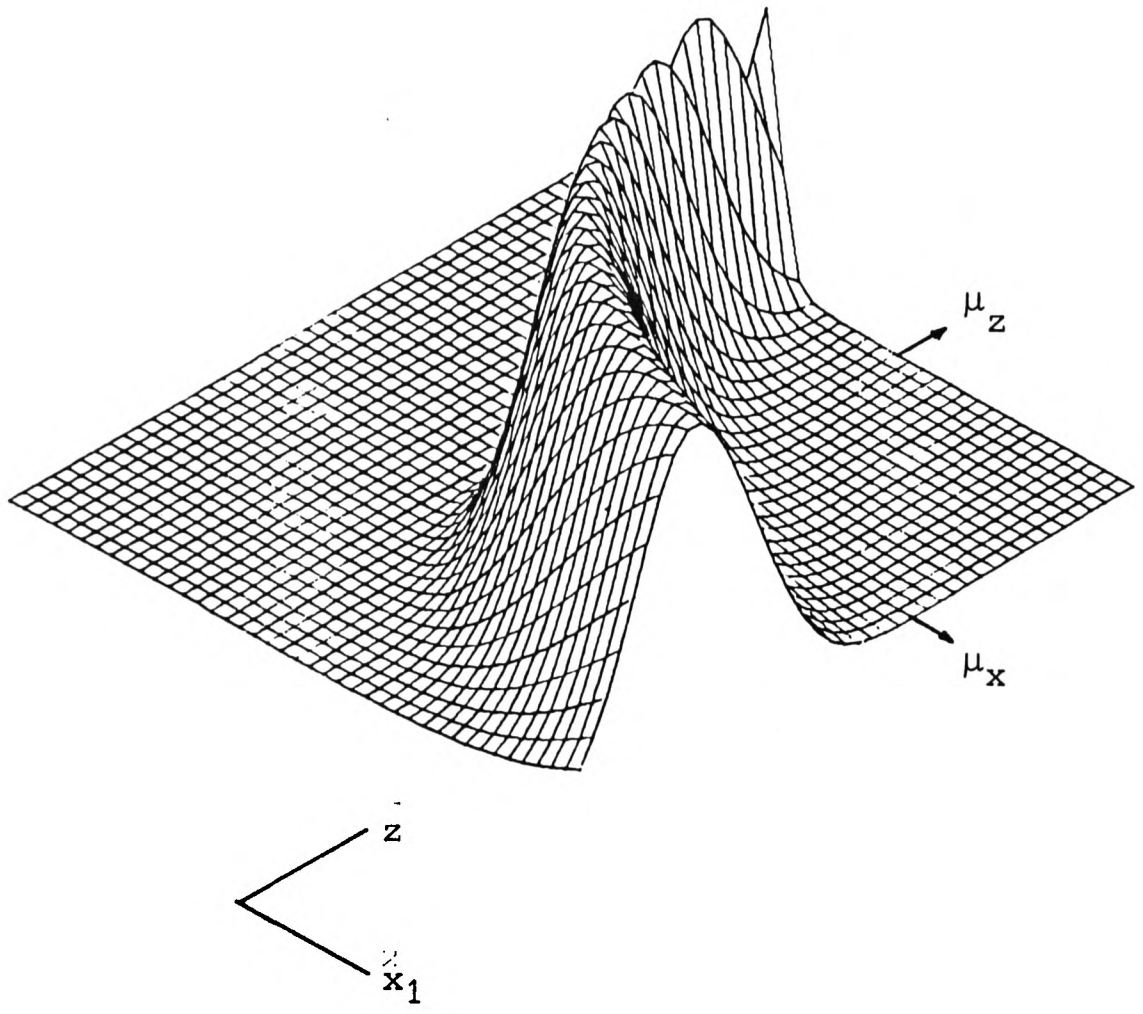
with assumed noise variance:

$$v_{\eta c}(i) = v_\eta + \tilde{v}_z(i) \qquad (4.49)$$

to account for current prior information about the bias z. The resulting one-dimensional conditional distribution for x_1 can then be used for linearisation and prediction of x_1 to provide new prior statistics $\tilde{m}_x$ and $\tilde{s}_x$ which can be combined with the old and unchanged $\tilde{m}_z$, $\tilde{s}_z$ and $\tilde{r}$ to give a new Normal two-dimensional prior distribution according to equation 4.26.

4.4.4 Summary And Results Of The Bias Estimator

The two-dimensional Bayes' algorithm for bias estimation is summarised as follows:



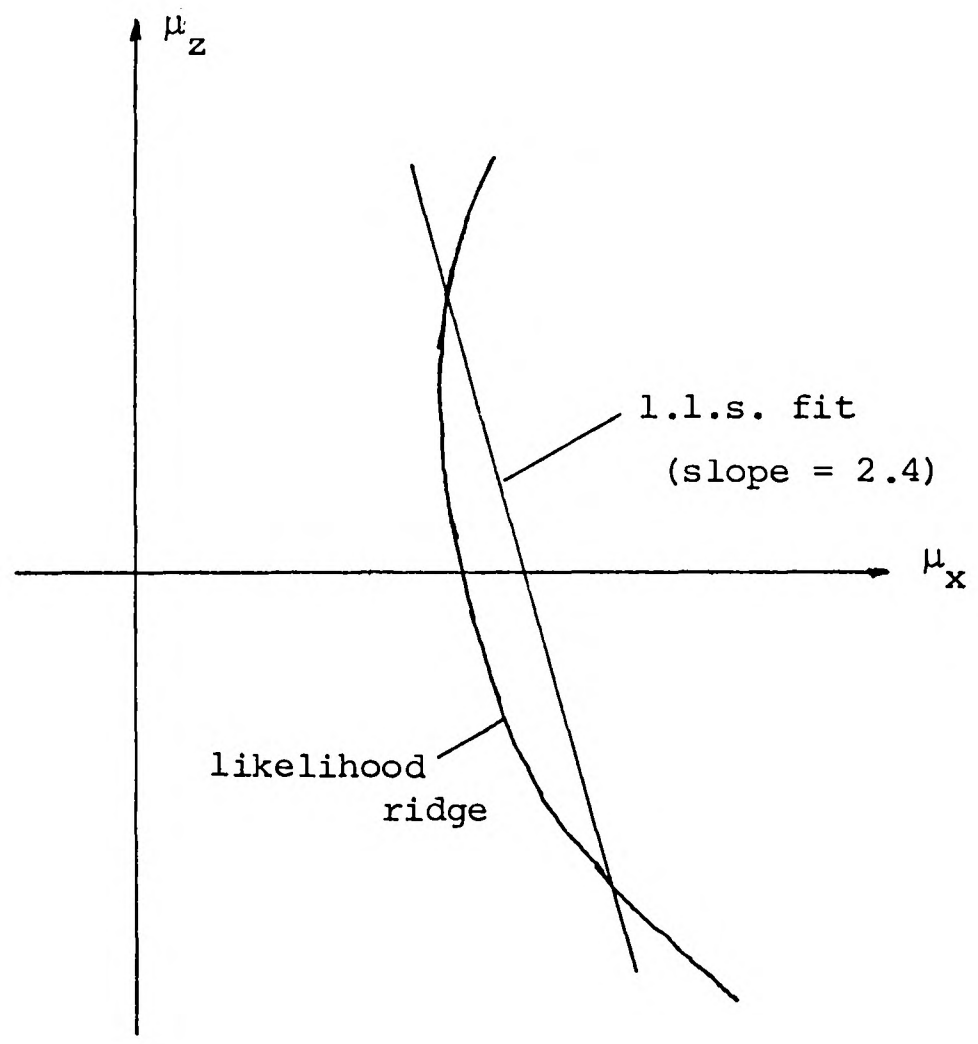


Fig 4.14 Alignement test of the likelihood ridge

1. Given a two-dimensional prior Normal distribution $p(x_1,z)$ at time i (equation 4.26) specified by the five sufficient statistics: $\tilde{m}_x(i)$, $\tilde{m}_z(i)$, $\tilde{s}_x(i)$, $\tilde{s}_z(i)$, $\tilde{r}(i)$

2. measure y(i)

3. compute predicted mean $\tilde{y}(i)$ and variance $\tilde{v}(i)$ of y(i) (equations 4.41) and test the integral of the diagnostic d(i) (equation 4.40)

4. if $\left| \sum d(i) \right| > D$ then reinitialise $p(x_1,z)$ to a prismatic distribution (equation 4.25); GO TO 7

5. Compute the alignement a(i) of the likelihood ridge (equations 4.45, 4.46)

6. if $A^{-1} < |a| < A$ then use corrected measurement $y_c(i)$ & $v_{\eta c}(i)$ (equations 4.48, 4.49) to drive one-dimensional Bayes' estimator for x_1 (as in section 4.2.3). Compute two new conditional statistics: $m_x(i)$ & $v_x(i)$. Set

$$m_z(i) = \tilde{m}_z(i), \quad v_z(i) = \tilde{v}_z(i), \quad r(i) = \tilde{r}(i)$$

GO TO 8

7. Compute two-dimensional Bayes' estimator of x_1 and z with five new conditional statistics (equations 4.31): $m_x(i)$, $m_z(i)$, $s_x(i)$, $s_z(i)$, r(i)

8. $m_x(i)$, $m_z(i)$, $s_x(i)$, $s_z(i)$, r(i) are the estimators of $x_1(i)$ and z(i)

9. use $m_x(i)$ and $v_x(i)$ as in section 4.2.3 to compute the linearised pseudo-measurement $y'(i)$, $v'_\eta(i)$ which drives the estimation and prediction of the multi-state model:

$$\underline{x}(i+1) = \underline{G}(\underline{x}(i), u(i), \underline{\xi})$$

$$y'(i) = x_1(i) + \eta'$$

The predicted statistics are: $\tilde{m}_x(i+1)$, $\tilde{s}_x(i+1)$ for x_1 (equations 4.33); $\tilde{m}_z(i+1)$, $\tilde{s}_z(i+1)$ for z (equations 4.35, 4.36) and $\tilde{r}(i+1)$ for the correlation coefficient (equation 4.39).

10. i = i + 1, GO TO 1

In the case of slowly varying bias, the tests are not performed as explained earlier and steps 4, 5 & 6 of the algorithm are not activated.

The bias estimation algorithm coupled to an EKF has been implemented and tested in the CAD simulation package which simulates the multi-state model of chapter 3 (section 3.4). The estimator results shown here (figures 4.15 to 4.22) are for jumping and for slowly varying bias (= 1 pH unit) for two setpoints (pH 8.5 & 12) and for two measurement noise standard deviations (s_η = 0.1, 0.2 pH units). The parameter of the drifting bias of equation 3.42 are: g_z = 0.999, α_z = 0. In all the figures, time-histories of the bias z(i), its estimate $m_z(i)$ and the standard deviation of its estimate $s_z(i)$ are superimposed on one pair of axes. Additionally, time-histories of the diagnostic d(i) which tests whether the bias has jumped, and the alignement parameter a(i) are shown for the jumping bias (figures 4.15 to 4.18).

It can be seen that the estimation of the bias has had different degrees of success. When the bias jumps, the estimate is good if the measurement noise is small (s_η = 0.1) and the setpoint is pH 8.5, (figure 4.15); the diagnostic shows clearly when the bias jumps, and the

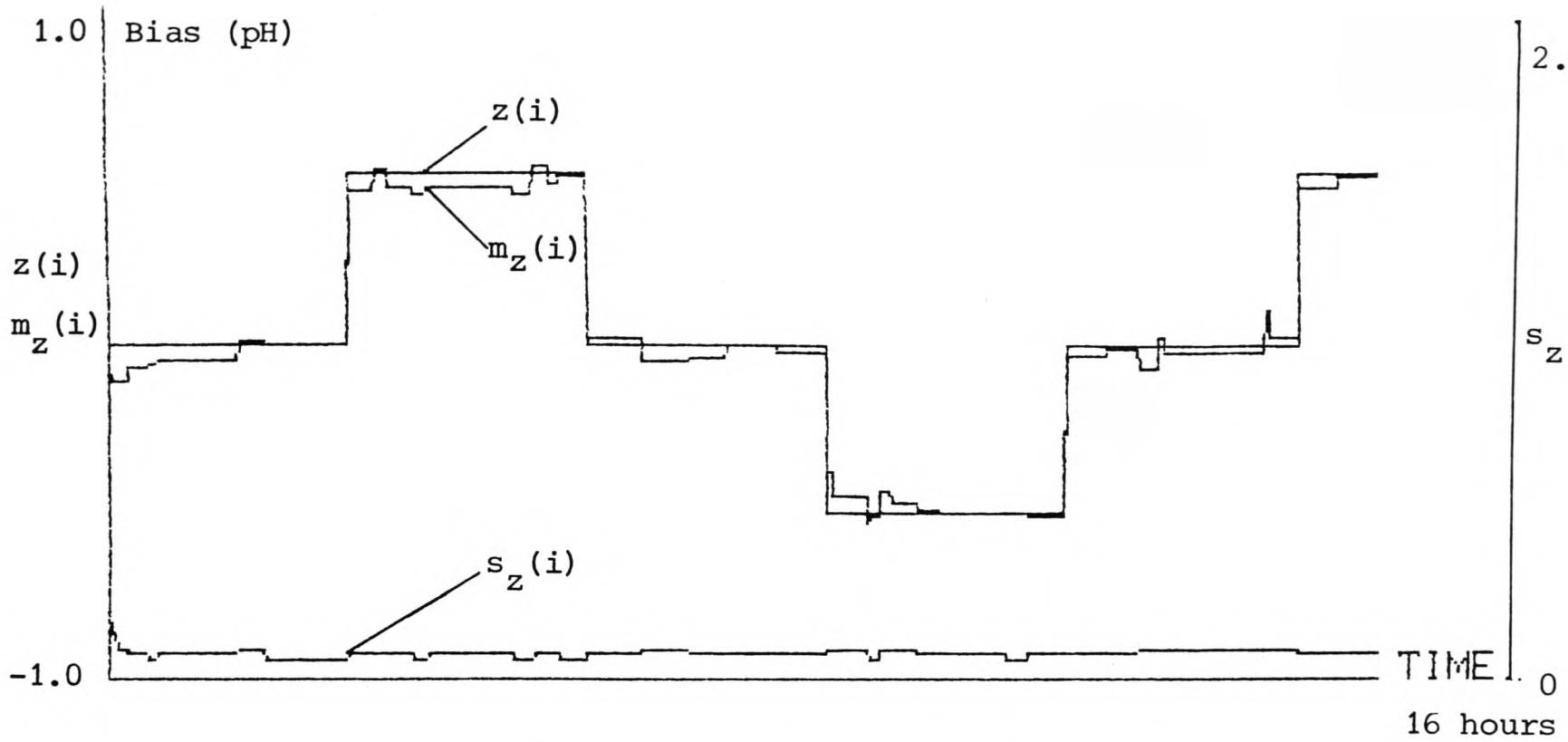
alignement test shows only a few two-dimensional estimations. For $s_\eta = 0.2$, figure 4.16, there is no significant deterioration in the estimation except for additional spikes in the estimate which lead to more two-dimensional estimation. The estimator is not so successful at a setpoint of pH 12 (figure 4.17, 4.18). Nonethless, the estimate m_z differs from the simulated bias z by an error $z - m_z$ which is within two standard deviations s_z of the estimate. The less succesful estimation may be due to the fact that at the far end of the pH non-linearity any small additional bias affects significantly the ionic concentration difference x_1 causing the variance of the pseudo-measurement noise to be large which in its turn disrupt the EKF. For the varying bias z(i), shown in figures 4.19 to 4.22, the estimate $m_z(i)$ follows closely the simulated value for the different setpoints and measurement noise with $s_z(i)$ showing the confidence in the estimate.

In section 4.4, a novel bias estimator has succesfully estimated constant or jumping bias and slowly varying bias on the pH measurement. It is based on the Linearised Estimator described in section 4.3 and uses two observabilty tests to improve the estimation of constant bias.

4.5 CONCLUSION

It has been demonstrated that Bayes' rule can contribute to better estimation for a particular non-linear system: the pH measurement. The estimator algorithm has shown to be robust in simulation; analysis to guarantee convergence of the algorithm could provide a theme for further research as will be discussed in chapter 9. A one-dimensional Bayes' rule has been implemented numerically for state estimation through the pH non-linearity and the resulting conditional statistics are "linearised" to drive an Extended Kalman Filter whose use is investigated in the next

chapter. The algorithm has been extended to a two-dimensional estimator which successfully estimated jumping and slowly varying bias on the pH measurement.



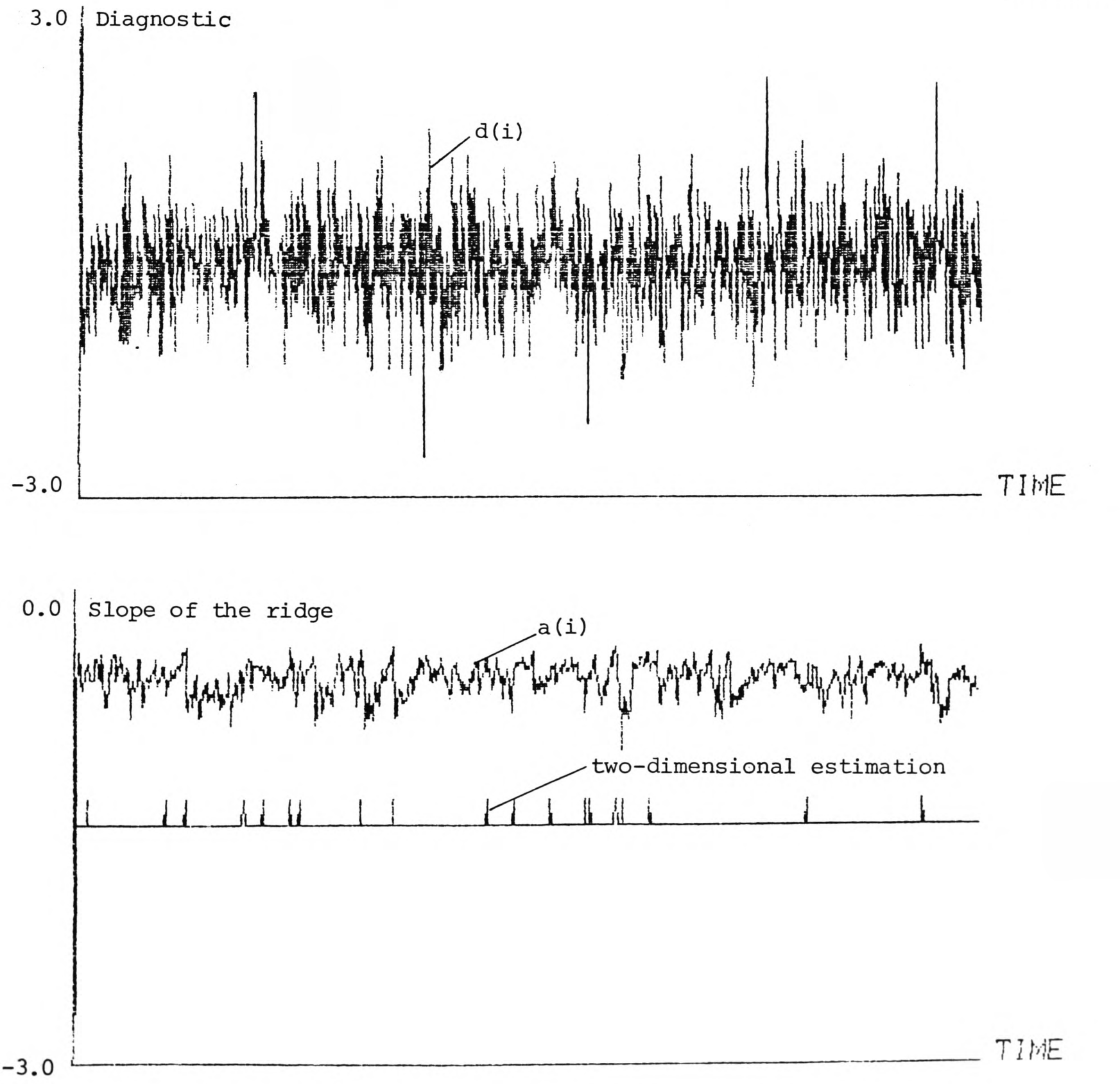


Fig 4.15 Bias estimation: jumping bias, setpoint=pH 8.5, s_η=0.1 pH units

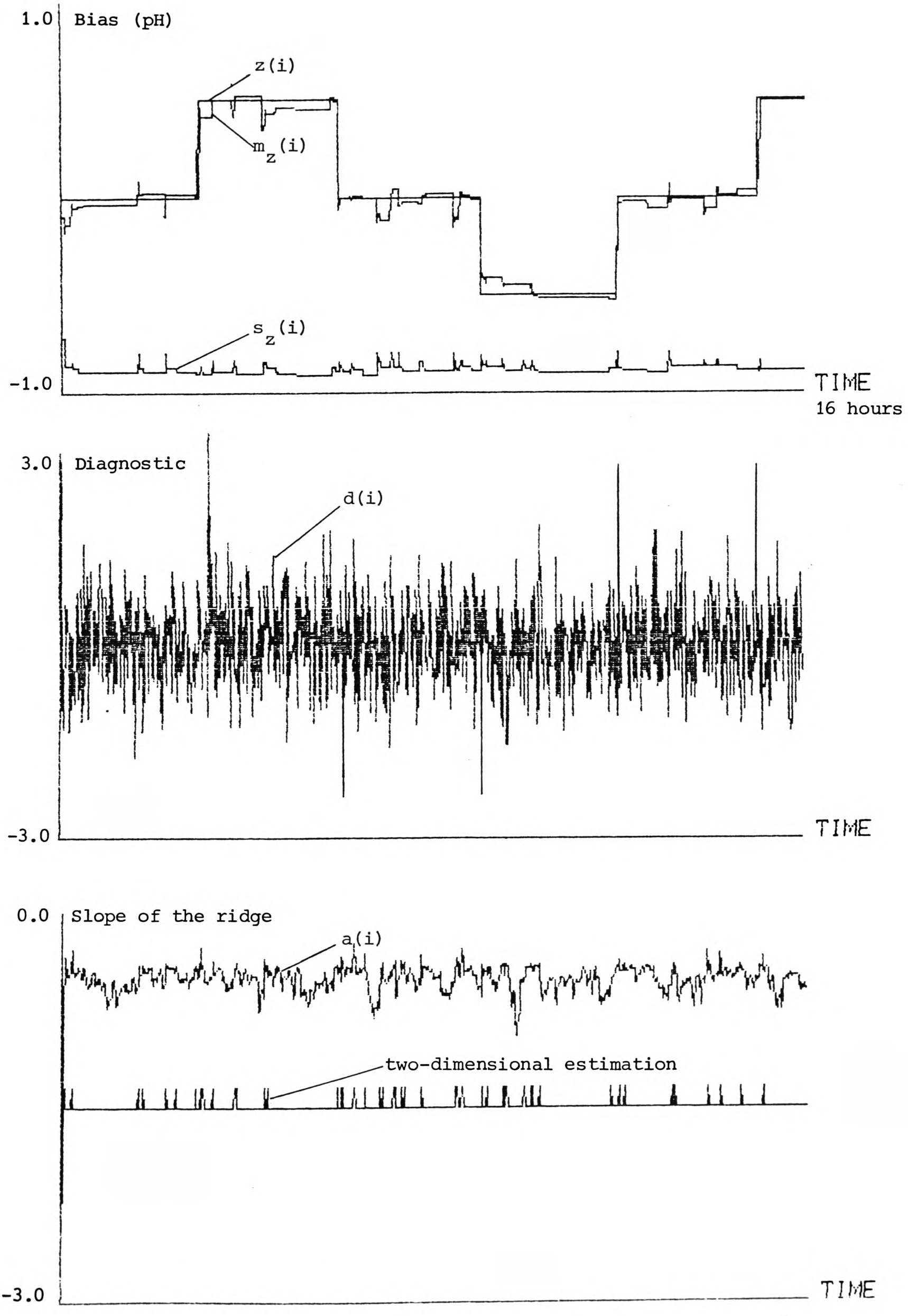


Fig 4.16 Bias estimation: jumping bias, setpoint=pH 8.5, s_η=0.2 pH units

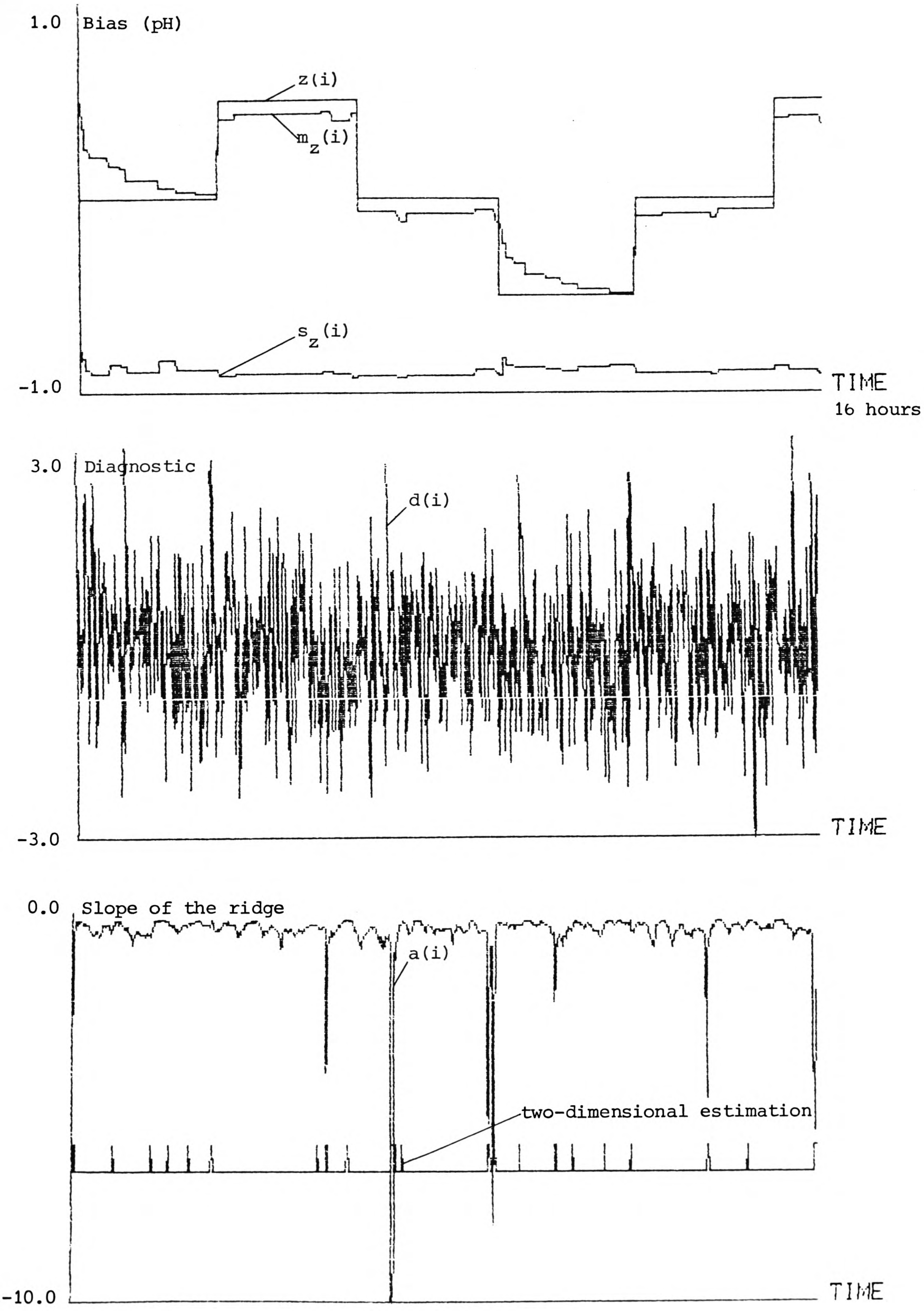


Fig 4.17 Bias estimation: jumping bias, setpoint=pH 12.0, s_η= 0.1 pH units

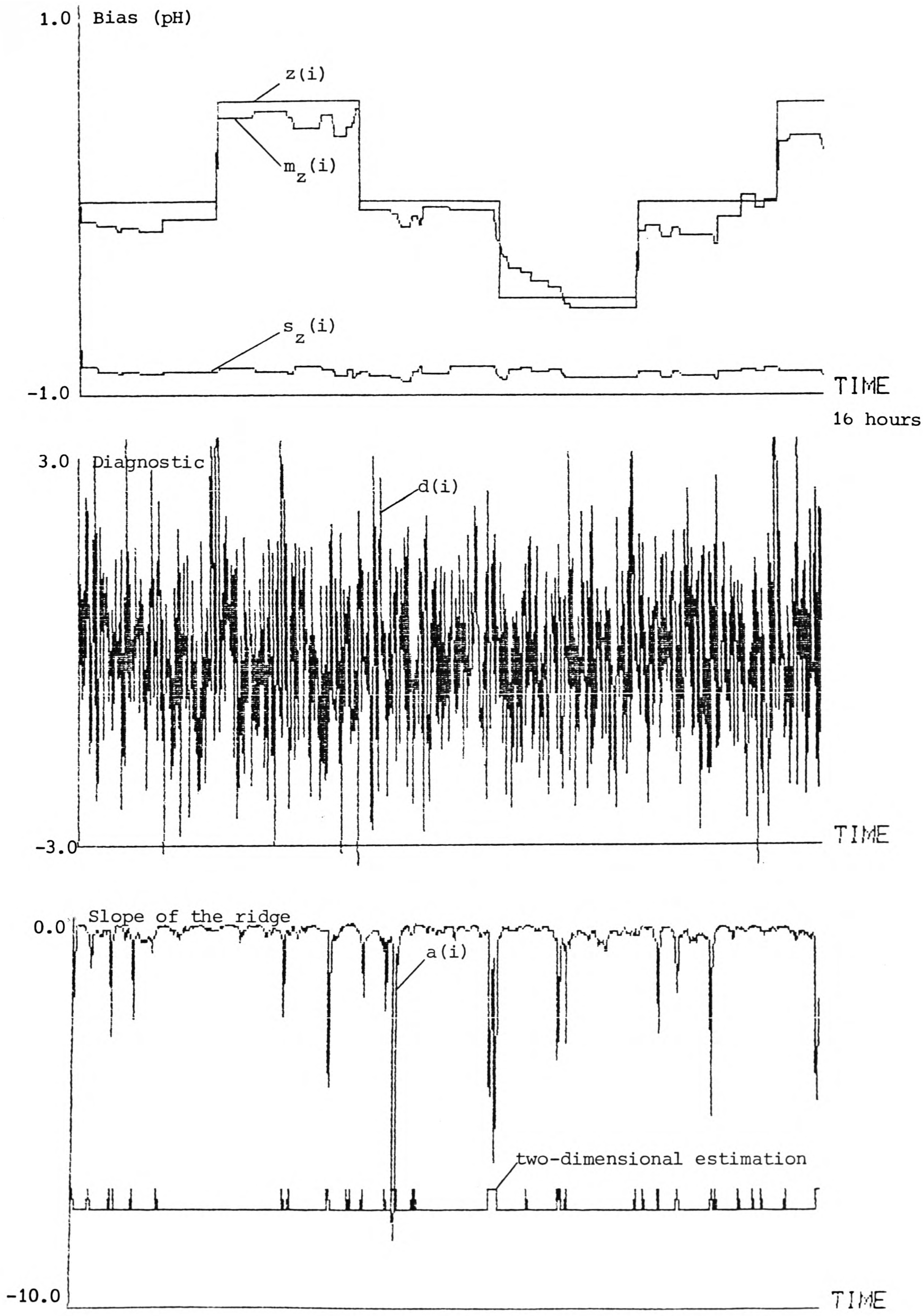


Fig 4.18 Bias estimation: jumping bias, setpoint=pH 12.0, s_η = 0.2 pH units

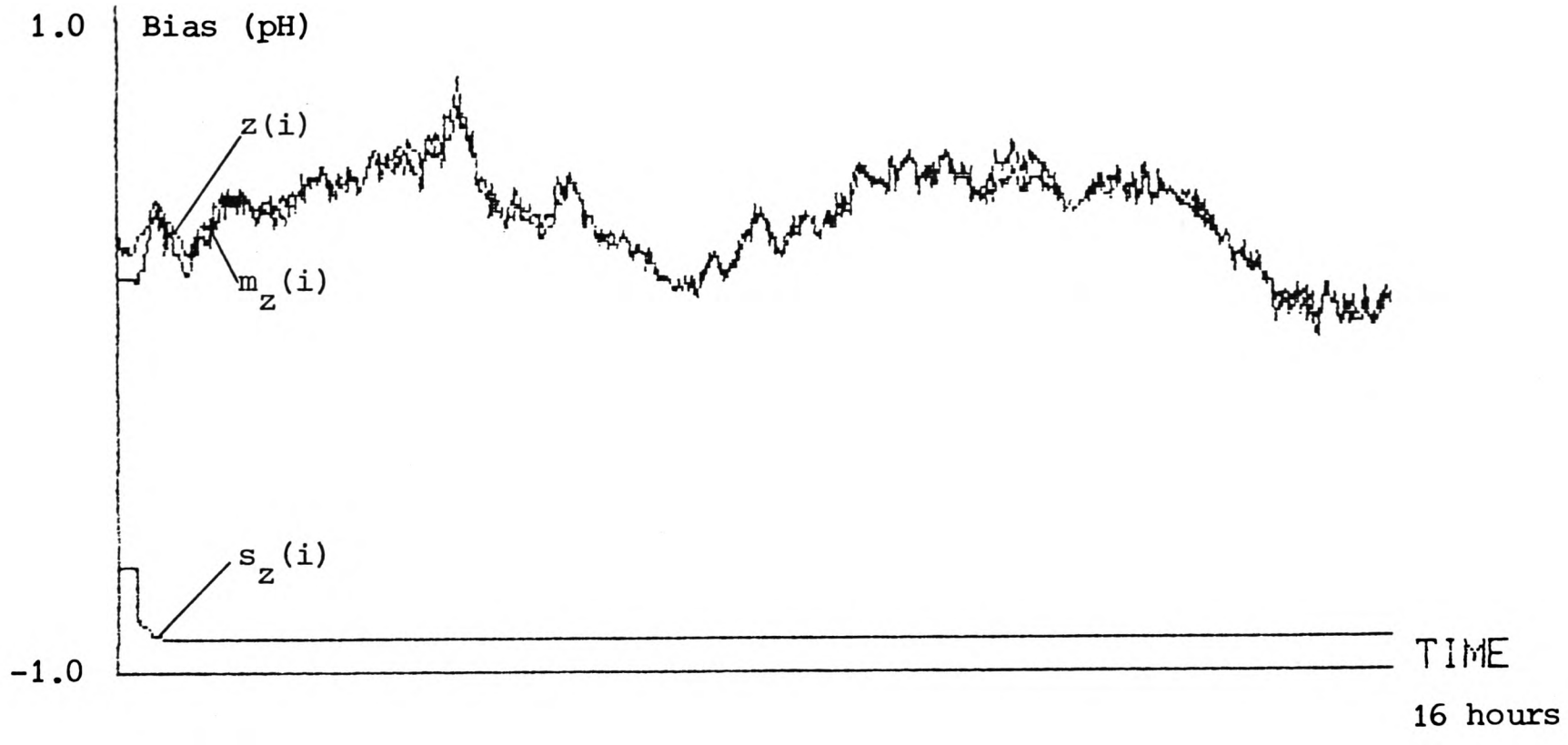


Fig 4.19 Bias estimation: variable bias, setpoint= pH 8.5, s_η= 0.1 pH units

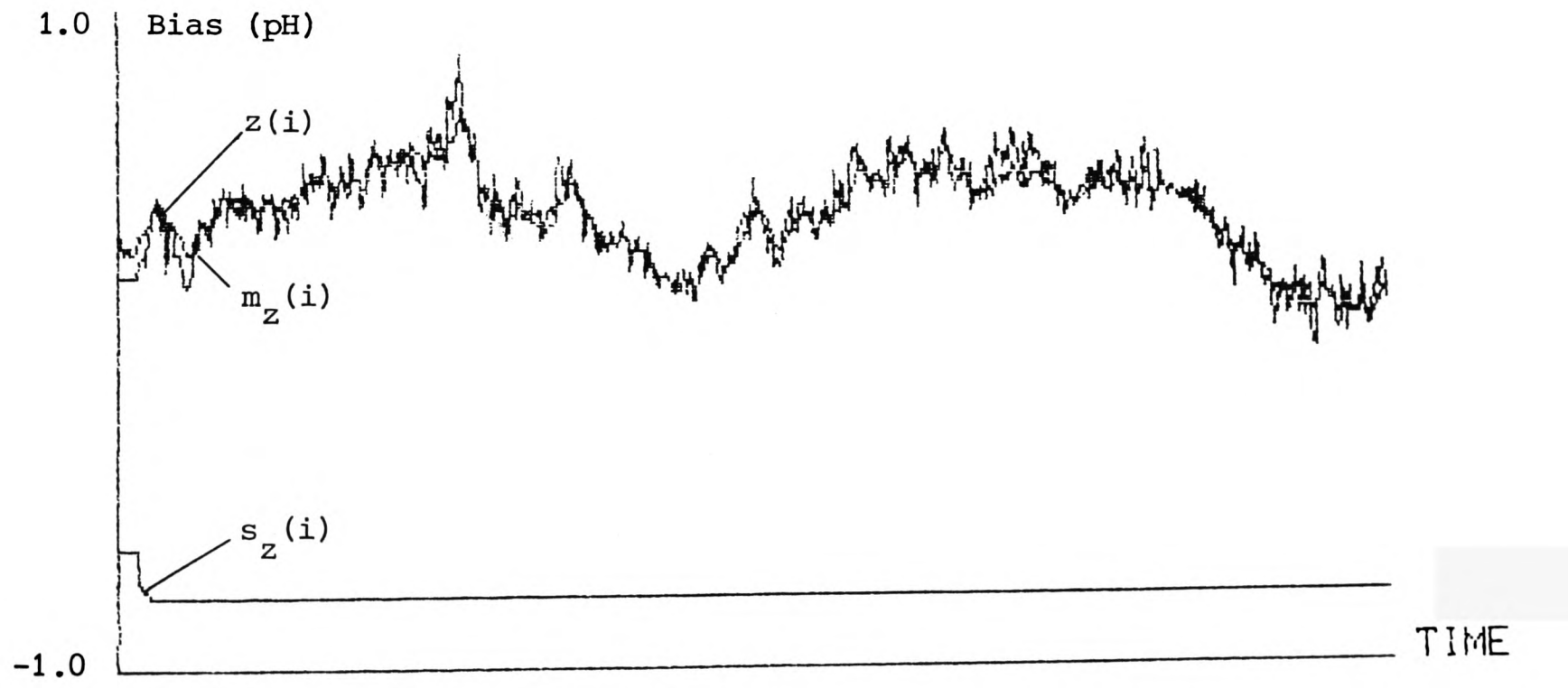


Fig 4.20 Bias estimation: variable bias, setpoint= pH 8.5, s_η= 0.2 pH units

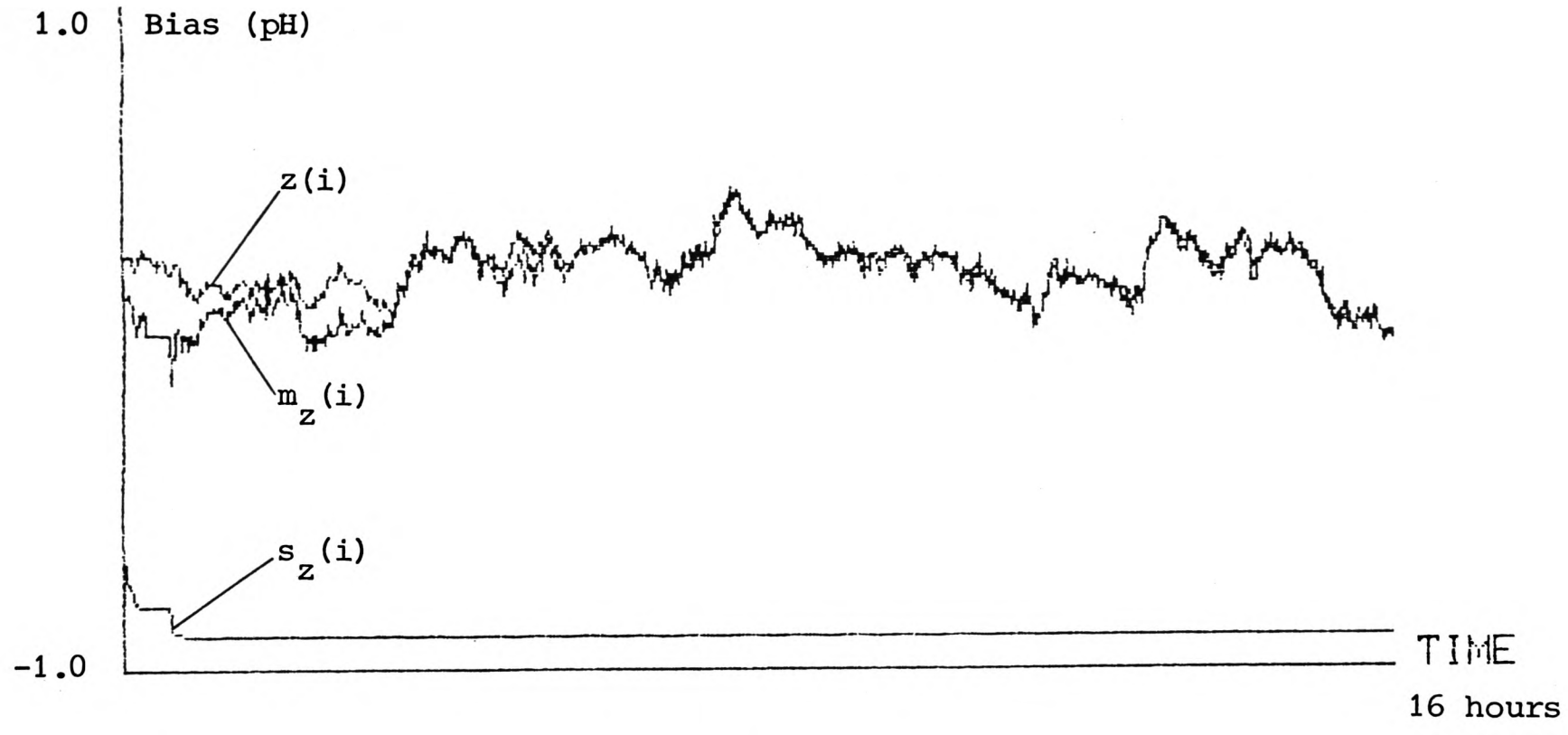


Fig 4.21 Bias estimation: variable bias, setpoint=pH 12.0, s_η=0.1 pH units



Fig 4.22 Bias estimation: variable bias, setpoint=pH 12.0, s_η=0.2 pH units

CHAPTER 5

STATE ESTIMATION OF THE pH MODEL

In this chapter, an Extended Kalman Filter (EKF) (Jazwinski 1970) is developed for the non-linear state estimation of pH regulation. The EKF employs the pre-specified state space model of pH regulation in a CSTR, which was derived in chapter 3, to implement a prediction/correction estimation scheme. The EKF is driven, not by the non-linear effluent pH measurement, but by a linearised pseudo-measurement of the effluent i.c.d. which is generated by the non-linear estimator of chapter 4.

The main feature of the state space model of chapter 3 is the separation of the chemical analysis of the neutralisation reaction from the tank dynamics and from the pH measurement. The CSTR model consists of three essential states: the i.c.d. of the regulated effluent pH and the flow and the i.c.d. of the influent disturbances. From the previous chapter, Bayes' rule and the Linearisation Estimator provides a pseudo-linear measurement which replaces the non-linear pH measurement and drives the state estimation filter. The neutralisation reaction for buffered reagents and the tank dynamics are non-linear elements of the model as was indicated in section 3.4.4. Therefore, an EKF which accounts for non-linear systems was used instead of a conventional linear Kalman Filter. The EKF produces estimates of the three states which may

provide feedforward information of the disturbances or may be used to drive stochastic control laws. Good estimates are conditional on the knowledge of the titration curve of the neutralisation process and on a bias-free pH measurement. These conditions are usually met in production processes using pH regulation (as discussed in chapter 1), but not in effluent treatment when estimates are often innacurate.

As discussed in section 3.4.2, because of probe fouling and poor calibration, the pH measurement may be subject to biases. When using the model-based EKF estimator, a biased measurement will affect the state prediction and will give poor estimation results unless the bias is accounted for. But section 4.4 has shown that even assuming a known titration curve, which is done here, it is not possible to estimate simultaneously the bias and the load disturbances. Therfore, in the development of the EKF equations, the measurement is assumed to be bias-free. Simulation results are used in section 5.5 to discuss this assumption.

This chapter and the next one attempt to answer the following questions:

1. Is the state-space model of chapter 3 completely observable for the EKF to estimate all the states?

2. How robust is the estimator to parametric changes in the model?

3. Can the EKF produce acceptable estimates of the disturbances which may be changing slowly or in a stepwise fashion?

4. Can the estimate be used to improve pH control in simulation prior to a full-scale application?

5. Can the extra cost in producing the state-space model, the EKF equations and the complex control laws be justified by improved performances?

In order to answer these questions, the EKF equations are developed in section 5.2 for the state space pH model of chapter 3 for strong and weak reagents. Observability of the pH model and construction of its observability matrix based on linear system theory are presented in section 5.3. Modelling errors to test the estimator robustness and to account for changes in the model parameters are computed and included in the EKF estimator in section 5.4. Section 5.5. discusses the performance of the estimator for three simulated processes, and compares results of the estimator with those of a full industrial application (Proudfoot 1983). Answers to the above questions one, two and three are summarised in the conclusion. Questions four and five, which relate to the controller performances, are answered in chapter 6.

5.1 INTRODUCTION

The Kalman Filter (Kalman & Bucy 1961) or the Extended Kalman Filter (Jazwinski 1970) uses a state space representation of a process model together with prior information about the process uncertainty to produce estimates of measured and unmeasured states and a measure of confidence in those states. The estimates can then be used as inputs to a classical or a stochastic controller.

Kalman filtering techniques were developed in the last twenty-five years as a result of research in the defence and aerospace industries. It is only recently that these techniques have been applied to process control with the vast majority of applications carried out in simulation

and on pilot plants. This is probably due to the complicated dynamic behaviour of the processes as well as their conservative management. Some of the reported applications include ship positionning (Balchen et al 1976), steel making (Solman et al 1974), kiln control (Dumont & Belanger 1978), and boiler control (Wallace & Clarke 1983).

Kalman filters have been applied to pH regulation in full-scale industrial processes by Jacobs et al (1980) and by Jutila (1983) as discussed in the survey of chapter 2. The Extended Kalman Filter developed in this chapter is for the neutralization of both strong and weak reagents of the general pH model derived in chapter 3; it was tested in simulation prior to it being used by Proudfoot (1983), as part of the current research, on an industrial scale for a buffered neutralization process. He uses the EKF for the estimation of influent disturbances of flow and concentration which are modelled by equations 3.46; the EKF is driven not by the Linearised estimator of chapter 4 but by an analytical inversion of the pH measurement. The estimates provide pseudo-feedforward measurements which are used to improve control. The quality of the estimation and the improvement to pH control are investigated in section 5.5.

5.2 DEVELOPMENT OF THE EKF EQUATIONS

In this section, an Extended Kalman Filter (EKF) is developed from the mathematical model of the pH system of chapter 3. The model which includes the chemistry of titration curves, the tank dynamics and the bias-free pH measurement is represented by equations 3.46:

$$x_1(i+k+1) = x_1(i+k) + \frac{\Delta}{V} x_2(i)(X_{in}(i) - x_1(i+k)) + \xi_1$$

$$x_j(i+1) = g_j x_j(i) + \alpha_j + \xi_j \qquad j=2,3$$

$$x_4(i+1) = x_1(i+k)$$

$$x_5(i+1) = x_1(i+k-1) \qquad (3.46)$$

.

.

$$x_{k+3}(i+1) = x_1(i+1)$$

$$y(i) = pH(x_1(i)) + \eta$$

where X_{in} accounts for the chemistry of strong and weak reagents.

Equations 3.46 can be summarised by:

$$\underline{x}(i+1) = G_1(\underline{x}(i),\underline{u}(i),\underline{\xi}(i),i) \qquad (3.29a)$$

$$\underline{y}(i) = G_2(\underline{x}(i),\underline{\eta}(i),i) \qquad (3.29b)$$

where $\underline{\xi}$ and $\underline{\eta}$ are assumed to be vectors of independent Normal random variables having zero-mean and covariance matrices $\underline{\Sigma}_1$ and $\underline{\Sigma}_2$ respectively so that $p(\underline{\xi}) = N(\underline{0},\underline{\Sigma}_1)$ and $p(\underline{\eta}) = N(\underline{0},\underline{\Sigma}_2)$.

The EKF equations for the model of equations 3.29 are given by Jacobs (1974). The state estimation update is:

$$\hat{\underline{x}}(i) = \tilde{\underline{x}}(i) + \underline{K}(i)(\underline{y}(i) - G_2(\tilde{\underline{x}}(i),\underline{0},i)) \qquad (5.1)$$

where the state prediction equals:

$$\tilde{\underline{x}}(i) = G_1(\hat{\underline{x}}(i-1),\underline{u}(i-1),\underline{0},i-1) \qquad (5.2)$$

and the gain matrix is given by:

$$\underline{K}(i) = \underline{\Sigma}(i)\underline{C}^T(\underline{B}_2\underline{\Sigma}_2\underline{B}_2^T)^{-1} \qquad (5.3)$$

The covariance matrix update is:

$$\underline{\Sigma}(i) = \tilde{\underline{\Sigma}}(i) - \tilde{\underline{\Sigma}}(i)\underline{C}^T(\underline{B}_2\underline{\Sigma}_2\underline{B}_2^T + \underline{C}\,\tilde{\underline{\Sigma}}(i)\underline{C}^T)^{-1}\,\underline{C}\,\tilde{\underline{\Sigma}}(i) \qquad (5.4)$$

where the covariance prediction equals:

$$\tilde{\underline{\Sigma}} = \underline{B}_1\underline{\Sigma}_1\underline{B}_1^T + \underline{A}\,\underline{\Sigma}(i-1)\,\underline{A}^T \qquad (5.5)$$

Elements of $\underline{A}$, $\underline{B}_1$, $\underline{B}_2$ and $\underline{C}$ are given by:

$$a_{j1} = \delta g_{1,j}/\delta x_1 \qquad (5.6)$$

$$b_{1,j1} = \delta g_{1,j}/\delta \xi_1 \qquad (5.7)$$

$$b_{2,j1} = \delta g_{2,j}/\delta \eta_1 \qquad (5.8)$$

$$c_{j1} = \delta g_{2,j}/\delta x_1 \qquad (5.9)$$

The partial derivatives are evaluated at $(\hat{\underline{x}}(i-1),\underline{u}(i-1),\underline{0},i-1)$ for G_1 and at $(\tilde{\underline{x}}(i),\underline{0},i)$ for G_2.

The state vector $\underline{x}(i)$ of the state-space model of equations 3.46 and its corresponding state estimate vector $\hat{\underline{x}}(i)$ are given by:

$$\underline{x}(i) = \begin{bmatrix} x_1(i+k) \\ x_2(i) \\ x_3(i) \\ x_4(i) \\ x_5(i) \\ \\ x_{k+3}(i) \end{bmatrix} \qquad \hat{\underline{x}}(i) = \begin{bmatrix} m_1(i) \\ m_2(i) \\ m_3(i) \\ m_4(i) \\ m_5(i) \\ \\ m_{k+3}(i) \end{bmatrix} \qquad (5.10)$$

In section 4.3, the Linearised Estimator reduces the non-linear effluent pH measurement y of equation 3.46 to a pseudo-linear measurement y' of effluent i.c.d. asssociated with a pseudo noise variance v'_η:

$$y'(i) = x_1(i) + \eta'(i) \qquad (4.21)$$

In case of small pH measurement noise η (standard deviation < 0.1 pH units) analytical inversion (Jacobs and Briggs 1984) of the pH measurement gives a good approximation which was used by Proudfoot (1983) in his application to the EKF.

From equations 3.46, G_1 (of equation 3.29a) is a non-linear function of X_{in} which is given by equations 3.30:

$$X_{in} = x_3 + uX_r/x_2 \qquad \text{for strong reagents} \qquad (3.30a)$$

$$X_{in} = f_1(f_1^{-1}(x_3) + uX_r/x_2) + \delta X \qquad \text{for weak reagents} \qquad (3.30b)$$

Therefore, the calculation of the elements of the $\underline{A}$ matrix from equation 5.6 is dependent upon the neutralization chemistry:

For strong reagents

$$\begin{aligned} a_{11} &= 1 - \frac{\Delta}{V} m_2 \\ a_{12} &= \frac{\Delta}{V}(m_3 - m_1) \\ a_{13} &= \frac{\Delta}{V} m_2 \end{aligned} \qquad (5.10)$$

For weak reagents

$$\begin{aligned} a_{11} &= 1 - \frac{\Delta}{V} m_2 \\ a_{12} &= \frac{\Delta}{V}(M_{in} - m_1 - f_2(R_{in})uX_r/m_2) \\ a_{13} &= \frac{\Delta}{V} m_2 f_2(R_{in}) f_2^{-1}(m_3) \end{aligned} \qquad (5.11)$$

where $M_{in} = f_1(f_1^{-1}(m_3) + uX_r/m_2)$

$R_{in} = f_1^{-1}(m_3) + uX_r/m_2$

$f_2(r) = df_1(r)/dr$

$f_2^{-1}(m) = df_1^{-1}(m)/dm$

For strong and weak reagents

$$a_{22} = g_2$$
$$a_{33} = g_3 \qquad (5.12)$$
$$a_{41} = a_{54} = a_{3+k,3+k-1} = 1$$

All the elements of $\underline{A}$ which have not been specified above (equations 5.10 to 5.12) are zero.

The system noise covariance matrix $\underline{\Sigma}_1$ is given by:

$$\underline{\Sigma}_1 = \begin{bmatrix} \text{var}(\xi_1) & 0 & 0 & 0 & . & 0 \\ 0 & \text{var}(\xi_2) & 0 & 0 & . & 0 \\ 0 & 0 & \text{var}(\xi_3) & 0 & . & 0 \\ 0 & 0 & 0 & 0 & . & 0 \\ . & . & . & . & . & 0 \\ . & . & . & . & . & 0 \\ 0 & 0 & 0 & 0 & 0 & 0 \end{bmatrix} \qquad (5.13)$$

From equation 5.7 $\underline{B}_1$ is given by:

$$\underline{B}_1 = \begin{bmatrix} 1 & 0 & 0 & 0 & . & 0 \\ 0 & 1 & 0 & 0 & . & 0 \\ 0 & 0 & 1 & 0 & . & 0 \\ 0 & 0 & 0 & 0 & . & 0 \\ . & . & . & . & . & 0 \\ . & . & . & . & . & 0 \\ 0 & 0 & 0 & 0 & 0 & 0 \end{bmatrix} \qquad (5.14)$$

The matrices $\dot{\underline{A}}$, $\underline{B}_1$, $\underline{\Sigma}$, $\tilde{\underline{\Sigma}}$ and $\underline{\Sigma}_1$ are square matrices of order 3+k.

From equation 3.46, G_2 (equation 3.29b) is linear and scalar and the vector $\underline{C}$ of order 3+k is given by:

$$\underline{C} = [\ 1 \quad 0 \quad 0\ ] \qquad \text{for } k = 0 \text{ (no time delay)} \qquad (5.15)$$
$$\underline{C} = [\ 0 \quad 0 \quad 0 \quad 1\ ] \qquad \text{for } k > 0$$

The measurement noise η' is a scalar; its variance v'_{η} is given by equation 4.22 of the Linearisation Estimator:

$$\underline{\Sigma}_2 = v'_{\eta} \tag{5.16}$$

$$\underline{B}_2 = 1 \tag{5.17}$$

For implementation in the CAD package, the EKF was written in the UDU^T format of Bierman (1977) which has been shown to be more robust to numerical instability (Bierman and Thornton 1977). The functions f_1, f_1^{-1}, f_2 and f_2^{-1} of equations 5.11 were implemented as a look-up table of titration curve data with linear interpolation between the data points.

5.3 OBSERVABILITY OF THE MODEL

In this section the observability of the non-linear system of equations 3.29 is examined. Observability results for the approximate linearised pH model of equations 5.10 and 5.11 are obtained for strong and weak reagents. These results are based on an extension of linear system theory.

The system of equation 3.29 is said to be completely observable at time i if, with the system in state $\underline{x}(i)$ it is possible to determine this state from the observation of the output $\underline{y}(i)$ over a finite time interval. The concept of observability of linear system was introduced by Kalman (1963) and is a prerequisite to the state estimation.

For a linear time-invariant system given by :

$$\underline{x}(i+1) = \underline{A}\,\underline{x}(i) + \underline{B}u(i) + \underline{\xi} \tag{5.18a}$$

$$\underline{y}(i) = \underline{C}x(i) + \underline{\eta} \tag{5.18b}$$

this definition of observability leads to the construction of an observability matrix $\underline{\Omega}$

$$\underline{\Omega} = \begin{bmatrix} C \\ CA \\ CA^2 \\ CA^3 \\ . \\ . \\ CA^{n-1} \end{bmatrix} \qquad (5.19)$$

which has full rank if and only if the system is completely observable.

There are no such general results about the observability of non-linear systems. However, observability criteria have been reported for a few specific time-varying non-linear systems (Hermann and Krener 1977, Gauthier and Bornard 1981), but none which could relate to the pH system of equations 3.46. Hence, the time-varying linearised system of equations 5.10 and 5.11 is analysed instead using linear system theory (equation 5.19). The ~~linearised~~ actual system is unlikely to be observable unless its linearization has an observability matrix $\underline{\Omega}$ ~~has~~ of full rank. A more rigorous observability analysis of the pH model can provide an area of future research.

Construction of the observability matrix:-

The observability matrix $\underline{\Omega}$ is constructed using equation 5.19 for the linearised model of equations 3.46. The elements of the $\underline{A}$ matrix are given by equations 5.10 and 5.12 for strong reagents and by equations 5.11 and 5.12 for weak reagents. For no time delay (k = 0), $\underline{\Omega}$ is given

by:

$$\underline{\Omega} = \begin{bmatrix} 1 & 0 & 0 \\ a_{11} & a_{12} & a_{13} \\ (a_{11})^2 & a_{12}(a_{11} + g_2) & a_{13}(a_{11} + g_3) \end{bmatrix} \quad (5.20)$$

$\underline{\Omega}$ is rank defficient if $g_2 = g_3$ because columns two and three can be made identical when each of their elements is divided by a_{12} for column two and a_{13} for column three. Hence, the vectors of $\underline{\Omega}$ are not linearly independent and the system is unobservable. This means that if the rate of change of the influent flow disturbance model x_2 and the influent i.c.d. disturbance model x_3 are the same, the pH model is not completely observable in a linear sense. Intuitively, this makes sense: an estimator cannot differentiate from the measurement y' (of equation 4.21) similar changes which may occur in x_2 or x_3, and it cannot attribute these changes to the correct disturbance.

The construction of the observability matrix $\underline{\Omega}$ is similar for time-delayed pH models ($k > 0$) and again the system is not completely observable if $g_2 = g_3$.

5.4 ROBUSTNESS OF THE EKF ESTIMATOR

In this section, robustness of the EKF estimator of section 5.2 is discussed with reference to its implementation in simulation to the pH model of section 3.4. Errors are intentionally introduced in some model parameters in order to test the robustness of the estimator. These modelling errors describe variations between the simulated pH model and the real pH system. The estimator is robust if it gives good estimates

for large modelling errors. The modified model paramaters are: the reactor volume and the time constants of the load disturbances. The modelling errors are analysed and computed in the form of a diagonal error matrix $\underline{E}$. The error matrix is added to the prediction covariance to account for the modelling differences thus preventing the EKF estimator from diverging.

In order to test the robustness of the EKF estimator in simulation for the pH model of equations 3.46, values of simulated parameters of the model are randomized away from their nominal values. The amount of randomization is charaterised by some modelling error Q, and each simulated parameter value P is computed from its nominal value P^0 (used by the estimator) according to

$$P = P^0(1 + Qr) \tag{5.21}$$

where r is an independent Gaussian random variable of probability distribution $p(r) = N(0.,1)$. The EKF estimator is robust if, when designed on the assumption that the parameters have their nominal values P^0, it gives good estimates when their actual values are P.

The randomized parameters of the pH model of equations 3.46 are the CSTR volume V and the time constants T_j of the Wiener processes x_2 and x_3; their corresponding nominal values are V^0 and T_j^0. The difference between the nominal and the simulated value of the tank volume V is to account for variations in the liquid level in the tank and for non-perfect mixing:

$$V = V^0(1 + \epsilon) \tag{5.22}$$

To allow for more flexibility in modelling the Wiener processes x_2 and x_3 of equations 3.41, the randomization of the time constants T_2 and T_3 is

made according to:

$$T_j = T_j^0(1 + \epsilon) \qquad j = 2,3 \qquad (5.23)$$

where ϵ in equations 5.22 & 5.23 is a normalised zero-mean random variable of variance $var(\epsilon) = Q^2$.

If the differences between nominal and actual parameters values are not considered in the EKF equations, the EKF estimates will diverge (Sage and Melsa 1971, Jazwinski 1974): i.e. the actual estimation errors between the states $\underline{x}$ and their estimates $\hat{\underline{x}}$ will greatly exceed the value predicted by the error variance $\underline{\Sigma}$.

Modelling errors

In this section, modelling errors arising from assumed uncertainties in the values of the parameters V and T_j are accounted for in the EKF equations. This is done by adding to the covariance prediction $\underline{\Sigma}$ of equation 5.5 a square matrix $\underline{E}$ (of dimension 3+k) whose elements are computed below. The effect of the additional term $\underline{E}$ is to increase artificially some selected terms of the covariance prediction in order to avoid the divergence of the filter:

$$\tilde{\underline{\Sigma}} = \underline{B}_1\underline{\Sigma}_1\underline{B}_1^T + \underline{A}\,\underline{\Sigma}(i-1)\,\underline{A}^T + \underline{E} \qquad (5.24)$$

The effect of the uncertainty in V on the state x_1 in equation 3.39 is computed as follows:

$$x_1(i+k+1) = x_1(i+k) + \frac{\Delta}{V}x_2(i)(X_{in}(i) - x_1(i+k)) + \xi_1 \qquad (3.39)$$

Replacing V with $V^0(1 + \epsilon)$ in 3.39:

$$x_1(i+k+1) = x_1(i+k) + \frac{\Delta}{V^0(1+\epsilon)} x_2(i)(X_{in}(i) - x_1(i+k)) + \xi_1 \quad (5.25)$$

For small ϵ, $(1+\epsilon)^{-1} \simeq (1-\epsilon)$; replacing in equation 5.25 and rearranging:

$$x_1(i+k+1) = x_1(i+k) + \frac{\Delta}{V^0} x_2(i)(X_{in}(i) - x_1(i+k)) + \xi_1 - \frac{\Delta}{V^0} x_2(i)(X_{in}(i) - x_1(i+k))\epsilon \quad (5.26)$$

The uncertainty in V due to the random variable ϵ can be calculated from equation 5.26:

$$e_{11} = \text{var}\{ \frac{\Delta}{V^0} x_2(i)(X_{in}(i) - x_1(i+k))\epsilon \} \quad (5.27)$$

where e_{11} is the element 1,1 of matrix $\underline{E}$ of equation 5.24. e_{11} is dependent upon x_{in} and is approximately given by (appendix III):

for strong reagents:

$$e_{11} = \{ \frac{\Delta}{V^0} (m_2(m_3 - m_1) + \sigma_{23} - \sigma_{12} + X_r u)Q \}^2 \quad (5.28)$$

for weak reagents:

$$e_{11} = \{ \frac{\Delta}{V^0} (m_2(M_{in} - m_1) - \sigma_{12})Q \}^2 \quad (5.29)$$

where m_1, m_2 & m_3 are the elements of the state estimate $\hat{\underline{x}}$ (equation 5.10), and σ_{12} & σ_{23} are the elements of the covariance matrix $\underline{\Sigma}$, and M_{in} is given by equation 5.11.

The calculation of the uncertainty in T_j (j=2,3) on the states x_2 and x_3 in equation 3.41 is computed as follows:

$$x_j(i+1) = g_j x_j(i) + \alpha_j + \xi_j \qquad j=2,3 \quad (3.41)$$

where g_j, α_j and $var(\xi_j)$ are given by:

$$g_j = (1-\Delta/T_j) \qquad \alpha_j = \bar{x}_j(1-g_j) \qquad var(\xi_j) = var(\mu_j)(1-g_j^2) \tag{3.42}$$

Replacing T_j with $T_j^0(1+\epsilon)$ in equation 3.42 and dropping the j subscript for convenience, we have for the rate of change of the process g:

$$g = \frac{\Delta}{T^0(1+\epsilon)} \tag{5.30}$$

Again, we can replace $(1+\epsilon)^{-1}$ with $(1-\epsilon)$ for small ϵ and rearranging equation 5.30:

$$g = g^0 + (1 - g^0)\epsilon \tag{5.31}$$

where $g^0 = 1 - \Delta/T^0$

Replacing g by g^0 from equation 5.31 for the offset α in equation 3.42:

$$\alpha = \bar{x}\,(1 - g^0 - (1 - g^0)\epsilon) \tag{5.32}$$

Rearranging equation 5.32:

$$\alpha = \alpha^0(1 - \epsilon) \tag{5.33}$$

where $\alpha^0 = \bar{x}\,(1 - g^0)$.

For the variance of the system noise $var(\xi)$, g is replaced by g^0:

$$var(\xi) = var(\mu)\left[1 - g_0^2 + \left[(2g^0(1 - g^0) + (1 - g^0)^2\epsilon\right]\epsilon\right] \tag{5.34}$$

Replacing g^0 by $1 - \Delta/T^0$ in the square brackets:

$$var(\xi) = var(\mu)\left[1 - g_0^2 + \left[(\Delta/T^0)^2\epsilon - 2(\Delta/T^0)^2 + 2\,\Delta/T^0\right]\epsilon\right] \tag{5.35}$$

For large T^0, $(\Delta/T^0)^2$ is small and may be neglected:

$$var(\xi) = var(\mu)\,(1 - g_0^2) + var(\mu)\,(2\,\Delta/T^0)\epsilon \tag{5.36}$$

The system noise ξ is hence represented by a sum of two terms: $\xi^0 + \xi^\epsilon$. ξ^0 is the system noise when $\epsilon = 0$ (no modelling errors); it is given by $var(\xi^0) = var(\mu)(1 - g_0^2)$. ξ^ϵ is the additional uncertainty due to the randomization ϵ; it is a zero-mean random variable of variance $var(\xi^\epsilon)$ given by:

$$var(\xi^\epsilon) = (2\ \Delta/T^0)^2\ Q^2 var(\mu) \qquad (5.37)$$

Replacing for g, α and ξ in equation 3.41:

$$x(i+1) = g^0 x(i) + \alpha^0 + \xi^0 \qquad (5.38)$$
$$+((1 - g^0)x(i) - \alpha^0)\epsilon + \xi^\epsilon$$

The uncertainty in T_j (j=2,3) due to the random variable ϵ can be calculated from equation 5.38:

$$e_{jj} = var\left[((1 - g_j^0)x_j(i) - \alpha_j^0)\epsilon\right] + var(\xi_j^\epsilon) \qquad (5.39)$$

where e_{jj} are the elements 2,2 & 3,3 of the error matrix $\underline{E}$ of equation 5.24. e_{jj} are approximately given by (appendix III):

$$e_{jj} = \left[((1 - g_j^0)m_j - \alpha_j^0)Q\right]^2 + (2\ \Delta/T^0)^2\ Q var(\mu) \qquad (5.40)$$

The remaining elements of ther error matrix $\underline{E}$ are zero.

5.5 SIMULATION RESULTS

The EKF estimator described in section 5.2 was used in simulation to test its performance and its robustness prior to its implementation on a full-scale industrial application. It was also tested to determine the effects on performance of unnaccounted features such as modelling errors and non-zero bias on the pH measurement. The simulation used is the CAD package PHDESIGN.

Figures 5.1 to 5.10 show simulated time-histories of the three essential states of the pH model of equations 3.46: outgoing i.c.d. x_1, incoming disturbances of flow x_2 and i.c.d. x_3. Also shown are their corresponding estimates m_1, m_2 and m_3, and the standard deviation of the estimates $\sqrt{\sigma_{11}}$, $\sqrt{\sigma_{22}}$ and $\sqrt{\sigma_{33}}$. The results presented here are for three different processes: process A (figures 5.1, 5.2), in which the titration curve is the theoretical strong reagents, and for which the disturbances are modelled by Wiener processes; process B (figures 5.3, 5.4), which has also Wiener model disturbances but which has a buffered titration curve shown in figure 1.3; and process C (figures 5.5, 5.6), which has the same buffered titration curve of process B, but for which the flow disturbances are plant recorded data.

Process C, which was introduced in section 1.1 and which provides a case study in chapter 8, is the full-scale neutralisation tank WB T103A of Caster Kellner Works at ICI. This industrial process provided a test-bed for the implemetation of the EKF estimator (Proudfoot 1983). Differences between the simulation results and those of the industrial process are discussed in section 5.5.3. Also, the effect of modelling errors on the robustness of the estimation and the effect of biased pH measurement on the state estimation are investigated in section 5.5.2 with the help of simulated results of figures 5.7 to 5.10.

5.5.1 Performance Of The EKF Estimator

Typical time-histories of Wiener models and their estimates are shown for two standard deviations of measurement noise on the effluent pH (s_η = 0.01, 0.1 pH units), for the strong reagents of process A (figures 5.1, 5.2) and for the weak reagents of process B (figures 5.3, 5.4). The estimates in all four cases are good and their standard deviations

reflect accurately the confidence in the estimates. For process A, the state x_1 and its estimate m_1 are indistinguishable; in figure 5.1, estimates of the flow m_2 and the i.c.d. m_3 seem correlated: a negative difference between x_2 and m_2 corresponds to a negative difference between x_3 and m_3, so that the products $x_2 x_3$ and $m_2 m_3$, i.e. the amount of acidity in the effluent, are equivalent. This may be due to the similarity of the values of Wiener time constants T_2, T_3 of equation 3.42 (T_2 = 80 mins., T_3 = 100 mins.). For process B, the estimate m_1 follows closely the state x_1 for both measurement noise values and the standard deviation of the estimate $\sqrt{\sigma_{11}}$, is relatively large because of the uncertainty in the buffered titration chemistry which is modelled in equations 3.46 by ξ_1. The flow estimate m_2 is good and the i.c.d. estimate m_3 is a smoothed version of the actual ic.d. x_3 with its mean level correctly estimated.

For all the four runs above, the modelling errors Q (equation 5.21) in the parameters is equal to 0.3, i.e. there is a 30% error in the parameter modelling. The estimates shown will provide good feedforward information for the inflow and incoming i.c.d. disturbances in a feddforward-feedback control configuration and good state estimation for a separated stochastic controller,as discussed in the next chapter.

Time-histories of simulated and estimated inflow and incoming i.c.d. for process C are show in figures 5.5 and 5.6 for the two pH measurement noise (s_η = 0.01, 0.1 pH units). It can be seen that the flow estimate m_2 is not fully able to follow the state x_2 and that the i.c.d. estimate m_3 is fairly constant at the mean value of the state x_3. Nonetheless, the standard deviations $\sqrt{\sigma_{22}}$ and $\sqrt{\sigma_{33}}$ are large and hence show their lack of confidence in the estimation. This performance of the estimator, which is not fully successful, is due to the inability of the Wiener

processes to represent large step-wise variations in the actual flow. The time constant T_2 of the flow Wiener model (equation 3.42) was chosen to be slower than that of the i.c.d. model and the standard deviation specified for the flow model was very large (180 $m^3hr.^{-1}$) while the standard deviation for the i.c.d. was very small because the incoming pH did not seem to vary by a large amount. Other choices of parameters values produced poor results. The chosen values above led the estimator to assume that all large and/or fast disturbances were due to changes in the flow and that the i.c.d. hardly changed. The EKF estimator exhibited the same performances in some instances on the full-scale trials on WB T103A (Proudfoot 1983). More comparisons between simulation and plant trials are discussed below in section 5.5.3.

5.5.2 Effect Of Modelling Errors And Bias

The effect of the introduction of modelling errors in the pH model of chapter 3 and the accounting of these errors in the EKF equations is shown in simulation for process A. Figure 5.7 shows time-histories of the states and their estimates when there is no modelling errors: Q (equation 5.21) equal zero. Figure 5.8 shows a comparable run but with 50% modelling (Q = 0.5) variation in the parameter values of the tank volume and the time constant of the Wiener processes. The estimates are good in the two runs which means that the calculation of the modelling error matrix $\underline{E}$ (equations 5.28, 5.29 & 5.40), which accounts for the parameter variations, is correct; hence, the EKF filter will not diverge for any errors in the modelling of the parameters.

As discussed in the introduction, the EKF estimator derived in section 5.2 assumes that there is no bias on the pH measurement. The effect of the bias on the state estimation was, however, investigated in

simulation for processes A & C because it gave an insight in understanding poor estimation behaviour on the full-scale trials. Figure 5.9 shows time-histories of the states and their estimates for process A when bias of value -1 pH units is present but unaccounted for in the estimation. The estimate m_1 is biased from x_1 and $\sqrt{\sigma_{11}}$ is much smaller than the difference between the state and the estimate; the same is true for the incoming i.c.d. x_3 and the flow estimate m_2 is out of phase with x_2. For process C (figure 5.10), results are similar and to some extent representative of poor performance of the EKF in plant trials (Proudfoot 1983): the mean value of the estimated flow is higher than the actual flow when a negative bias is present and the mean value of the estimated incoming i.c.d. is lower than the actual i.c.d.. This is because more reagent is being used to control at what is actually a higher pH set point and the EKF assumes that this is due to a combination of more inflow and more concentrated influent.

5.5.3 Full-scale Implementation Of The EKF

The EKF was implemented on-line on the full-scale process after the above simulation results showed good disturbance estimation, making improvement due to feedforward control likely if the pH measurement was bias-free. The on-line trials indicated that state estimation of the disturbances could provide a small improvement when the estimates were used in a feedforward configuration, although robustness to large disturbances was lost (Proudfoot and Jacobs 1984). The improvement was small because the process was buffered a great deal and could be well controlled by feedback alone.

Some of the unsuccessful performance of the on-line estimator could be explained in simulation. One reason illustrated earlier, is the inability of the Wiener models to represent accurately the actual inflow and i.c.d. when they changed in a step-wise manner and at the same rate in the full-scale trials making them unobservable simultaneously (section 5.3). Another reason for poor state estimation is the presence of bias on the pH measurement probe which has shown to affect the estimates considerably (figures 5.9, 5.10). On the full-scale process, the pH measurement was assumed to be bias-free but poor calibration of the probes would have led to significant biases.

Further understanding of EKF performance is achieved by considering the pH model which was used in simulation. The model is fairly accurate as discussed in section 3.5 and its simulation results are comparable with those obtained on-line (chapter 8; Case Study 1), but nonetheless, the model cannot represent bad engineering designs. These may include measurement lag on the pH probes and innacurate reagent deliveries which affect the state estimation. The pH model is also not able to represent variations in the process titration curve and step-wise disturbances which again may affect the estimator. These model difficulties could provide an area of future research as will be discussed in chapter 9.

5.6 CONCLUSION

In this chapter, an EKF estimator was derived for the non-linear pH model of chapter 3. Observability of the model was discussed with reference to linear system theory and it was proven that the model is not completely observable if the rates of change of the disturbances are the same. Robustness of the estimator was also tested for variations in the model parameters. Simulation results have shown that the estimator can

produce good estimates provided that the pH measurement is bias-free and that the titration curve is known. These estimates can give a valuable information on influent disturbances which could be used in control as will be discussed in the next chapter. However, the practicality of the estimation scheme on a full-scale industrial process has not been fully investigated because the chosen process lacked the required condition of bias-free pH measurement. Nevertheless, a small improvement in control performance using the EKF estimator has been reported.

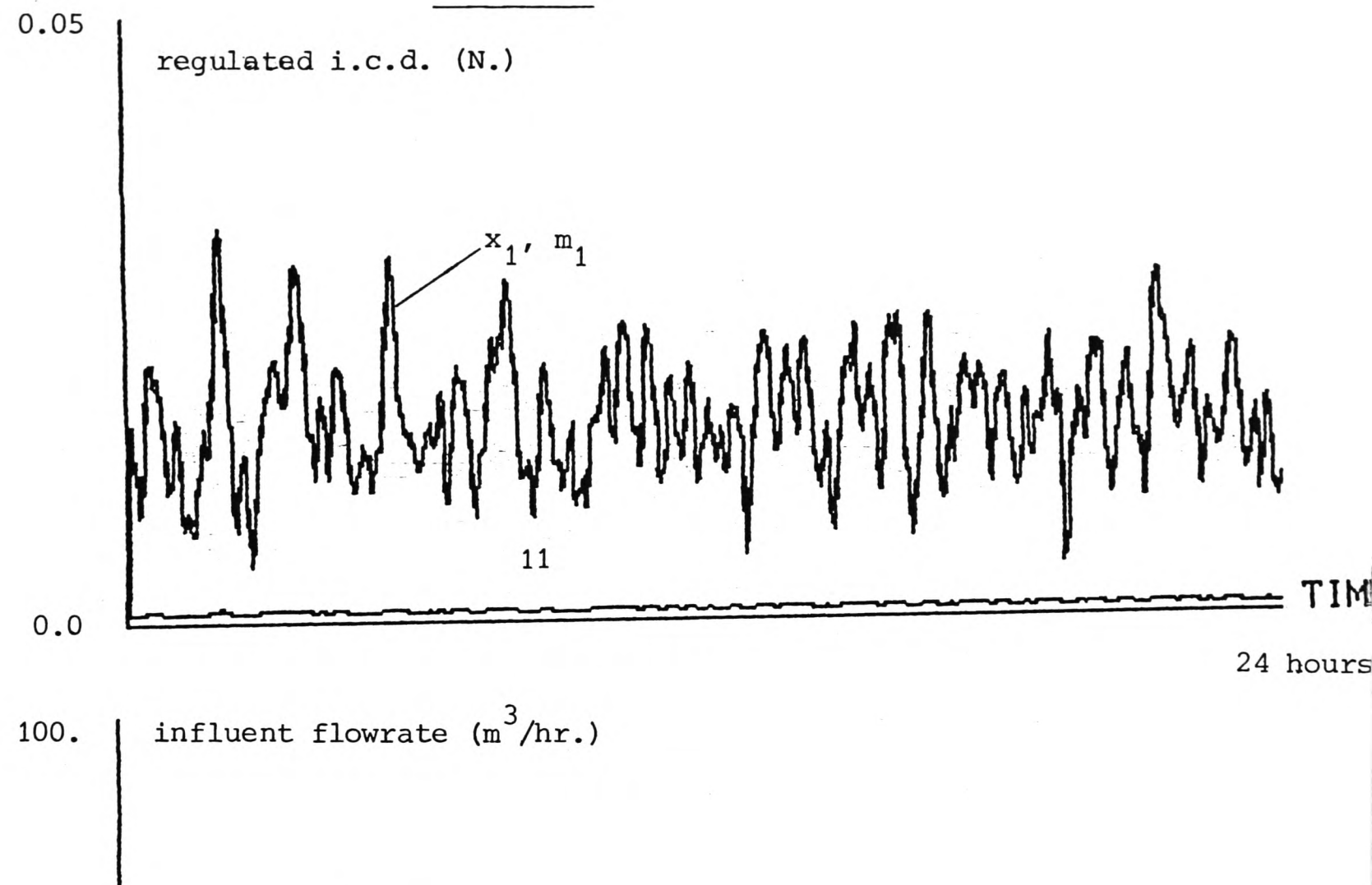


Fig 5.1 State estimation: Q= 0.3, s =0.01 pH units

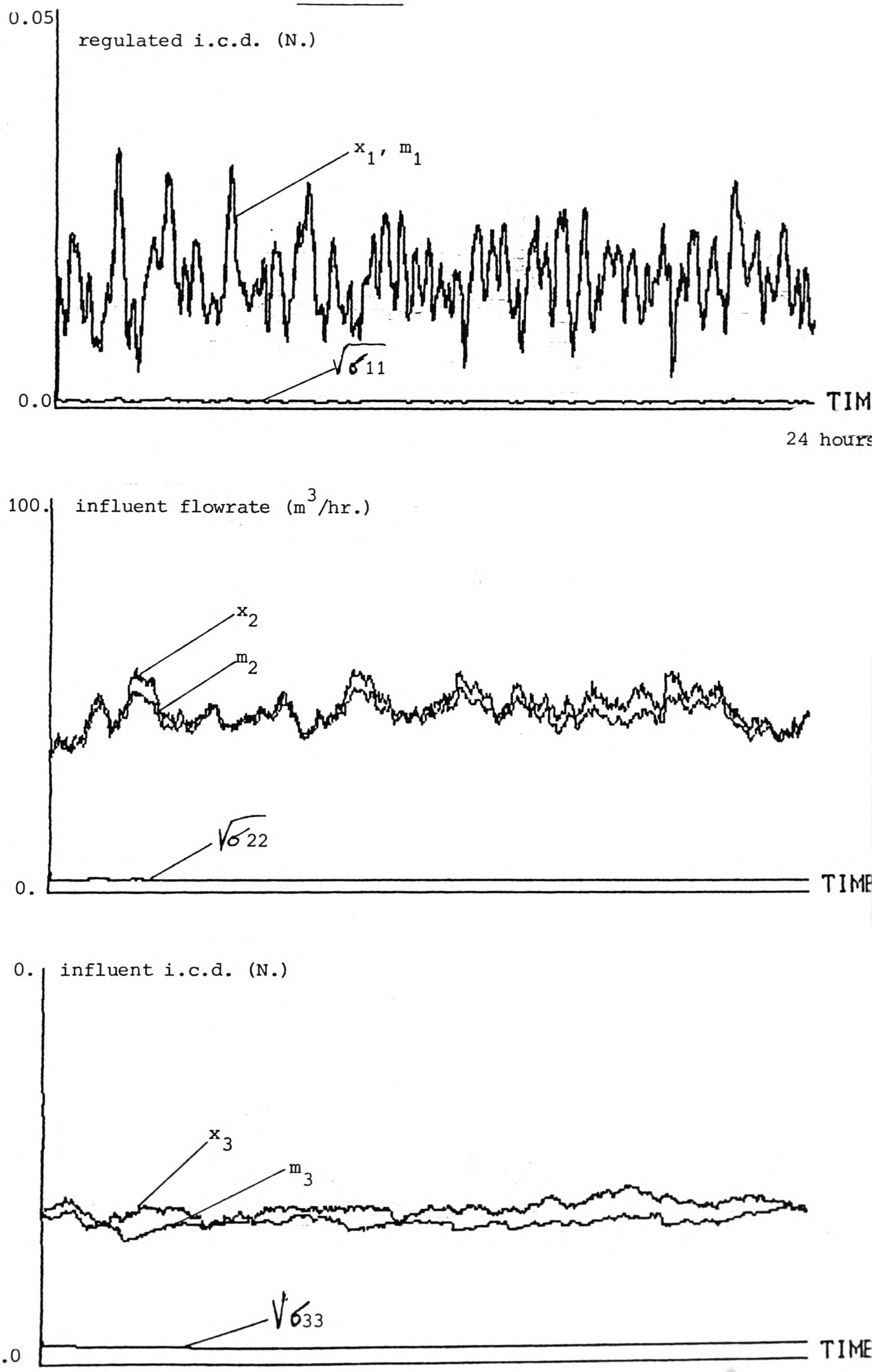
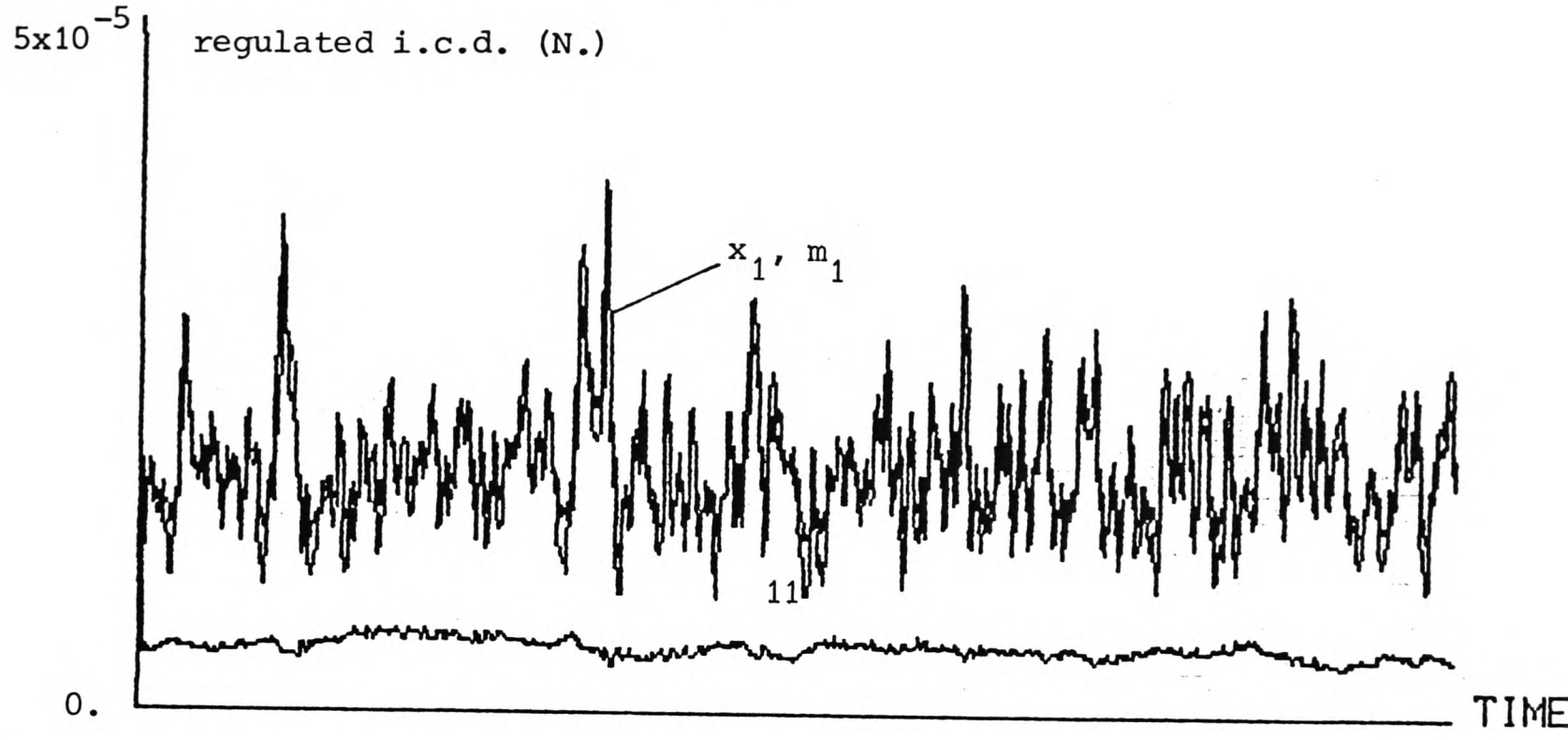
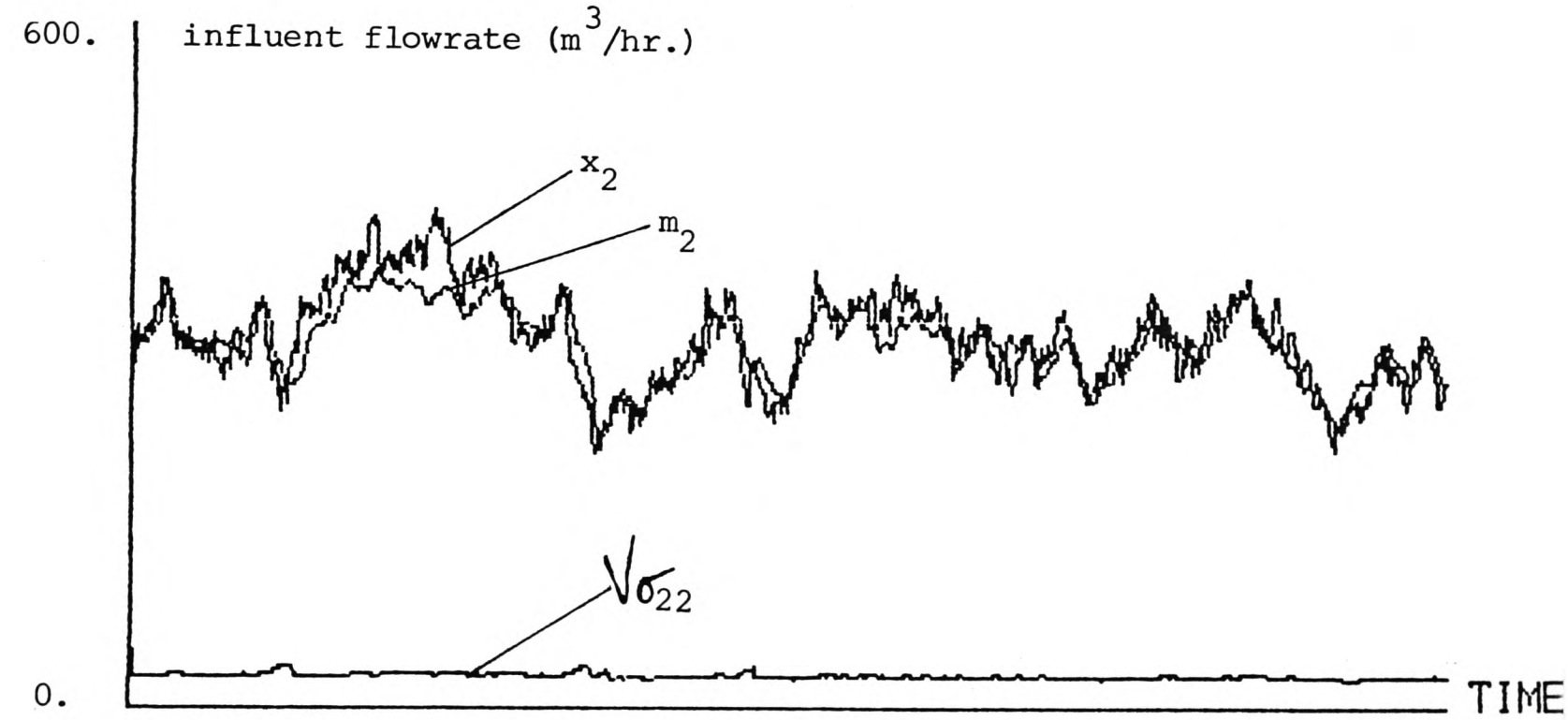


Fig 5.2 State estimation: Q= 0.3, s = 0.1 pH units





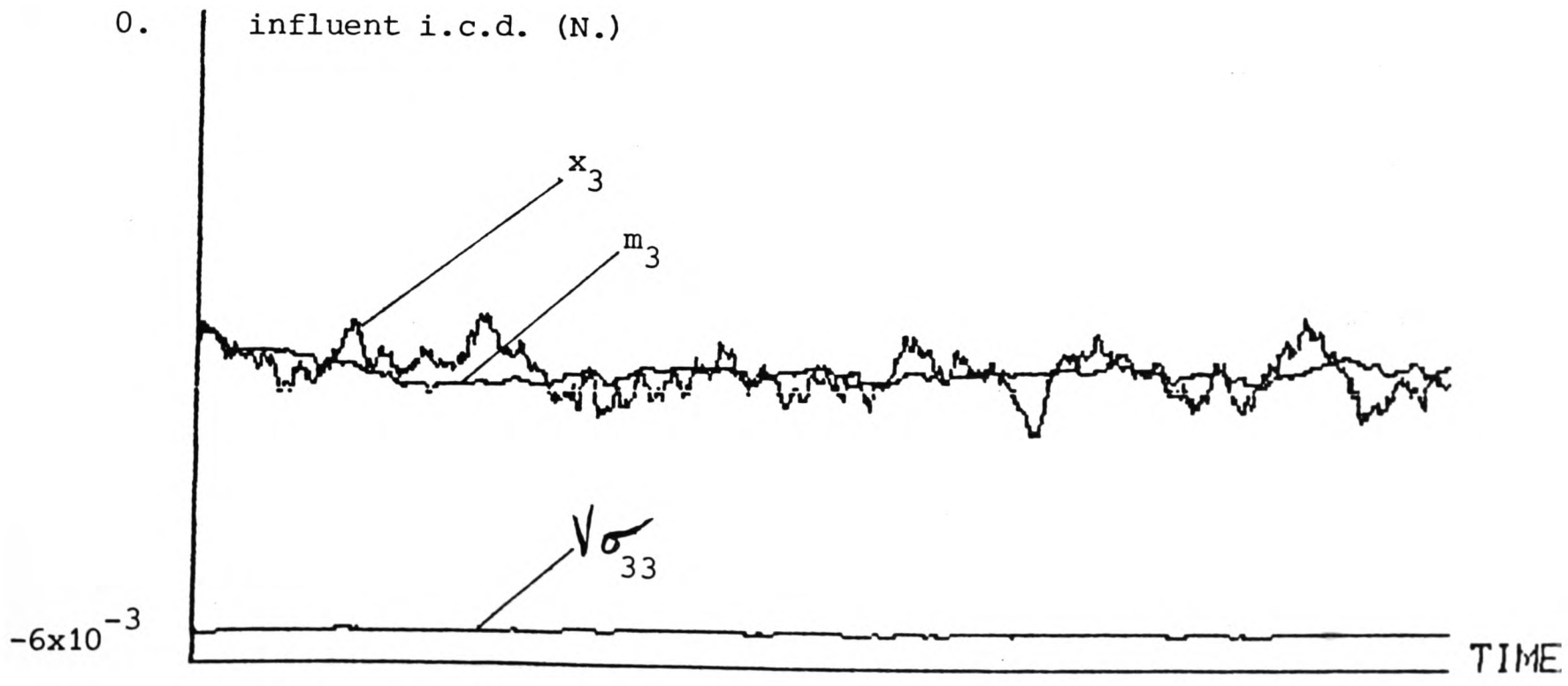
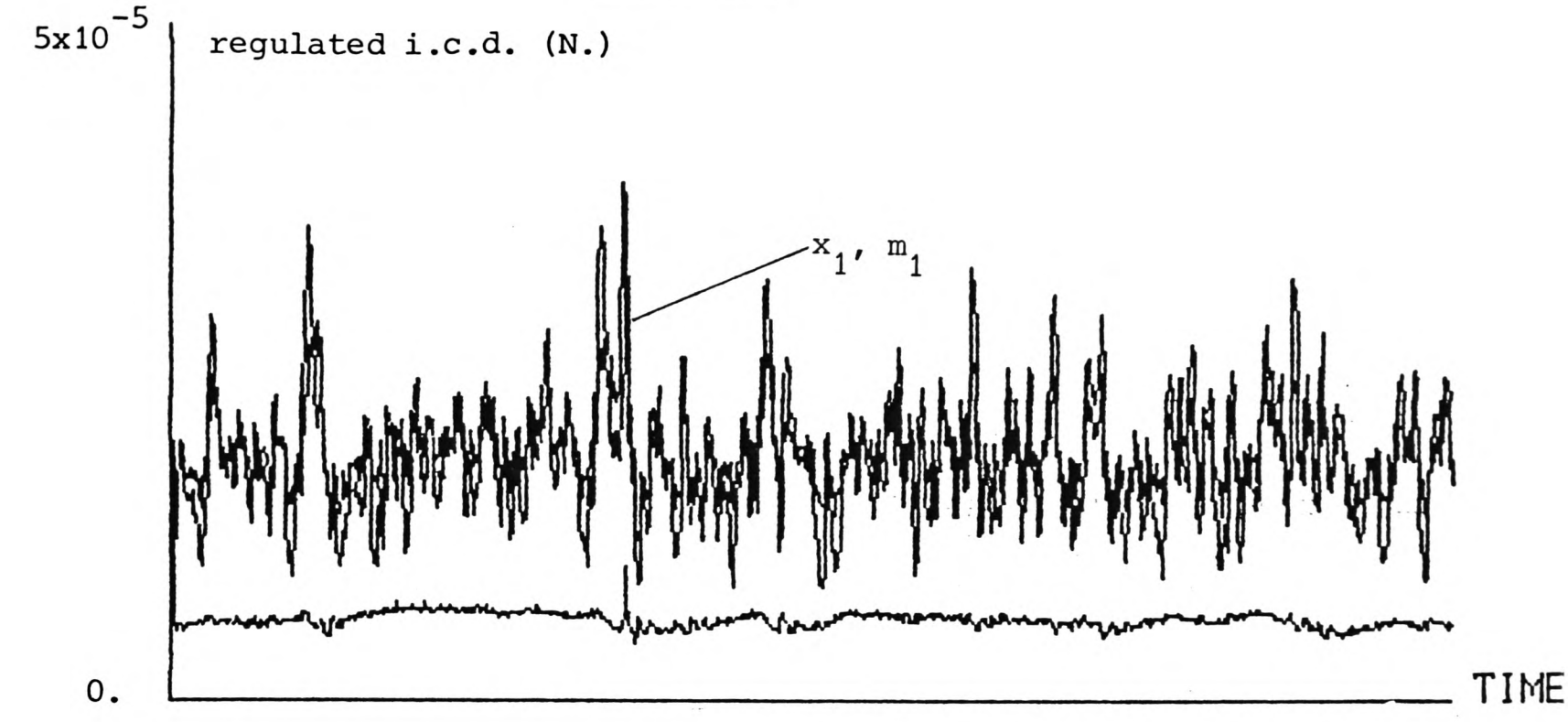
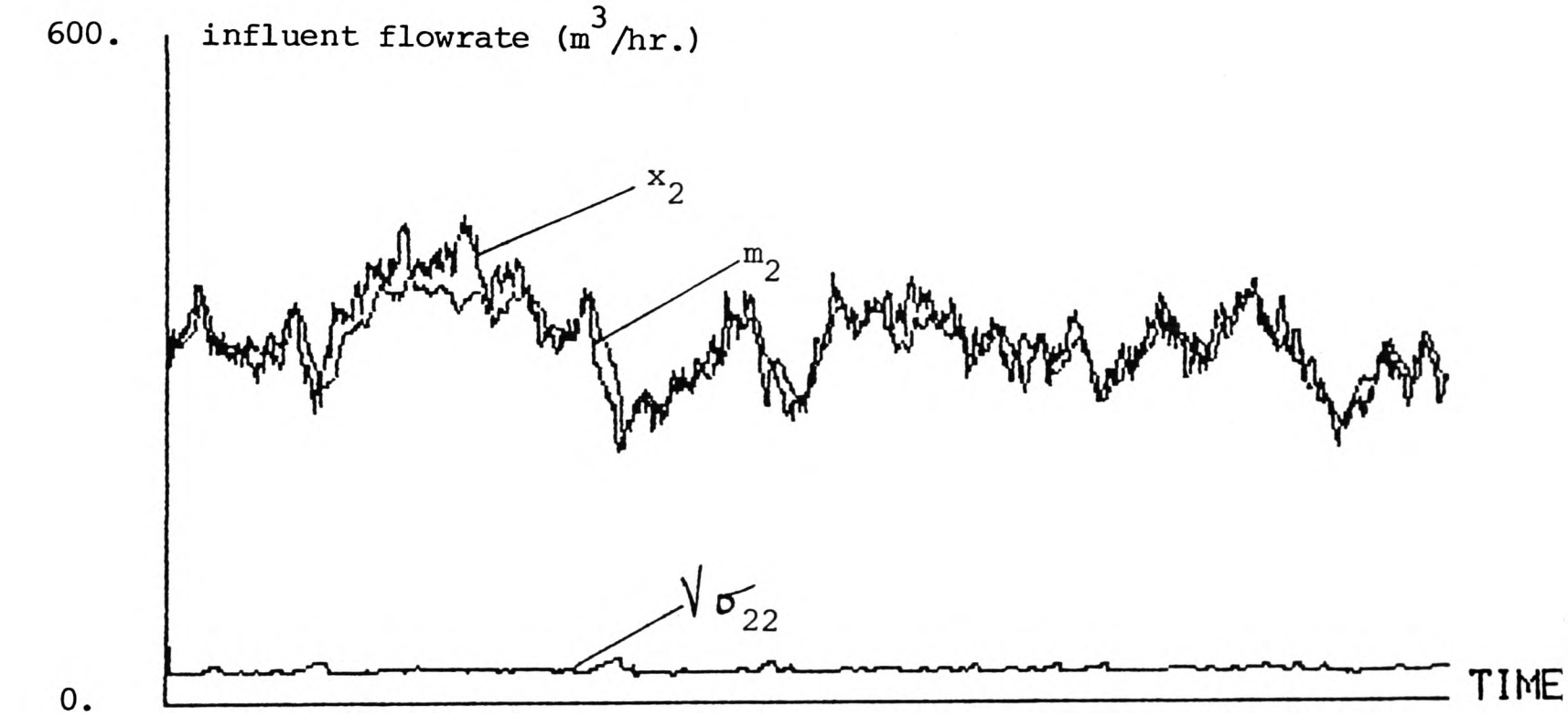


Fig 5.3 State estimation: Q= 0.3, s = 0.01 pH units

PROCESS B





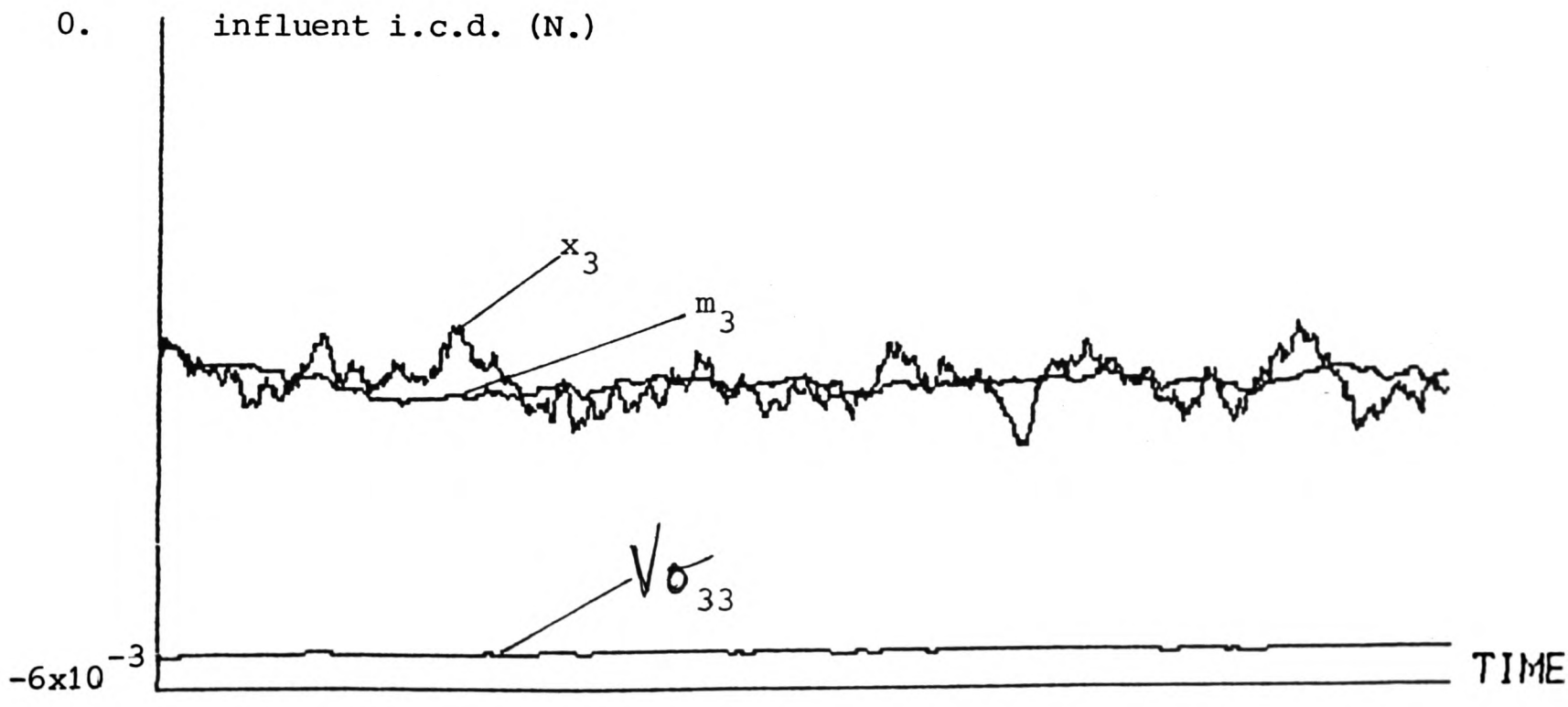


Fig 5.4 State estimation: Q= 0.3, s = 0.1 pH units

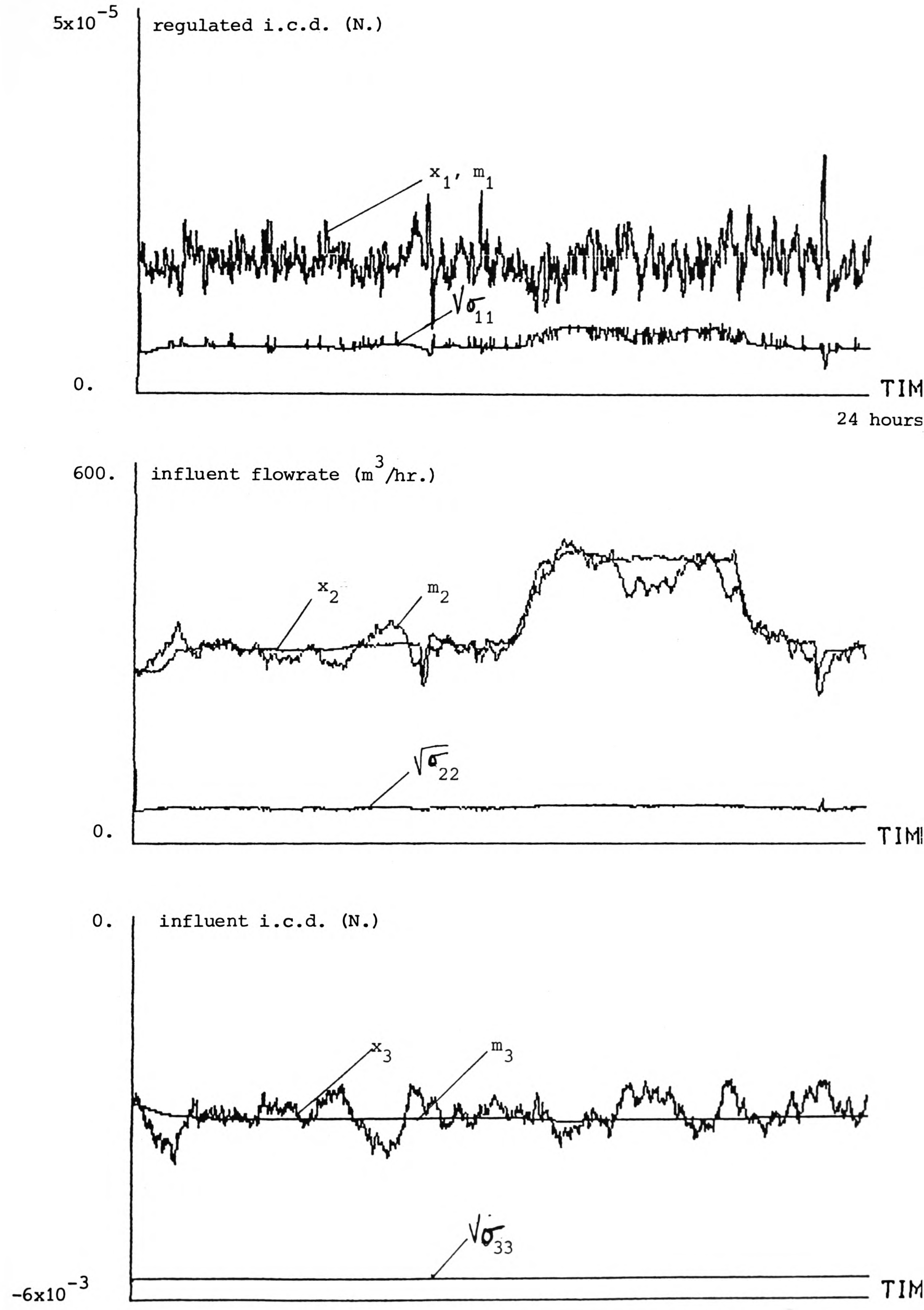


Fig 5.5 State estimation: Q= 0.3, s = 0.01 pH units

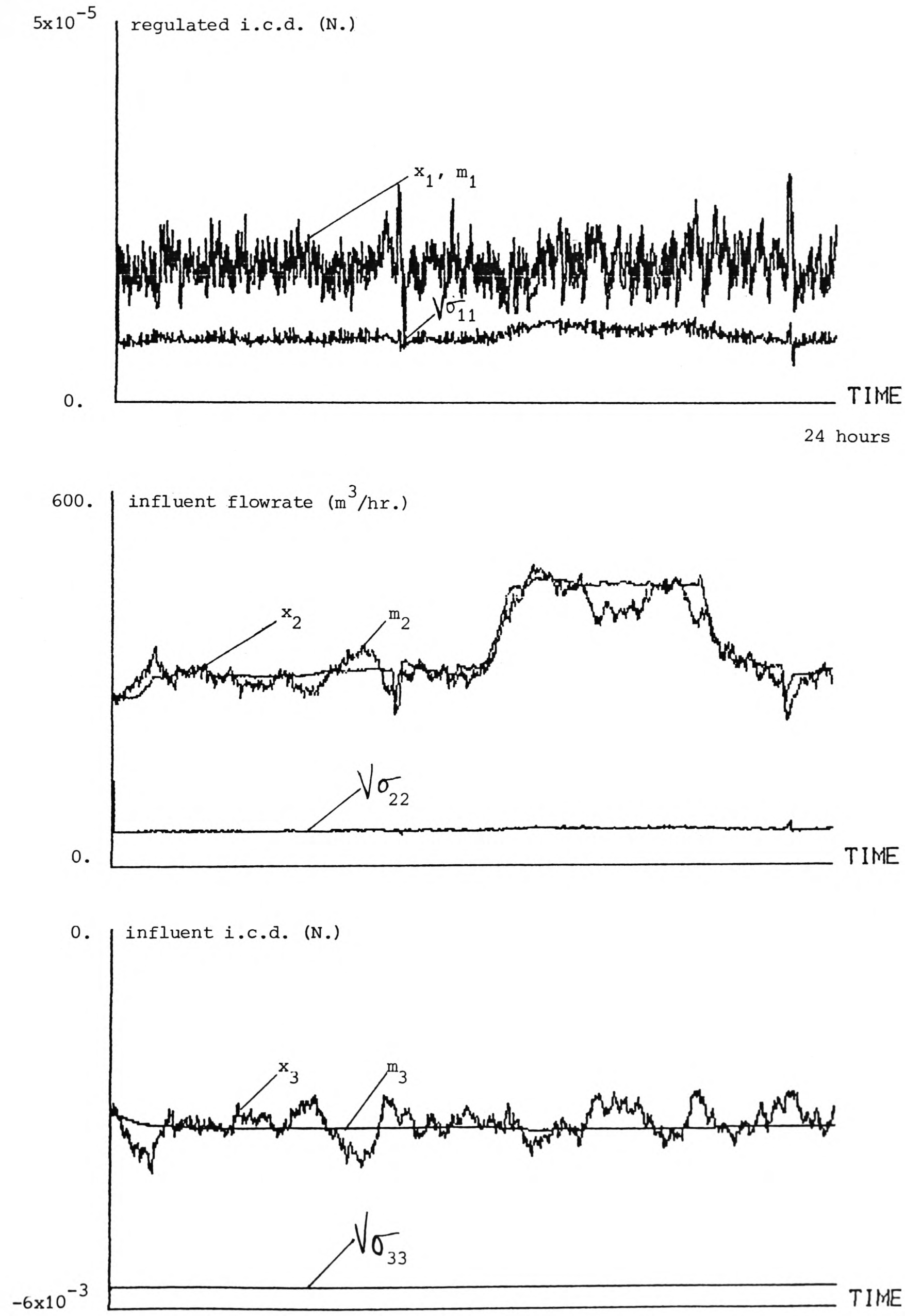
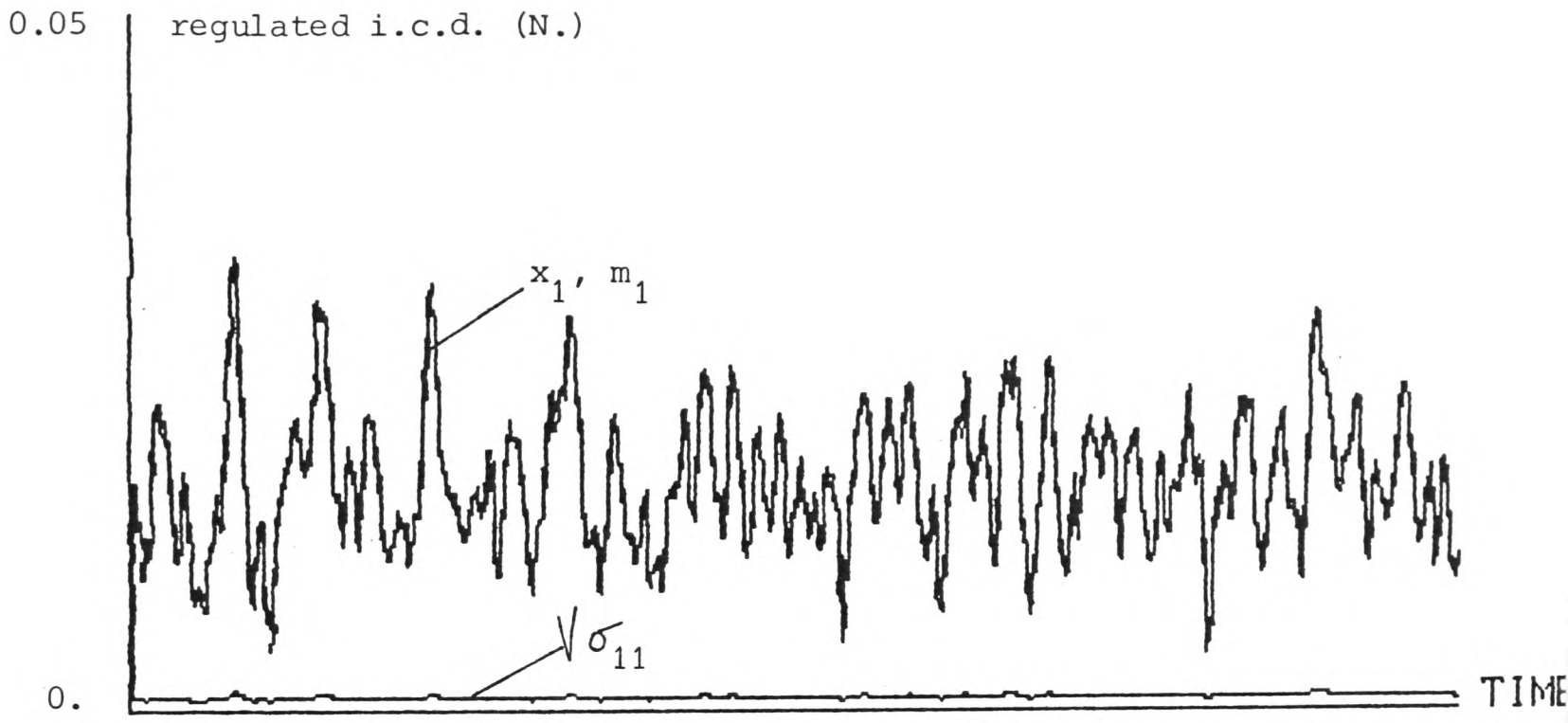
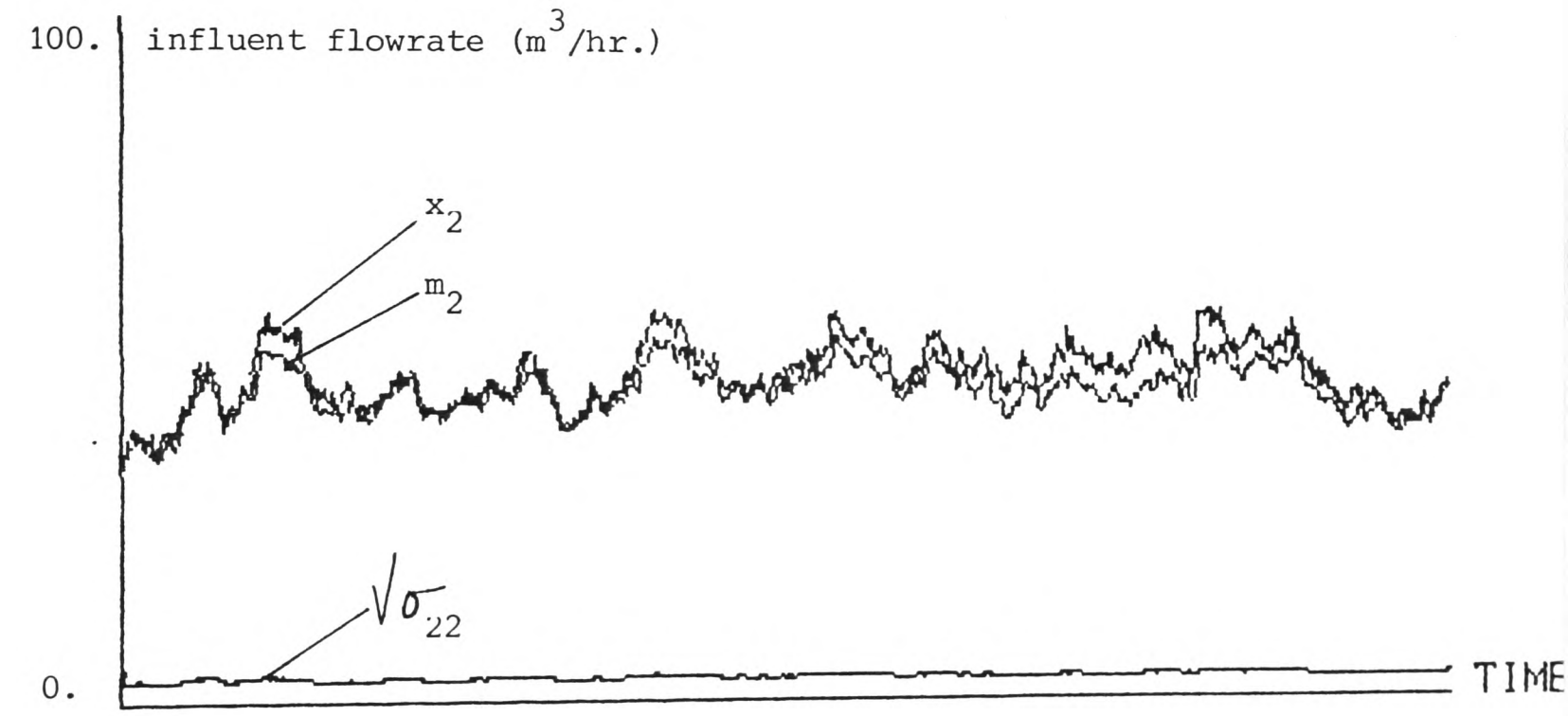


Fig 5.6 State estimation: Q= 0.3, s = 0.1 pH units





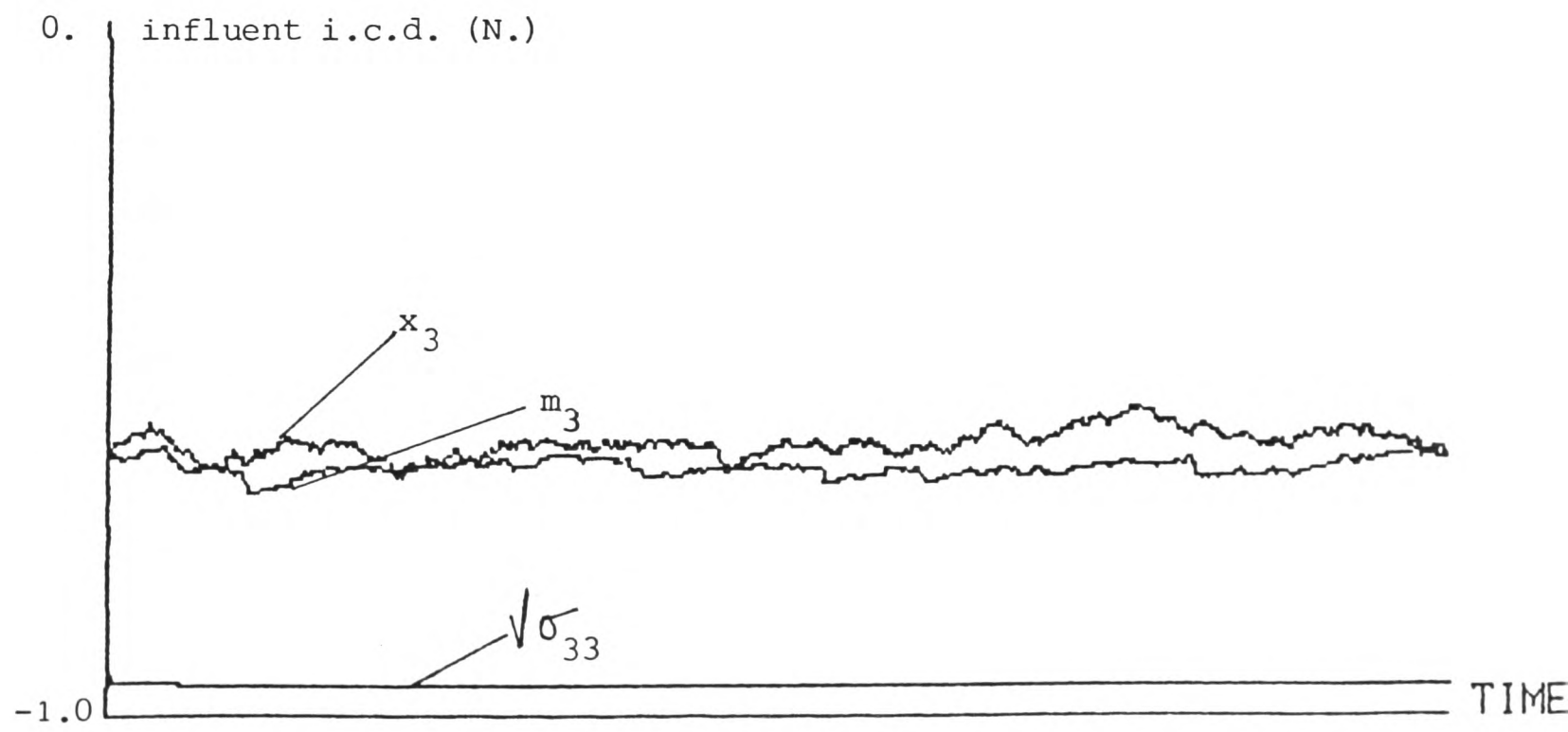


Fig 5.7 Effect of modelling errors on state estimation: Q= 0.

PROCESS A

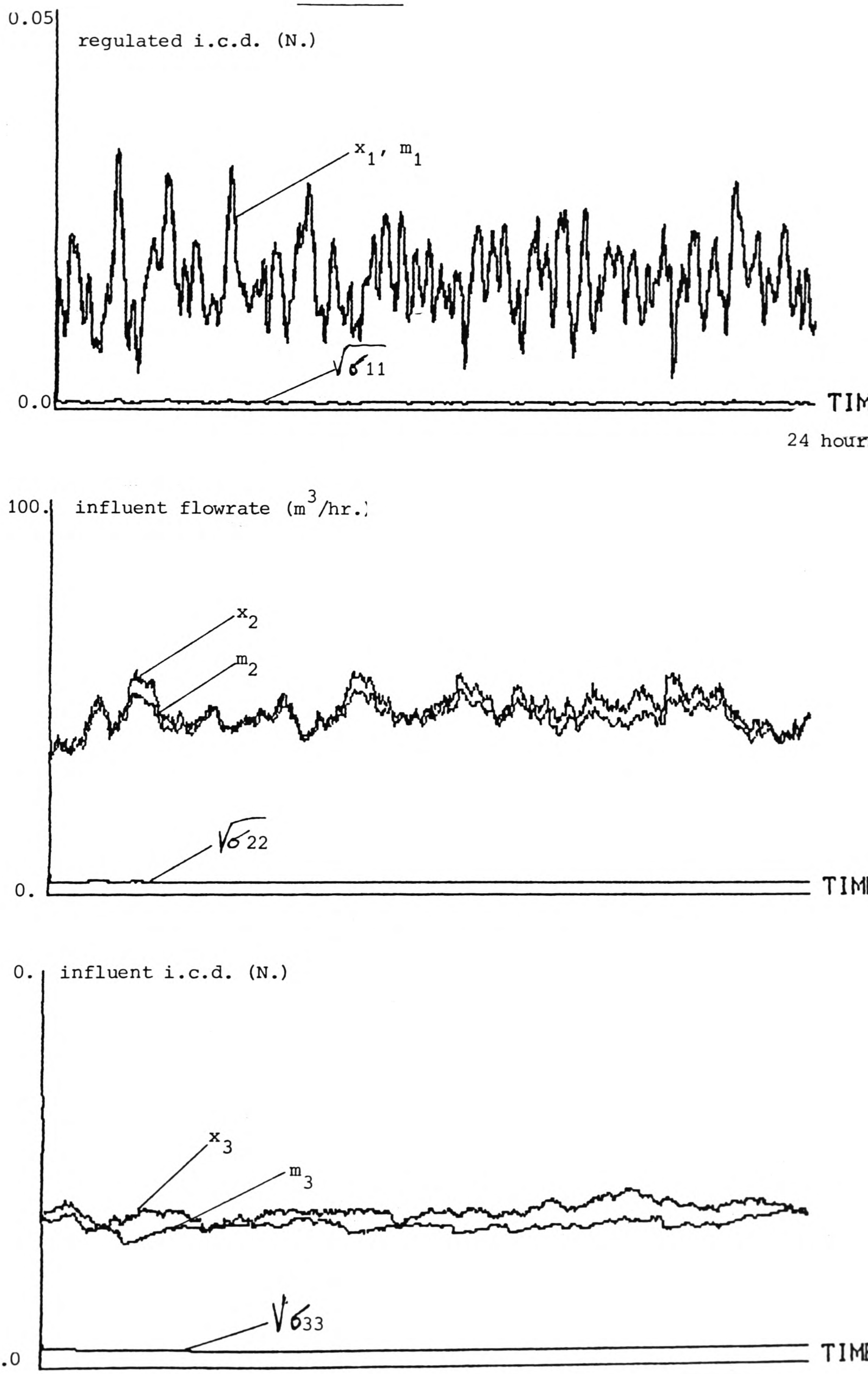


Fig 5.8 Effect of modelling errors on state estimation: Q=0.5

PROCESS A

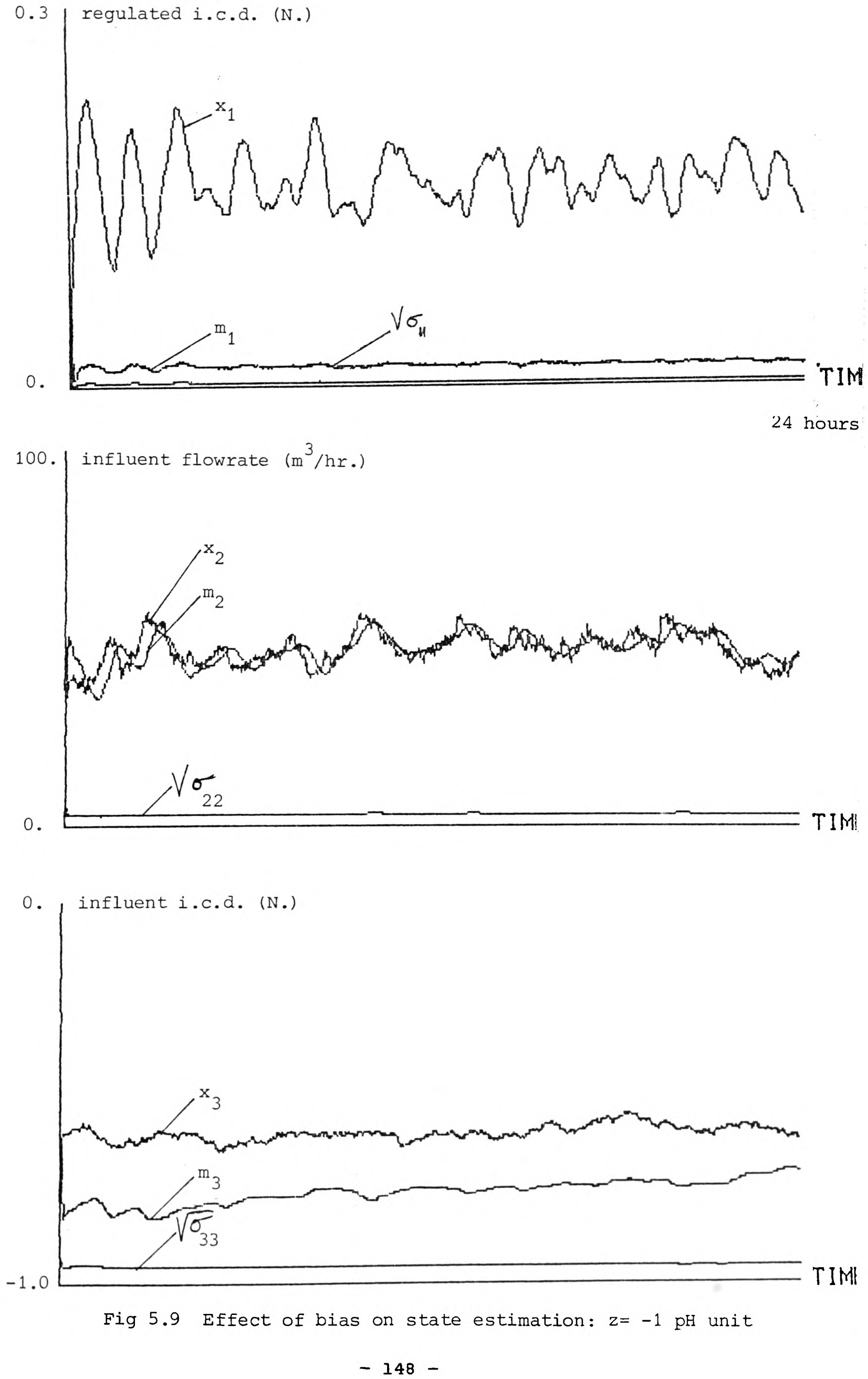
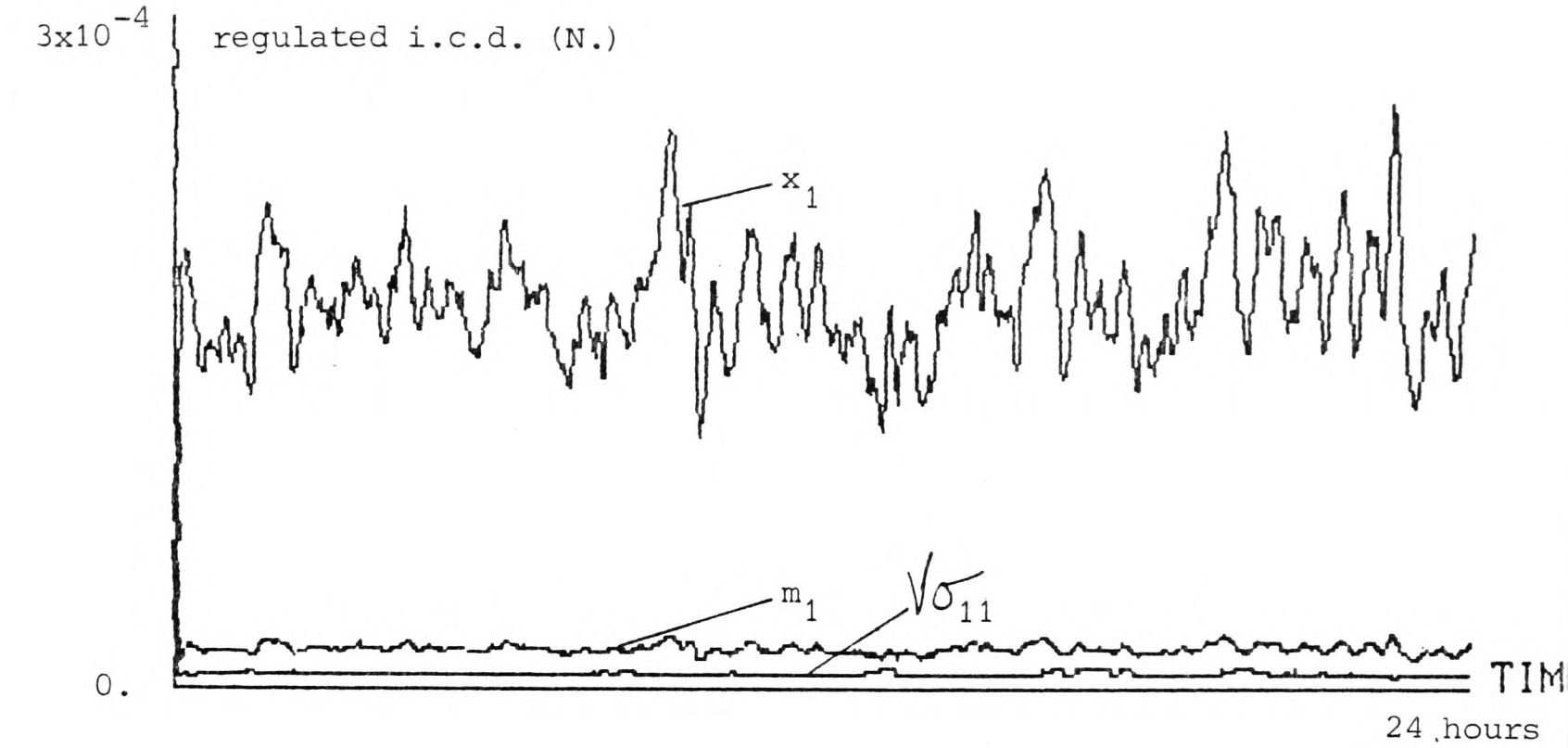
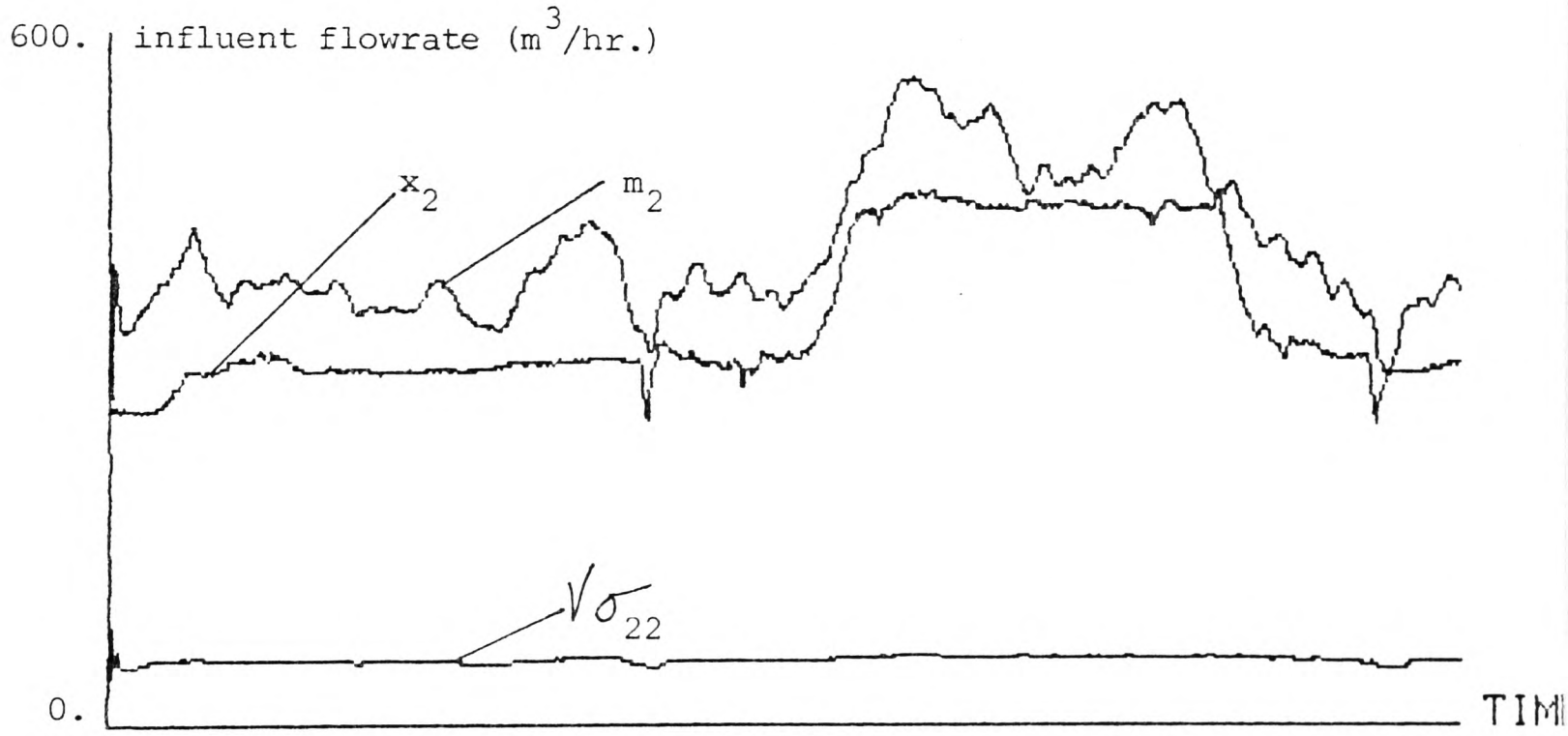


Fig 5.9 Effect of bias on state estimation: z= -1 pH unit





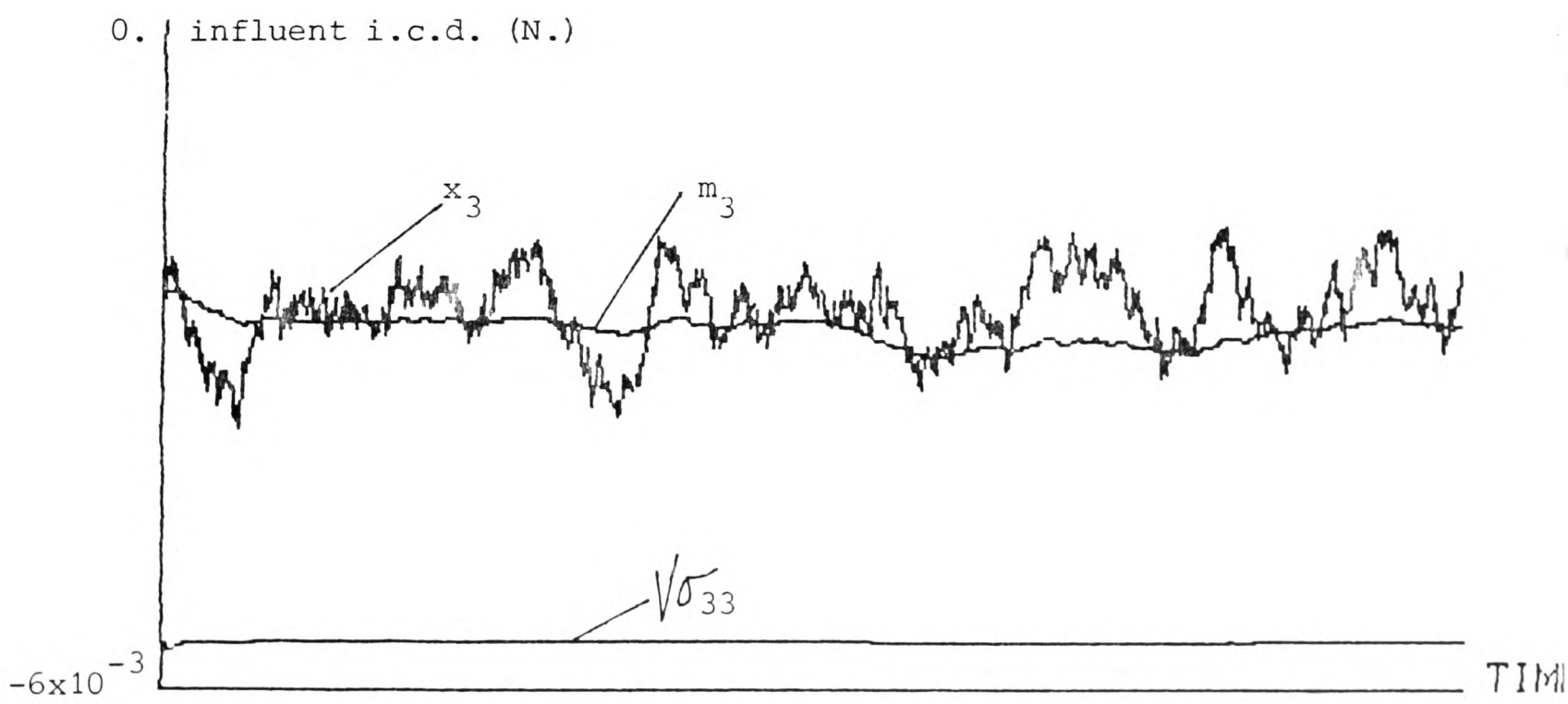


Fig 5.10 Effect of bias on state estimation: z= -1 pH unit

CHAPTER 6

CONTROL STRATEGIES FOR pH REGULATION

This chapter reports on two contributions: i) comparison of a large number of classical and stochastic control algorithms for pH regulation, ii) a novel cautious controller which is developed by the author.

Section 6.1 introduces the classical and stochastic controllers used in the chapter. Three cost functions which provide quantitative comparisons of the controllers are defined in section 6.2. Classical controllers are discussed in section 6.3 and the cautious controller is derived in section 6.4.

6.1 INTRODUCTION

Two different approaches to pH regulation in CSTR's were mentioned in chapter 1 and will be discussed in detail in this chapter; they are: the classical approach (section 6.3) and the stochastic approach (section 6.4).

Classical controllers use error-actuated feedback; additional feedforward signals about load disturbances in the form of influent flow and acidity may be used to improve performances. The error signal driving the controller can be generated as an error in pH or as an error

in ionic concentration difference as will be discussed in section 6.3.1. If, in some cases, feedforward measurements are not available, a state estimation filter (derived in chapter 5) may provide estimates of load disturbances which can be used as synthetic feedforward signals (section 6.3.2).

Simulated feedback controllers include:

(i) Standard three-term control with integral desaturation (PID)

(ii) Self-tuning three-term control (ST-PID) (Proudfoot 1983)

(iii) Generalised k-incremental minimal variance self-tuning control (K-STC) (Clarke et al 1983)

(iv) Pole placement self-tuning control (P-STC) (Wellstead et al 1979, Clarke 1982, Proudfoot 1983)

The three-term PID controller is widely used in industry and is included here to provide a basis for comparison and to assess the extent of the improvement which may be achieved by using more complex control algorithms. The ST-PID is a self-tuner with parameters interpreted as those of a PID regulator. The ST-PID and K-STC are implicit selftuners in the sense that the controller parameters are estimated directly. The P-STC is an explicit selftuner in which an estimator estimates the model parameters of the controlled process; these are subsequently used as the basis for the design of the controller. The implementation of the feedback controllers is assessed in section 6.3.3. The three self-tuning controllers are certainty-equivalent (Patchell and Jacobs 1971) controllers: they do not take into consideration the fact that their estimated parameters are not equal to the true ones and may be inaccurate.

On the other hand, the stochastic controller derived in section 6.4 is a cautious (Jacobs and Patchell 1972) controller: it uses estimates generated by the Extended Kalman Filter of chapter 5 and is aware of the resulting uncertainty. It takes a more cautious control action. The control algorithm is derived by minimizing a cost function which can be defined in terms of ionic concentration difference (section 6.4.2) or of pH. Caution arises in the controller when the pH cost function is minimized as is explained in section 6.4.3. Its effect is to move the operating pH set point of the controller to a region of lesser slope on the pH non-linearity where control is easier. The caution reproduces what a plant operator would do when he readjusts the operating point if control is not satisfactory.

To provide quantitative comparisons for the different controllers, statistical results (section 6.2) in the form of root mean square error in pH, average excess acidity below set point and average reagent flow are calculated for each simulated run. An example is used to assess the effect of a biased pH measurement on the quality of control.

A control strategy which summarises different regulation techniques for pH processes is presented in section 6.5. This strategy is based on the knowledge of the process titration curve and the feedforward signals, and on the presence of bias on the pH measurement. The strategy provides guidelines to the implementation of suitable controllers.

Simulation comparisons of all twenty-five controllers which are presented in this chapter were carried out on the interactive simulation package PHDESIGN.

6.2 pH COST FUNCTIONS

In this section, three pH cost functions are defined and the effect of biased measurement on their values is investigated. The three cost functions are: the Root Mean Square Error (RMSE) in pH, the Average Excess Acidity (AEA) below set point in pH, and the Average Reagent Flow (ARF) in m^3hr^{-1}. The cost functions are selected in order to evaluate the performance of the different control schemes in the light of constraints on acceptable pH control and on running costs.

the cost functions are recorded for all simulation runs and are displayed with the simulated time-histories. They are designed to reflect the quality of pH control and reagent economy.

The cost functions are given by:

$$1) \quad \text{RMSE (pH)} = J_1 = \left\{ \frac{1}{N} \sum (pH_0 - pH(x_1(i))^2 \right\}^{0.5} \qquad (6.1)$$

where N is the total number of control samples in the simulation run, pH_0 is the target value in pH, and $pH(x_1)$ is the actual effluent pH leaving the neutralization vessel;

$$2) \quad \text{AEA (pH)} = J_2 = \frac{1}{N} \sum P(i) \qquad (6.2)$$

where $P(i) = pH_0 - pH(x_1(i))$ for $pH(x_1) \leq pH_0$

$P(i) = 0$ for $pH(x_1) > pH_0$

$$3) \quad \text{ARF } (m^3hr^{-1}) = J_3 = \frac{1}{N} \sum u(i) \qquad (6.3)$$

where u(i) is the amount of reagent used at each control sample.

The actual effluent pH is used in the cost function instead of the measured pH because the evaluation of the controller performances should be in terms of the actual pH leaving the vessel and not the measured one. A difference between the two exists when there is some bias on the pH measurement which as discussed in section 4.1 may be due to probe fouling and/or poor calibration.

The cost functions defined in this section will provide a comparison of the performance of the different controllers described in section 6.3 and 6.4.

6.3 CLASSICAL CONTROLLERS

In this section, the classical control techniques introduced in section 6.1 are discussed. These techniques are summarised in figure 6.1. At the center of the classical control scheme lies the feedback controller which may be a PID regulator or a self-tuning regulator. Their individual merits are briefly discussed in section 6.3.3; a thorough description is available elsewhere (Proudfoot 1983). The performance of the feedback controller may be improved upon by an additional feedforward controller which can be driven either by measurement of load disturbances of inflow and incoming i.c.d. or by their estimates. The feedforward controller is derived in section 6.3.2. The feedback controllers of section 6.3.3 are driven by an error between the measured variable and the target value. The error can be calculated (section 6.3.1) either in terms of pH or in terms of ionic concentration difference. the error is also calculated if the pH measurement is biased and when the bias estimator of section 4.4 is activated. The effect of the bias on the quality of pH regulation under feedback control is also discussed. Simulation results are presented for all the different

controllers in section 6.3.4.

6.3.1 Error Signals For Feedback Controllers

In this section, the error signal driving the feedback controllers is calculated for bias-free and biased pH measurement as an error in pH or in i.c.d. Also, an example shows how a non-zero bias on the feedback measurement affect the pH regulation.

For bias-free pH measurement, the error is calculated as follow:

1) error in pH

$$e_{pH} = pH_0 - y \qquad (6.4)$$

where pH_0 is the target value of pH and y is the measured pH. This corresponds to what is usually done in practice with standard analog hardware. It makes no attempt at linearization. It can be used successfully (Proudfoot 1983) in neutralizing systems of buffered reagents in which the system non-linearity is not very severe.

2) error in ionic concentration difference X

$$e_X = X_0 - x \qquad (6.5)$$

with X_0, x obtained from pH_0 and y by inverting analytically the pH non-linearity of section 3.3 (figure 1.1). If there were no measurement noise, this would eliminate the pH non-linearity as discussed in section 4.2. Even when some noise is present, it may provide sufficient linearization of the pH measurement and improvement of performance to justify the expense of its implementation. Hewkin (1979) reports on a successful full-scale application of the analytical inversion for neutralization of strong reagents.

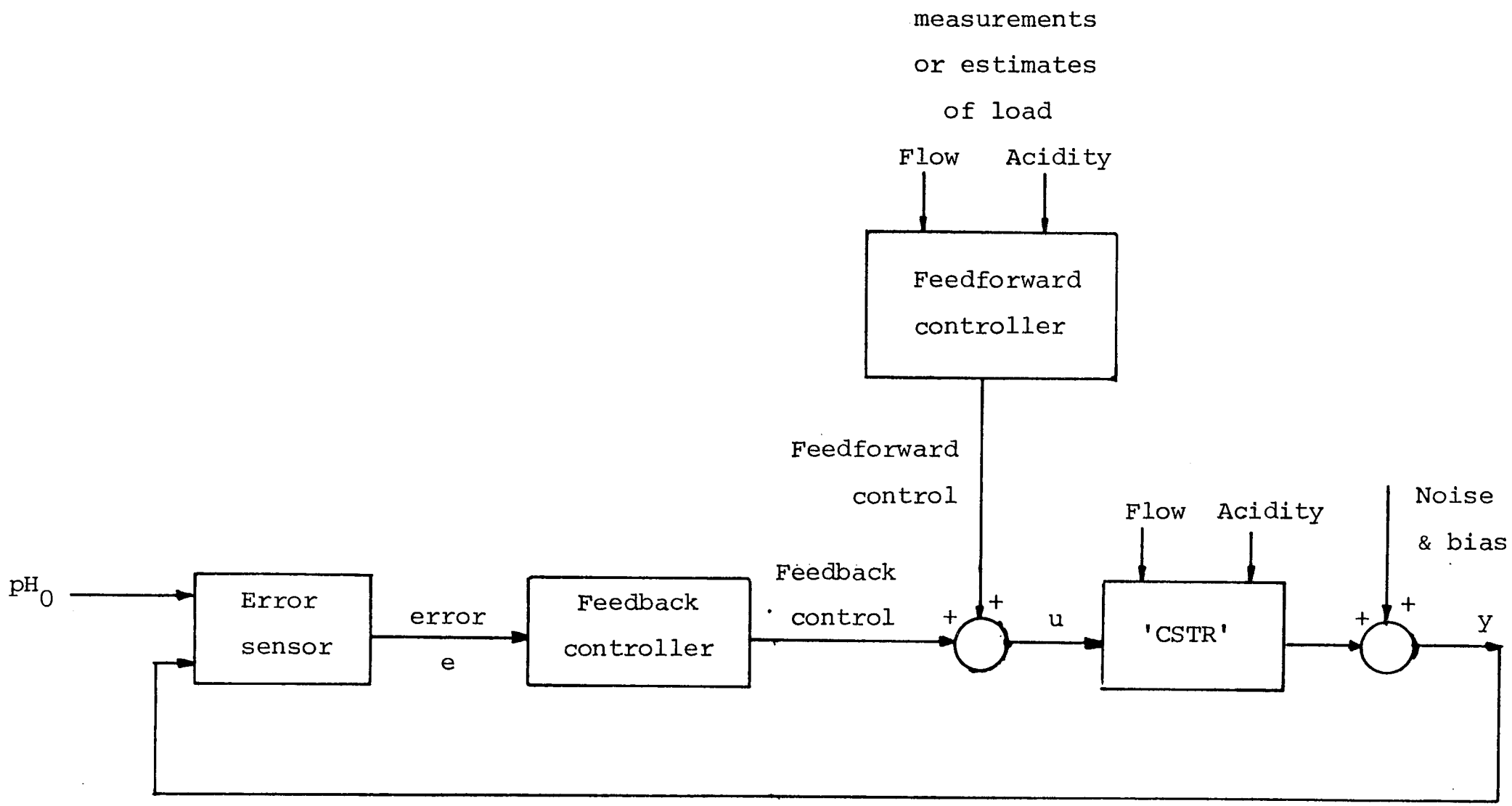


Fig 6.1 Structure of classical controllers

The measured variable of the feedback controller used in the calculation of the error was assumed to be bias-free. But, as discussed earlier in section 4.1, this may not be the case, and the pH measurement may be corrupted by additive bias. The bias estimator of section 4.4 coupled to the EKF estimator of section 5.2 can then be used to estimate the bias and the ionic concentration difference of the effluent. First, it is shown how the signal driving the feedback controller is calculated, then an example illustrates the improvement in regulation when the bias is estimated.

In the presence of non-zero bias, the error signal driving the controller is given by:

1) error in pH

$$e_{pH} = pH_0 - (y - m_z) \qquad (6.6)$$

where m_z is the bias estimate given by equation 4.31b.

2) error in X

$$e_X = X_0 - m_{k+3} \qquad (6.7)$$

where m_{k+3} is the estimate of the delayed (by k samples) effluent i.c.d. given by equation 5.10.

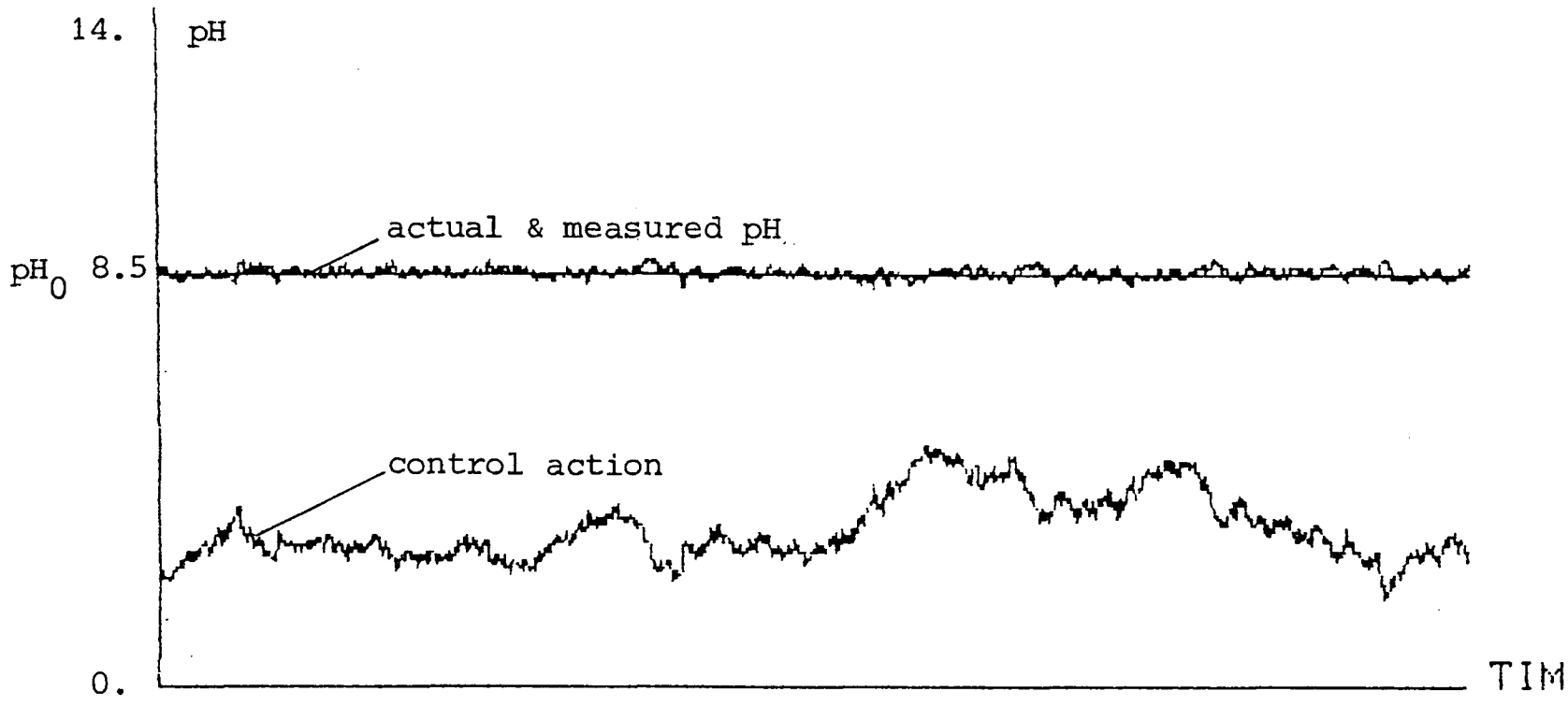
It was shown in section 5.5.2 how the bias on the measurement affects the state estimation; here, the effect of the bias on the cost functions and on the quality of regulation is illustrated by an example in figure 6.2. The example shows three simulation runs of a particular neutralization process: run A is when no bias is present, run B is when a constant bias (= -0.5 pH units) on the pH measurement exists but is not estimated, and

run C is when the bias is present and estimated using the Bayes' algorithm of section 4.4. Time histories of actual pH, measured pH, and control action are displayed for each run.

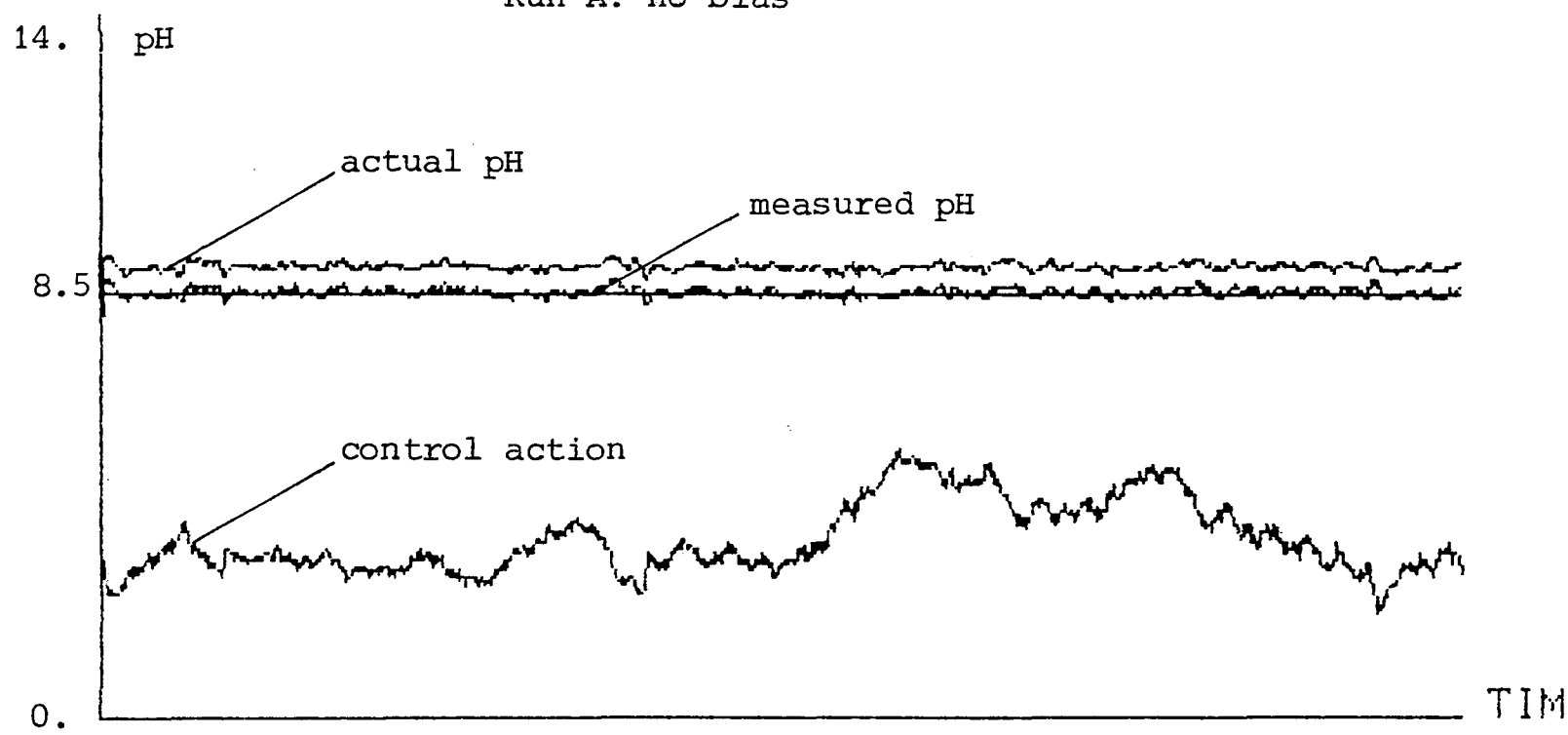
The values of the cost functions for the three runs are tabulated below:

	RMSE(pH)	AEA(pH)	ARF(m^3hr^{-1})
Run A	0.089	0.036	0.117
Run B	0.504	0.0	0.127
Run C	0.099	0.036	0.117

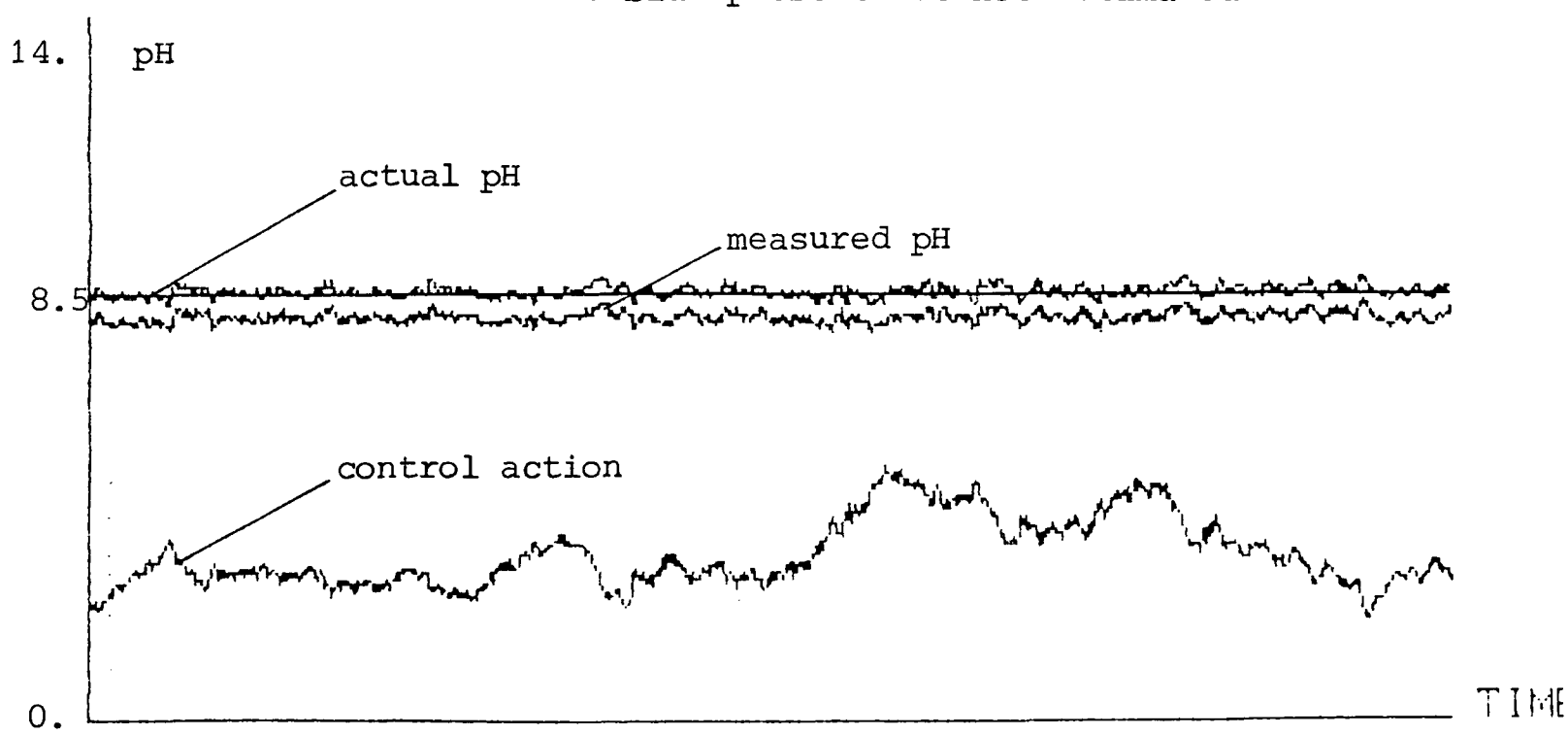
In run A, the control is good at the pH target value of 8.5 with a RMS error of 0.089; the time-histories of the actual pH and the measured pH are approximately the same because the measurement is bias-free (the difference between the two is due to the measurement noise). Time histories of run B show what might appear as good control of the measured pH at the required target value of pH 8.5, but the actual value of the pH is about pH 9. This is reflected in the value of the RMS error (= 0.504) and in the bigger amount of reagent needed to control the pH at a setpoint of 9 (ARF = 0.127). Run C, in which the bias is estimated, shows the actual pH controlled at the required value of pH 8.5 while the measured pH is levelled at pH 8. The RMS error of run C indicates that there is significant improvement in the quality of control over run B and that there is a slight deterioration in performance over run A. A confirmation that the effluent pH is controlled at the required value is given by the ARF which is the same value as in run A.



Run A: no bias



Run B: Bias present but not estimated



Run C: bias present and estimated

Fig 6.2 Effect of bias on regulation: z= -0.5 pH units

Simulation results in section 6.3.4, of two neutralization processes one of buffered reagents and the other of strong reagents, show the effect of the linearization on pH control. It did not improve performance significantly for the buffered process while the strong reagent process could not be successfully controlled at the required set point without it.

6.3.2 The Feedforward Controller

In this section, the feedforward controller is derived for strong and weak reagents, and for measured and estimated load disturbances. the incorporation of the feedforward control with the feedback is also described.

The feedforward control action $u_{FF}(i)$ is found by calculating the control action which is necessary to make (in equation 3.38) the steady state value of the effluent i.c.d. x_1 equal to the i.c.d. X_0. This gives:

$$X_0 = X_{in}(x_2, x_3, X_r, u_{FF}) \qquad (6.8)$$

where X_{in} account for the chemistry of neutralization and is given by equations 3.30. The feedforward control u_{FF} is given by:

$$u_{FF} = x_2(X_0 - x_3)/X_r \qquad \text{for strong reagents} \qquad (6.9)$$

$$u_{FF} = x_2(f_1^{-1}(X_0) - f_1^{-1}(x_3))/X_r \qquad \text{for buffered reagents} \qquad (6.10)$$

When the measurement of the load disturbances, y_2 for the inflow and y_3 for the incoming pH (equations 3.43), are available, y_2 and $pH^{-1}(y_3)$ replace x_2 and x_3 respectively in equation 6.9 or 6.10; $pH^{-1}(.)$ is the analytical inversion of the pH non-linearity. If the feedforward

measurements y_2 and y_3 are unavailable or too noisy, the EKF estimator of section 5.2 provides synthetic feedforward signals by producing on-line estimates of the load disturbances. These estimates m_2 and m_3, given by equation 5.10, are then substituted for x_2 and x_3 in equation 6.9 or 6.10. Only the mean values of the measurements or the estimates are used in equation 6.9 or 6.10 so as to keep the feedforward calculation simple. Any innacuracies are compensated for by the feedback controller.

The calculation of the feedforward control for buffered reagents is conditional on the knowledge of the titration curve because of the presence of the function $f_1^{-1}(.)$ in equation 6.10. $f_1^{-1}(.)$ is given by the titration data points and is implemented as a look-up table. If the titration curve is variable or unknown, it may be estimated from the amount of reagent needed for control and from the feedback and feedforward signals. This estimation procedure can provide an important area of future research as will be discussed in chapter 9.

The feedforward control $u_{FF}(i)$ is added to the feedback control $u_{FB}(i)$ as in figure 6.2 to give the total control action (reagent flow rate) u(i):

$$u(i) = u_{FB}(i) + u_{FF}(i) \qquad (6.11)$$

with the following limits on each control:

$$0 \leq u_{FF} \leq u_{max}$$

$$-u_{max} \leq u_{FB} \leq u_{max}$$

$$0 \leq u \leq u_{max}$$

where u_{max} is the maximum reagent flow allowed. This limits the total control action u(i) between 0 and u_{max} and the feedback controller can clip the feedforward completely.

Simulation results in section 6.3.4 show the effect of the feedforward on regulation performance and the difference in the quality of control when measured and estimated feedforward are used.

6.3.3 The Feedback Controllers

In this section, the four feedback controllers introduced in section 6.1 are briefly described. They are: the three-term fixed-parameter PID regulator, the three-term selftuner ST-PID, the K-incremental selftuner K-STC, and the pole-placement selftuner P-STC.

All feedback controllers have as their input an error signal (section 6.3.1) and as their output a signal used to manipulate the process through an actuator. The relationship between the input and the output signals may be independent of the process as in the PID regulator, or it may be a function of estimates of the process parameters as in the selftuners.

i) The fixed-parameter PID regulator:

PID regulators are widely used in industry in general and in pH regulation in particular (as surveyed in chapter 2) because they give acceptable performance, are robust, and are easy to use.

The classical PID algorithm has the following form:

$$u(t) = K \left\{ e(t) + \frac{1}{T_i} \int e(t)dt + T_d \frac{de}{dt}(t) \right\} \qquad (6.12)$$

where

u(t) is the control action at time t,

e(t) is the error between the setpoint and the measured output,

K is the controller gain,

T_i, T_d are the integral and derivative terms respectively.

The PID regulator of equation 6.12 may show a very large increase in the integral term $\int e(t)dt$ with a sustained deviation from the setpoint. This is termed as integral "wind-up" and can be overcome by desaturating the integral store.

Manual tuning of the PID parameters for pH regulation is difficult and time consuming. Controller settings for linear systems recommended by Ziegler and Nichols (1944) cannot be used for pH because of the large variations of the process gain of the pH system (section 1.2). Other alternatives to the PID are the selftuning regulators which automatically tune the controller parameters according to the process variations.

ii) The selftuning regulators:

The three selftuning regulators have been implemented in the CAD simulation package PHDESIGN. Their application to pH regulation is briefly described here. The self-tuning PID regulator was the most common used of all feedback controllers in simulation because of its ease of use and its robustness. It proved to be so satisfactory that it was used wherever a fixed-parameter PID regulator needed to be implemented. The ST-PID has also been used to validate the simulation (as will be shown in chapter 8) of the pH model of chapter 3 and to demonstrate that selftuning can lead to improved performance (section 6.3.4) over a conventional PID control. It was also used to provide good feedback control in CAD studies both of process configurations and controller configuration (Chapter 8, case study 2).

The other selftuners implemented in simulation are the general implicit K-incremental selftuner (K-STC) and the general explicit pole-placement selftuner (P-STC). The P-STC needed more computing power than the other two selftuners but gave better performance (section 6.3.4) because it can handle the uncertain time-delays caused by fluctuating flow rate through the neutralization process. The performance of the K-STC matched that of the PID selftuner and the latter was preferred because of its simplicity.

The computer coding of all three selftuners were taken "off the shelf" (from Proudfoot (1983) and from the selftuning control group at the Department of Engineering Science) to be implemented in the CAD package after slight modifications. The performance of the selftuning controllers is compared in the next section with that of the fixed-parameter PID for two simulated neutralization processes to show how much improvement automatic tuning can bring to pH regulation.

6.3.4 Simulation Results Of Classical Controllers

Simulation results for of the different classical controllers of section 6.3 are presented in this section. Quantitative and qualitative comparisons are carried out in order to determine the benefits of feedforward and selftuning control over the fixed-paramater PID feedback. Two neutralization processes are used as simulation test-bed: process A in which the titration curve is the theoretical strong reagent (as defined in section 3.2.2), and process B which has a buffered titration curve. Performance comparisons are for one operating point for process A, and ~~for~~ two for process B. The two processes were used earlier in section 5.5 as a test-bed for the investigation of the Kalman filter estimation of load disturbances. These disturbance estimates will be used here as synthetic feedforward measurements as discussed in section

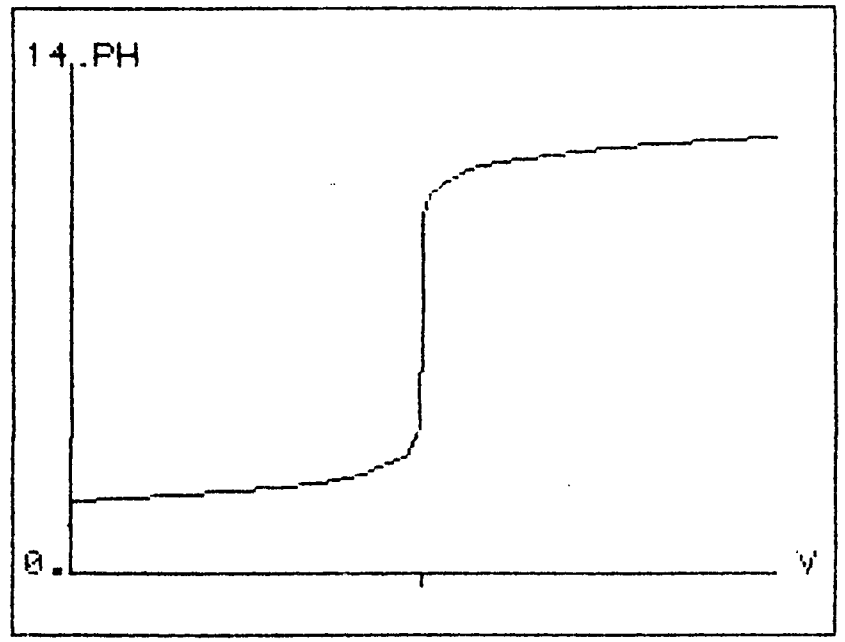
6.3.2. The parameters of the processes are displayed in figures 6.3 and 6.4. The displays are generated by the CAD package PHDESIGN.

The simulation results for processes A and B are shown in tables 6.1 to 6.3, in the form of the cost functions defined earlier in section 6.2. The results are for four feedback controllers, driven by the error in i.c.d. in process A, and by the error in pH in process B, with and without the additional feedforward signals of measured or estimated load disturbances. The inclusion of the performances of the raw feedback (without feedforward) is given so that any improvement due to feedforward control can be assessed. The simulation runs for each process are comparable because all runs use identical sequences of random variables.

The results of classical controllers are classified in the tables according to, horizontally, the a priori information about the disturbances, and vertically, the complexity of the feedback controllers. The simplest controller is the PID regulator, and when no information on the load is available, the controller is used in feedback configuration only. When some feedforward information (such as rate of change, mean value, and standard deviation) of the inflow and the incoming i.c.d. exists, the EKF of chapter 5 generates estimates of the load disturbances which can be used as estimated feedforward. Finally if the disturbance measurements are obtainable, they are used instead of the estimates in the feedforward controller. The quality of the measured feedforward control is a function of the quality of the measurements: low measurement noise and bias-free measurement should lead to good feedforward control. In the simulation runs, it is assumed that the disturbance measurements are good and representative of the different loads. Nonetheless, the effect of noisy measurement can be assessed using the CAD package as discussed in section 6.2 which showed the effect

PLANT A G3 STRONG REAG.

PH SET POINT	12.000
REACTOR VOL. (M3)	15.000
MAX. TIME DELAY (MIN.)	1.000
DELAY : T. CONST. RATIO	0.100
REACTOR TEMP. (C)	25.00
REAGENT CONC. (N.)	17.650
MAX. REAGENT FLOW (M3/HR.)	9.000
STRONG (0) - BUFF.(1) REAG.	0



DISTURBANCES : WIENER PROCESSES OR PLANT DATA

	T. CONST.(MIN.)	MEAN	STAND. DEV.
FLOW (M3/HR.)	0.800E+02	0.480E+02	0.495E+01
CONC. (N.)	0.100E+03	-0.600E+00	0.600E-01

MEASUREMENTS:

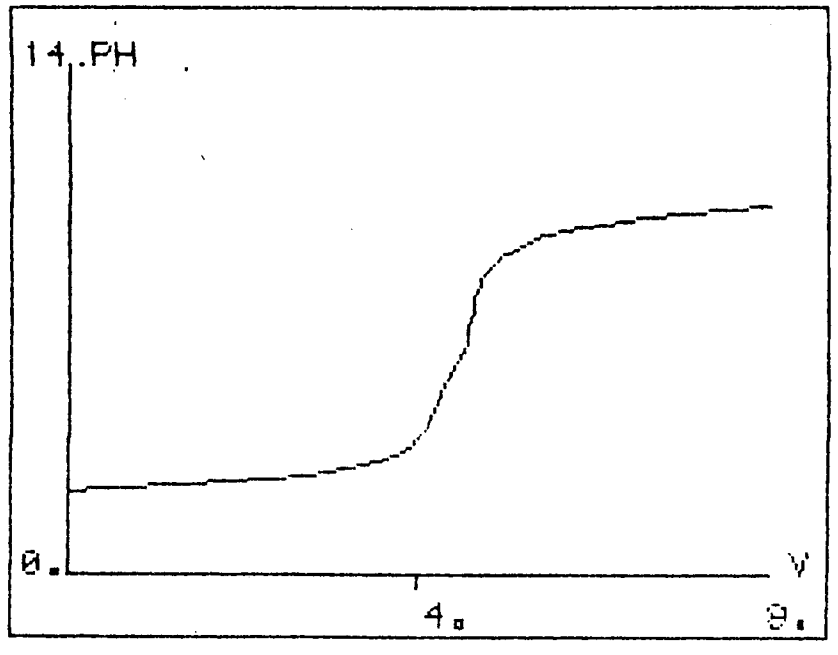
	SD. NOISE	FILTER (MIN.)	PRESENT	BIAS
PH OUT (PH)	0.01	0.10	1	0.00 - 0
FLOW IN (M3/HR)	2.00	3.00	0	
PH IN (PH)	0.01	1.50	0	

SIMULATED pH PROCESS: HE,HC,DP,DT,MP,MT,RE,CO,OQ ? HC

Fig 6.3 Process A

FLANT B WBT103 A P.DATA

PH SET POINT	8.500
REACTOR VOL. (M3)	40.000
MAX. TIME DELAY (MIN.)	1.500
DELAY : T. CONST. RATIO	0.100
REACTOR TEMP. (C)	50.00
REAGENT CONC. (N.)	5.200
MAX. REAGENT FLOW (M3/HR.)	0.500
STRONG (0) - BUFF.(1) REAG.	1



DISTURBANCES : WIENER PROCESSES OR PLANT DATA

	T. CONST.(MIN.)	MEAN	STAND. DEV.
FLOW (M3/HR.)		*** PLANT DATA ***	
CONC. (N.)	0.600E+02	-0.316E-02	0.500E-03

MEASUREMENTS:

	SD. NOISE	FILTER (MIN.)	PRESENT	BIAS
PH OUT (PH)	0.01	0.10	1	0.00 - 0
FLOW IN (M3/HR)	5.00	3.00	0	
PH IN (PH)	0.01	1.50	0	

SIMULATED pH PROCESS: HE.HC.DP.DT.MP.MT.RE.CO.OQ ? HC

Fig 6.4 Process B

of a biased effluent pH measurement on regulation.

The complexity of the four feedback controllers increases from the PID, whose fixed parameters are the same as the initial ones of the ST-PID, through the implicit PID and k-incremental selftuners to the more complex implicit pole placment. In order to justify the cost of implementation, one would expect that the more complex the controller, the better its performance. Hence, the P-STC coupled to measured feedforward control (lower right side corner of the tables) should produce the "best" results, which is the case in all three tables. Best results mean smallest Root Mean Square Error and smallest Average Excess Acidity. The ratio of the quality of control (measured as RMSE), of the most complex self-tuner (the P-STC) with the measured feedforward control to that of the simplest raw feedback controller (the PID) provides a measure of the improvement complex controllers may bring. A high ratio for a particular process means that implementation of complex controllers and possibly feedforward measurements can be justified.

Process A:

For process A (figure 6.3), a setpoint of pH 12 is selected. The error (section 6.3.1) driving the feedback controllers is calculated as an error in ionic concentration difference (i.c.d.) amounting to a linearization of the pH measurement. The error in i.c.d. was chosen after preliminary results showed that the pH could not be controlled without the linearization. This is because the linearization reduces the highly non-linear process titration curve to a straight line as discussed in section 3.2.2.

Controller configurations

	Raw Feedback	+ Estimated Feedforward	+ Measured Feedforward
PID	0.114	0.100	0.100
ST-PID	0.105	0.087	0.086
K-STC	0.102	0.079	0.077
P-STC	0.099	0.057	0.056

Root Mean Square Error (RMSE) in pH

Controller configurations

	Raw Feedback	+ Estimated Feedforward	+ Measured Feedforward
PID	0.052	0.046	0.046
ST-PID	0.048	0.039	0.039
K-STC	0.047	0.035	0.034
P-STC	0.046	0.029	0.028

Average Excess Acidity (AEA) in pH

Average Reagent Flow (ARF) in m^3hr^{-1} = 1.61 for all twelve runs.

TABLE 6.1 Quantitative comparisons of classical controllers

Process A; pH setpoint = 12.0

The simulation results of process A are shown as Root Mean Square Error and Average Excess Acidity in table 6.1. It is seen that with feedback alone, there is about 10% improvement in performance from any selftuner over the fixed-parameter PID. The use of feedforward (whether estimated or measured) produces a noticeable improvement in RMSE over feedback alone, with the largest improvement (from 0.099 to 0.056) when it is coupled to the implicit pole-placement selftuner. There is a slight improvement in performance from the estimated to the measured feedforward. The size of the improvement shows that the estimate of inflow and incoming i.c.d. which were generated by the EKF in chapter 5, are good, and are comparable to their measurements.

The improvement ratio, defined earlier in this section, for process A, of the pole placement with measured feedforward (RMSE = 0.056, AEA = 0.028) compared to the PID with no feedforward (RMSE = 0.114, AEA = 0.052) is equal to two.

Process B:

Process B (figure 6.4), is a simulation of the full-scale neutralization reactor T103A of Caster Kellner works at ICI. The process was introduced in section 1.1 when outlining the objective of the ICI project, and will be discussed in detail in chapter 8. The flow disturbances used in the simulation of this process are plant recorded data. Comparisons of the controllers are carried out for two different target values: pH 8.5 and pH 8. The setpoint pH 8.5 was chosen so as to compare the simulation results with the full-scale trials in which the operating target value was usually pH 8.5. The value of pH 8 was chosen as corresponding to a more difficult control region in order to see if

selftuning control and/or the addition of feedforward signals would give any improvement over the fixed-parameter PID. Because the process titration curve was well buffered, it was believed that the linearization of the pH measurement will not improve performance and the error driving the feedback controller was selected as the error in pH (section 6.3.1). This was confirmed by preliminary simulation runs.

Comparable results of process B are shown in tables 6.2 and 6.3 for setpoint pH 8.5 and pH 8 respectively for the four feedback controllers with and without feedforward control. It is seen (table 6.2) that at a set point of pH 8.5, using feedback alone, all three selftuners produce better performance than the fixed-parameter PID, but there is little to choose between any of them. It can also be seen that the use of estimated feedforward produces some improvement for all controllers and that using measured feedforward gives slightly better performance still. For the case of the pole-placement controller, the RMSE (0.038) is identical in each case this being the smallest of all four controllers.

The improvement in performance from the raw PID regulator (RMSE = 0.087, AEA = 0.035) to the pole placement + measured feedforward (RMSE = 0.038, AEA = 0.015) is over twice as large.

At a set point of pH 8 (table 6.3), the process is more non-linear and hence more difficult to control. The fixed-parameter PID with no feedforward shows a relatively large RMSE of 0.26. Time-histories of this run are displayed in figure 6.5a and show the actual pH dipping into the acid region after 10 hours of simulation because of the load change. On the other hand, the estimates of all three selftuners have adapted to this load variations resulting in better control (RMSE < 0.1). The addition of feedforward (estimated or measured) to feedback control also

Controller configurations

	Raw Feedback	+ Estimated Feedforward	+ Measured Feedforward
PID	0.260	0.110	0.094
ST-PID	0.097	0.087	0.084
K-STC	0.096	0.100	0.098
P-STC	0.092	0.077	0.066

Root Mean Square Error (RMSE) in pH

Controller configurations

	Raw Feedback	+ Estimated Feedforward	+ Measured Feedforward
PID	0.101	0.047	0.037
ST-PID	0.040	0.037	0.034
K-STC	0.038	0.038	0.038
P-STC	0.037	0.029	0.026

Average Excess Acidity (AEA) in pH

Average Reagent Flow (ARF) in m^3hr^{-1} = 0.111 for all runs except for Raw Feedback PID for which ARF = 0.112

TABLE 6.3 Quantitative comparisons of classical controllers

Process B; pH setpoint = 8.0

Controller configurations

	Raw Feedback	+ Estimated Feedforward	+ Measured Feedforward
PID	0.087	0.064	0.053
ST-PID	0.054	0.052	0.048
K-STC	0.056	0.054	0.051
P-STC	0.055	0.038	0.038

Root Mean Square Error (RMSE) in pH

Controller configurations

	Raw Feedback	+ Estimated Feedforward	+ Measured Feedforward
PID	0.035	0.025	0.021
ST-PID	0.021	0.019	0.017
K-STC	0.022	0.022	0.020
P-STC	0.020	0.015	0.015

Average Excess Acidity (AEA) in pH

Average Reagent Flow (ARF) in m^3hr^{-1} = 0.117 for all twelve runs.

TABLE 6.2 Quantitative comparisons of classical controllers

Process B; pH setpoint = 8.5

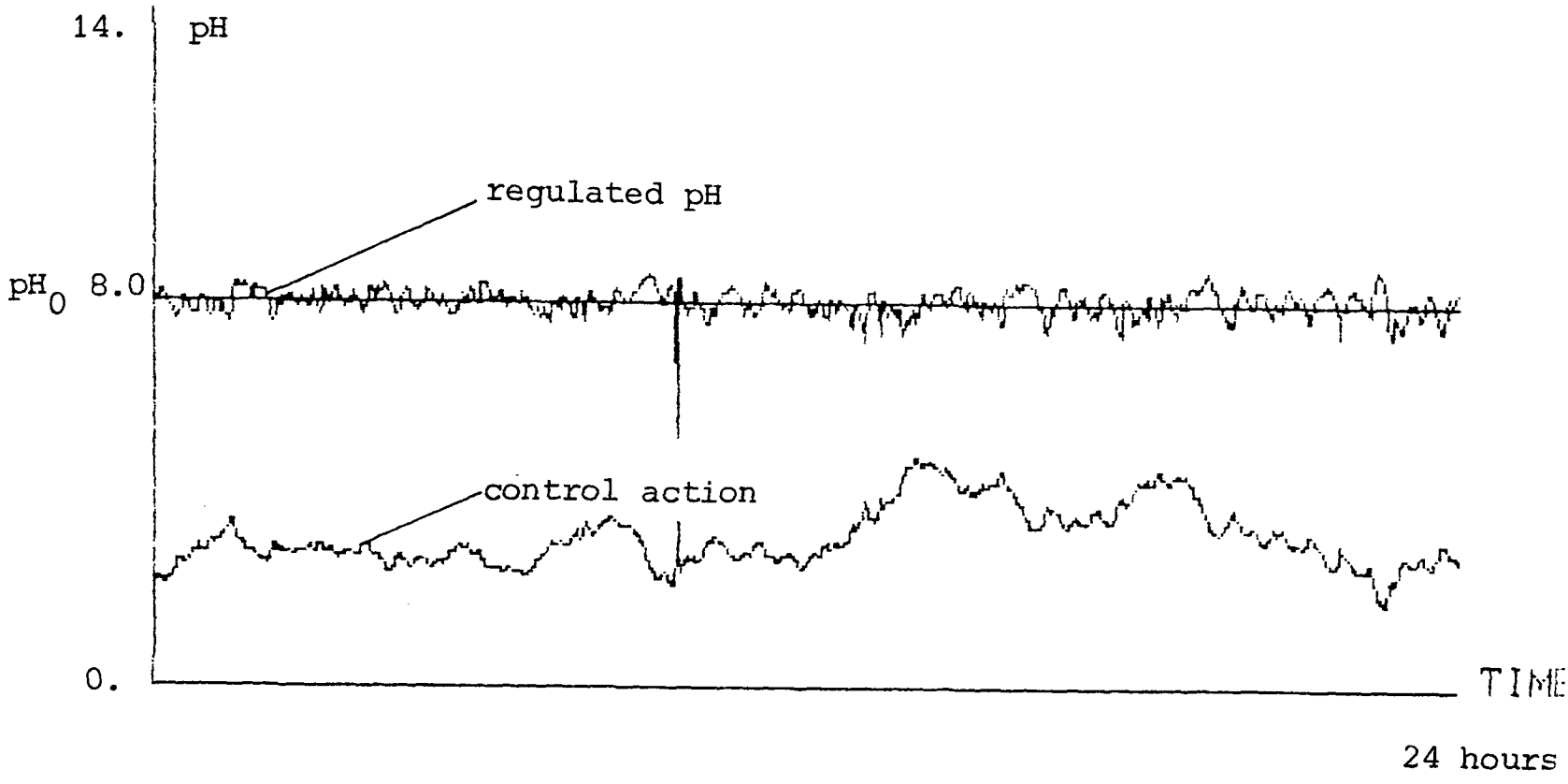
produced some improvement because the controller was aware (from the feedforward signals) of the load change and was able to take a more appropriate corrective action resulting in an even smaller RMSE. Figure 6.5b shows qualitatively, the improvement over the raw PID (figure 6.5a) when using the pole-placement selftuner with additional measured feedforward.

The improvement ratio for a setpoint of pH 8 of the P-STC with measured feedforward (RMSE = 0.066, AEA = 0.026) to the raw PID regulator (RMSE = 0.260, AEA = 0.101) is equal to about four. It is also noted that the amount of reagent used (ARF) when control was poor under PID (0.112) was slightly more than for any other controller (0.111).

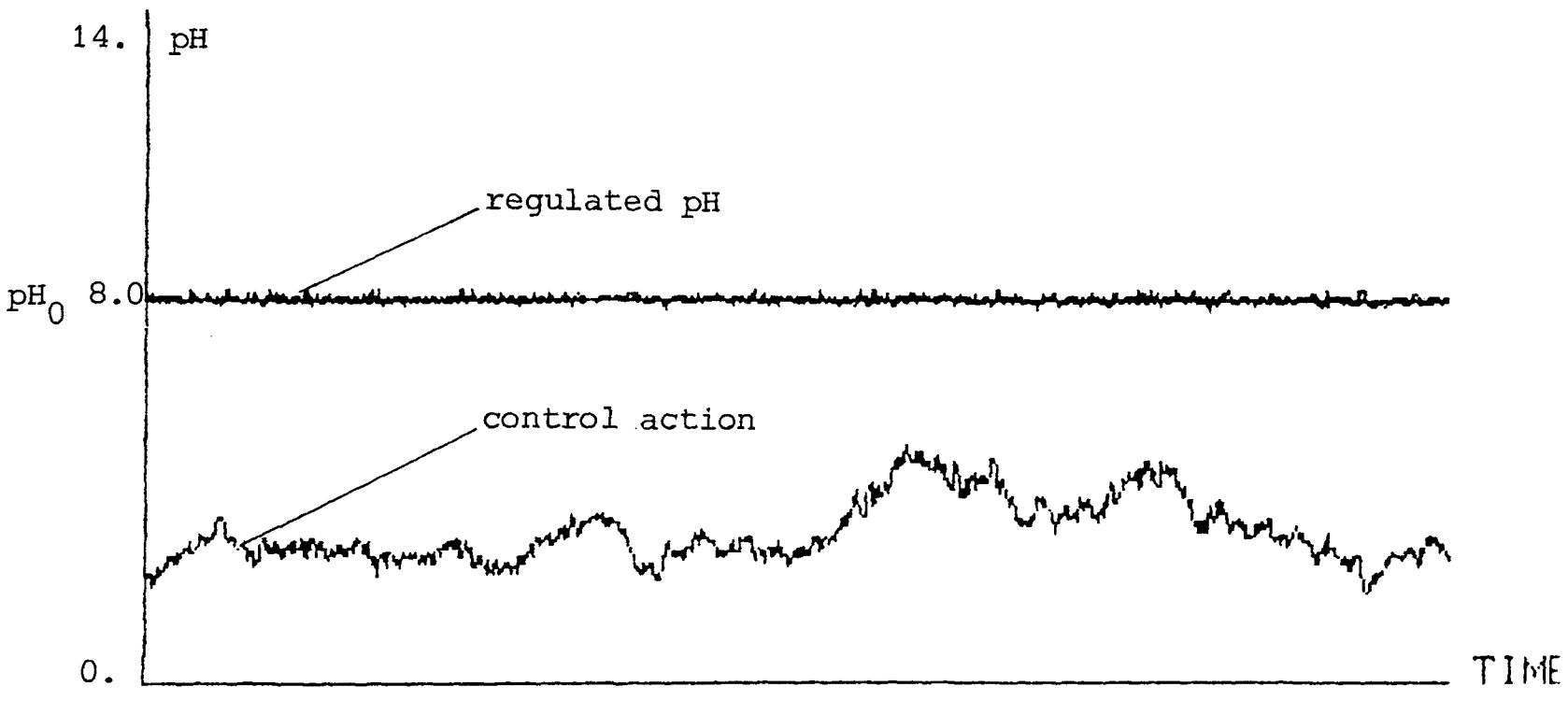
6.3.5 Discussion Of Results

The results of classical controllers presented here show that improvement in performance over a fixed-parameter PID regulator is possible if one uses more complex feedback control and has access to feedforward information. The improvement is dependent on each process and its parameters; it varies from a factor of two for weakly non-linear pH systems, such as process A after linearization or process B at setpoint pH 8.5, to a factor of four for the more non-linear pH system of process B at setpoint pH 8.

The performance of the pole-placement selftuner coupled to measured feedforward has been the best of all classical controllers at the cost of a more complex feedback algorithm. This good performance is because the pole-placement algorithm is estimating an explicit model, and thus could handle the uncertain time-delays caused by fluctuating flow rate through



a. Raw PID: r.m.s. error = 0.260 pH units



b. P-STC + measured feedforward
r.m.s. error = 0.066 pH units

Fig 6.5 pH regulation of process B

the neutralization process. There is little to choose between the still satisfactory performance of the other two selftuners: dynamics of the controlled process were sufficiently simple that they can be well matched by the selftuner PID and so there is little need for the more complex general k-incremental selftuner.

The results of classical controllers shown in this section have confirmed that if a controlled process can be satisfactorily regulated using a fixed-parameter PID, then a selftuner can achieve a better performance and show more robust behaviour to load changes than a conventional controller. The results also show good feedforward measurements result in better control, and that moreover, estimated feedforward signals can improve upon the performance of the feedback controller if no feedforward measurements are available.

6.4 STOCHASTIC CONTROL

In this section, a novel cautious stochastic controller is derived for the pH model of chapter 3. The controller is derived by minimizing a performance index which can be defined in terms of ionic concentration difference (i.c.d.) or in terms of pH. The controller is driven by the state estimates of the pH model generated by the Extended Kalman Filter (derived in section 5.2) coupled to the Linearised Bayes' Estimator of chapter 4. The control law is cautious because it takes into account the uncertainties about the state estimates in the form of their covariance matrix. In order to show the effect of caution, the stochastic control action u(i) may be regarded as a sum of two components, a certainty-equivalent control u^{ce}, plus caution:

$$u(i) = u^{ce}(i) + u^{caution}(i) \qquad (6.13)$$

where $u^{ce}(i)$ is the control action when there is no uncertainty and $u^{caution}(i)$ provides an indication of the control which allows for the state uncertainties.

The stochastic controller, unlike the classical controllers of section 6.3, does not differentiate between feedback and feedforward signals. Its general structure is shown in figure 6.6, and the controller is separated into two operations: state estimation and control. Because the pH system, for which the controller is designed, is non-linear these two operations cannot be performed optimally and the stochastic controller is thus a suboptimal controller.

Section 6.4 is arranged as follows: The performance indices for which the stochastic control is derived are defined for i.c.d. and for pH in section 6.4.1. This lead to the derivation of two control laws: an i.c.d. control law in section 6.4.2 and a pH control law in section 6.4.3. Simulation results of the stochastic controller are compared with those of the classical controllers in section 6.4.4.

6.4.1 The Performance Indices

The discrete-time pH model of section 3.4, for which the performance indices are defined, is restated here:

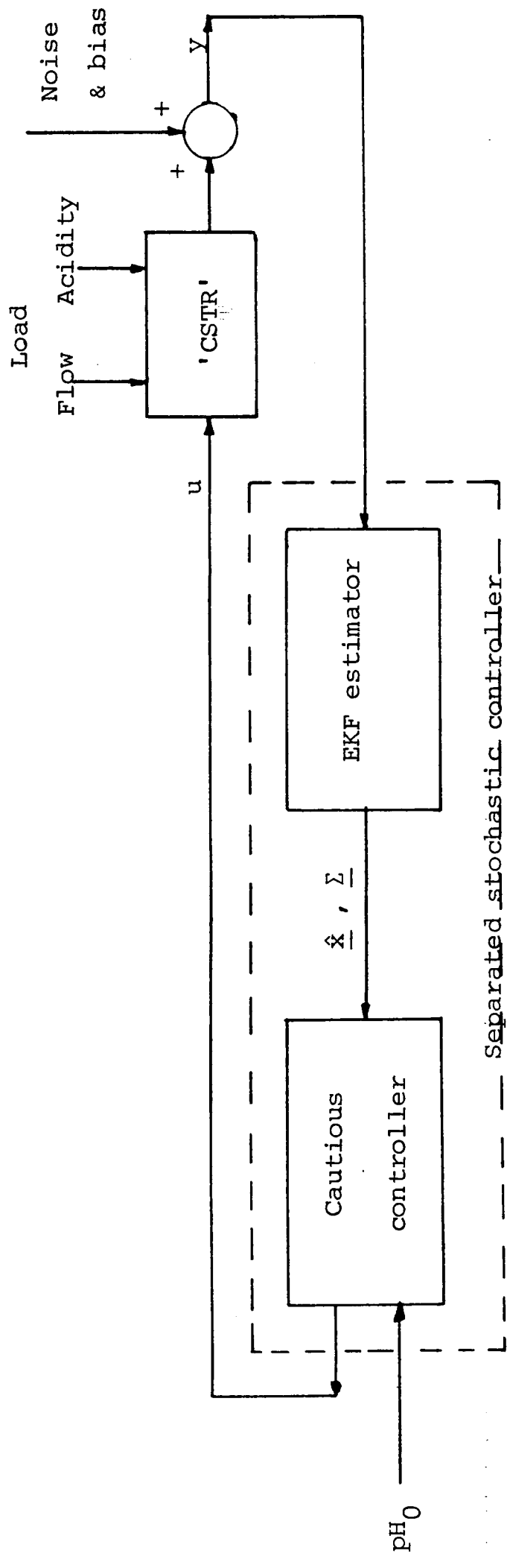


Fig 6.6 Structure of the stochastic controller

$$x_1(i+k+1) = x_1(i+k) + \frac{\Delta}{V} x_2(i)(X_{in}(i) - x_1(i+k)) + \xi_1$$

$$x_j(i+1) = g_j x_j(i) + \alpha_j + \xi_j \qquad j=2,3$$

$$x_4(i+1) = x_1(i+k)$$

$$x_5(i+1) = x_1(i+k-1) \qquad (3.46)$$

.

.

$$x_{k+3}(i+1) = x_1(i+1)$$

$$y(i) = pH(x_1(i)) + \eta$$

where X_{in} accounts for the chemical analysis of the neutralization reaction, and is given by:

$$X_{in} = x_3 + uX_r/x_2 \qquad \text{for strong reagents} \qquad (3.30a)$$

$$X_{in} = f_1(f_1^{-1}(x_3) + uX_r/x_2) + \delta X \qquad \text{for weak reagents} \qquad (3.30b)$$

The cost function for a generalised minimum variance controller for a given process is defined by (Iserman 1981):

$$J = E\left[\{\Phi_0 - \Phi(i+k+1)\}^2 + qu^2(i) \middle| u(i), i\right] \qquad (6.14)$$

where Φ_0 and $\Phi(i+k+1)$ are the process target value and controlled output, and q is a weighting factor on the control action u(i). This weighting factor is included (Clarke and Hastings-James 1971) in the cost function in order to prevent the cancellation of the zeros of the process and to limit excessive control input. q is particularly useful for non-minimum phase plants which have unstable zeros. However, because the pH process modelled by equations 3.46 is not non-minimum phase and its control input is limited, q is set to zero. This leads to a minimum variance control law in which the objective of the control action u(i) is to minimise the

error between the controlled output $\Phi(i+k+1)$ and the target value Φ_0 in the cost function:

$$J_{\Phi} = E\left[\left\{\Phi_0 - \Phi(i+k+1)\right\}^2 \middle| u(i), i\right] \qquad (6.15)$$

Φ_0 and $\Phi(i+k+1)$ can either be in terms of ionic concentration difference (i.c.d.) X or in terms of pH, giving the two cost functions:

$$J_X = E\left[\left\{X_0 - x_1(i+k+1)\right\}^2 \middle| u(i), i\right] \qquad (6.16)$$

$$J_{pH} = E\left[\left\{pH_0 - pH(x_1(i+k+1))\right\}^2 \middle| u(i), i\right] \qquad (6.17)$$

where x_0 & pH_0 are the target value in i.c.d. and pH respectively; x_1 is the i.c.d. of the controlled effluent and the function pH(.) is given by equation 3.28. The state $x_1(i+k+1)$ rather than $x_1(i)$ appears in the cost functions because in the discrete-time system of equations 3.46, $x_1(i+k+1)$ is the state affected by u(i) (of $X_{in}(i)$). The resulting control action u(i) minimises the k steps ahead output $x_1(i+k+1)$ of $pH(x_1(i+k+1))$, where k represents the integer time-delay in the controlled process. Hence, the controller is termed the suboptimal k-step ahead controller.

The pH cost function J_{pH} of equation 6.17 is the one used to calculate the control action u(i) in the cautious controller, because pH is the measured variable and the quality of control (section 6.2) is quantified in terms of deviations from pH setpoint. Furthermore, a pH control law would take into account the asymmetry of the pH non-linearity about the operating point.

The i.c.d. control law for the i.c.d. cost funtion J_X is also derived

because its results are needed to calculate the pH control law.

6.4.2 The i.c.d. Control Law

In this section, a cautious i.c.d. control law for strong and weak reagents is derived using the cost function of equation 6.16. The control action u(i) is made of two terms: a certainty equivalent control and a cautious term.

Replacing for $x_1(i+k+1)$ from equations 3.46 into the cost function J_X of equation 6.16:

$$J_X = E\left[\left\{X_0 - x_1(i+k) - \frac{\Delta}{V} x_2(i)(X_{in}(i) - x_1(i+k)) + \xi_1\right\}^2 \middle| u(i), i\right] \qquad (6.18)$$

where $X_{in}(i)$ is given by equations 3.30 for strong and weak reagents.

i) Strong Reagents:

Substituting $X_{in}(i)$ from equation 3.30a into equation 6.18:

$$J_X = E\left[\left\{X_0 - x_1(i+k) - \frac{\Delta}{V}(x_2(i)(x_3(i) - x_1(i+k)) + u(i)X_r) + \xi_1\right\}^2 \middle| u(i), i\right] \qquad (6.19)$$

Minimising J_X by calculus with respect to u(i) gives the k-step ahead control law:

$$u(i) = E\left[\frac{V}{\Delta}(X_0 - x_1(i+k)) + x_2(i)(x_1(i+k) - x_3(i))\right] \Big/ X_r \qquad (6.20)$$

Replacing the expected values of the states by their estimates (equation 5.10) generated by the Kalman filter:

$$E[x_1(i+k)] = m_1(i)$$

$$E[x_2(i)x_1(i+k)] = m_2(i)m_1(i) + \sigma_{12}(i)$$

$$E[x_2(i)x_3(i)] = m_2(i)m_3(i) + \sigma_{23}(i)$$

where m_1, m_2 & m_3 are the estimates given by the EKF (equation 5.1) and σ_{12} & σ_{23} are the corresponding elements of the covariance matrix Σ given by equation 5.4. Hence, the i.c.d. cautious controller for strong reagents is given by:

$$u(i) = \left[\frac{V}{\Delta} (X_0 - m_1(i)) + m_2(i)(m_1(i) - m_3(i)) + \sigma_{12}(i) - \sigma_{23}(i) \right] / X_r \qquad (6.21)$$

The certainty-equivalent controller u^{ce} may be obtained from equation 6.21 by neglecting all the covariance terms:

$$u^{ce}(i) = \left[\frac{V}{\Delta} (X_0 - m_1(i)) + m_2(i)(m_1(i) - m_3(i)) \right] / X_r \qquad (6.22)$$

Substracting equation 6.22 from equation 6.21 yields the caution term:

$$u^{caution}(i) = (\sigma_{12}(i) - \sigma_{23}(i))/X_r \qquad (6.23)$$

The caution term is due to the non-linearity in the modelling of the tank dynamics of the pH model in equations 3.46: $x_2(i)(x_1(i+k) - x_3(i))$.

ii) Weak Reagents:

Substituting $X_{in}(i)$ from equation 3.30b into equation 6.18:

$$J_X = E \left[\{ X_0 - x_1(i+k) - \frac{\Delta}{V} (x_2(i)(f_1(f_1^{-1}(x_3(i)) + u(i)X_r/x_2(i))) - x_1(i+k)) + \xi_1 \}^2 \,|\, u(i), i \right] \qquad (6.24)$$

Minimising equation 6.24 with respect to u(i) gives the i.c.d. k-step ahead controller for buffered reagents:

$$u(i) = \left[f_1^{-1}\left\{ \frac{1}{m_2}\left(\frac{V}{\Delta}(X_0 - m_1) + m_2 m_1 + \sigma_{12} \right)\right\} - f_1^{-1}(m_3) \right] \sqrt{\frac{X_r}{m_2}\left(1 + \sigma_{22}/m_2^2\right)} \qquad (6.25)$$

where the index (i) has been dropped from the left-hand-side of equation 6.25. The certainty-equivalent controller is obtained by neglecting the uncertainties in the estimates:

$$u^{ce}(i) = \left[f_1^{-1}\left\{ \frac{1}{m_2}\left(\frac{V}{\Delta}(X_0 - m_1) + m_2 m_1 \right)\right\} - f_1^{-1}(m_3) \right] m_2/X_r \qquad (6.26)$$

The effect of the caution cannot be extracted from equation 6.25 readily; but, it may be seen to be due to two non-linearities in the model of equations 3.46: the modelling of the tank dynamics and the chemistry of neutralization. It is possible to derive the certainty-equivalent controller for strong reagents (equation 6.22) from that for weak reagents (equation 6.26) by substituting the non-linear function $f_1^{-1}(.)$ of equation 6.26 with a linear function of slope unity (section 3.2.2) for the strong reagents controller.

The caution element in the i.c.d. controller for strong and for weak reagents is because of the non-linearities of the model state equations. An additional element of caution is introduced in the stochastic controller if one considers the non-linearity of the pH measurement.

6.4.3 The pH Control Law

In this section, a cautious pH control law is derived for the pH cost function of equation 6.17. The caution arises in the controller because numerical calculation of an optimal operating point leads to an effective setpoint which is directly influenced by the confidence in the state estimates. The effect of this interaction is that reduced quality of estimation results in the optimal operating point moving to a region of lesser slope where control is easier. The caution is equivalent to the manual tuning of the operating point by the plant operator if control is not satisfactory.

The optimal operating point is calculated numerically in units of i.c.d. for each setpoint pH_0: it is equal to the i.c.d. target value X_0 plus a caution term which is proportional to the quality of estimation. This optimal operating point is then used instead of X_0 in the k-step ahead controllers derived in the previous section for strong and weak reagents.

The pH cost function of equation 6.17

$$J_{pH} = E\left[\left\{pH_0 - pH(x_1(i+k+1))\right\}^2 \middle| u(i),i\right] \qquad (6.17)$$

can be written in the form:

$$J_{pH} = E\left[\left\{\ G(x_1(i+k+1))\ \right\}^2 \middle| u(i),i\right] \qquad (6.27)$$

where $G(x_1(i+k+1)) = pH_0 - pH(x_1(i+k+1))$ (6.28)

Hence,

$$J_{pH} = \int_{x_1} p(x_1(i+k+1)|u(i),i)\left\{\ G(x_1(i+k+1))\ \right\}^2 dx_1 \qquad (6.29)$$

The probability distribution of the prediction $p(x_1(i+k+1)|u(i),i)$ is assumed to be Normal with its mean equal to the predicted state $\tilde{x}_1(i+k+1)$ given by the EKF state prediction (equation 5.2). From equation 5.10, $\tilde{x}_1(i+k+1)$ corresponds to $\tilde{m}_1(i+1)$ in the state prediction vector $\underline{\tilde{x}}(i+1)$. The variance of the distribution is the variance $\tilde{\sigma}_{11}(i+1)$ of the predicted state $\tilde{m}_1(i+1)$; $\tilde{\sigma}_{11}(i+1)$ is the element 1,1 of the state prediction covariance $\underline{\tilde{\Sigma}}(i+1)$ which is given by equation 5.5. The probability distribution is hence written as:

$$p(x_1(i+k+1)|u(i),i) = N(\tilde{m}_1(i+1);\tilde{\sigma}_{11}(i+1)) \qquad (6.30)$$

The pH cost function of equation 6.29 is given by:

$$J_{pH} = \frac{1}{c}\int_{x_1} \{ G(x_1(i+k+1)) \}^2 \exp\left[-(x_1(i+k+1) - \tilde{m}_1(i+1))^2/2\tilde{\sigma}_{11}(i+1)\right] dx_1 \qquad (6.31)$$

where c is a normalising constant independent of $\tilde{m}_1$ and the function $G(x_1(i+k+1))$ is given by equation 6.28. Minimizing J_{pH} of equation 6.31 is equivalent to sliding the Normal distribution $p(x_1(i+k+1)|u(i),i)$ along the horizontal axis of x_1, as shown in figure 6.7, until the integral with its product with $\{ G(x_1(i+k+1)) \}^2$ is minimised.

Values of $\tilde{m}_1(i+1)$ which minimise J_{pH} are the optimal operating points in i.c.d. They were computed numerically for values of the standard deviation $\sqrt{\tilde{\sigma}_{11}(i+1)}$ ranging from 0 to 10^{-2} and for values of setpoint pH_0 ranging from pH 2 to pH 12. Figure 6.8 illustrates the relationship between the optimal values of $\tilde{m}_1$ and a range of $\sqrt{\tilde{\sigma}_{11}}$ (0 to $2\text{x}10^{-2}$) for selected values of pH_0 (8.5, 9.0, 9.5). This relationship may be approximated by a family of two connected straight lines. Each pair of lines is characterised by a slope s and a threshold value t. The values

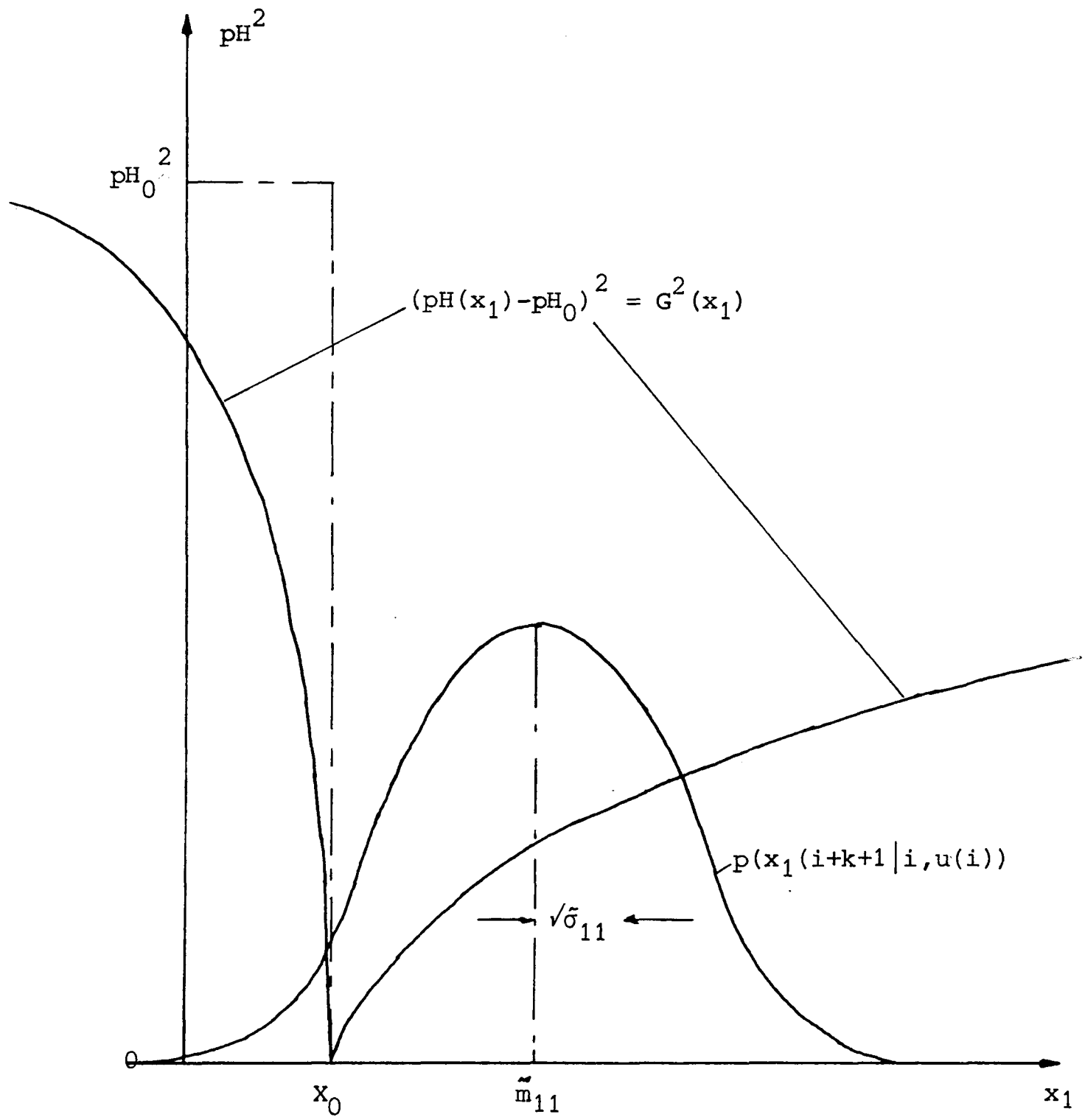


Fig 6.7 Minimization of the pH cost function J_{pH}

of slope and threshold of these lines are plotted each as a function of the different pH setpoints in figure 6.9 (for the slope s) and in figure 6.10 (for the threshold t). Both functions are symmetric about pH 7. A least square fit of the values gives the following relationships between the required setpoint pH_0 and s & t which define the optimal values of $\tilde{m}_1$:

for $7.5 \leq pH_0 \leq 12.0$

$$s = 0.925pH_0 - 5.8 \qquad (6.32a)$$

$$t = 1.32x10^{-(13-pH_0/1.2)} \qquad (6.32b)$$

for $2.0 \leq pH_0 \leq 6.5$

$$s = -0.925pH_0 + 7.2 \qquad (6.33a)$$

$$t = 5.4x10^{-(2+pH_0/1.2)} \qquad (6.33b)$$

For a given setpoint pH_0, the slope s and the threshold t are calculated from the above relationships. If the value of the standard deviation of the prediction $\sqrt{\tilde{\sigma}_{11}}$ is less than the threshold t, the optimal value of the operating point X_{opt} is set equal to the setpoint in i.c.d. X_0 in the i.c.d. control laws (equations 6.21 and 6.25): because the covariance element $\tilde{\sigma}_{11}$ is very small and the confidence in the prediction is large, there is little need to introduce additional caution and the pH control law reverts to the i.c.d. control law of section 6.4.2. If $\sqrt{\tilde{\sigma}_{11}}$ is equal or larger than the threshold, the optimal operating point X_{opt} is equal to the i.c.d. setpoint X_0 plus an additional caution element; this element relates the slope s and the threshold t, calculated earlier for a given pH_0, to the confidence in the prediction:

$$X_{opt} = X_0 + s(\sqrt{\tilde{\sigma}_{11}(i+1)} - t) \qquad \text{for } \sqrt{\tilde{\sigma}_{11}(i+1)} \geq t \qquad (6.34)$$

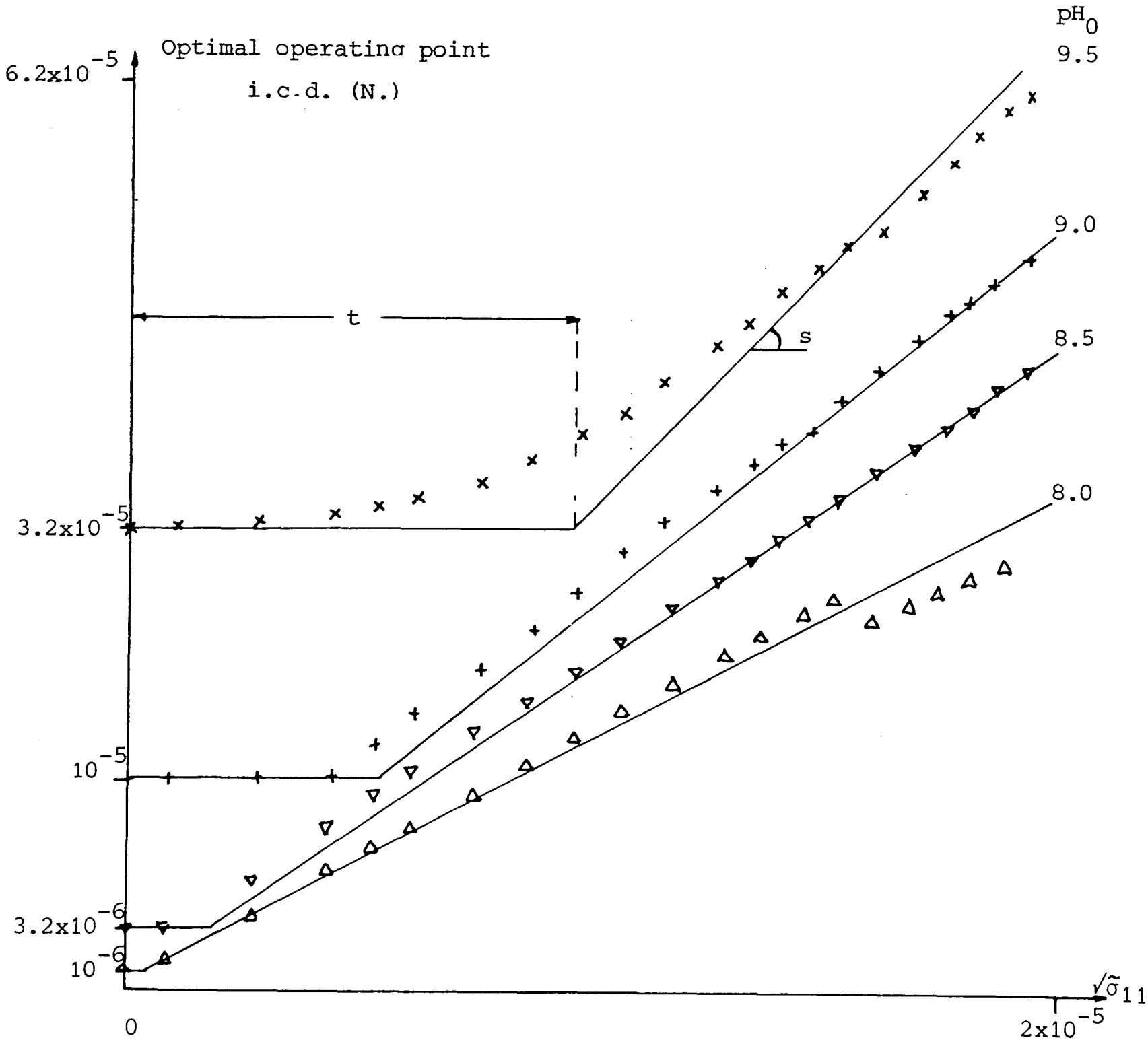


Fig 6.8 Numerical values of the optimal operating point

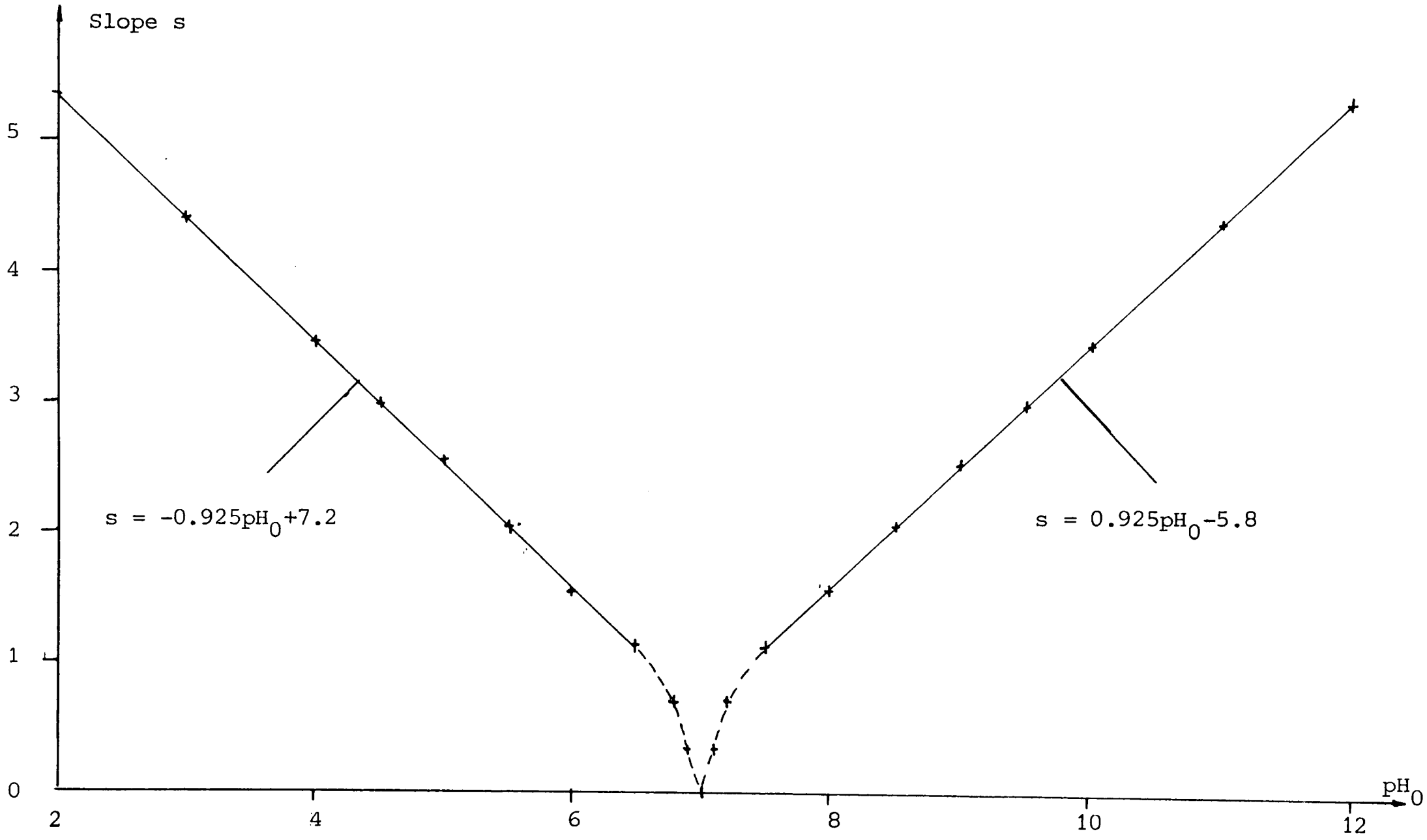


Fig 6.9 Relationship between the slope s and the setpoint pH_0

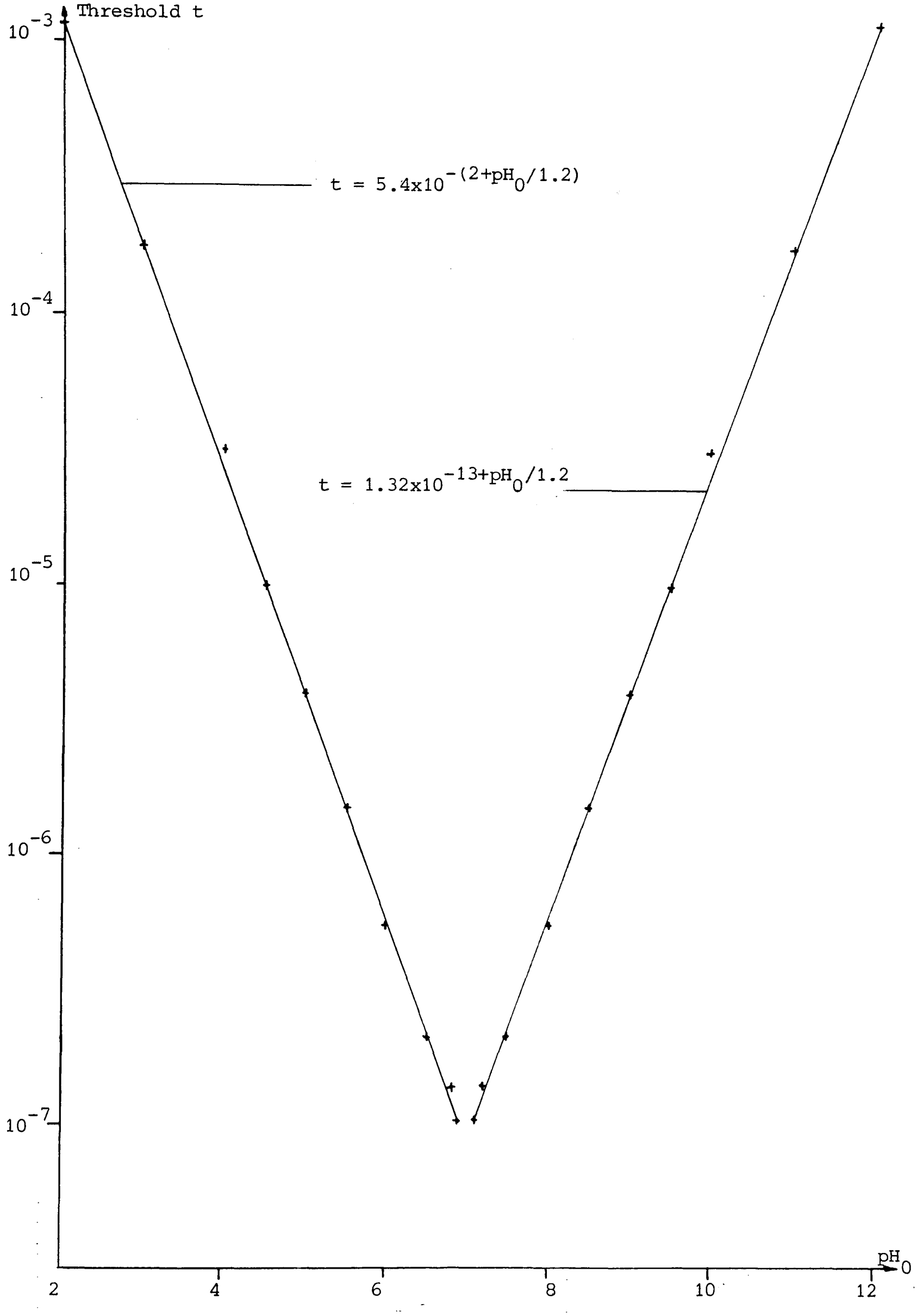


Fig 6.10 Relationship between the threshold t and the setpoint pH_0

$$X_{opt} = X_0 \qquad \text{for } \sqrt{\tilde{\sigma}_{11}(i+1)} < t$$

Thus the optimal operating point X_{opt} is directly influenced by the confidence in the current state prediction. When the prediction is bad, X_{opt} moves to a region on the pH non-linearity where control is easy. For a target value of pH > 7, s (from equation 6.32) is positive resulting in X_{opt} being larger than X_0, and the optimal operating point which is the effective setpoint is greater than pH_0. If on the other hand, the required setpoint pH_0 is less than 7, s (from equation 6.33) is negative, and the effective setpoint is less than pH_0. In both cases, the slope of the pH non-linearity is less steep at the effective setpoint than at the required one.

The cautious behaviour of the pH control law is due to the asymmetry of the pH non-linearity about the chosen target value pH_0. At pH_0 equal to pH 7, the slope s (from figure 6.9) equal zero making the optimal operating point X_{opt} equal to the i.c.d. target value X_0, and no caution is introduced. For $pH_0 > 12$ and $pH_0 < 2$, the value of the threshold t (figure 6.10) is large and, unless the estimates are very poor, $\sqrt{\tilde{\sigma}_{11}(i+1)} < t$ is true making X_{opt} again equal to X_0.

In conclusion, the caution due to the pH control law is ineffective if the target value is either very close to pH 7 or very far from it. In most cases, the pH target value lies between these two extremes, and the the performance of the stochastic controller compares favourably with more classical control techniques as will be shown in the next section.

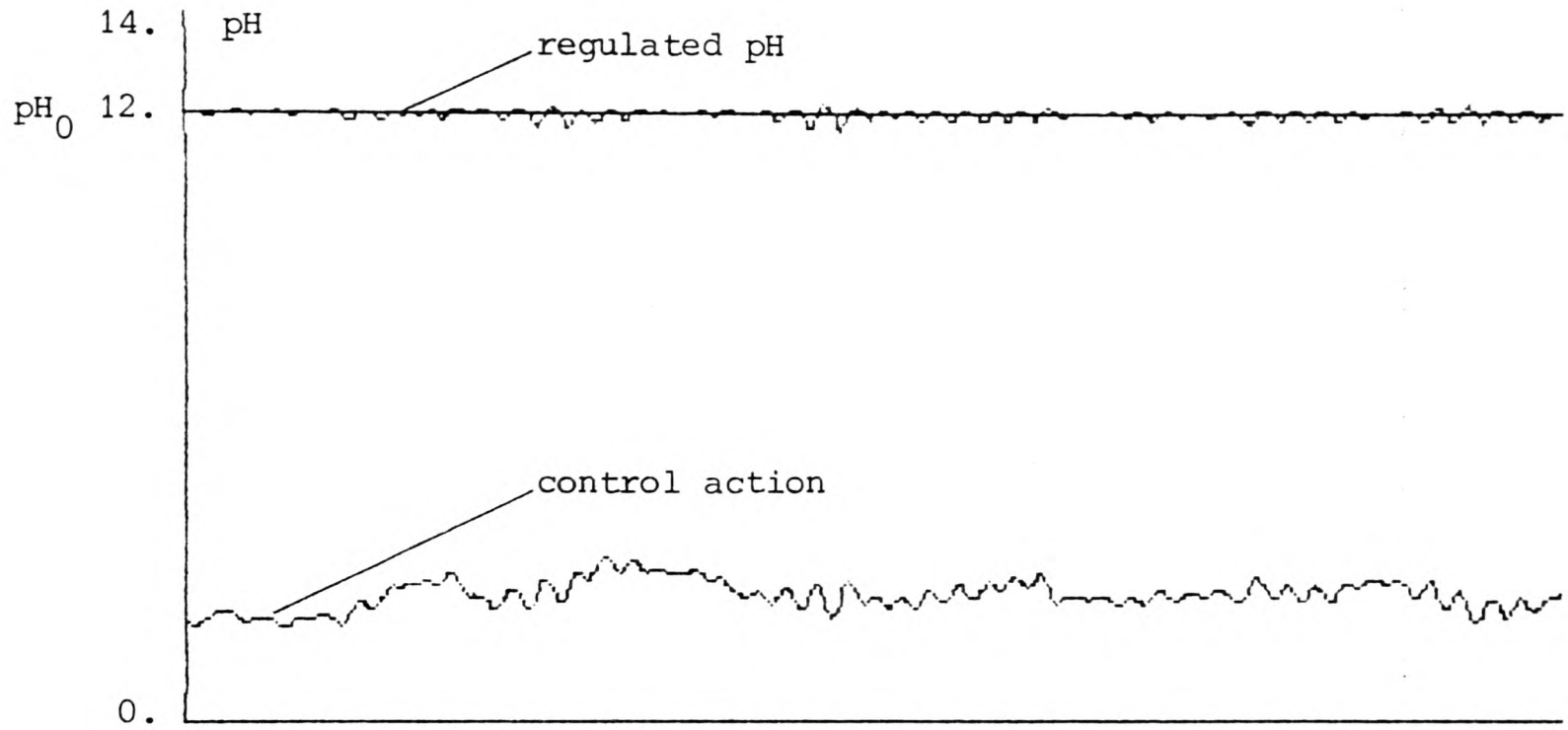
6.4.4 Simulation Results Of The Stochastic Controller

In this section, simulation results of the cautious stochastic controller are presented for two neutralization processes. The results are comparable with those of the classical controllers discussed in section 6.3. The neutralization processes which provide the experimental test-bed for the cautious controller are the one used to investigate the classical control algorithms in section 6.3.4: process A is a strong reagent process while process B is a weak reagent one.

Process A:

The stochastic controller results for process A are shown in figure 6.11: time-histories of the controlled pH and the corresponding control action for regulation at pH 12 are displayed; also shown are the values of the different cost functions (RMSE, AEA, ARF) for this particular run. These values are directly comparable with those of the classical controllers shown in table 6.1. The RMS error of the stochastic controller (0.072) is smaller than for any of the raw feedback. This is not surprising because the stochastic controller uses additional information about the process disturbances in the form of their estimates. The performance of the novel controller is also better (in terms of smaller RMSE) than most of the feedback controllers with estimated or measured feedforward, the exception being the more complex pole-placement feedback controller.

The Average Excess Acidity (AEA), which measures the error in pH below the setpoint, of the stochastic controller (0.031) is comparable with that of the classical controllers. This means that the optimal operating point of the stochastic controller (section 6.4.3) is the same as the



R.M.S.E. = 0.072 pH units

A.E.A. = 0.031 pH units

A.R.F. = 1.61 m^3/hr.

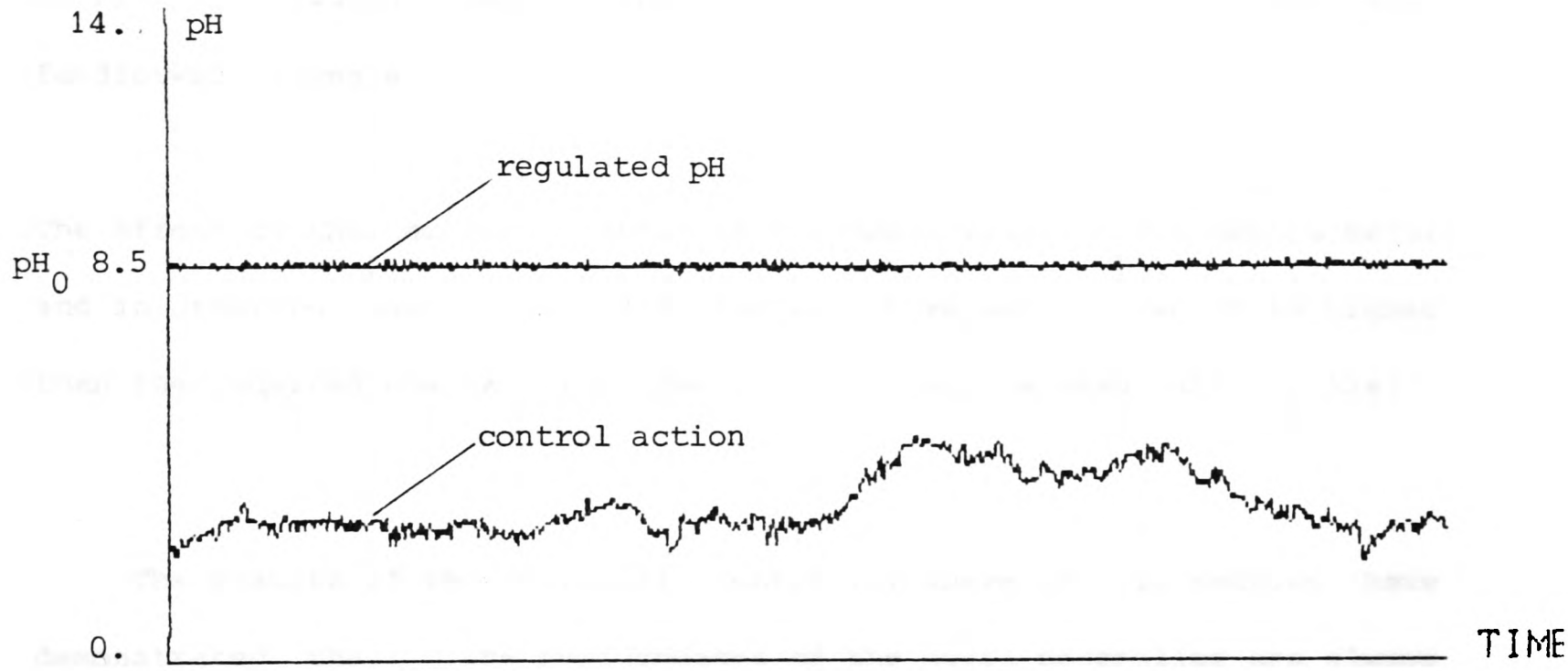
Fig 6.11 Stochastic cautious controller: process A
setpoint = 12.0

chosen target of pH 12, and that there is little caution exercised by the stochastic algorithm. One would expect this behaviour because the target value is far from the neutral point of pH 7 and the caution element due to the pH control law is almost non-existent. Finally, the improvement in performance of the stochastic controller over that of most classical controllers was brought upon using the same amount of reagent (ARF = 1.61).

Process B:

For process B, two target values for the stochastic k-step ahead controller were selected: pH 8.5 (figure 6.12) and pH 8 (figure 6.13). Its performance compares with that of the classical controllers shown in tables 6.2 and 6.3. It can be seen (figure 6.12) that at a setpoint of pH 8.5, the cautious controller has a RMS error of 0.049 pH units which is smaller than for any raw feedback algorithm. The performance of the cautious algorithm is also better than most feedback controllers with estimated feedforward with the exception of the pole-placement. When compared with feedback + measured feedforward, the k-step ahead controller is better than both the fixed-parameter PID and the K-STC but worse than the ST-PID (marginally) and the P-STC.

The effect of the caution due to the pH control law (section 6.4.3) is apparent for the chosen target value of pH 8.5. The Average Excess Acidity for the cautious controller (0.012) is much smaller than for any of the classical controllers, even though the value of the RMSE (0.049) is about the same. This means that the effective setpoint (the optimal operating point) of the stochastic controller is higher than the required target value making the control easier. This also shown in the slightly



R.M.S.E. = 0.049 pH units

A.E.A. = 0.012 pH units

A.R.F. = 0.118 m^3/hr.

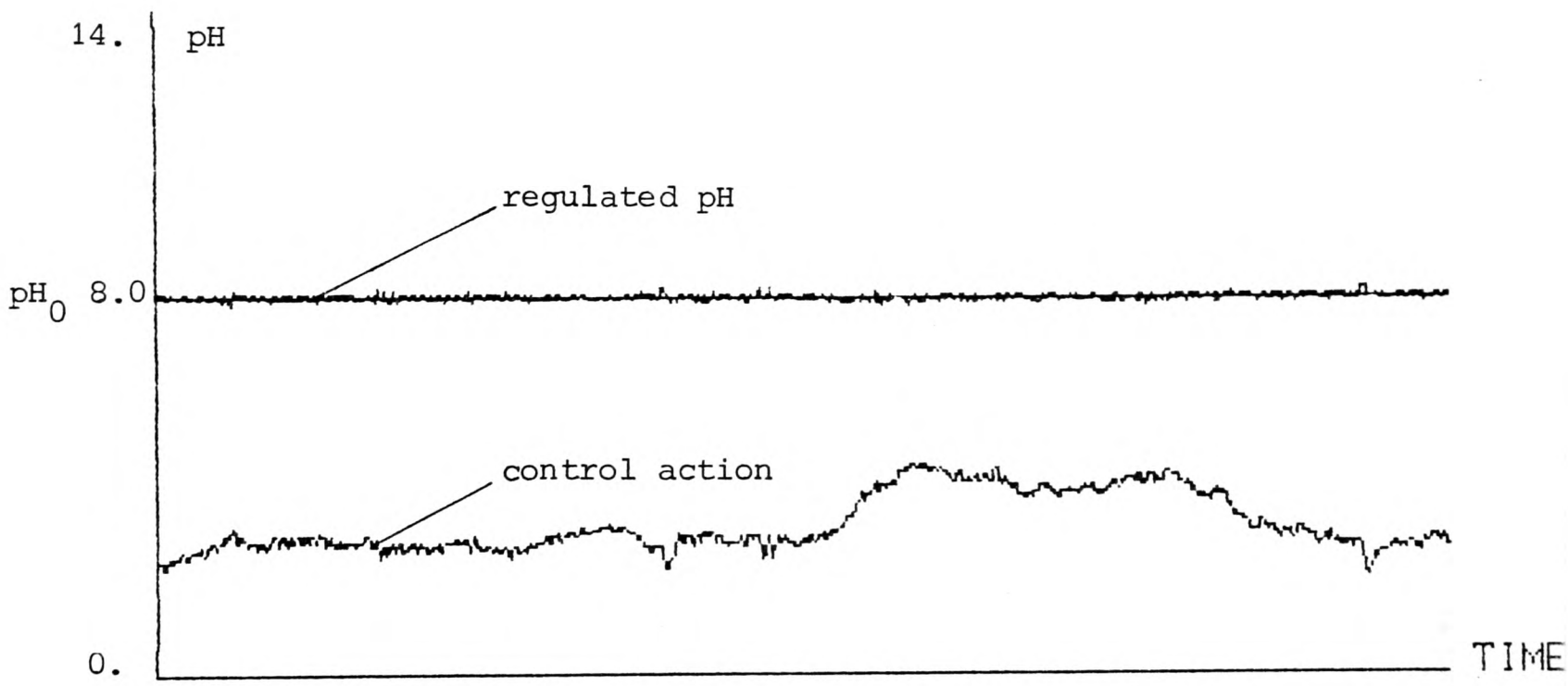
Fig 6.12 Stochastic cautious controller: process B
setpoint = 8.5

larger amount of reagent used (ARF = 0.118) to regulate the pH.

At a setpoint of pH 8 (figure 6.13), the performance of the stochastic controller is similar to that at pH 8.5. The RMS error (0.087) is smaller than for feedback alone, and the performance is better than for the PID and the K-STC plus estimated or measured feedforward. The performance of the novel controller is comparable with that of the ST-PID + measured feedforward, and worse than the pole-placement with feedforward signals.

The effect of the caution is shown in the small value of the AEA (0.027); and in order to regulate the pH at the effective setpoint which is higher than the required one, a larger amount of reagent is used (ARF = 0.114).

The results of the stochastic controller shown in this section have demonstrated that: the performances of the novel controller are always better than those of classical feedback alone; that they are often better than those of the classical controllers plus estimated feedforward; and that they are sometime better than those of the classical controllers plus measured feedforward. The estimated feedforward algorithm uses the same estimation procedure as that of the stochastic controller, but the implementation of the latter is significantly less complex than for any of the selftuners. Hence, from the simulation results presented here, the novel stochastic controller can provide a useful alternative, at a lower implementation cost, to more classical control algorithms if some information about the process disturbances and about the titration curve is available.



R.M.S.E. = 0.087 pH units

A.E.A. = 0.027 pH units

A.R.F. = 0.11 pH units

Fig 6.13 Stochastic cautious controller: process B
setpoint = 8.0

6.5 CONCLUSION

From the simulation results presented in section 6.3.4, it can be concluded that the selftuners provide a more robust control than does the PID with the explicit pole-placement giving the best performance; this is because the pole-placement is robust to uncertain time-delays (section 6.3.5). The simulations also show that good feedforward measurements of the load disturbances result in better control. In the case when no feedforward measurements are available, improved performance over feedback control can still be achieved using estimates of the disturbances generated by a state estimator as feedforward signals. Better performance (section 6.4.4) than that of classical controllers is also often possible if these estimates are used instead to drive the novel cautious controller.

The estimation and control techniques for pH, presented in this chapter and in the previous two, can be summarised in a pH control strategy which provides some guidelines to the most appropriate control configuration that can be implemented. The strategy is based on whether or not information available a priori exists for three elements: The process disturbances, the titration curve, and the bias on the pH measurement. The a priori information exists in the form of good feedforward measurements of the disturbances, a correct experimental titration curve and the value of the bias (which may be zero) on the pH. Hence, there are eight cases to control.

The available information for each process is considered before listing these cases. A priori information about two of the elements is necessary to calculate (estimate) the third. With available feedforward measurements and a constant titration curve, the value of the bias can be

successfully estimated as was shown in chapter 4. If, on the other hand, the bias and the titration curve are known, the EKF of chapter 5 can estimate the load disturbances. Also, for the development of an estimation scheme for the titration curve one would require to know about the disturbances and about the bias; such estimator can provide an area of future research as will be discussed in chapter 9.

Thus, based on a priori knowledge of the three specified elements, the control strategy (summarised in table 6.4) recommended for the eight cases is stated as follows: in the four cases, where one or none of the elemets is known, only a feedback controller can be used because the feedforward requires both the titration curve and the measurement of the disturbances; any estimation to supplement the missing elements is not possible. The feedback controller recommended in such cases is the pole-placement selftunerbecause it is robust to variable time-delays. In case 5, only the disturbances are unknown; they can be estimated and their estimates are used as synthetic feedforward in addition to the feedback control. An alternative in this case, is the cautious controller in which the estimates directly drive a suboptimal control law. If computer space for the controller implementation is critical, the simple caution algorithm is the most suitable algorithm. In case 6, only the bias is unknown; however, it can be estimated, and its estimate is used to correct the feedback signal in a feedback + measured feedforward configuration. Case 7 is when the titration curve alone is not available: parts of it may be estimated and used to generate the feedforward control action in addition to the feedback. The last case, case 8 is when the titration curve, the disturbances and the bias are known; no estimation is necessary and the recommended control structure is that of the pole-placement coupled to the measured feedforward.

Info. on bias	Info. on disturbances	
	NO	YES
NO	Case 1 estimation is not possible feedback only	Case 3 estimation is not possible feedback only
YES	Case 2 estimation is not possible feedback only	Case 7 estimation of titration curve feedback + measured feedforward

NO information on titration curve

Info. on bias	Info. on disturbances	
	NO	YES
NO	Case 4 estimation is not possible feedback only	Case 6 estimation of bias feedback + measured feedforward
YES	Case 5 estimation of disturbances feedback + estimated feedforward or cautious control	Case 8 estimation is not required feedback + measured feedforward

Information on titration curve is available

TABLE 6.4 Control strategies based on a priori information

Finally, this chapter has also demonstrated (section 6.3.5) that the improvement in performance due to complex controllers is process dependent and cannot be investigated by analysis alone. The CAD package PHDESIGN proved to be a valuable tool in understanding the mechanism of each controller and in assessing their performances. The package has also provided a useful comparison of simulated performances under various control algorithms and the ~~the~~ best achievable regulatory performance for a particular neutralization process.

CHAPTER 7

PHDESIGN: CAD PACKAGE FOR DESIGNING pH CONTROL SYSTEMS

This chapter describes the computer package PHDESIGN which was developed to simulate pH regulation in a common class of unit processes. The package has provided the experimental facility for the development and the implementation of a range of algorithms performing classical control, stochastic control and non-linear estimation. The package has been described in several articles (Jacobs et al 1984, Jacobs and Badran 1984a,b).

Chapter 7 is arranged as follows: section 1 introduces the package and describes its scope for new and existing processes. Section 2 summarises the simulated mathematical model and the available control algorithms. Section 3 describes the package structure and its interactive features. Section 4 concludes the chapter. A user manual is provided in appendix IV.

7.1 INTRODUCTION

The simulation package PHDESIGN has been developed to provide for experimental facility for the design studies presented in the thesis. The simulated mathematical model has been described in chapter 3 and will

be briefly summarised in this chapter. A selection of conventional and novel algorithms for classical control, adaptive control and on-line estimation is included so that their performances can be compared and the likely return on their implementation costs can be assessed. The algorithms have been derived in chapters 4, 5 and 6, and will only be mentioned in section 7.2. The simulation is sufficiently accurate in detail, sensitive to uncertainty and well provided with interactive features that the package can be used as a general purpose tool for designing real pH plant. Questions which can be answered include:

(i) For a given existing plant:-

(a) What seems to be the best achievable regulatory performance?

(b) How do performances compare under various control algorithms which may be more or less expensive to implement?

(c) Would the return from improved instrumentation or from implementing a complex algorithm justify the costs?

(d) To what extent might performance be improved by changing some operating condition, such as target value of pH?

(ii) For proposed new plant how would efficiency and cost of control vary with:-

(a) Operating conditions?

(b) Values of parameters, such as tank volume?

(c) Number of unit processes; for example n cascaded neutralisation stages rather than just one?

The package already has been used, in collaboration with major chemical engineering companies (section 1.1), in one case study, to achieve improved control of existing plant, and in another, to help design new plant. The two case studies are described in chapter 8.

7.2 THE MATHEMATICAL MODEL AND THE CONTROL ALGORITHMS

This section briefly describes the mathematical pH model which provides the basis of the simulation and which has been derived from first principles in chapter 3. The section also summarises the selection of estimation and regulation algorithms presented earlier in the thesis and included in the CAD package. They are: non-linear estimators of bias-free and biased pH measurements (derived in chapter 4), state estimation of load disturbances (chapter 5), and the classical and stochastic controllers presented in chapter 6.

7.2.1 The Mathematical Model

The simulation is based on a continuous stirred-tank reactor (CSTR), figure 1.1, where an influent stream of variable acidity and flow-rate is neutralised by mixing with concentrated reagent. A feedback signal in the form of measured pH of effluent drives the controller which adjusts reagent flow-rate. Two principal dynamic effects (section 3.4) are simulated: the exponential time constant of flow through a holding tank and a distance-velocity lag which accounts for dead-times in the reagent flow and mixing. Neutralisation processes using in-line mixers or recycle loops may be represented by this dynamic model and can be simulated using the package. Multi-tank systems can also be simulated as a succession of individual tanks. Case study 2 of chapter 8 shows how the CAD package was used in modelling and simulating pH neutralization in such a multi-tank system. The numerical integration interval used to simulate these continuous-time dynamics can be made small and is independent of the sampling interval of simulated discrete-time control.

In the simulation, the process titration curve is explicitly modelled as

the combination of its two separate underlying factors: the severe and constant nonlinearity of the pH measurement (section 3.3), and the variable reaction chemistry (section 3.2) which determines ionic concentrations as a function of volumetric ratios of reagents present.

Four sources of uncertainty are simulated:

1. Random noise on the feedback and feedforward measurements. The simulation is of white noises passed through anti-aliasing filters such as are necessary for discrete-time measurement and control of continuous-time processes.

2. Variable bias on the pH feedback signal to represent probe ageing or fouling.

3. Random loading in the form of unpredictable changes to influent flow-rate and acidity. These can be simulated either by generating stochastic variables having user-specified statistics or by storing and reproducing actual time-histories of plant disturbances.

4. Modelling errors between nominal and actual values of plant parameters.

Randomisation is optional so that comparative studies can be made in which different controllers or estimators see identical sequences of 'random' variables.

7.2.2 Control Algorithms

Control algorithms which were developed in chapter 6 and tested in the package are mostly classical controllers which use error-actuated feedback, with feedforward an optional extra as described in section 6.3.

The error signal driving the feedback controller can be generated (section 6.3.1) as either an error in pH or an error in ionic concentration difference. The simulated feedback controllers (section 6.3.3) include a fixed-parameter PID and three selftuners. All feedforward controllers can be driven either by measurements of load flow and acidity or, if the necessary instrumentation is assumed to be unavailable, by online estimates of these load variables.

Estimates of the load flow and concentration as well as of the regulated effluent concentration are generated by the nonlinear estimator of section 4.3 which drives the extended Kalman filter of chapter 5 tailored to the mathematical model. An alternative version (derived in section 4.4) is included which can estimate the value of a non-zero bias on the pH feedback measurement.

The package provided also a test-bed for the design and testing of the novel suboptimal cautious stochastic controller (section 6.4), in which the Kalman filter estimates of the load disturbances drive the pH control law of section 6.4.3. Also simulated is a manual controller which delivers a constant amount specified by the user of neutralizing reagent. In total, twenty-five controllers are simulated.

7.3 STRUCTURE AND INTERACTIVE FEATURES

In this section, the structure and the user-interaction of the CAD package are described. The structure consists of linked modules which appears to the user as a single program. The interaction is driven by menus of options and provides for file storage of many processes with their controllers and for graphical output of simulated time histories.

7.3.1 The Structure

The package is written entirely in ANSI FORTRAN-77 and uses a subset of GINO graphic routines. It has been implemented on a VAX 11/780 with Tektronix-compatible terminals. It is approximately 10,000 lines of well-commented and structured source code divided into 140 modules. The main module consists of three major subroutines: the first one specifies the process and the controller, the second simulates the specified process and the controller, and the third displays graphically the different simulated time histories. The simulation module is the core of the package. It includes the following operations: first the process variables are randomized and the ~~the~~ controller parameters initialized; then, at each integration interval, the reaction chemistry and the tank dynamics are simulated and a pH measurement is taken; estimation of load flow and acidity is optional and is carried out at each control interval before computation of the control action. The simulated results are logged for display, and the process simulation is complete when the control loop has been executed the required number of times.

7.3.2 The Interactive Features

Interactive features of the package are designed to be user-friendly. They make it easy for the user to specify, modify and store mathematical models of controlled processes, to store the most recently tuned value of controller parameters, and to run simulations and record the results.

Each process is specified by:

1. A name

2. Values of model parameters such as tank volume V, distance-velocity lag, temperature, statistics or time-histories of flows, disturbances, noises and bias

3. A titration curve, usually in the form of experimentally determined points not necessarily at the operating temperature of (2) above.

4. Values of controller parameters tuned to match the controlled process

5. Values of simulation parameters such as numerical integration interval, control sampling interval, overall run-time.

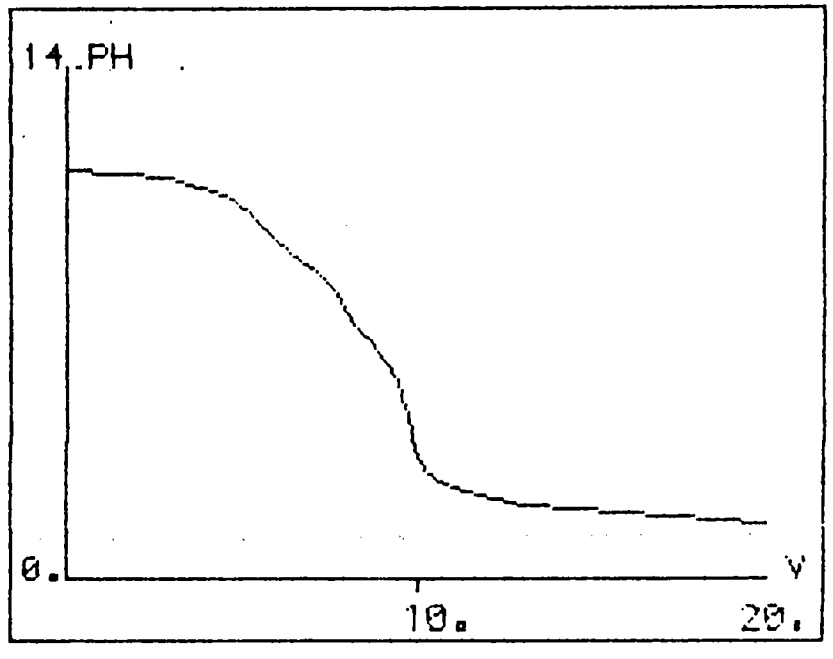
Figure 7.1 is a typical display summarising (1), (2) and (3) above and showing the process titration curve.

The interaction is driven by menus which prompt the user to specify or modify process characteristics, titration curve data and controller parameters. The files maintain information about specific processes, with options for the user to create new entries, to modify and overwrite existing entries and to delete unwanted entries. The overwrite option provides a mechanism for controller development; it automatically files values of controller parameters which have been obtained by trial and error during a session of simulation. Hence well-tuned controller parameters can be recalled at the start of each run.

The package interacts with the user through lists of two letter mnemonics including HElp which displays the current menu of options. Figure 7.2 summarises the interaction at four levels. At Level 1 the user specifies

PLANT 7 FEED BRINE PH

PH SET POINT	2.500
REACTOR VOL. (M3)	25.000
MAX. TIME DELAY (MIN.)	1.500
DELAY : T. CONST. RATIO	0.050
REACTOR TEMP. (C)	20.00
REAGENT CONC. (N.)	-8.800
MAX. REAGENT FLOW (M3/HR.)	1.000
STRONG (0) - BUFF.(1) REAG.	1



DISTURBANCES : WIENER PROCESSES OR PLANT DATA

	T. CONST.(MIN.)	MEAN	STAND. DEV.
FLOW (M3/HR.)		*** PLANT DATA ***	
CONC. (N.)	0.180E+03	0.178E-02	0.500E-03

MEASUREMENTS:

	SD. NOISE	FILTER (MIN.)	PRESENT	BIAS
PH OUT (PH)	0.01	0.10	1	0.00 - 0
FLOW IN (M3/HR)	5.00	2.00	0	
PH IN (PH)	0.01	2.00	0	

SIMULATED pH PROCESS: HE,HC,DP,DT,MP,MT,RE,CO,OQ ? HC

Fig 7.1 Display of process parameters

a controlled process by either calling a stored (OLd) process or inputting a NEw process. At Level 2 he can display and modify the process specifications and the titration curve or proceed directly to choose a controller. Controller and run-time parameters can be displayed and modified at Level 3. At Level 4 simulation results in form of time-histories are displayed. Overwrite and quit options are available from all levels.

The data entry is flexible and robust: it will allow floating point and integer conversion and it will not fail on typing errors but will prompt the user to reenter the data.

Control with any of the available algorithms can be simulated as an interactive computing job. Even the most complex combination, pole-placement self-tuning with bias estimation, runs at about 200 control sample intervals per minute of CPU time on the VAX.

Simulation results, such as those presented throughout the thesis, are stored in the form of time-histories of all significant simulated variables such as flow-rates, acidities, pH, controls, bias, estimates and their estimated standard deviations from the nonlinear estimator and from the self-tuning controllers. These time-histories can be displayed on the VDU one at a time or concurrently and can be hard-copied (figure 7.3). Options for ordinate rescaling are included in the package. Statistical results (section 6.2) in the form of root mean square error in pH, average excess acidity below the setpoint and average reagent flow are also computed and displayed.

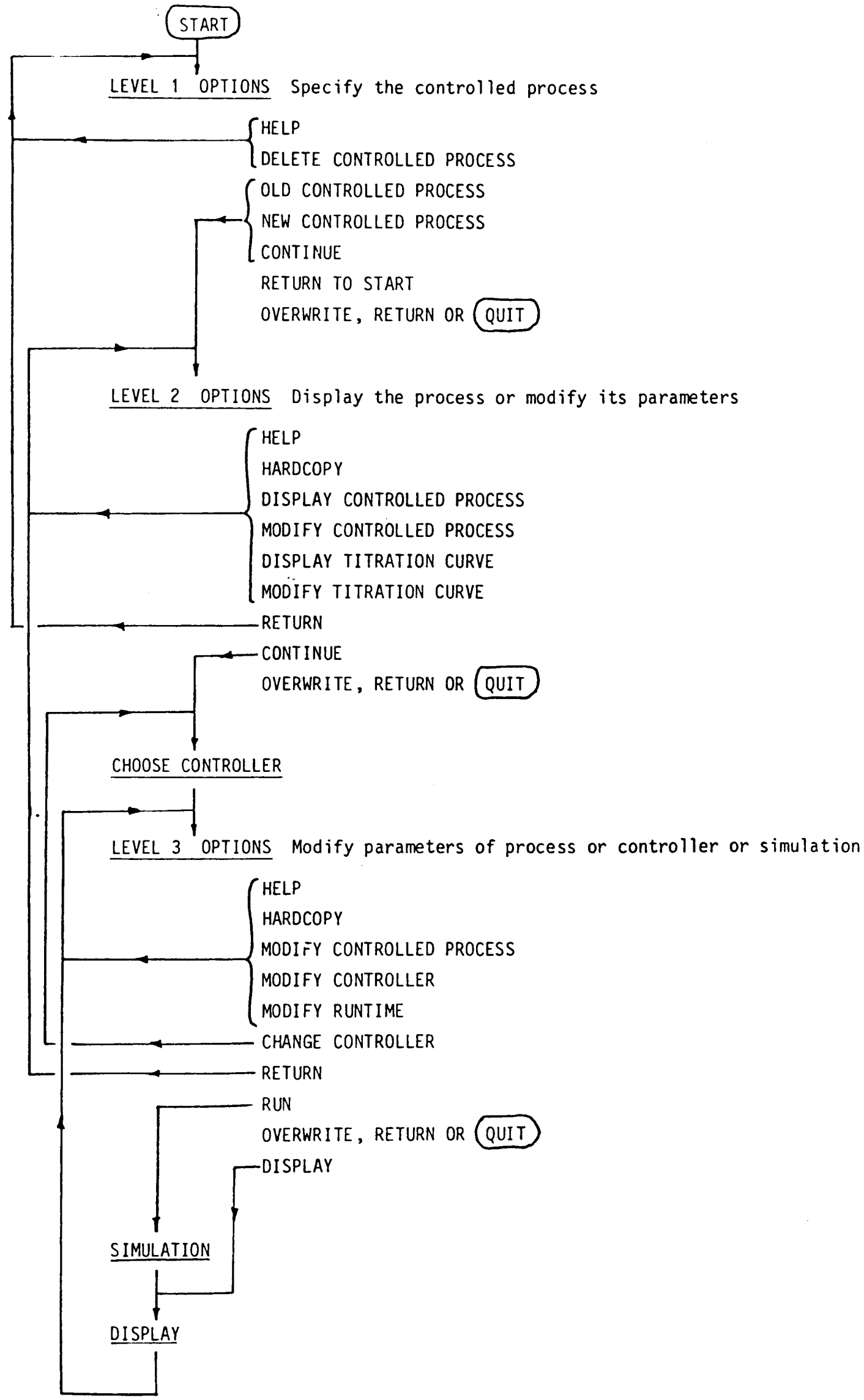
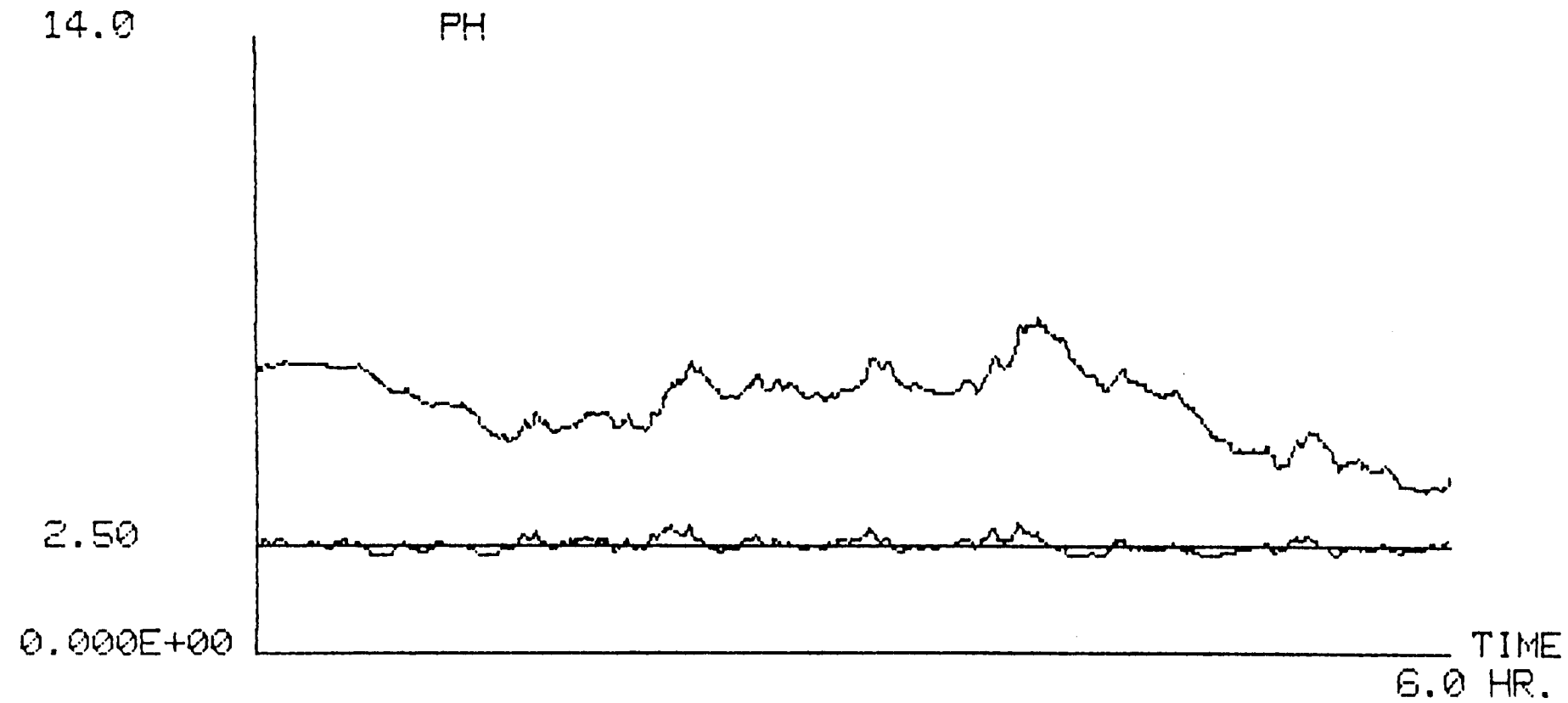


Fig 7.2 PHDESIGN: interactive features

PLANT 7 FEED BRINE PH



ACTUAL PH OUT TOTAL CONTROL ACTION

ST-PID on pH

PERFORMANCE INDICES :	RMSE (pH)	AEA (pH)	ARF (M3/H.)
	0.140	6.698E-02	0.821

PH,Y1-Y3,F1-F3,X1-X3,M1-M3,S1-S3,XZ,MZ,SZ,DZ,TZ,UT,UF,UO,PY,PE,P1-P14
DISPLAY OPTIONS: HE,LE,CY,HC,OQ,RE ? HC

Fig 7.3 Displayed time-histories

7.4 CONCLUSION

A CAD package has been developed which simulates a range of control algorithms peforming pH regulation in a common class of unit process. Its combination of an accurate mathematical model of titration chemistry plus modern algorithms for adaptive control and nonlinear estimation plus interactive simulation provides an up-to-date design tool which is believed to be unique. The package has been used to generate most of the results (in the form of time-histories and tables) presented in the thesis. Examples to show the scope of the package in improving existing pH control systems and in designing new systems will be described in the next chapter. For future research and development, the simulation package should be valuable in designing a wide variety of pH regulation systems including, but not restricted to, those which might use an on-line micro-computer capable of implementing the simulated algorithms.

CHAPTER 8

CASE STUDIES IN pH REGULATION

This chapter describes two collaborative projects with the chemical industry: i) evaluation of the advantages of modern control to pH regulation of effluent waste for ICI; ii) a design study of pH control in a Unilever production process.

8.1 CASE STUDY 1: ICI

The ICI project and its objectives were introduced in chapter 1. The author's work consisted of: 1) investigation of the pH control strategy presented in chapter 6; 2) development of the simulation package presented in chapters 6. ICI provided an experimental facility in the form of a full-scale industrial process. The process is the neutralisation tank T103A of the Waste Brine Treatment Plant (WBTP) in Runcorn, Cheshire.

First, the experimental facility is described and the process is modelled and simulated. Then, it is shown that the simulation results are comparable with those of the full scale plant thus validating the simulation and the model. Finally, based on good simulation results, modern controllers are recommended for implementation on the

neutralisation tank resulting in better pH regulation. The implementation of the different controllers was carried out by Proudfoot (1983).

8.1.1 The Neutralisation Tank T103A

In the neutralisation vessel T103A, incoming acid effluent at approximately pH 2.5 is neutralised by addition of sodium hydroxide (NaOH) reagent, to a setpoint between pH 8 and pH 9. This tank was chosen as a test-bed for the research work because the conventional analog PI controller often could not regulate the pH at the required setpoint. Large load changes resulted in unsatisfactory performance of the controller whose parameters had to be retuned every few hours. Additionally, the existing controller acted directly on the non-linear reagent valve. In order to linearise the reagent flow loop, a cascaded flow controller was installed on the valve.

Major disturbances to the vessel are variations in flow and in concentration of the incoming effluent. Flow into the vessel normally varies between 220 m^3h^{-1} and 400 m^3h^{-1}, but can rise rapidly to as much as 600 m^3h^{-1} for periods of several hours. There are other disturbances associated with the plant which can vary the flow by up to 100 m^3h^{-1} over a relatively short time (0.5 hour). The ionic concentration of the effluent is usually steady because its pH is controlled upstream of T103A. But in some cases, when the load increases, the incoming concentration can vary significantly. The vessel volume is 40 m^3 and the maximum reagent delivery is 0.5 m^3h^{-1}. There are no direct feedforward measurements of the influent flow or pH on T103A; however, there exists a flow measurement on the plant which provides, after numerical manipulation, typical recordings of flow disturbances into the

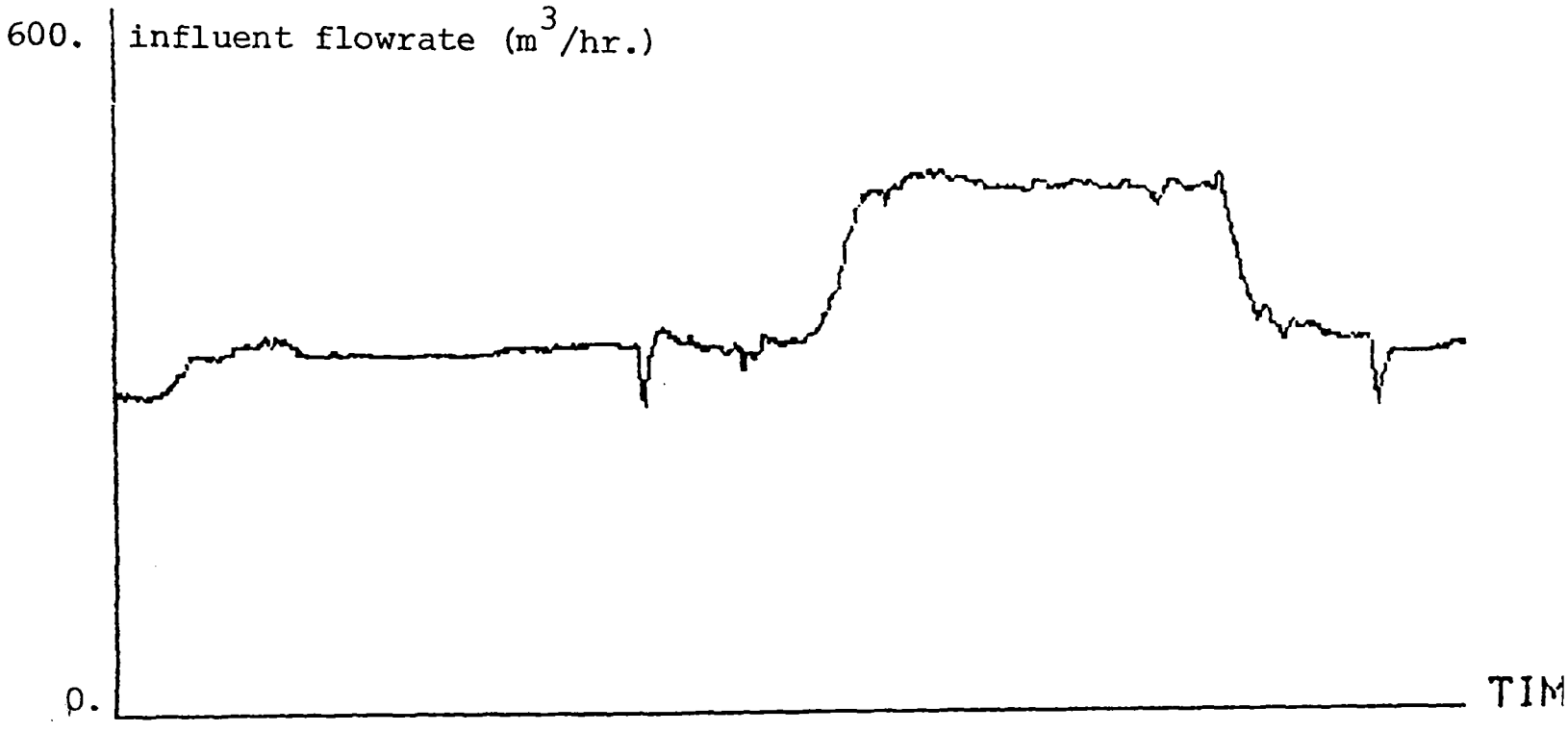
neutralisation tank.

The mixing of influent and reagent in the vessel can be approximated (section 3.4) by a variable first order lag T and a pure time-delay of approximately 0.1T. The main non-linearity in the system is a buffered titration curve. For the simulation of the process model, the incoming concentration can be satisfactorily modelled as a stochastic Wiener process (equation 3.41), whereas the abrupt changes of flow could not. For this reason, recordings of real flow data from an upstream measurement on the plant is used to simulate the inflow. Time-histories of simulated inflow and incoming pH are shown in figure 8.1 for a 24-hour period. The parameters of the simulated model were shown in figure 6.4.

8.1.2 Simulation And Full-scale Trials

Figure 8.2 shows that the simulation of the CAD package matches the behaviour of the real process. Time-histories of regulated pH at a target value of pH 8.5 under conventional PI control and of the corresponding reagent (NaOH) flow are shown for the real process and the simulation. The time-histories have similar shapes even though the simulated load disturbances (as indicated by the NaOH flow) could not be identical with the (unmeasured) real disturbances. The two pH outputs are characterised by the inability of the controller, due to the poor tuning of its parameters, to cope with large variations in the load. This similarity was only obtained when real flow data was used in simulation. The simulated r.m.s. error in pH over 24 hours had a value (0.337) close to that (0.343) of the real system.

A good simulation of the real process and its load disturbances having been established, the package was used to explore possibilities for



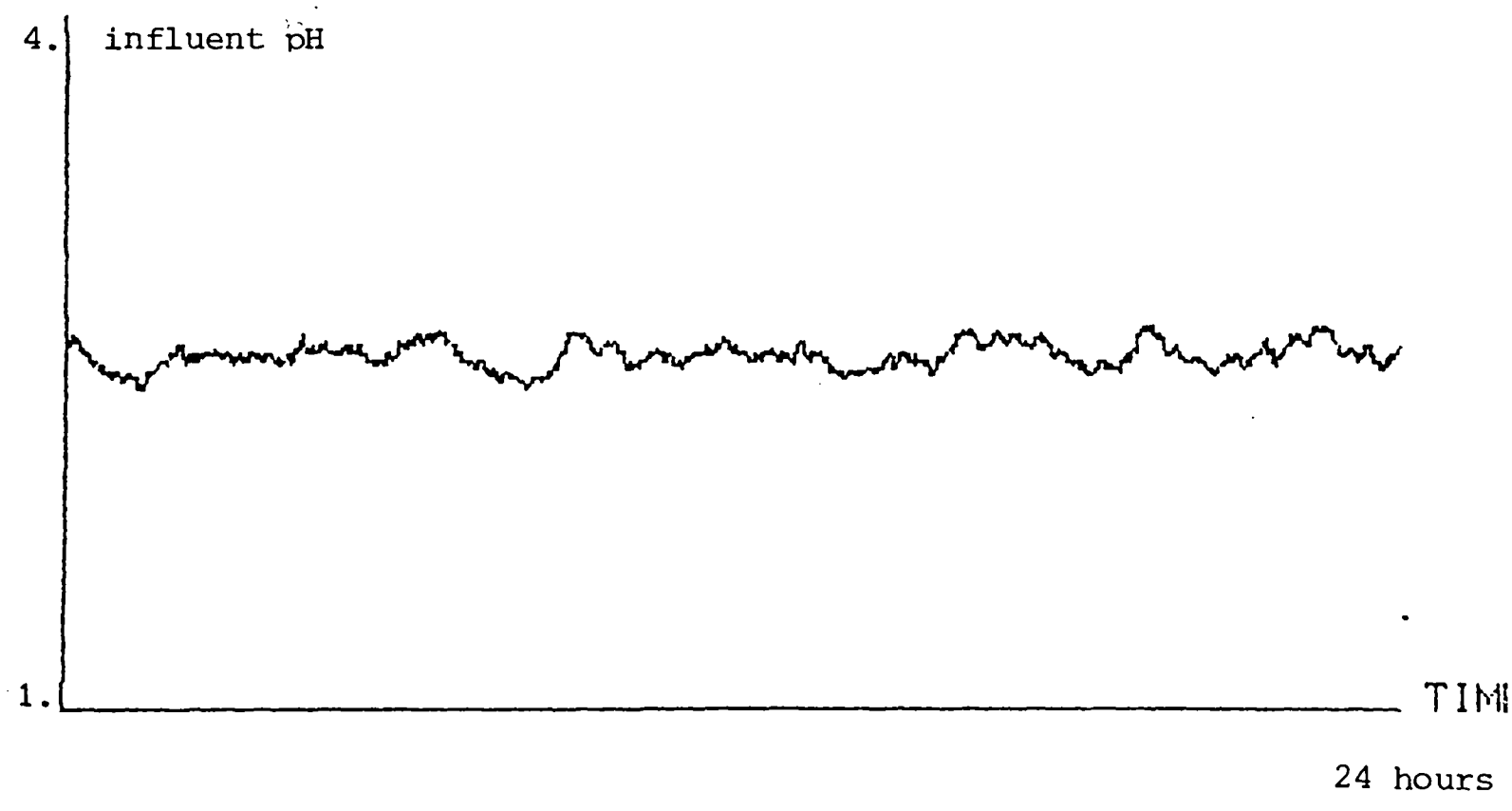


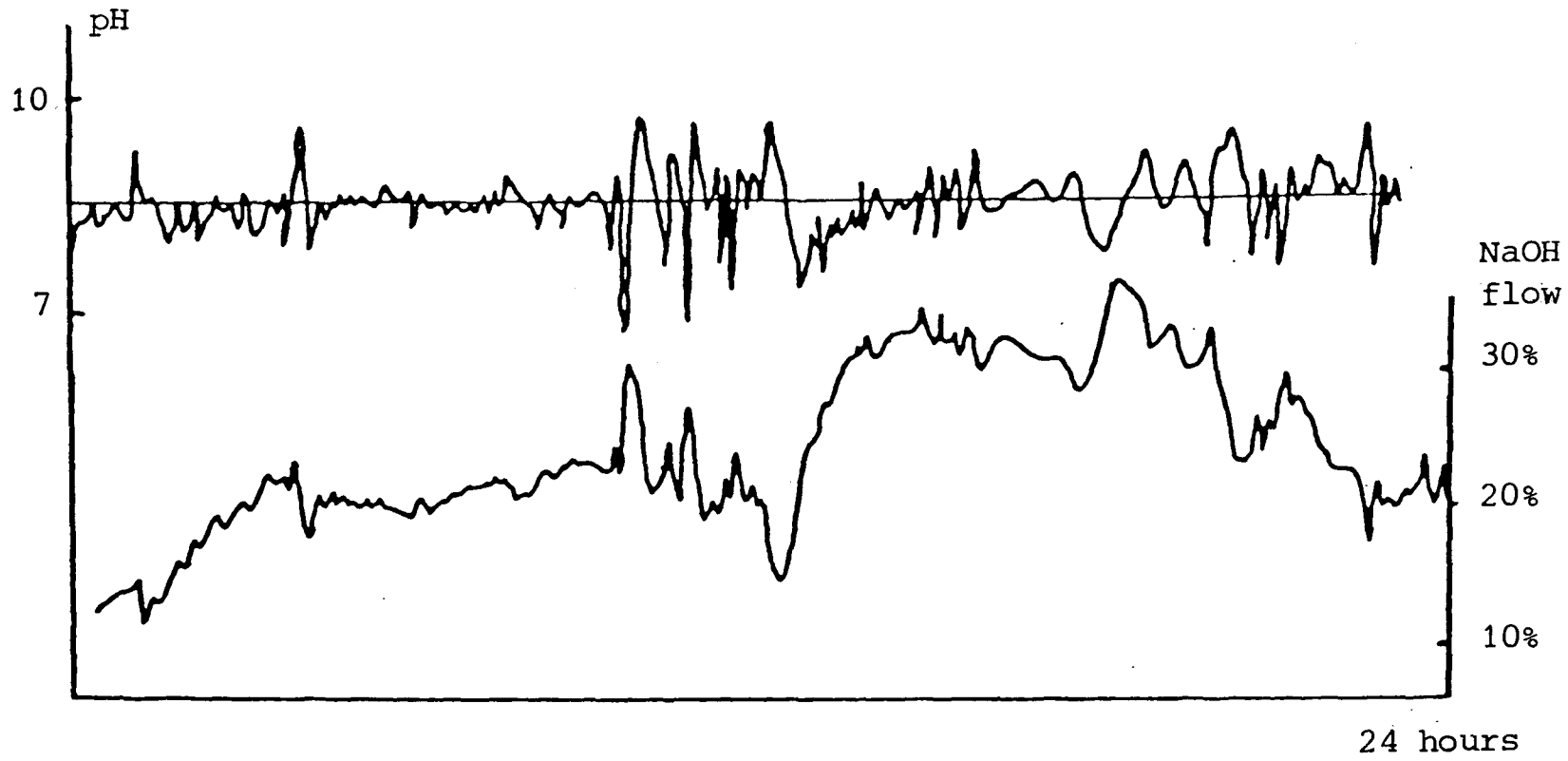
Fig 8.1 Simulated load disturbances into T103A

achieving better control. Figure 8.3a shows simulated time histories, with the same load disturbances as in figure 8.2b, which indicate that regulation could be substantially improved and rms error reduced by a factor of about five (to 0.059) by using a self-tuning PI control. Figure 8.2b shows the corresponding improved performance of the real plant (rms error 0.07) achieved when the self-tuning PI control was implemented (Proudfoot et al 1983).

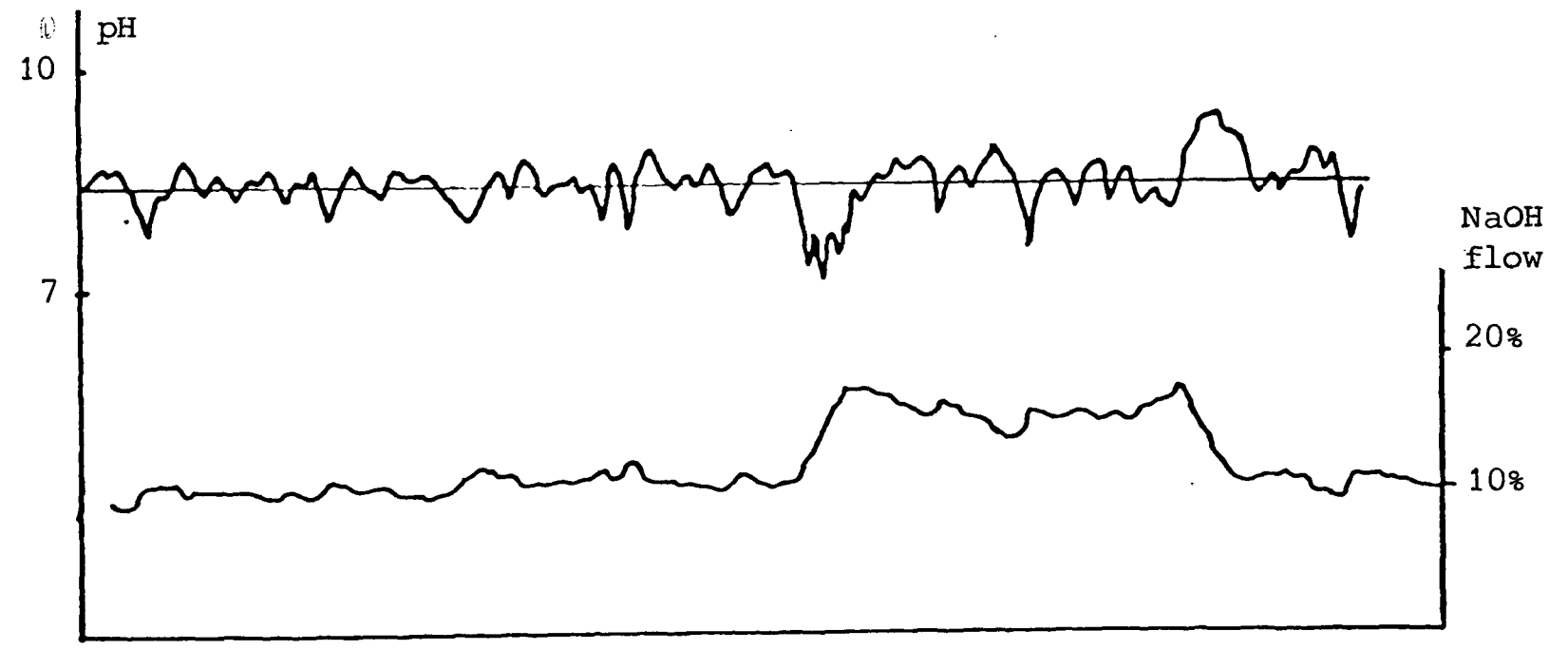
Prior to their on-line implementation, other controllers were tested in simulation for performance and robustness. Comparisons between simulation and on-line trials for the feedback controllers discussed in section 6.3 are presented in table 8.1 as RMS errors. The results of the on-line trials are reproduced here from Proudfoot (1983).

It can be seen that (table 8.1) results of the on-line trials agree with those of the simulation which were presented in section 6.3.4: better performance over long periods is achieved when selftuners are used. Discrepancies in the RMSE between simulation and on-line trials is mainly due to the variations in the load disturbances over the days averaged during the trials.

There were no feedforward measurements of inflow or incoming pH on the vessel T103A. Instead, their estimates were generated by the Kalman filter algorithm derived in chapter 5. This algorithm was initially tested in simulation, and the results were presented in section 6.3.5; it was shown that improvement in regulation is possible if these estimates are used as synthetic feedforward. Based on these results, the algorithm was commissioned on line. However, the estimates on the full-scale process were not accurate enough to be used as feedforward signals, because of bias on the feedback measurement (as discussed in section 5.5.3). Nevertheless, a small improvement in the quality of pH

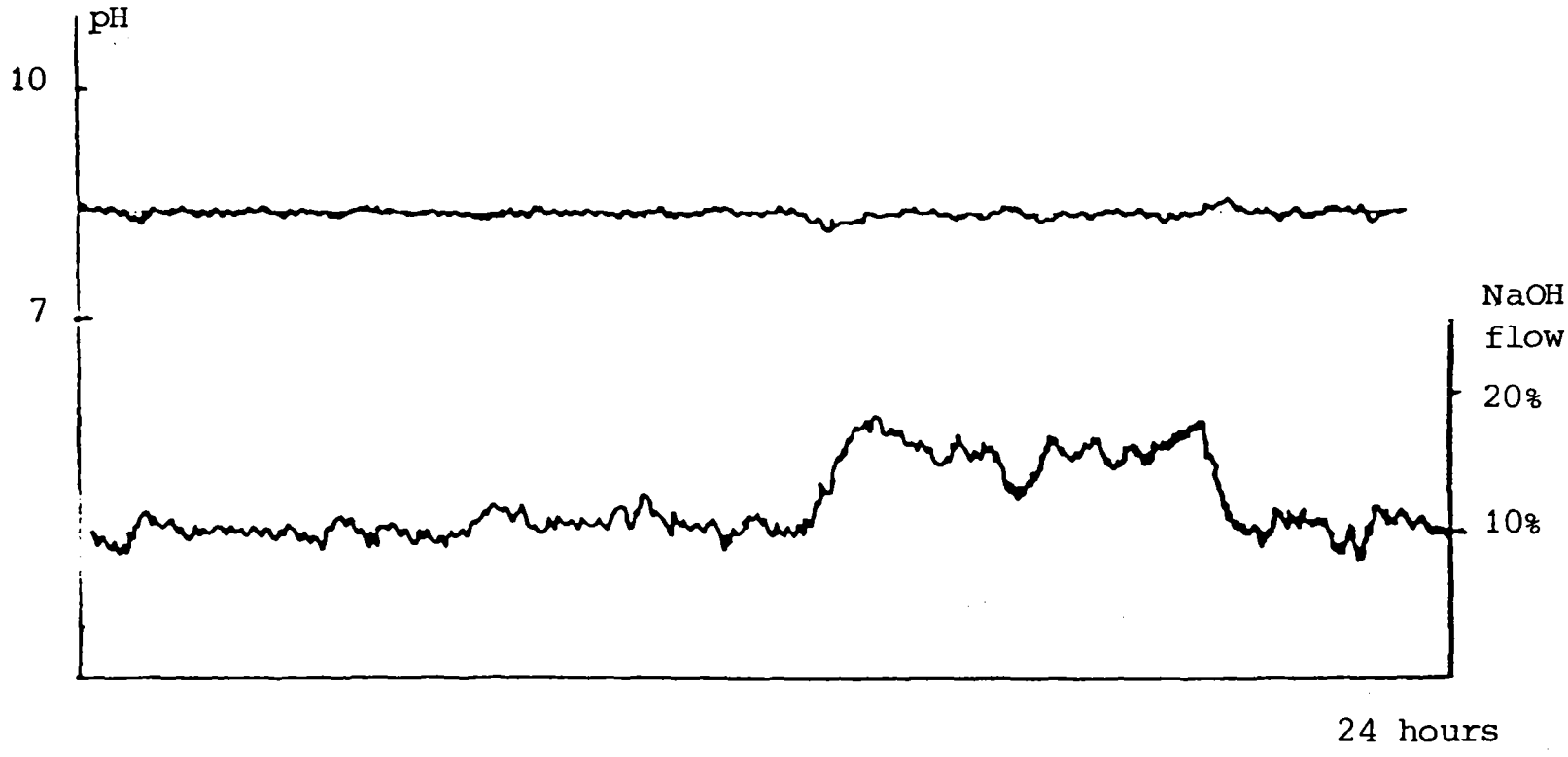


a. Real plant data: r.m.s. error = 0.343 pH

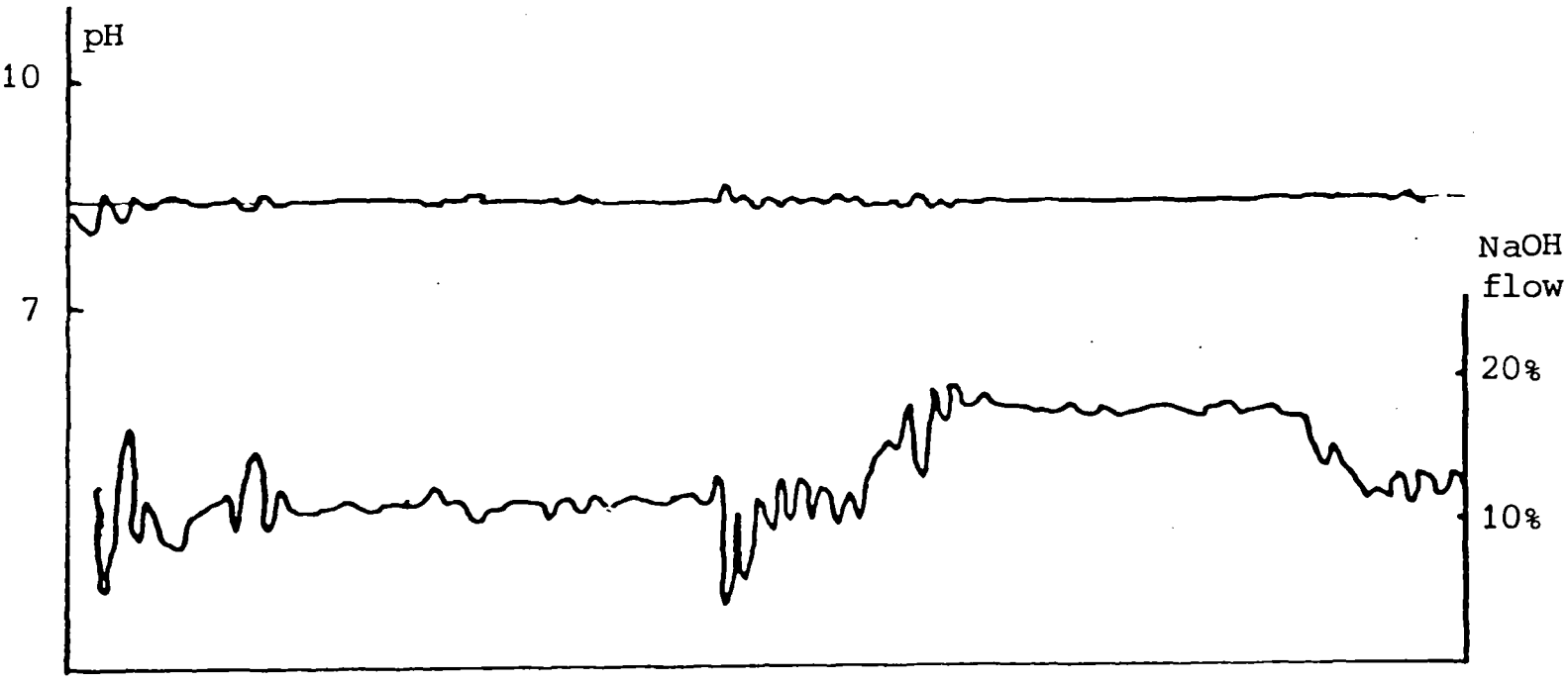


b. CAD simulation: r.m.s. error = 0.337 pH

Fig 8.2 Waste Brine neutralisation under conventional PI control



a. CAD simulation: r.m.s. error = 0.059 pH



b. Real plant data: r.m.s. error = 0.07 pH

Fig 8.3 Waste Brine neutralisation under self-tuning PI control

Controller	Simulation:	On-line trials:	
	averaged RMSE over 2 days run	averaged RMSE	number of days for average
PI	0.083	0.100	1 day run
ST-PI	0.065	0.104	65
ST-PID	0.064	0.114	41.5
K-STC	0.064	0.128	23
P-STC	0.054	0.093	21

TABLE 8.1 Comparisons of simulation and on-line trials

regulation in the vessel has been reported (Proudfoot 1983) when the Kalman filter scheme was implemented.

A result of the ICI study has been that improved performance, such as that of figure 8.3, was routinely achieved in the real neutralisation vessel resulting in considerable reagent savings.

8.2 CASE STUDY 2: UNILEVER

The Unilever project was introduced in section 1.1.2. Its objective was to achieve improved pH control on a pilot plant by using the simulation package PHDESIGN to study different structures of neutralisation system for a sulphonation product. The study was divided in three stages:

1. to develop a model of the pilot plant which can be incorporated in the simulation package; and to simulate the model under different controllers, in a single stage neutralisation in order to study the effect of varying the process parameters.

2. to recommend an optimum and realisable one- or two-stage neutralisation system based on simulation results of the model. Its parameters would be pre-specified by Unilever.

3. to simulate current and optimum designs for an existing full-scale neutralisation process.

The verification of the simulations against experimental results is a necessary step for Unilever before implementing any regulation schemes the study may recommend.

8.2.1 Single-stage Neutralisation

The process under study is a neutralisation of acid (pH 1.0) using reagent base in a mixing vessel coupled to a recycle loop as shown in figure 8.4. The process is modelled as a CSTR with a time constant T and a time delay τ whose values are computed below from the process volumes and flow rates.

The process model

The neutralisation of acid with base is modelled from equation 3.27 according to the chemical analysis presented in section 3.2. The flow f_1 and the ionic concentration difference x_1 of the stream into the recycle loop (figure 8.4) are given by:

$$f_1 = f_a + u \simeq f_a \qquad \text{because } u \ll f_a \qquad (8.1a)$$

$$x_1 = X(X^{-1}(x_a) + ux_r/f_1) \qquad (8.1b)$$

where X(.) depends on the titration chemistry.

The dynamics of the various elements of the system are modelled by:

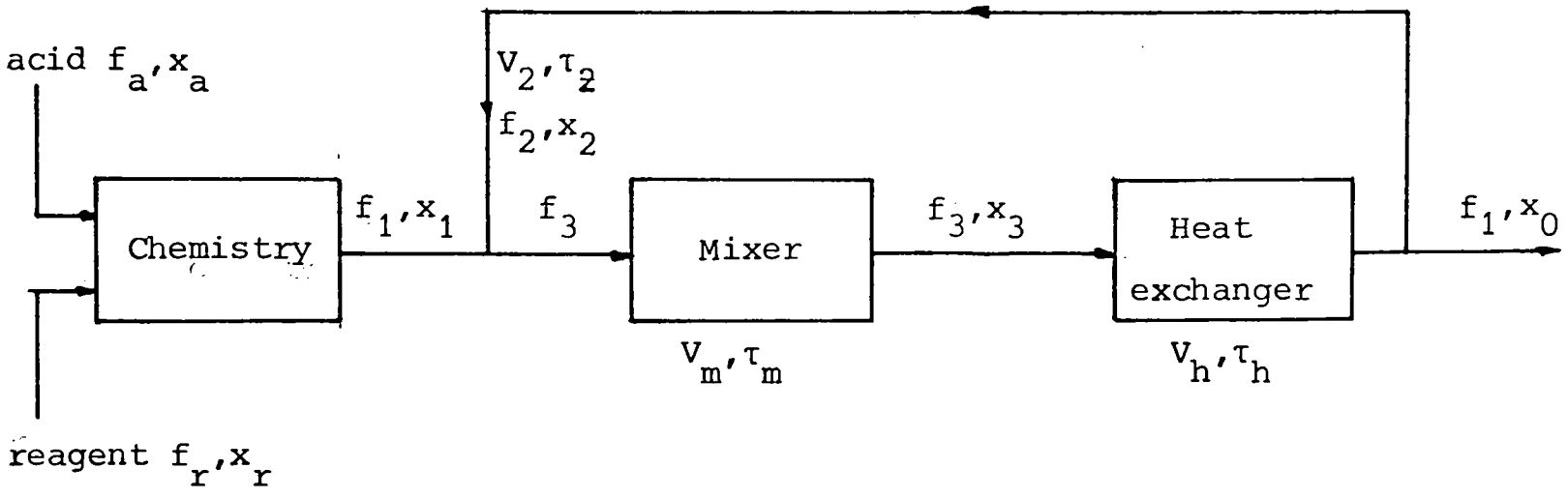
mixer:
$$V_m \frac{dx_3(t+\tau_m)}{dt} = f_1x_1 + f_2x_2 - f_3x_3(t+\tau_m) \qquad (8.2)$$

heat exchanger:
$$x_0(t) = x_3(t-\tau_h) \qquad (8.3)$$

recycle pipe:
$$x_2(t) = x_0(t-\tau_2) = x_3(t-\tau_2-\tau_h) \qquad (8.4)$$

Taking the Laplace transform and substituting for x_2 in the mixer equation:

$$f_3x_3(s) = \frac{f_1\exp(-s\tau_m)}{1 + sT_m}x_1(s) + \frac{f_2\exp(-s\tau_t)}{1 + sT_m}x_3(s) \qquad (8.5)$$



Neutralisation in a recycle loop

f_i = flow of element i

x_i = ionic concentration differnce of element i

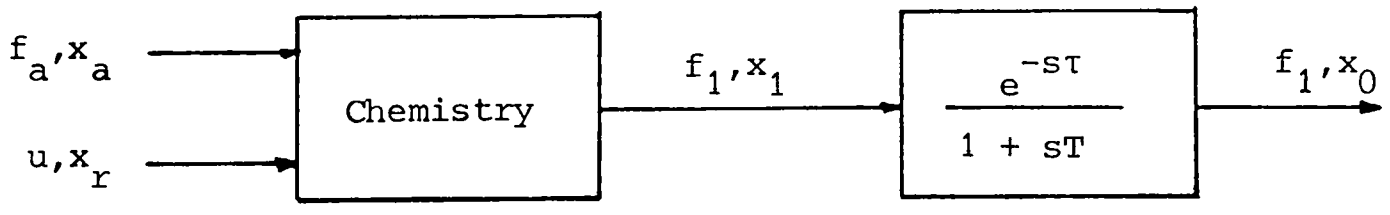
V_i = volume of element i

τ_i = time delay associated with V_i

$f_1 = f_a + u$

$f_3 = f_1 + f_2$

R = recycle ratio = f_3/f_1 $\qquad 1 \leq R < \infty$



$\tau = \tau_m + \tau_h$

$T = (V_m + V_2 + \frac{R-1}{R} V_h)/f_1$

figure 8.4: CSTR representation of the recycle loop

where $T_m = V_m/f_3$ and $\tau_t = \tau_m+\tau_h+\tau_2$.

The recycle ratio R of the recycle loop is defined by:

$$R = (f_1+f_2)/f_1 = f_3/f_1 \qquad 1 \leq R < \infty \qquad (8.6)$$

Replacing the flows by R in equation 8.5 and rearranging:

$$x_3(s)\cdot\left\{(1 + sT_m) - \frac{R-1}{R}\exp(-s\tau_t)\right\} = \frac{1}{R}\exp(-s\tau_m)\, x_1(s) \qquad (8.7)$$

Assuming that at steady state, $s\tau_t \ll 1$ which gives $\exp(-s\tau_t) \simeq 1 - s\tau$.

Substituting in equation 8.7:

$$x_3(s)\left\{1 + s[(R - 1)\tau_t + RT_m]\right\} = e^{-s\tau}m\, x_1(s) \qquad (8.8)$$

Substituting for x_3 from equation 8.3:

$$x_0(s)\,(1 + sT) = e^{-s\tau}\, x_1(s) \qquad (8.9)$$

Equation 8.9 represents a first order dynamic system of time constant T and time delay τ given by:

$$T = RT_m + (R - 1)(\tau_m + \tau_h + \tau_2) \qquad (8.10)$$

$$\tau = \tau_m + \tau_h \qquad (8.11)$$

Usually, $\tau_m \ll \tau_2$; hence, τ_m can be dropped from equation 8.10:

$$T = RT_m + (R - 1)(\tau_h + \tau_2) \qquad (8.12)$$

T_m, τ_h and τ_2 are given by:

$$T_m = \frac{V_m}{f_3} \quad ; \quad \tau_h = \frac{V_h}{f_3} \quad ; \quad \tau_2 = \frac{V_2}{f_2}$$

Replacing in equation 8.12 to represent the time constant T by the

process volumes and flow rates:

$$T = (V_m + V_2 + \frac{R-1}{R} V_h)/f_1 \qquad (8.13)$$

The recycle loop can thus be represented, for simulation purpose, by a time constant T and a time delay τ given by equation 8.13 and 8.11 respectively.

Using the CSTR process model, simulation results are obtained which show how the quality of pH regulation (r.m.s. error of output pH) depends on controller structure, on target value of pH and on two design parameters. These results are for pre-specified load disturbances and titration curve. The two design parameters are: signal-to-noise ratio on feedforward measurements, quoted in terms of proportional size of noise, and volume of the CSTR, quoted as the time constant T (V/F). Four pH set points simulated are 8, 9, 10, 11. Acceptable pH performance is equivalent to about an r.m.s. error of 0.4 pH units.

Three controller structures are investigated:-

1. Feedforward without feedback but with good knowledge of the titration characteristics (figure 8.5). It is seen that the r.m.s.error is proportional to the target value for a noise to signal ratio greater than 5%. It can also be seen that acceptable regulation is practically impossible at a target value of pH 8.

2. Feedback without feedforward (figure 8.6). The feedback controller is the selftuner PID (Proudfoot 1983) which was presented in section 6.3. The plateaux on the r.m.s. error curves for pH 8 and pH 9 are mainly due to the presence of

buffering on the titration curve at these pH values. The curves for pH 10 and pH 11 level off at an acceptable value of r.m.s. error for a time constant T of 5 minutes. However, for lower target values, the curves start levelling off at much larger values of T.

3. Combined feedforward and feedback (figure 8.7). There are no noticeable difference in performance after the addition of feedforward signals regardless of their accuarcy. For this particular process, feedforward control seems unecessary.

The results show that tight regulation (r.m.s. error < 0.4 pH units) to target near to neutrality (pH 8) would require either very accurate feedforward measurements (better than ±0.5%) for good feedforward control or a very large CSTR (T of order 1 hour) for good feedback control. The addition of feedforward to a feedback scheme yields little improvement because of the small variations in the load disturbances. The results also show that good regulatory performance can be achieved on the pilot plant (which has a time constant = 5 mins.) at a setpoint of pH 10. Because the required target value is pH 8, this single-stage neutralisation cannot be recommended. Thus, the next step of the study is to investigate two-stage configurations.

8.2.2 Two-stage Neutralisation

A two-stage configuration is investigated using the same load disturbances and titration curve as in section 8.2.1. The single-stage results obtained in section 8.2.1 showed that good feedback control is possible in a tank with a small time constant (figure 8.6) if the target value is pH 10. Thus, overneutralisation to pH 10 in a 5 minutes time

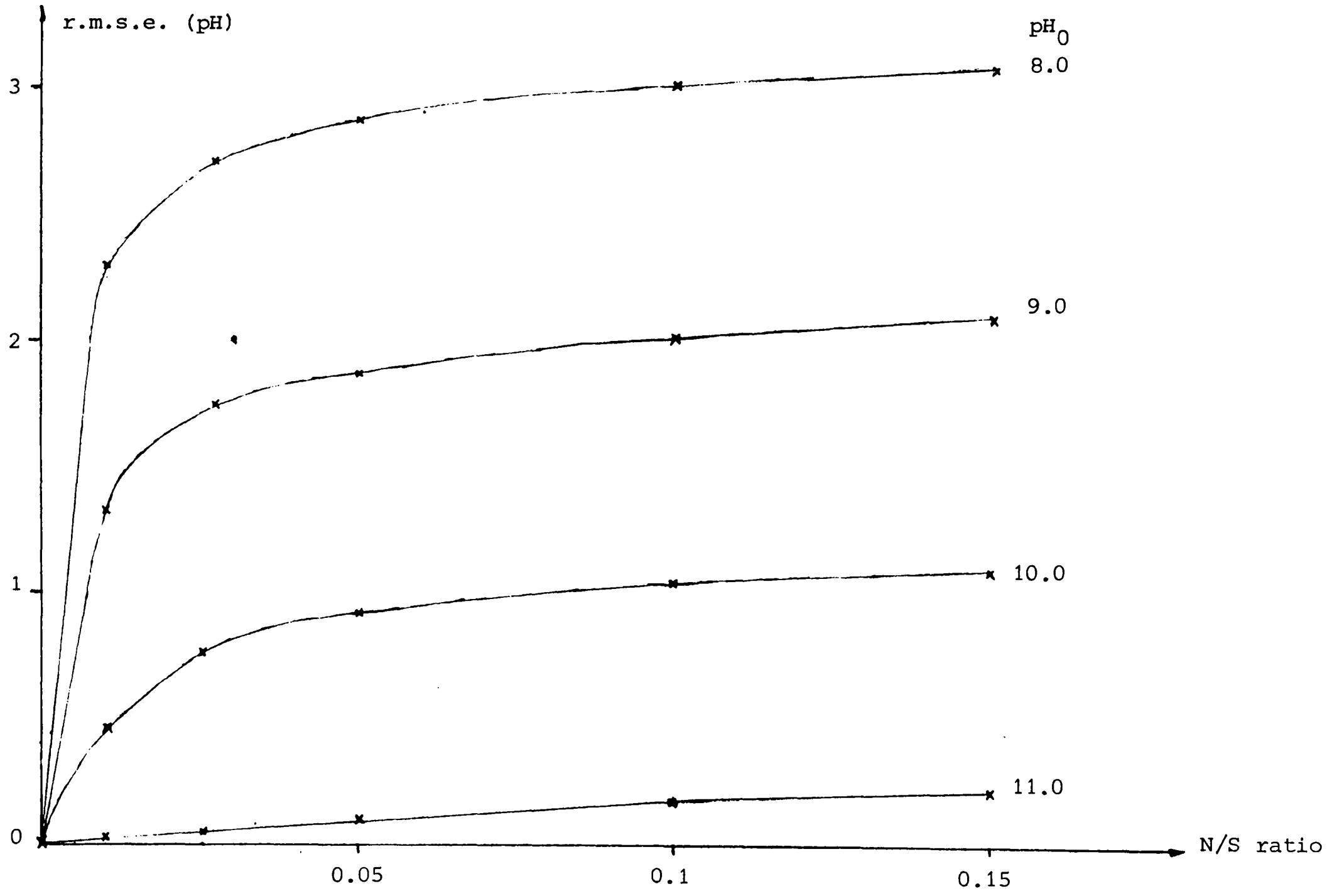


Fig 8.5 Single-stage neutralisation: feedforward control

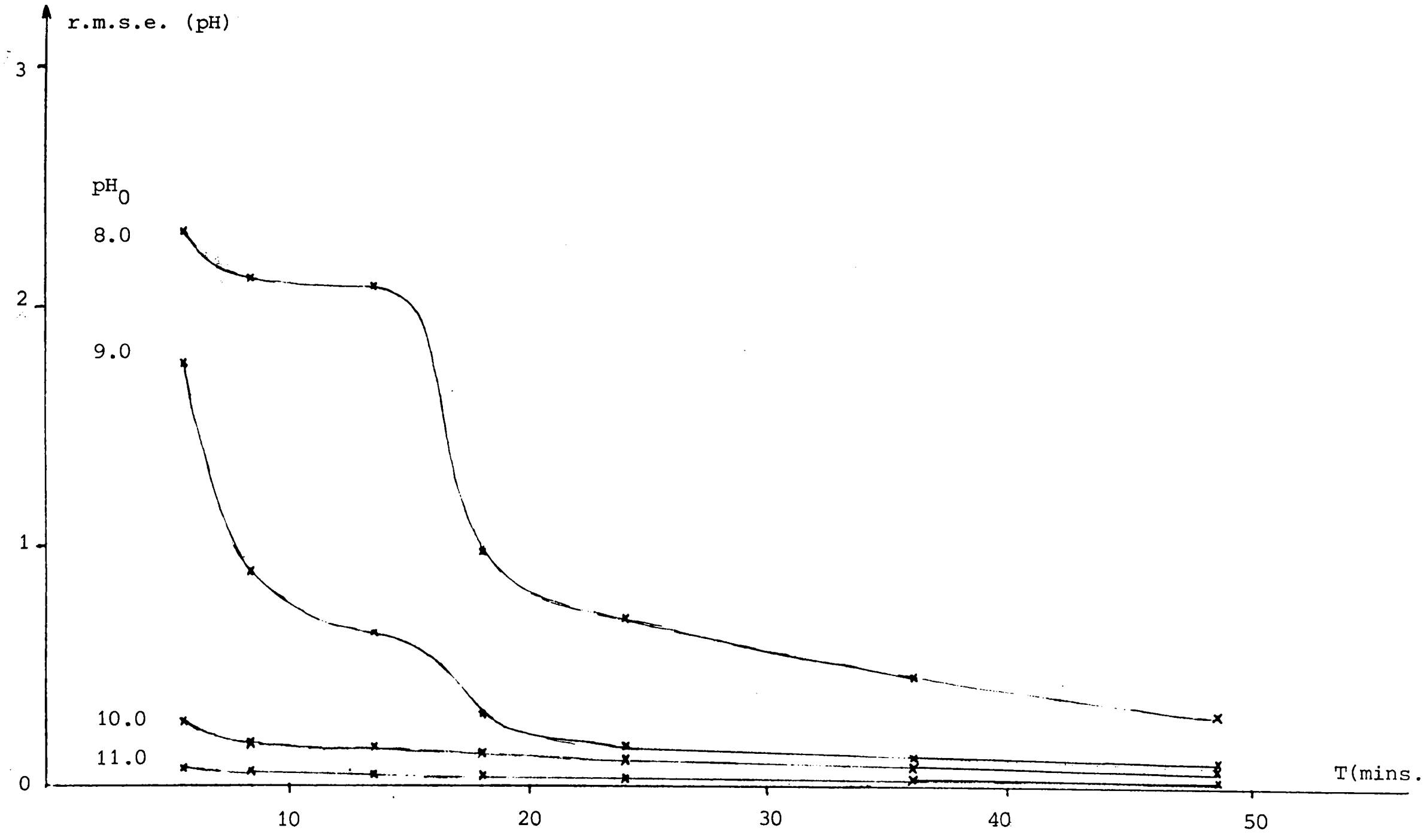


Fig 8.6 Single-stage neutralisation: feedback control

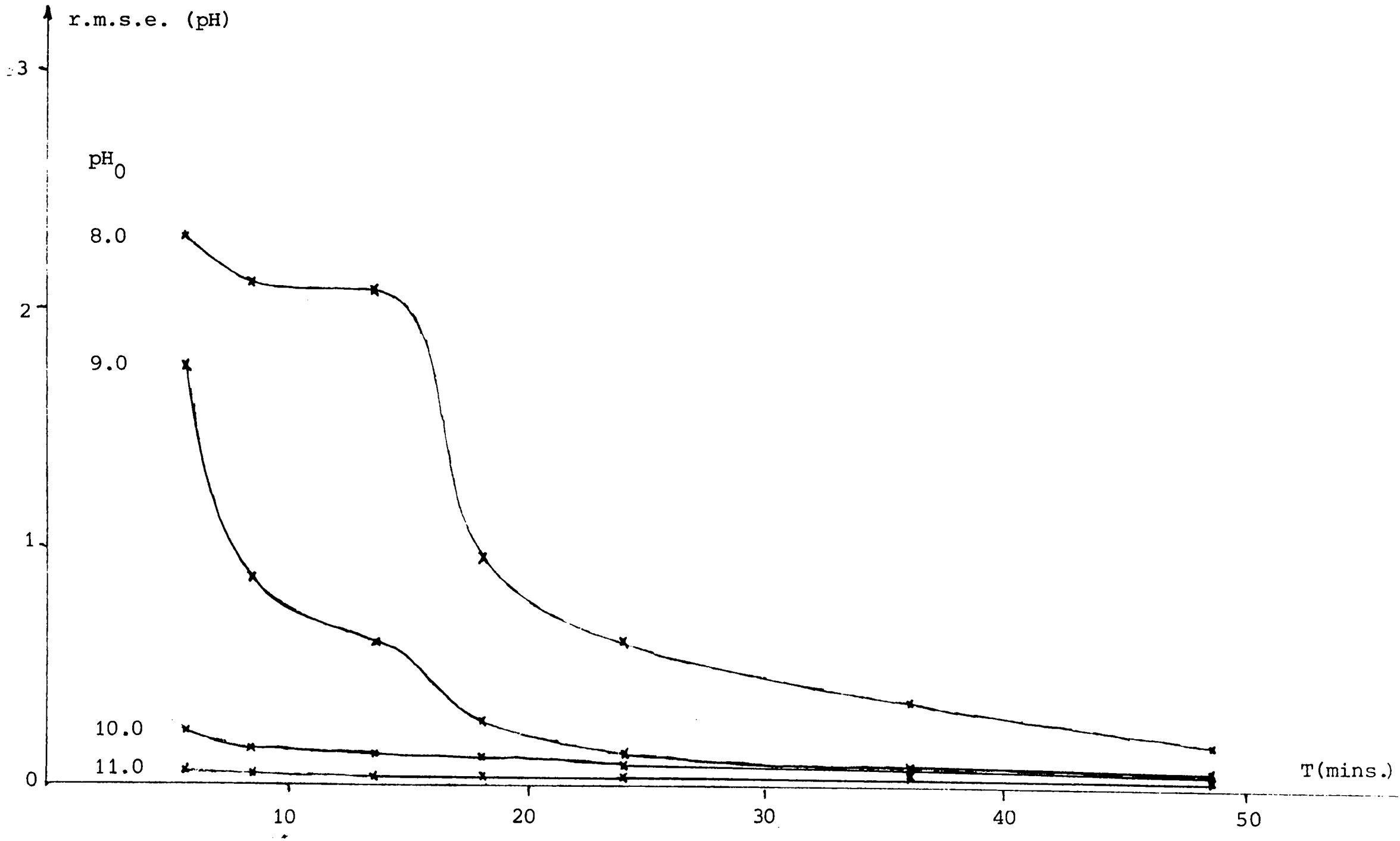


Fig 8.7 Single-stage neutralisation: feedback + feedforward control

N/S ratio of feedforward signals = 0.01, 0.05

constant tank was considered as the first stage in the two-stage system, with a final setpoint of pH 8 in the second stage. Overneutralisation in the first stage was chosen instead of underneutralisation (say to pH 4), because the physical properties of the influent product are greatly affected if the pH is below pH 7.

The two-stage system investigated (figure 8.8) is one in which the influent acid to the first stage is used as neutralizing reagent in the second stage. With such a configuration, a problem may arise: the reagent acid in the second stage may cause large variations of the influent acid flow into the first stage. However, preliminary two-stage simulation results have shown that the amount of acid influent taken to neutralise the second stage does not exceed 3% of the total. This additional perturbation to the first stage is small compared to the previously simulated flow disturbances which were of the order of 10% of nominal flow. The output of a single-stage simulation was therefore used as input for a single-stage simulation of the second stage. Stability analysis, presented in appendix E, of the two-stage configuration indicates that the reagent line to the second stage should not cause stability problems in the coupled system.

The results obtained (figure 8.9) using a selftuner PID, show how the quality of pH regulation (r.m.s. error in pH) in the second stage depends on the target value of pH and on the time constant of that stage. Three target values (8.0, 8.5 and 9.0) are simulated for time constants T ranging from 2.5 minutes to 10 minutes. It can be seen that when T = 4 minutes, the r.m.s. error levels off at 0.3 pH units for a target value of pH 8. This shows that the pH can be well regulated to the required target value of pH 8 in the second stage.

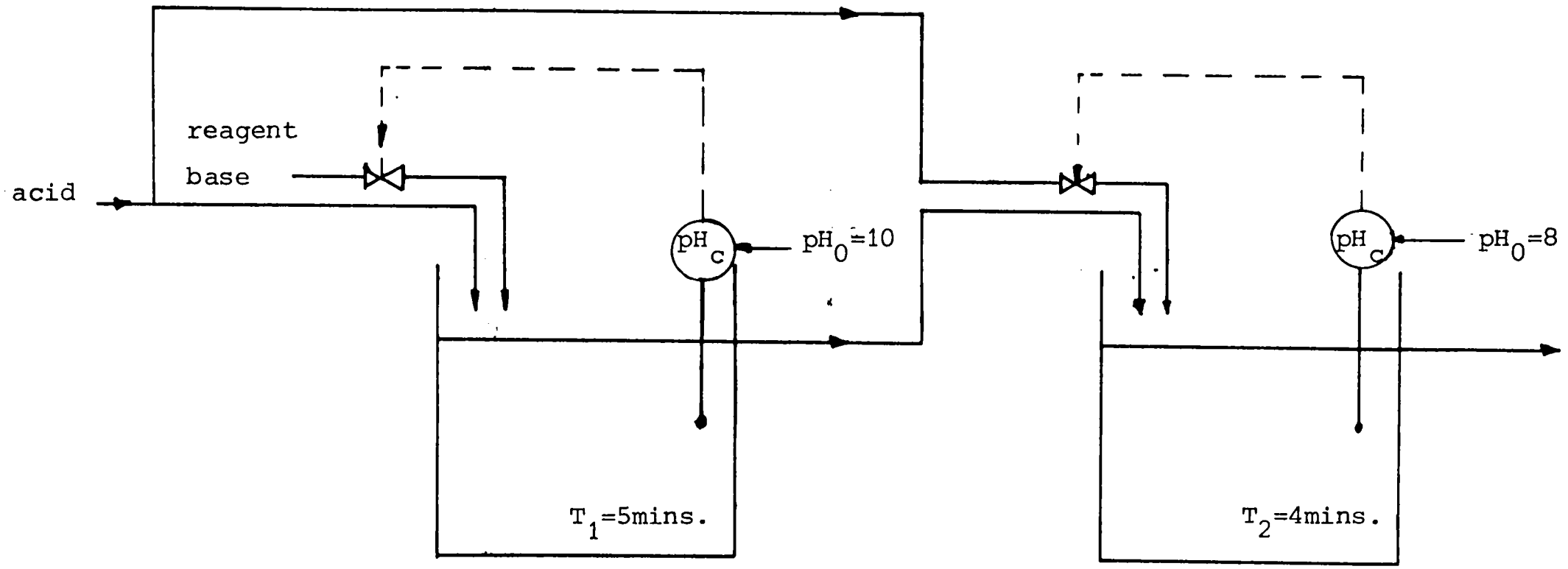


Fig 8.8 Two-stage neutralisation

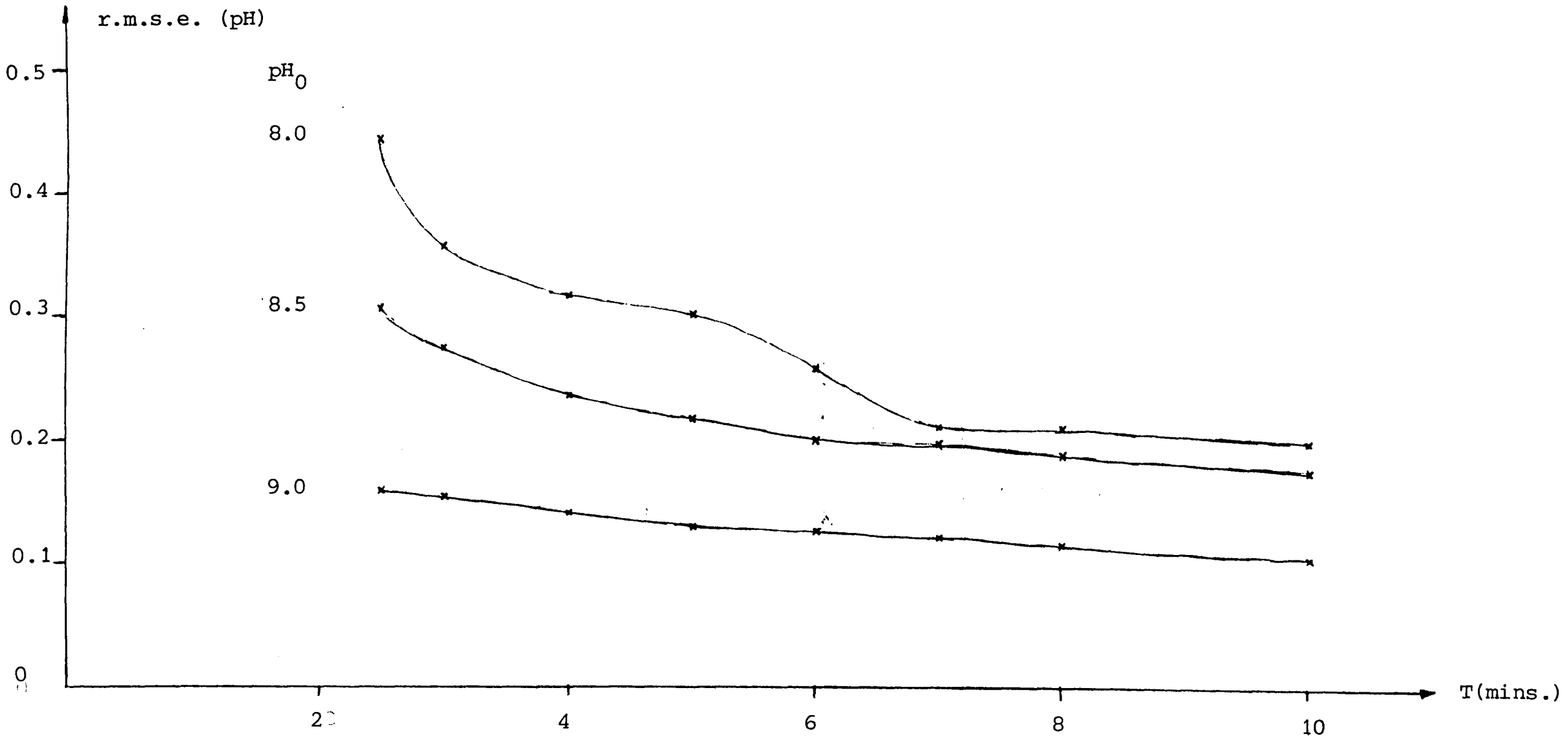


Fig 8.9 Two-stage neutralisation: feedback control

Thus, a recommended pH neutralisation system for the specified process is feedback control of a two-stage neutralisation each with a time constant of approximately 5 minutes. The target values in the first and second stages are pH 10 and pH 8 respectively.

8.2.3 Simulation Of A Full-scale Neutralisation Process

Simulation results for four different schemes to regulate pH in an existing plant are presented. Influent acid (pH 1.5) is neutralised in a recycle loop using concentrated base to a target value of pH 11.5. The schemes are:

1. Existing two-stage neutralisation (scheme A) with each stage time constant and open-loop base and acid flow rates specified by Unilever (figure 8.10). A constant addition of base in the first stage lifts the pH well above the target value to pH 13; the addition of acid in the second stage is too small to lower the pH to the required target value making impossible further feedback regulation using base.

2. Two-stage neutralisation (scheme B) with open-loop base and acid flow rates tuned to permit subsequent feedback regulation using base (figure 8.11). Half the amount of base in scheme A is added in the first stage to take the pH marginally above the target value of pH 11.5. Constant acid addition in the second stage lowers the pH below the target value, thus allowing closed-loop regulation using base.

3. One-stage feedback control (section 8.2.1) with base regulation, with tank time constant as in scheme A above (figure 8.12). The tank time constant is large enough for the selftuner PID to regulate the pH within acceptable levels

4. Optimal two-stage feedback control with base regulation in the first stage and acid regulation from the influent in the second as in section 8.2.2 but with same tank time constants as in schemes A & B above (figure 8.13). The amount of neutralising acid used in the second stage is small compared to the simulated influent disturbances. The selftuner PID is the feedback controller in both stages, and the target value in the first stage is pH 11.75.

The figures show time-histories of regulated pH and of base reagent flow into the second tank. Values of r.m.s. error in pH were as follows:

Scheme A	0.952
Scheme B	0.352
One stage feedback control	0.198
Two-stage feedback control	0.093

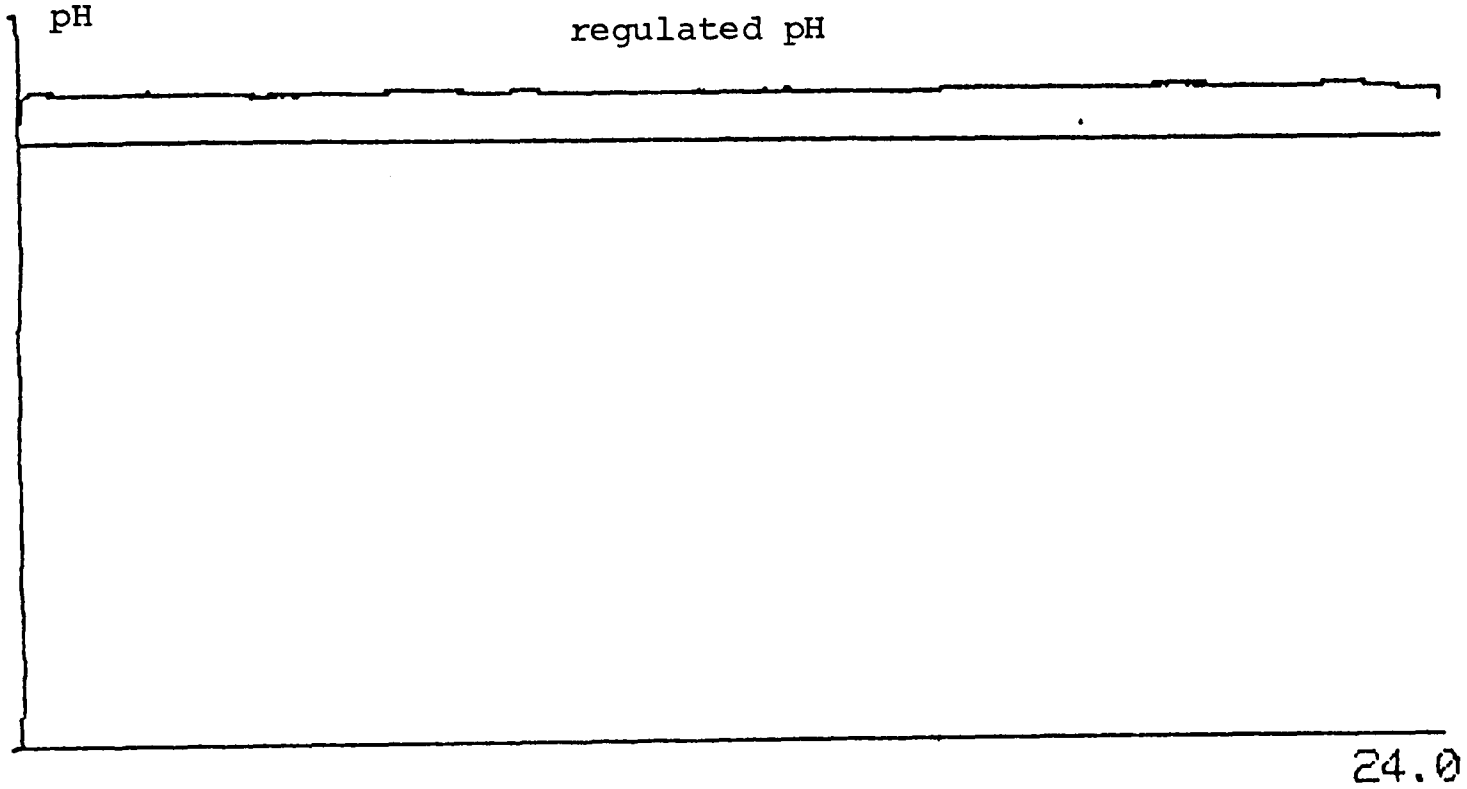
These simulation results show that scheme A & B are not well designed, and it is believed that the performance of the plant can be significantly improved by using feedback control. Actual time-histories from the process would provide a starting point for further studies.

8.3 CONCLUSION

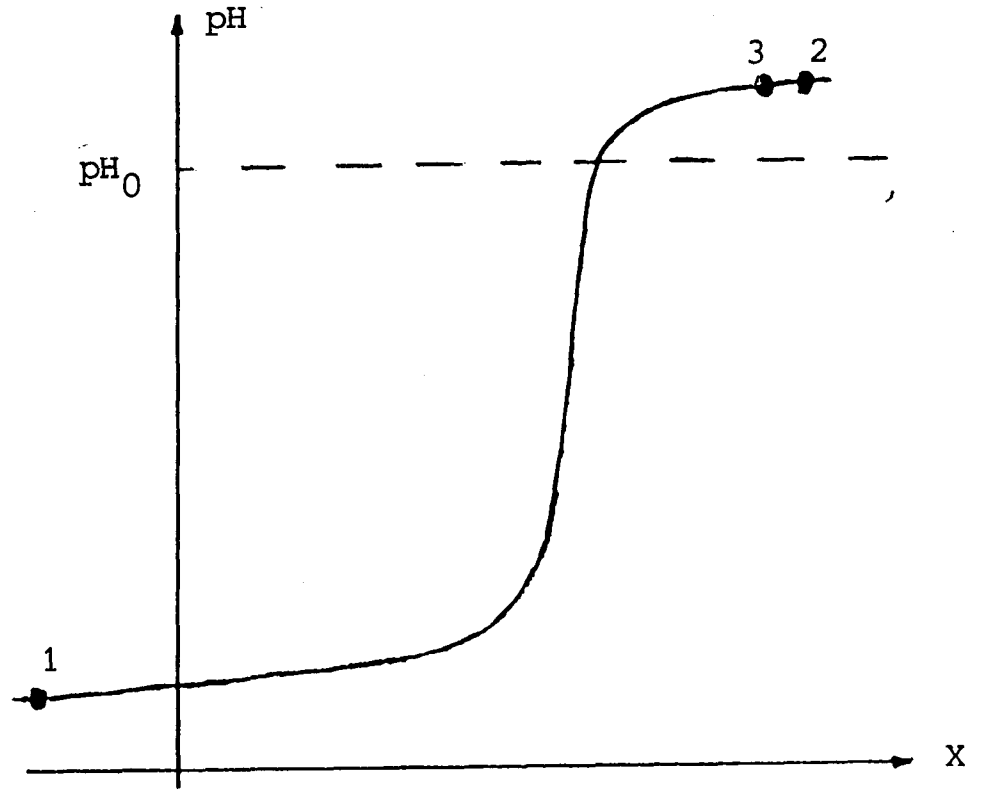
This chapter has shown how the simulation package has been used to investigate pH regulation for two chemical industries, and to provide recommendations to improve control performances. For ICI, control of pH in the neutralisation vessel improved considerably; the actual target

value was reduced by one pH unit which lead to savings in the cost of neutralisation. The package is now used within ICI to improve control of other existing pH systems by recommending alternative control techniques and operating conditions.

For Unilever, simulation results established key factors in plant design: residence time, operating target values, necessity of feedforward signals. Based on these results, a pH neutralisation system for a pilot plant has been recommended. Different control systems for an existing plant were also simulated, and recommendations were made to Unilever which will enable the company to rule out unpromising schemes.



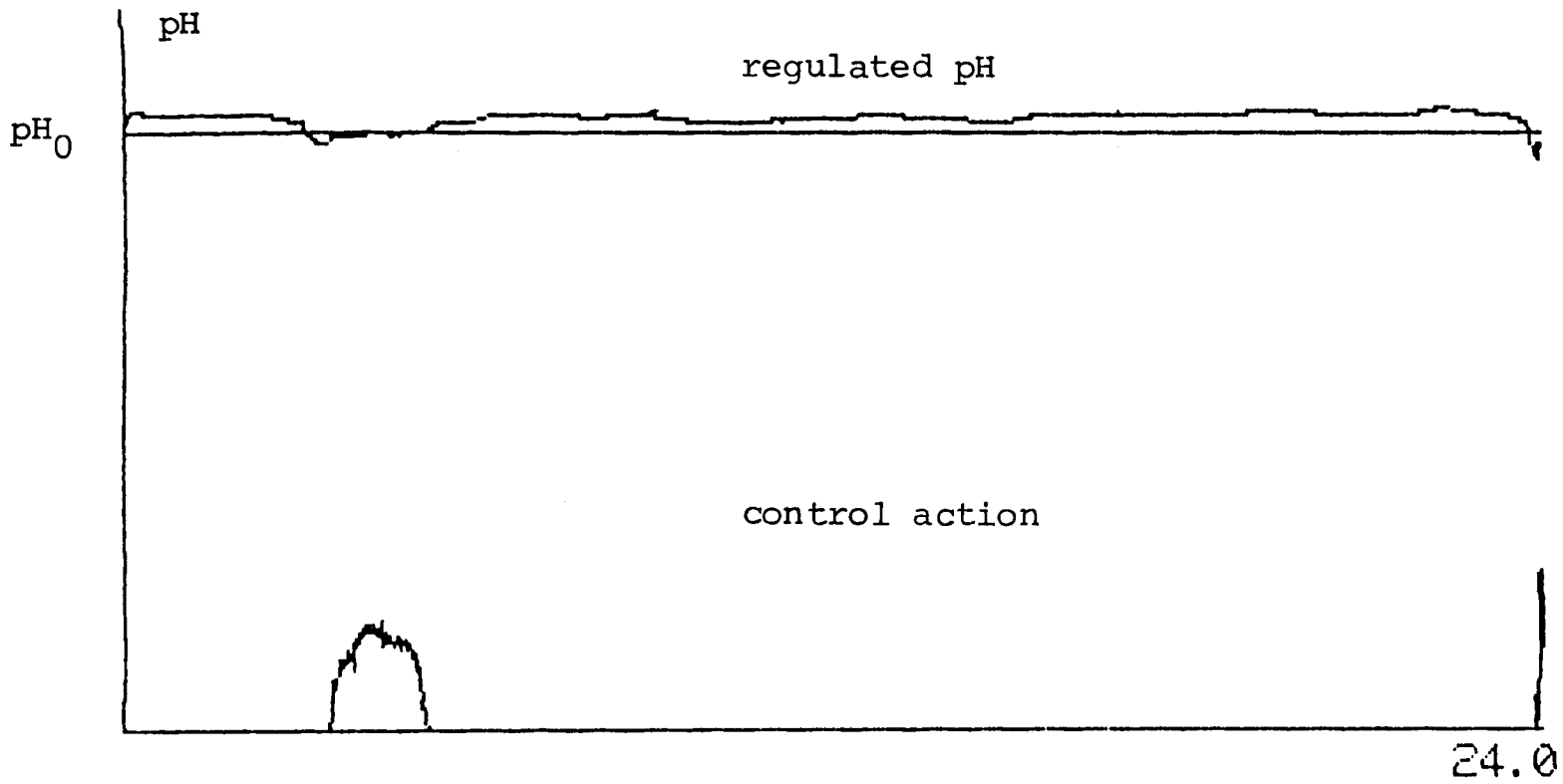
r.m.s. error = 0.952 pH units



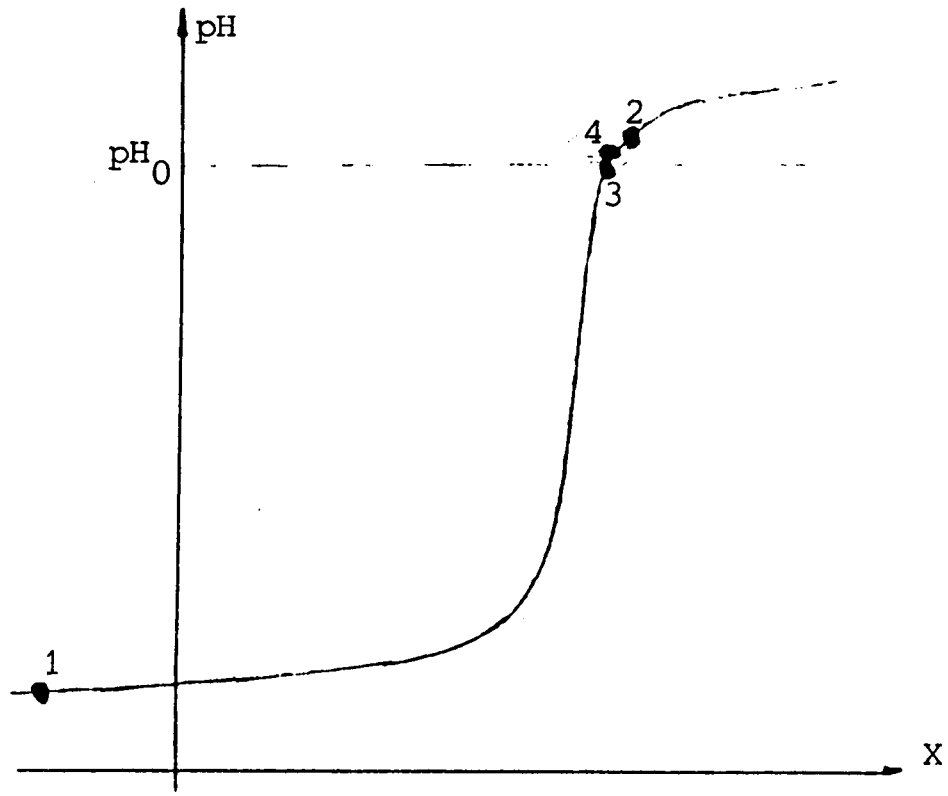
1. Influent
2. After constant base addition ($1 m^3 h^{-1}$)
3. After constant acid addition ($0.064 m^3 h^{-1}$

Further regulation toward set point is impossible using base

Fig 8.10 Existing two-stage neutralisation (scheme A)

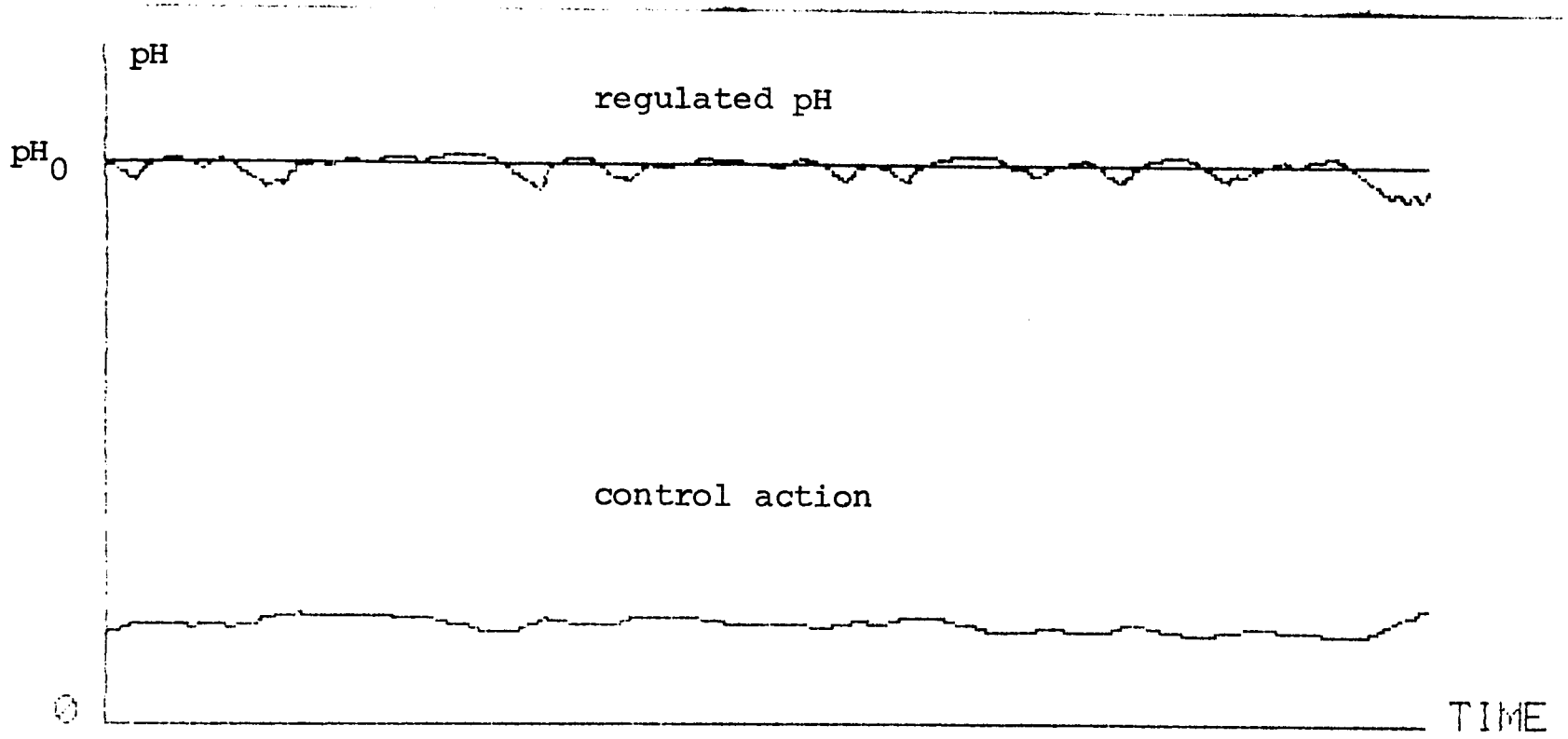


r.m.s. error = 0.352 pH units

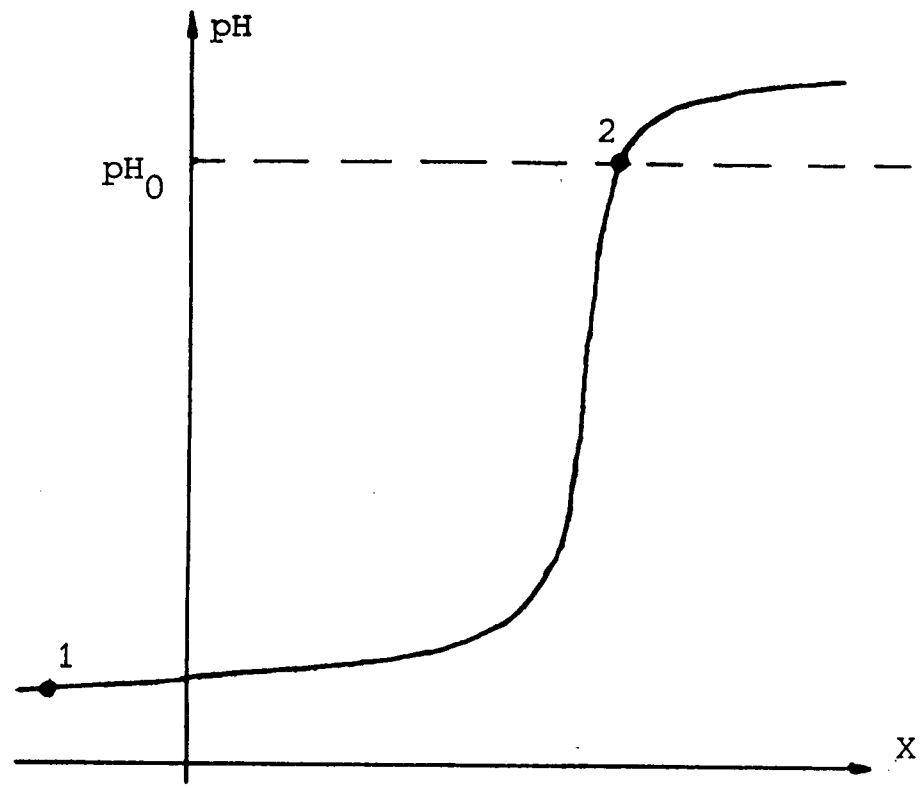


1. Influent as in fig 8.10
2. After constant base addition ($0.5 m^3 h^{-1}$)
3. After constant acid addition as close below set point as safely possible
4. Regulation using base

Fig 8.11 Modified two-stage neutralisation (scheme B)

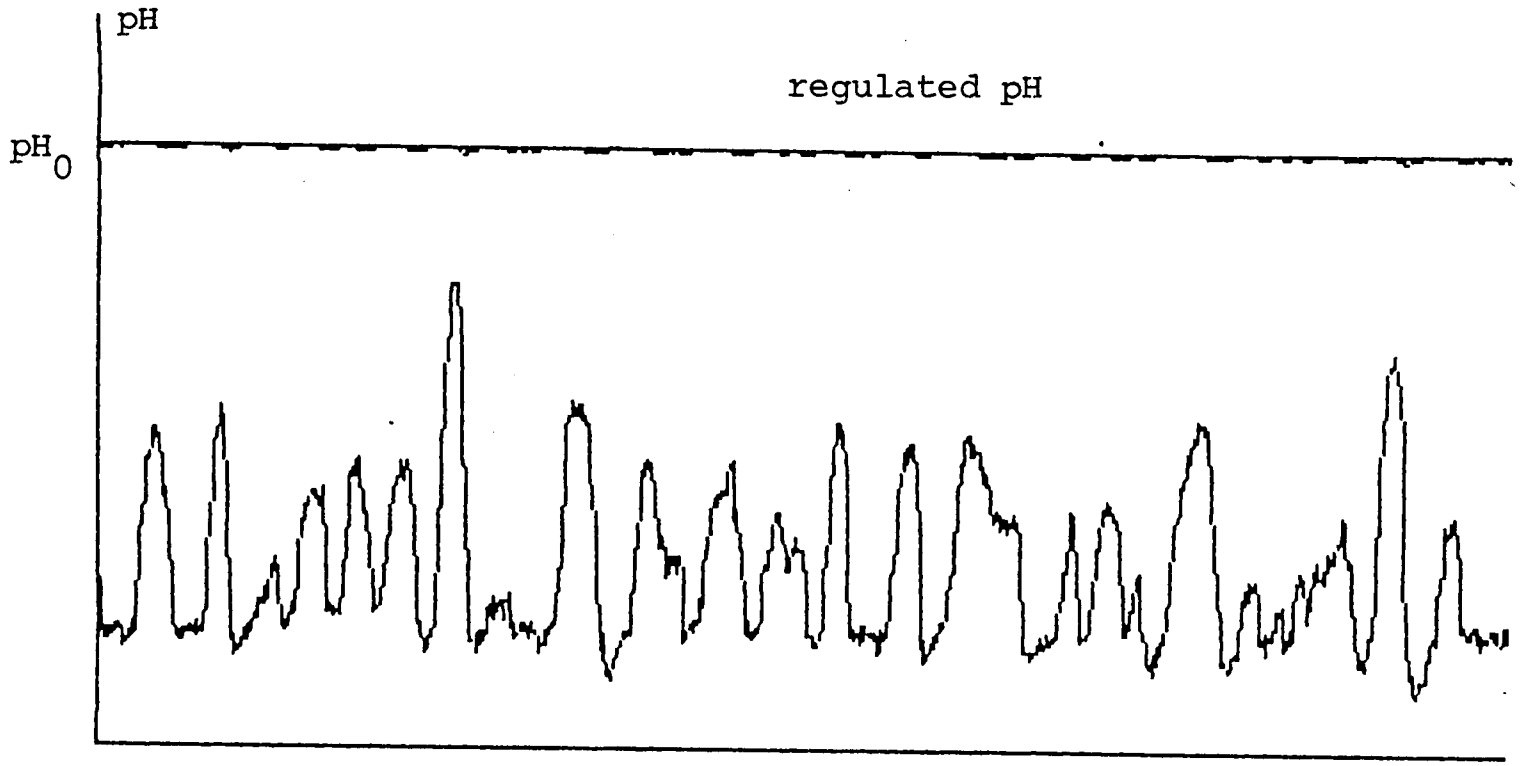


r.m.s. error = 0.198 pH units

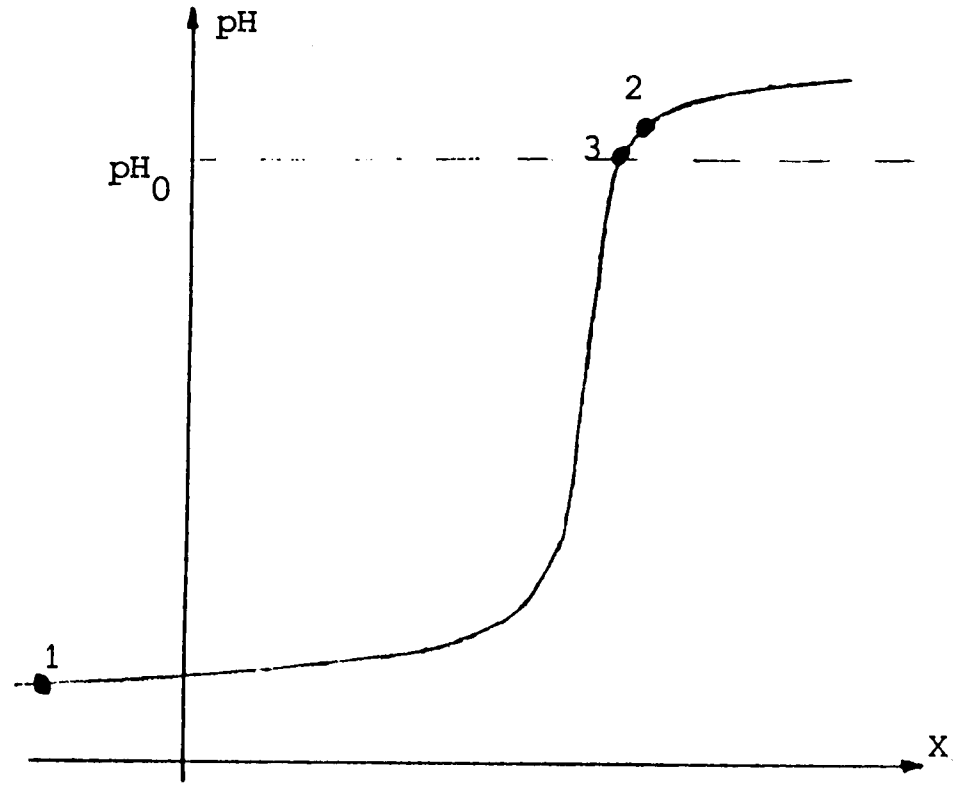


1. Influent as in fig 8.10
2. Regulation using base

Fig 8.12 One-stage feedback control



r.m.s. error = 0.093 pH units



1. Influent as in fig. 8.10
2. First-stage feedback control using ba
3. Second-stage feedback control using acid from influent.

Fig 8.12 Two-stage feedback control

CHAPTER 9

CONCLUSIONS

This concluding chapter reviews in section 9.1 the contribution of the thesis to the development of models, estimators and controllers of pH. The chapter also outlines in section 9.2 possible directions of further research. Section 9.3 concludes the chapter and the thesis.

9.1 REVIEW

The work described in the thesis comprised varied areas of resarch all linked by one control methodology for a particular non-linear system: pH. This methodology included at the start the construction of an accurate model, then the design of non-linear estimators tailored to the model and the development of estimator-based controllers, and finally the production of a realistic and interactive simulation package to test the model, the estimators and the controllers prior to their implementation on a full-scale process. The methodology is necessary because analysis alone is not sufficient to evaluate and assess the merit of the different algorithms for systems as non-linear as pH.

In the introduction to the thesis, chapter 1, the four specific contributions were stated: i) a new model of pH neutralization, ii) the

application of a non-linear estimator to bias-free and biased pH measurement, iii) a novel cautious stochastic controller, and iv) a comparison of a variety of control algorithms for pH regulation. This section describes how these contributions have been achieved and summarises the results of each contribution.

i) Modelling techniques have been used to construct a non-linear mathematical model of effluent neutralization in CSTR. The model, which is described in chapter 3, can distinguish between the inherent non-linearity of the pH measurement and the variable and often uncertain non-linearity of the titration chemistry. The contribution of the author is in developing from the process titration curve a novel three-dimensional function (equation 3.19) of the chemical analysis of neutralization. This function has been reduced to an approximate two-dimensional relationship (equation 3.27) and successfully incorporated in the mathematical model. The model has been derived using theoretical and experimental results and has been validated (chapter 8, case study 1) by comparing simulated outputs with real process outputs.

ii) The successful application of the non-linear Bayes' estimator to a noisy pH measurement of the effluent resulted in the linearisation of the pH non-linearity and the extraction of the effluent concentration from the pH measurement. The non-linear estimator (described in chapter 4) was used in conjunction with a model based Kalman filter estimator tailored to the mathematical model of neutralization. The estimator gives accurate estimates of the load disturbances to the CSTR provided that the pH measurement is not biased. The estimates have been used in simulation and on an industrial process, as synthetic feedforward signals to improve upon the feedback regulation of pH. However, the practicality

of the estimation scheme on the industrial process has not been fully investigated because the chosen process lacked the required condition of bias-free pH measurement. Nevertheless, a small improvement in regulatory performance using the non-linear estimator has been reported.

A novel version of the Bayes' estimator was developed to estimate non-zero bias on the pH measurement. The bias estimator used Bayes' rule in combination with two observability tests to estimate successfully, in simulation, variable step-wise and drifting bias. Good bias estimation is conditional on good feedforward measurements of the disturbances. The estimate of the bias provides a corrected value of the actual effluent pH which can be used for feedback control. The bias estimator was not tested on the industrial scale process because the process lacked the required feedforward measurements.

iii) A novel stochastic controller (described in chapter 6) has been developed for the pH process of chapter 3 and succesfully implemented in simulation. The controller, driven by the estimates of the process disturbances, explicitly accounts for their uncertainties in the form of a caution term. Reduced quality of estimation increases the importance of the caution term and forces the controller to regulate the pH at an optimally tuned target value where control is easier. The optimal target value is calculated numerically and is directly influenced by the confidence in the estimates. The performance of the cautious controller compares favourably with more classical control techniques with the added benefit that manual tuning of its parameters is not required. The simulation results presented in the thesis (sections 6.3.4, 6.4.4) have demonstrated that the performance of the novel controller is always better than that of any raw feedback (PID or selftuning) controller; it

is also often better than that of combined feedback-feedforward controllers. The cautious controller is easier to implement than any selftuner with estimated feedforward (as discussed in section 6.4.4); hence, the caution controller can provide a useful alternative to more classical control algorithms for a certain class of pH processes.

iv) The CAD simulation package (described in chapter 7) which was develop to simulate the neutralization model, includes a variety of modern and conventional control algorithms. The modern algorithms include three selftuning controllers, the non-linear estimators and the novel cautious controller. The conventional algorithms include a hand-tuned PID control, analytical linearisation of the pH measurement and the use of estimated or measured feedforward signals. The contribution of the author is in bringing together in the simulation package up to twenty-five pH control laws whose performance can be compared and the likely return of their implementation assessed.

Such comparisons have been carried out in the thesis to neutralisation processes of strong and buffered reagents. The simulation results for the different controllers have shown that improvement in performance over the PID is possible with the use of selftuners and with access to feedforward information. The amount of improvement is particular to each process, but in general, the pole-placement selftuner coupled to measured feedforward showed the best performance at the cost of a more complex feedback algorithm. For low cost implementation, the PID selftuner or the cautious controller can still provide good pH regulation.

The linearisation of the pH measurement is also a deciding factor in achieving good control: the simulation results show that the

linearisation was essential for tight pH regulation for a strong reagent process, while it did not improve control performance for a buffered process. No general conclusion on the effect of the linearisation can be drawn from these results because the non-linearity of each pH process is dependent on all the process parameters including the titration curve.

Based on the value and the amount of a priori information about the process, a pH control strategy has been proposed. The strategy (section 6.5) summarises the results of modelling, estimation and control techniques developed in the thesis. Information about the process titration curve, the disturbances, and the bias on the pH measurement has provided guidelines to the control configurations that can be implemented as well as their relative limitations.

9.2 FUTURE RESEARCH

The various areas of research described in the thesis can provide specific fields of future investigation which are outlined in this section.

An area of future research is the extension of the work reported here to account for pH systems in which the titration curve is variable or unknown. Although these systems were not specifically encountered during the course of the thesis, they are common (Proudfoot and McAlpine 1984) in treatment of waste effluent ~~for~~ from different processes. The future work may be based on that of Jutila (1983) in which the pH chemical model is characterized by the presence of hypothetical chemical species which can be chosen by static fitting of the titration curve. In order to limit the computing power required for the non-linear curve fitting, only specific parts of the titration curve need to be estimated. However,

before trying such complicated schemes, it would be worthwile to determine whether a selftuner such as the pole-placement can regulate the pH effectively.

The regulation of effluent pH using lime is widely used in industry because of its low cost. Lime reacts very slowly and its reaction kinetics introduces a major variable time-delay in the control system and affects the quality of pH regulation. Ways of improving pH regulation for such process can provide a second area of research. As a starting point, the pole-placement selftuner would probably provide a robust pH regulation.

Another area of future research is to investigate pH regulation using an in-line mixer. In general, in-line mixers cost less than CSTR's but are characterised by relatively large time-delays. The simulation package PHDESIGN can be used for this investigation in the same manner as described in chapter 8 for the modelling and the pH regulation in recycle loops.

A different area of research can be the study of the convergence properties of the non-linear estimator of chapter 4. Although the estimator has provided accurate estimates of effluent concentration and bias, its convergence has not yet been proved.

A more practical future research area would be application of the bias estimator and the stochastic cautious controller on a pilot plant or on a full-scale pH neutralization process. The two algorithms are robust and have performed well in simulation. They can be applied to processes which are difficult to control because of large disturbances or noisy and

biased pH measurements.

9.3 CONCLUSION

The conclusion from the thesis is that pH regulation, for existing and new processes, can benefit from good engineering practice and also from modern control technology. For existing plant, good practice includes accurate measurement of pH to prevent biases, accurate control of reagent flow, exploitation of feedforward signals, linearization to eliminate known non-linearities. For designs of new plant good engineering practice influences choice of system layout, sizing of mixing vessels and piping, choice of operating target values. Modern control technology includes use of selftuners, use of non-linear estimators and stochastic controllers if suitable data is available. Even with good practice and modern control technology, there is a limit to the quality of neutralization which can be achieved. This limit varies from plant to plant and can only be determined experimentally because of the uncertainties and the non-linearities of the pH systems. The computer package PHDESIGN can provide a tool for predicting the limit as well as for designing controllers to achieve the required performance.

APPENDIX A

CALCULATION OF THEORETICAL TITRATION CURVES

Examples illustrating the calculation of theoretical titration curves in aqueous solutions are shown here for strong and for weak reagents.

Water dissociates into hydrogen ions and hydroxyl ions according to:

$$H_2O \rightarrow H^+ + OH^- \qquad (A.1)$$

with the dissociation constant of the water K_w governing the concentration of the ions in solution:

$$[H^+]\,[OH^-] = K_w = 10^{-14} \text{ at } 25°C \qquad (A.2)$$

The bracketed terms represent the concentration of the species in Normality.

A.1 STRONG ACIDS AND BASES

Consider a reaction between sodium hydroxide NaOH, and hydrochloric acid HCl. Both are strong reagents and are completely dissociated in solution:

$$HCl + NaOH + H_2O \rightarrow H^+ + OH^- + Na^+ + Cl^- \qquad (A.3)$$

The ionic concentrations satisfy the principle of electroneutrality:

$$[H^+] + [Na^+] = [OH^-] + [Cl^-] \qquad (A.4)$$

Assuming complete ionization of acid and base, $[Na^+]$ must equal the original concentration of base x_B, and $[Cl^-]$, the original concentration of acid x_a:

$$[H^+] + x_B = [OH^-] + x_A \qquad (A.5)$$

Substituting for $[OH^-]$ from equation A.2:

$$x_A - x_B = [H^+] - \frac{10^{-14}}{[H^+]} \qquad (A.6)$$

Equation A.6 can then be used to relate acid and base concentration to pH:

$$x_A - x_B = 10^{-pH} - 10^{pH-14} \qquad (A.7)$$

A.2 WEAK ACIDS AND BASES

Consider the addition of a weak base such as ammonia NH_3 to the mixture of HCl and NaOH previously investigated:

$$HCl + NaOH + NH_3 + H_2O \rightarrow H^+ + OH^- + Na^+ + Cl^- + NH_4^+ \qquad (A.8)$$

Only a fraction of the weak base will ionize, the remainder being in equilibrium with the product of its ions, obeying the relationship:

$$K_C = [NH_4^+][OH^-]/[NH_3] \qquad (A.9)$$

A charge balance on the system is as follows:

$$[H^+] + [Na^+] = [OH^-] + [Cl^-] + [NH_4^+] \qquad (A.10)$$

Here again, x_B and x_A may be substituted for $[Na^+]$ and $[Cl^-]$ due to complete ionization. The initial concentration of the third reagent, ammonia, is given as x_C and is the sum of the undissociated base and the ammonia ion:

$$x_C = [NH_3] + [NH_4^+] \qquad (A.11)$$

The concentration of undissociated NH_3 may be found from equation A.9:

$$[NH_3] = [NH_4^+][OH^-]/K_C \qquad (A.12)$$

Then,

$$x_C = [NH_4^+] + [NH_4^+][OH^-]/K_C \qquad (A.13)$$

Solving for $[NH_4^+]$,

$$[NH_4^+] = \frac{x_C}{1+[OH^-]/K_C} \qquad (A.14)$$

Making all the appropriate substitutions in equation A.10:

$$x_A - x_B = [H^+] - \frac{10^{-14}}{[H^+]} + \frac{x_C}{1+10^{-14}/[H^+]K_C} \qquad (A.15)$$

For convenience, equation A.15 can be restated in terms of pH:

$$x_A - x_B = 10^{-pH} - 10^{pH-14} + x_C/(1 + 10^{pK_C+pH-14}) \qquad (A.16)$$

where pK_C (like pH) is the negative logarithm to the base 10 of K_C.

In equations A.7 and A.16, values are selected for x_A, x_C and pH, and x_B is calculated resulting in a titration curve relating pH to x_B for a given x_A and x_C.

APPENDIX B

IMPLEMENTATION OF THE pH NON-LINEARITY

This appendix discusses the numerical implementation on a digital computer of the relationship between the i.c.d. X and pH as defined by equations 3.28. The appendix also discusses the implementation of the derivative of this relationship needed in equation 4.17.

B.1 THE pH NON-LINEARITY

The relationship between X and pH is shown in figure 1.1 and is defined by:

$$pH(X) = -\log_{10}\left(-\frac{X}{2}\left(1+\sqrt{\left(1+4K_w/X^2\right)}\right)\right) \qquad \text{if } X < 0 \qquad (3.28a)$$

$$pH(X) = -\log_{10}\left(-\frac{X}{2}\left(1-\sqrt{\left(1+4K_w/X^2\right)}\right)\right) \qquad \text{if } X > 0 \qquad (3.28b)$$

Equations 3.28 are computed by taking the first three terms of the Taylor's series expansion of the square root:

$$pH(X) = -\log_{10}\left[-X - \frac{K_w}{X}\left(1 + \frac{K_w}{X^2}\left(2\,\frac{K_w}{X^2} - 1\right)\right)\right] \qquad X < 0 \qquad (B.1a)$$

$$pH(X) = -\log_{10}\left[\frac{K_w}{X}\left(1 + \frac{K_w}{X^2}\left(2\,\frac{K_w}{X^2} - 1\right)\right)\right] \qquad X > 0 \qquad (B.1b)$$

B.2 THE DERIVATIVE OF THE pH NON-LINEARITY

The derivative of the pH non-linearity is needed in the Extended Kalman Filter of section 4.3.3:

$$H_{EKF} = \frac{dpH(X)}{dX} \tag{4.17}$$

Differentiating equations 3.28 with respect to X:

$$\frac{dpH(X)}{dX} = -\frac{1}{\ln 10}\,(X^2 + 4K_w)^{-1/2} \qquad X < 0 \tag{B.2a}$$

$$\frac{dpH(X)}{dX} = \frac{1}{\ln 10}\,(X^2 + 4K_w)^{-1/2} \qquad X > 0 \tag{B.2b}$$

The derivative of the pH function is computed by taking the first three terms of the Taylor's series expansion of equations B.2, and rearranging:

$$\frac{dpH(X)}{dX} = -\frac{1}{\ln 10}\left[\frac{1}{X}\left(1 - 2\frac{K_w}{X^2}\left(1 + 3\frac{K_w}{X^2}\right)\right)\right] \qquad X < 0 \tag{B.3a}$$

$$\frac{dpH(X)}{dX} = \frac{1}{\ln 10}\left[\frac{1}{X}\left(1 - 2\frac{K_w}{X^2}\left(1 + 3\frac{K_w}{X^2}\right)\right)\right] \qquad X < 0 \tag{B.3b}$$

APPENDIX C

CALCULATION OF MODELLING ERRORS

In this appendix, modelling errors arising from uncertainties in the value of the tank volume and the time constants of the disturbances are calculated as an error matrix $\underline{E}$. These errors are accounted for in the EKF equations in section 5.4.

C.1 MODELLING ERRORS IN THE TANK VOLUME

The uncertainty in the volume V can be calculated from equation 5.27:

$$e_{11} = \mathrm{var}\{ \frac{\Delta}{V^0} x_2(i)(X_{in}(i) - x_1(i+k))\epsilon \} \qquad (5.27)$$

where e_{11} is the element 1,1 of the modelling error matrix $\underline{E}$; ϵ is a normalised zero-mean independent random variable of variance $\mathrm{var}(\epsilon) = Q^2$; x_{in} accounts for the neutralisation chemistry and is given by equations 3.30:

$$X_{in} = x_3 + uX_r/x_2 \qquad \text{for strong reagents} \qquad (3.30a)$$

$$X_{in} = f_1(f_1^{-1}(x_3) + uX_r/x_2) + \delta X \qquad \text{for weak reagents} \qquad (3.30b)$$

In order to simplify the calculation of the variance in equation 5.27, the random term $x_2(i)(X_{in}(i) - x_1(i+k))$ is replaced by a random variable

χ:

$$\chi = x_2(i)(X_{in}(i) - x_1(i+k)) \qquad (C.1)$$

Replacing for χ in equation 5.27:

$$e_{11} = \left[\frac{\Delta}{V^0}\right]^2 \text{var}\{\chi\epsilon\} \qquad (C.2)$$

χ and ϵ are random variables; hence, e_{11} is approximately computed (Papoulis 1965) by:

$$e_{11} \simeq \left(\frac{\Delta}{V^0}\right)^2 (m_\chi)^2 v_\epsilon + (m_\epsilon)^2 v_\chi + 2 m_\chi m_\epsilon v_{\chi\epsilon} \qquad (C.3)$$

where m_χ & m_ϵ and v_χ & v_ϵ are the mean and variance of χ and ϵ respectively, and $v_{\chi\epsilon}$ is their covariance. But, $m_\epsilon = 0$ and $v_\epsilon = Q^2$; substituting these values in equation C.3:

$$e_{11} = \left\{\frac{\Delta}{V^0} m_\chi Q\right\}^2 \qquad (C.4)$$

Replacing m_χ from equation C.1 for strong and for weak reagents, we obtain equations 5.28 and 5.29.

for strong reagents:

$$e_{11} = \left\{\frac{\Delta}{V^0} (m_2(m_3 - m_1) + \sigma_{23} - \sigma_{12} + X_r u)Q\right\}^2 \qquad (5.28)$$

for weak reagents:

$$e_{11} = \left\{\frac{\Delta}{V^0} (m_2(M_{in} - m_1) - \sigma_{12})Q\right\}^2 \qquad (5.29)$$

where m_1, m_2 & m_3 are the elements of the state estimate $\hat{\underline{x}}$ (equation 5.10), and σ_{12} & σ_{23} are the elements of the covariance matrix $\underline{\Sigma}$, and M_{in} is given by:

$$M_{in} = f_1(f_1^{-1}(m_3) + uX_r/m_2)$$

C.2 MODELLING ERRORS IN THE DISTURBANCES

The calculation of the uncertainty in the disturbance time constants T_j (j=2,3) can be calculated from equation 5.39:

$$e_{jj} = \text{var}\left[((1 - g_j^0)x_j(i) - \alpha_j^0)\epsilon\right] + \text{var}(\xi_j^{\epsilon}) \qquad (5.39)$$

where e_{jj} are the elements 2,2 & 3,3 of the error matrix $\underline{E}$; ϵ is again a normalised zero-mean independent random variable of variance $\text{var}(\epsilon) = Q^2$; $\text{var}(\xi_j^{\epsilon})$ is given by equation 5.37:

$$\text{var}(\xi_j^{\epsilon}) = (2\ \Delta/T^0)^2\ Q^2 \text{var}(\mu_j) \qquad (5.37)$$

Again, in order to simplify the calculation of the variance in equation 5.39, the random term $((1 - g_j^0)x_j(i) - \alpha_j^0)$ is replaced by a random variable χ:

$$\chi = ((1 - g_j^0)x_j(i) - \alpha_j^0) \qquad (C.5)$$

Replacing for χ in equation 5.39:

$$e_{jj} = \text{var}\{\chi\epsilon\} + \text{var}(\xi_j^{\epsilon}) \qquad (C.6)$$

χ and ϵ are random variables; hence, $\text{var}\{\chi\epsilon\}$ of equation C.6 can be approximately computed (Papoulis 1965) as in equations C.3 and C.4:

$$e_{jj} = \{m_\chi Q\}^2 + \text{var}(\xi_j^{\epsilon}) \qquad (C.7)$$

Substituting for m_χ from equation C.5 and for $\text{var}(\xi_j^{\epsilon})$ from equation 5.37, equation C.7 is written as equation 5.40:

$$e_{jj} = \left[((1 - g_j^0)m_j - \alpha_j^0)Q\right]^2 + (2\ \Delta/T^0)^2\ Q\text{var}(\mu) \qquad (5.40)$$

The remaining elements of the error matrix $\underline{E}$ are zero.

APPENDIX D

PHDESIGN: USERGUIDE

PHDESIGN: CAD OF SYSTEMS FOR REGULATING pH

USER GUIDE

by W. A. Badran and O. L. R. Jacobs

Dept. of Engineering Science, University of Oxford

November 1983.

1.0 INTRODUCTION

PHDESIGN is a CAD package which simulates pH regulation in a common class of unit process. A range of algorithms performing classical control, adaptive control and on-line estimation is included. The package is accurate in detail and well provided with interactive features. It can be used in two different ways:

(i) to design improved controls for existing processes,

(ii) to explore control aspects of proposed new process.

The simulation is based on a continuous stirred-tank reactor (CSTR), having the standard configuration of fig. 1, where an influent stream of variable acidity and flow-rate is neutralised by mixing with concentrated reagent. A feedback signal in the form of measured pH of effluent drives the controller which adjusts the reagent flow-rate. Feedforward signals measuring influent acidity and flow rate may or may not be available.

The program is written in ANSI FORTRAN 77 and uses a subset of GINO graphic routines with Tektronix-compatible terminals. It has been implemented on a VAX 11/780. Detailed descriptions of the package can be found elsewhere [1-4].

2.0 INPUT FROM THE USER

The user must specify process characteristics, titration curve data and controller parameters. Process disturbances in influent flow-rate and acidity are simulated either by generating stochastic variables or by storing influent flow rate and pH data and reproducing them as actual time-histories.

The process and the controller parameters are stored in two files: PH#.DAT and CT#.DAT where # is a number identifying the simulated process. Up to a hundred processes can be filed in this way. A directory of filed processes, PHCONT.DAT, contains the process number, a brief process description, the user name, and the date at which the process parameters were last modified and stored.

3.0 OUTPUT FROM THE SIMULATION

Simulation results are stored in the form of time-histories of all significant simulated variables such as flow-rates, acidities, pH, controls, bias, estimates and their estimated standard deviations from the on-line estimator and from the different controllers. At the end of a run, these time-histories can be displayed on the VDU one at a time or concurrently and can be hard-copied. Options for ordinate rescaling are included in the package. Statistical results in the form of root mean square error in pH (RMSE) and of average reagent flow (ARF) are also computed and displayed.

If the program is interrupted while running two temporary files PH0.DAT and CT0.DAT are created; they contain the process and controller parameters of the current run. They are subsequently deleted on sucessful completion of the program.

4.0 USER INTERACTION

The interaction is driven by menus which prompt the user to specify or modify process characteristics, titration curve data and controller parameters. The files maintain information about specific processes, with options for the user to create new entries, to modify and overwrite existing entries and to delete unwanted entries. The overwrite option provides a mechanism for controller development; it automatically files values of controller parameters which have been obtained by trial and error during a session of simulation. Hence well-tuned controller parameters can be recalled at the start of each run.

The package interacts with the user through lists of two letter mnemonics including HElp which displays the current menu of options. Fig. 2 summarises the interaction at four levels. At Level 1 the user specifies a controlled process by either calling a stored process or inputting a new process. At Level 2 he can display and modify the process specifications and the titration curve or proceed directly to choose a controller. Controller and run-time parameters can be displayed and modified at Level 3. At Level 4 simulation results in form of time-histories are displayed. Overwrite and quit options are available from all levels.

PHDESIGN is run from the computing system by typing either

```
$ PHDESIGN
```

or `$ RUN PHDESIGN`

and is quit by the command OQ (Overwrite and Quit) followed by QU (QUit).

When PHDESIGN is invoked, the welcome message:

```
WELCOME TO PHDESIGN
C.A.D. for pH systems
```

```
DO YOU WANT INSTRUCTIONS ? (Y,N)
```

is displayed. By entering "Y", a brief introductory message appears explaining the purpose of the program:

PHDESIGN

PHDESIGN is a C.A.D. package of systems for regulating pH.
The user specifies the pH process and chooses the controller.
After each run, time histories of the different simulated variables are displayed.
The program interacts with the user through lists of two-letter mnemonics of which HE(lp) displays the current options available.

This stays on the screen until the user, prompted by the program, presses <RETURN>.

4.1 Level 1: Specify Process

This level specifies the controlled pH process. The commands available are:

HE - print this message
RE - REturn to welcome message
NE - input NEw process from keyboard
OL - get OLd process from disk
DE - DElete old process from disk
CO - COntinue with specified process
OQ - Overwrite and Quit options

HE and RE are self-explanatory. NE prompts the user to input a new process; example 1 in section 6 describes a typical session when using this command. OL and DE will list the existing processes and will prompt the user to choose one from the list. CO will proceed to the next level with an already chosen process; if no process was chosen the program will prompt the user to do so before proceeding. OQ options are described in section 4.5.2.

4.2 Level 2: Display and Modify Process

At this level, the specified process and the titration curve may be displayed and modified. The commands are:

HE - print this message
RE - REturn to specify pH process
CO - COntinue to specify controller
HC - HardCopy
DP - Display Process specifications
DT - Display Titration curve
MP - Modify Process specifications
MT - Modify Titration curve
OQ - Overwrite and Quit options

RE returns to Level 1 to specify a different process. CO continues to choose the controller (section 4.3); if a controller has been chosen previously, the program monitor goes to Level 3 to display the controller parameters (section 4.4). HC produces a hardcopy of the screen. DP displays, as in fig. 3, the controlled process parameters such as set point, tank volume, time delay, disturbance statistics and measurement filters and bias; the titration curve is also drawn on the screen. Display of titration curve data, DT, is described in the following section. Modification of the process specification, MP, and of titration curve, MT, are discussed in examples 2 and 3 of section 6.

4.2.1 Display Titration Curve: Option DT - The titration curve display options allow the user to plot the titration curve data on different axes. The options are:

HE - print this message
P1 - X-Xs/Xr vs. Vr/Vs
P2 - X vs. VrXr/Vs
P3 - pH vs. r
HC - HardCopy
RE - REturn to simulated pH process

where X is the ionic concentration difference ($[OH^-]-[H^+]$) of the mixture
Xs is the ionic concentration difference ($[OH^-]-[H^+]$) of the sample
Xr is the ionic concentration difference ($[OH^-]-[H^+]$) of the reagent
Vs is the volume of the sample
Vr is the volume of the reagent
r = VrXr/VsXs

P1 and P2 plot the titration chemistry without the logarithmic non-linearity of the pH measurement so as to show any nonlinear effect of the chemistry of buffered solutions [5,6]. The evaluation of $[OH^-]$ here depends on temperature, which is part of the user-specified data. P3 plots pH of the mixture as a

function of a non-dimensional ratio r. HC produces a hardcopy of the screen and RE returns the program monitor to Level 2 options.

4.3 Choose Controller

When choosing a control algorithm, the user must specify whether the controller configuration is manual (MA) with a constant control to be specified by the user, classical using error-actuated feedback and possibly also some feedforward (CL) or stochastic using the separated estimation and control structure of optimal control theory (ST). Other options are to return to the Level 2 options by issuing the command RE or to proceed to the overwrite and quit options by issuing the command OQ (section 4.5.2).

CONTROLLER CONFIGURATION

MA - MAnual control
CL - CLassical control
ST - STochastic control
RE - REturn to specify pH process
OQ - Overwrite and Quit options

When a classical control configuration is chosen, the user will then specify if the error signal driving feedback control is in units of pH, EP, or in units of acidity (ionic concentration difference), EX so that the nonlinearity of pH measurement is removed.

ERROR CONFIGURATION

EP - Error in pH
EX - Error in X

Feedforward measurements of flow-rate and acidity of influent are optional: NF option does not use any feedforward signals in control; EF option provides online estimates of influent flow-rate and acidity which are used as synthetic feedforward signals assuming that no measurements are available; real feedforward instrumentation on the influent stream is simulated and used for control when MF option is selected.

FEEDFORWARD CONFIGURATION

NF - No Feedforward
EF - Estimated Feedforward
MF - Measured Feedforward

Finally, a feedback controller may be chosen from:-

i) standard three-term PID control, option PI;

ii) self-tuning three-term PID control, option SP;

iii) generalised k-incremental minimal variance self-tuning control, option KS;

iv) pole placement self-tuning control, option PS.

FEEDBACK CONFIGURATION

PI - PId control
SP - St-Pid control
KS - K-Stc control
PS - P-Stc control

After the controller is selected, the program monitor goes to Level 3 to display and modify the controller parameters.

4.4 Level 3: Display and Modify Controller

Options at this level display and modify controller and runtime parameters.

The commands are:

HE - print this message
RE - REturn to simulated pH process
CC - Change Controller
HC - HardCopy
MC - display and Modify Controller parameters
MR - display and Modify Run time specifications
MP - Modify Process specifications
DI - DIsplay options
RU - RUn simulation
OQ - Overwrite and Quit options

RE returns to Level 2 to display the process parameters. CC changes the chosen controller. HC produces a hardcopy of the screen. MC modifies controller parameters (example 4, section 6) and MR modifies runtime parameters (example 5). Also at this level, the option to modify the process parameters, MP, is included. DI takes the program monitor to Level 4 to display already existing results without running the simulation.

On typing RU, the program simulates the chosen process with the specified controller; the message:

PROGRAM RUNNING

appears on the screen.

After successful completion of the run, the user is prompted to display the simulated results.

4.5 Level 4: Display Simulated Results

Time-histories of 40 simulated variables can be displayed using the first 40 options (from PH to P14) available at this level:

PH - actual output pH
Y1 - measurement of output pH
Y2 - measurement of input flow
Y3 - measurement of input pH
F1 - filtered measurement of output pH
F2 - filtered measurement of input flow
F3 - filtered measurement of output pH
X1 - simulated output conc.
X2 - simulated input flow
X3 - simulated input conc.
M1 - estimated output conc.
M2 - estimated input flow
M3 - estimated input conc.
S1 - standard deviation of est. output conc.
S2 - standard deviation of est. input flow
S3 - standard deviation of est. input conc.
XZ - simulated bias on measurement of pH
MZ - estimated bias on measurement of pH
SZ - standard deviation of est. bias on measurement of pH
DZ - diagnostic for bias estimation
TZ - test for bias estimation
UT - total control action
UF - feedforward control action
UO - "optimal" control action to achieve set point in a single step
PY - stc : phiy
PE - stc : estimation error
P1 - P14 - stc parameters

HE - print this message
RE - REturn to controller options
HC - HardCopy
LE - LEave plot on the screen
CY - Change Y-axis for plots
OQ - Overwrite and Quit options

The remaining options are: HE,RE,HC,LE,CY,OQ. HE is the help message. RE

returns to Level 3 to display controller parameters; from Level 3 the user can return to Level 4 without running the simulation by issuing the command DI. Each variable is plotted one at a time by default. The option LE allows the user to overwrite the default and to plot more than one variable on the same axes: fig. 4 shows a hardcopy of two time-histories, Y1 (measurement of output pH) and UT (total control action), concurrently displayed. Name of variables and of the controller are also shown together with three performances indices: Root Mean Square Error in pH (RMSE), Average Excess Acidity below set point (AEA) and Average Reagent Flow (ARF).
Options for ordinate rescaling, CY, and for overwrite and quit,OQ , are described below.

4.5.1 Scale Y-axis Option (CY): - Maximum and minimum values of Y-axis for each variable have default values which can be modified by using the CY option. In order to change the values, the user inputs the corresponding number of the variable. He is then prompted to enter the maximum and the minimum values of the ordinate which will remain unchanged until they are modified again.

To exit from the CY option and to return to Level 4 the user, prompted by the program, presses <RETURN>

4.5.2 Overwrite and Quit Option (OQ): - Overwrite and quit options are available from all four levels. The commands are:

HE - print this message
RE - REturn to preceeding options
OC - Overwrite and save Controller specifications
OP - Overwrite and save Process specifications
QU - QUit program

RE returns to the level from which OQ was called. OC overwrites the controller file CT#.DAT with the current controller and runtime parameters. OP overwrites the process file PH#.DAT with the current process parameters; it also updates the table of content file PHCONT.DAT.

QU quits the CAD package PHDESIGN.

5.0 PROGRAM LIMITATIONS

PHDESIGN is not completely fool-proof. Its users are assumed to have some general knowledge of computing and of control.

The data entry is flexible and robust: it will allow floating point and integer conversion and it will not fail on typing errors but will prompt the user to reenter the data.

Specific limitations of the package are explained in detail in the examples of section 6.

6.0 EXAMPLES

There are five examples of typical sessions:

i) Input a new process, option NE;

ii) Modify process specifications, option MP;

iii) Modify titration curve data, option MT;

iv) Modify controller parameters, option MC;

v) Modify runtime parameters, option MR.

In all the examples note:

- what the user types in is underlined.
- when inputting new data or modifying old data pressing the <RETURN> key will keep the default value unchanged.

```
                    NEW PROCESS SPECIFICATIONS                  PROCESS:  7
                    --------------------------

PROCESS NAME (MAX. 15 CHARAC.)
                          OLD =
                          NEW = ? USER GUIDE EX.
USERNAME (MAX. 6 CHARAC.)
                          OLD =
                          NEW = ? USER
STRONG (0) - BUFFERED (1) REACTION
          OLD=  0.0000E+00  NEW= ? 1
PH SET POINT
          OLD=  0.0000E+00  NEW= ? 8.5
REACTOR VOLUME  M3
          OLD=  0.0000E+00  NEW= ? 40.0
DELAY : T. CONST. RATIO
          OLD=  0.0000E+00  NEW= ? 0.1
MAX. TIME DELAY  MINS.
          OLD=  0.0000E+00  NEW= ? 1.5
REACTOR TEMP. DEGREE C
          OLD=  0.0000E+00  NEW= ? 50.
REAGENT CONC. (+VE BASE, -VE ACID)
          OLD=  0.0000E+00  NEW= ? 5.2
MAX. REAGENT FLOW  M3/HR.
          OLD=  0.0000E+00  NEW= ? 0.5
SIM. (0) -  ACTUAL (1.2.3) DISTURBANCES
          OLD=  0.0000E+00  NEW= ? 1
DISTURBANCE FILENAME    OLD =
                        NEW = ? FLOW.DAT
```

1 - user-specified titration curve

Flag	Flow in	pH in
1	plant data	simulated
2	simulated	plant data
3	plant data	plant data

NEW PROCESS SPECIFICATIONS

PROCESS: ?

```
WIENER MODEL FLOW: T. CONST.  MINS.
         OLD=  0.0000E+00  NEW= ? 60.
WIENER MODEL CONC: T. CONST.  MINS.
         OLD=  0.0000E+00  NEW= ? 120.
WIENER MODEL FLOW: MEAN  M3/HR.
         OLD=  0.0000E+00  NEW= ? 360.
WIENER MODEL CONC: MEAN  N. (+VE,-VE)
         OLD=  0.0000E+00  NEW= ? -3.16E-3
WIENER MODEL FLOW: S. DEV.  M3/HR.
         OLD=  0.0000E+00  NEW= ? 40.
WIENER MODEL CONC: S. DEV.  N.
         OLD=  0.0000E+00  NEW= ? 5.E-4
ONE (0) - THREE (1) MEASUREMENT(S)
         OLD=  0.0000E+00  NEW= ? 1
BIAS: NO (0) - CONST. (1) - VARIABLE (2,3)
         OLD=  0.0000E+00  NEW= ?
PH OUT : BIAS  PH
         OLD=  0.0000E+00  NEW= ?
PH OUT : T. CONST. MEAS. FILTER  MINS.
         OLD=  0.0000E+00  NEW= ? 0.1
FLOW IN: T. CONST. MEAS. FILTER  MINS.
         OLD=  0.0000E+00  NEW= ? 3.
PH IN  : T. CONST. MEAS. FILTER  MINS.
         OLD=  0.0000E+00  NEW= ? 1.5
PH OUT : S. DEV.   MEAS. NOISE  PH
         OLD=  0.0000E+00  NEW= ? 0.01
FLOW IN: S. DEV.   MEAS. NOISE  M3/HR.
         OLD=  0.0000E+00  NEW= ? 5.
PH IN  : S. DEV.   MEAS. NOISE  PH
         OLD=  0.0000E+00  NEW= ? 0.01
```

NEW TITRATION SPECIFICATIONS

PROCESS: 7

NUMBER OF POINTS IN TITRATION CURVE :
N OLD= 38 NEW= ?

1- V,PH =?0.,2.26
2- V,PH =?0.5,2.32
3- V,PH =?1.5,2.46
4- V,PH =?2.5,2.65
5- V,PH =?3.0,2.78
6- V,PH =?3.7,3.06
7- V,PH =?3.9,3.18
8- V,PH =?4.3,3.61
9- V,PH =?4.4,3.81
10- V,PH =?4.5,4.03
11- V,PH =?4.57,4.4
12- V,PH =?4.61,4.62
13- V,PH =?4.65,4.83
14- V,PH =?4.69,5.05
15- V,PH =?4.73,5.24
16- V,PH =?4.77,5.41
17- V,PH =?4.81,5.58
18- V,PH =?4.85,5.76
19- V,PH =?4.89,5.92
20- V,PH =?4.93,6.08
21- V,PH =?4.97,6.26
22- V,PH =?5.01,6.47
23- V,PH =?5.05,6.95
24- V,PH =?5.08,7.36
25- V,PH =?5.13,7.75
26- V,PH =?5.17,8.02
27- V,PH =?5.21,8.2
28- V,PH =?5.25,8.33
29- V,PH =?5.35,8.58
30- V,PH =?5.45,8.78
31- V,PH =?5.55,8.94
32- V,PH =?5.65,9.06
33- V,PH =?5.85,9.26
34- V,PH =?6.05,9.4
35- V,PH =?6.25,9.52
36- V,PH =?6.75,9.73
37- V,PH =?7.25,9.87
38- V,PH =?7.75,9.99
39- V,PH =?8.75,10.15

TEMPERATURE OF TITRATION CURVE :
TEMP OLD= 0.0000E+00 NEW= ? 50.
VOLUME OF SAMPLE :
VSAMPL OLD= 0.0000E+00 NEW= ? 100
STRENGTH OF REAGENT (NORM. -VE,+VE)
NREAG OLD= 0.0000E+00 NEW= ? 0.05

```
                    MODIFY PROCESS OPTIONS                          PROCESS: 7
                    ----------------------

 1 - PNAME  - PROCESS NAME (MAX. 15 CHARAC.)                    USER GUIDE EX.
 2 - PUSER  - USERNAME (MAX. 6 CHARAC.)                         USER
 3 - IBUFF  - STRONG (0) - BUFFERED (1) REACTION                      1.000000E+00
 4 - SPPH   - PH SET POINT                                            8.500000E+00
 5 - VOLUM  - REACTOR VOLUME  M3                                      4.000000E+01
 6 - TDFACT - DELAY : T. CONST. RATIO                                 1.000000E-01
 7 - TDMAX  - MAX. TIME DELAY  MINS.  .                               1.500000E+00
 8 - TEMP   - REACTOR TEMP. DEGREE C                                  5.000000E+01
 9 - NREAG  - REAGENT CONC. (+VE BASE, -VE ACID)                      5.200000E+00
10 - UMAX   - MAX. REAGENT FLOW  M3/HR.                               5.000000E-01
11 - IDIST  - SIM. (0) -  ACTUAL (1,2,3) DISTURBANCES                 1.000000E+00
12 - DISTFN - DISTURBANCES FILENAME                                   FLOW.DAT
13 - TX2    - WIENER MODEL FLOW: T. CONST.  MINS.                     6.000000E+01
14 - TX3    - WIENER MODEL CONC: T. CONST.  MINS.                     1.200000E+02
15 - MX2    - WIENER MODEL FLOW: MEAN  M3/HR.                         3.600000E+02
16 - MX3    - WIENER MODEL CONC: MEAN  N. (+VE,-VE)                  -3.180000E-03
17 - SX2    - WIENER MODEL FLOW: S. DEV.  M3/HR.                      3.333860E+01
18 - SX3    - WIENER MODEL CONC: S. DEV.  N.                          5.000000E-04
19 - IBIAS  - ONE (0) - THREE (1) MEASUREMENT(S)                      0.000000E+00
20 - IBSIM  - BIAS: NO (0) - CONST. (1) - VARIABLE (2,3)              0.000000E+00
21 - BIAS   - PH OUT : BIAS  PH                                       0.000000E+00
22 - TYF1   - PH OUT : T. CONST. MEAS. FILTER  MINS.                  1.000000E-01
23 - TYF2   - FLOW IN: T. CONST. MEAS. FILTER  MINS.                  3.000000E+00
24 - TYF3   - PH IN  : T. CONST. MEAS. FILTER  MINS.                  1.500000E+00
25 - SN1    - PH OUT : S. DEV.   MEAS. NOISE  PH                      1.000000E-02
26 - SN2    - FLOW IN: S. DEV.   MEAS. NOISE  M3/HR.                  5.000000E+00
27 - SN3    - PH IN  : S. DEV.   MEAS. NOISE  PH                      1.000000E-02

        INPUT option number or press RETURN to continue 4
 SPPH    OLD=   8.500       NEW= ? 8.0
```

TITRATION CURVE SPECIFICATIONS

PLANT 7 USER GUIDE EX.

1-V =	0.00	PH=	2.26	14-V =	4.69	PH=	5.05	27-V =	5.21	PH=	8.20
2-V =	0.50	PH=	2.32	15-V =	4.73	PH=	5.24	28-V =	5.25	PH=	8.33
3-V =	1.50	PH=	2.46	16-V =	4.77	PH=	5.41	29-V =	5.35	PH=	8.58
4-V =	2.50	PH=	2.65	17-V =	4.81	PH=	5.58	30-V =	5.45	PH=	8.78
5-V =	3.00	PH=	2.78	18-V =	4.85	PH=	5.76	31-V =	5.55	PH=	8.94
6-V =	3.70	PH=	3.06	19-V =	4.89	PH=	5.92	32-V =	5.65	PH=	9.06
7-V =	3.90	PH=	3.18	20-V =	4.93	PH=	6.08	33-V =	5.85	PH=	9.26
8-V =	4.30	PH=	3.61	21-V =	4.97	PH=	6.26	34-V =	6.05	PH=	9.40
9-V =	4.40	PH=	3.81	22-V =	5.01	PH=	6.47	35-V =	6.25	PH=	9.52
10-V =	4.50	PH=	4.08	23-V =	5.05	PH=	6.95	36-V =	6.75	PH=	9.73
11-V =	4.57	PH=	4.40	24-V =	5.09	PH=	7.36	37-V =	7.25	PH=	9.87
12-V =	4.61	PH=	4.62	25-V =	5.13	PH=	7.75	38-V =	7.75	PH=	9.98
13-V =	4.65	PH=	4.83	26-V =	5.17	PH=	8.02	39-V =	8.75	PH=	10.15

40- TEMPERATURE OF TITRATION CURVE = 50.00
41- VOLUME OF SAMPLE = 100.00
42- STRENGTH OF REAGENT (NORM. -VE,+VE) = 0.050

INPUT option number or press RETURN to continue 35
V OLD= 6.750 NEW= ?
PH OLD= 9.730 NEW= ? 9.7

```
                CLASSICAL CONTROL SPECIFICATIONS
                --------------------------------

                ST-PID on pH


 1 - T.CONST. OF INV. REF. MODEL (MINS.)                    0.000E+00
 2 - T.CONST. OF FILTER ON PHIY (MINS.)                     0.000E+00
 3 - T.CONST. #1 OF C FILTER (MINS.)                        0.000E+00
 4 - T.CONST. #2 OF C FILTER (MINS.)                        0.000E+00
 5 - FORGETING FACTOR                                        1.00
 6 - INIT. COV. DIAG. FOR U DATA                            1.000E+03
 7 - INIT. COV. DIAG. FOR Y DATA                            1.000E+03
 8 - ASSUMED TIME DELAY                                      1.00
 9 - INITIAL GAIN                                           0.000E+00
10 - INITIAL INTEGRAL TIME (MINS.)                          1.000E+07
11 - INITIAL DERIVATIVE TIME (MINS.)                        0.000E+00
12 - INITIAL DERIVATIVE FILTER (MINS.)                      0.000E+00
13 - TIME FOR ESTIMATION ONLY (MINS.)                       0.000E+00
14 - ESTIMATION FLAG                                        1.00
15 - CONTROL FLAG                                           1.00
16 - NUMBER OF ESTIMATED PARAMETERS                         4.00
17 - LIMIT ON MAX. EST. GAIN                                1.00
18 - LIMIT ON MIN. EST. GAIN                               0.000E+00
19 - ESTIMATION DEADBAND AROUND SETPOINT                   0.000E+00
20 - ESTIMATION: NO (0) - 3 STATES (1) - BIAS (2)          0

        INPUT option number or press RETURN to continue 1
PPID     OLD=  0.0000E+00  NEW= ? 5.
```

RUN-TIME SPECIFICATIONS

1	RANDOM NUMBER INITIALISATION	1
2	INTEGRATION STEP LENGTH (SEC)	3.00
3	CONTROL SAMPLE (SEC)	30.0
4	TOTAL RUN TIME (HR)	3.00
5	MODELLING ERRORS (PERCENT)	35.0

INPUT option number or press RETURN to continue **4**

TTIME OLD= 3.000 NEW= ? **24.**

7.0 REFERENCES

[1] Badran W.A. (1984) On designing algorithms for controlling pH, D.Phil thesis, University of Oxford

[2] Jacobs O.L.R., Badran W.A. and C.G. Proudfoot (1983) CAD of systems for regulating pH, to be published in The Chemical Engineer

[3] Jacobs O.L.R. and W.A. Badran (1983) CAD of pH control systems, submitted for IFAC Congress Budapest

[4] Jacobs O.L.R. and W.A. Badran (1984) CAD of pH control systems, PROMECON Conference London

[5] Shinskey F.G. (1973) pH and pion control, Wiley

[6] Jacobs O.L.R. (1984) pH regulation, Encyclopedia of Systems and Control Pergamon

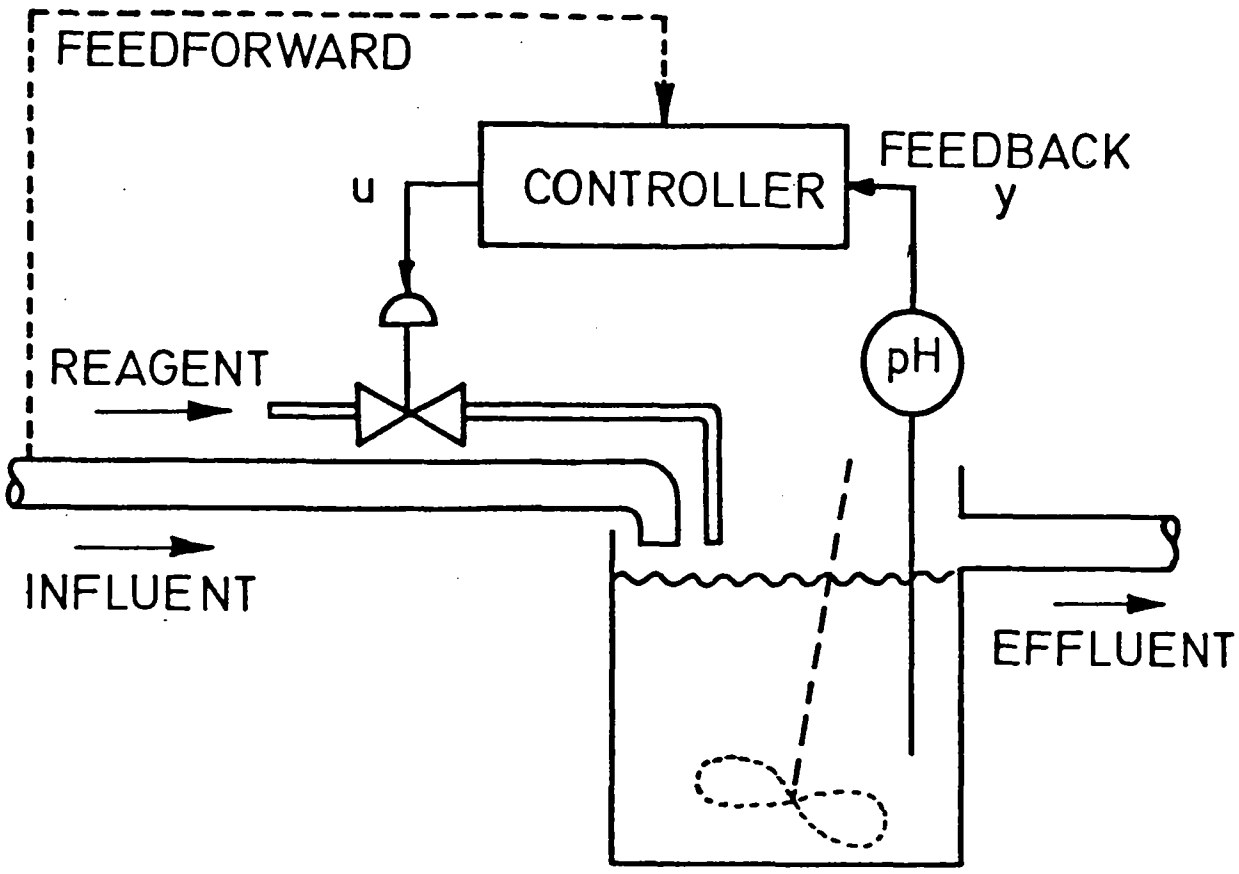


Fig. 1 pH regulation in a continuous stirred-tank reactor

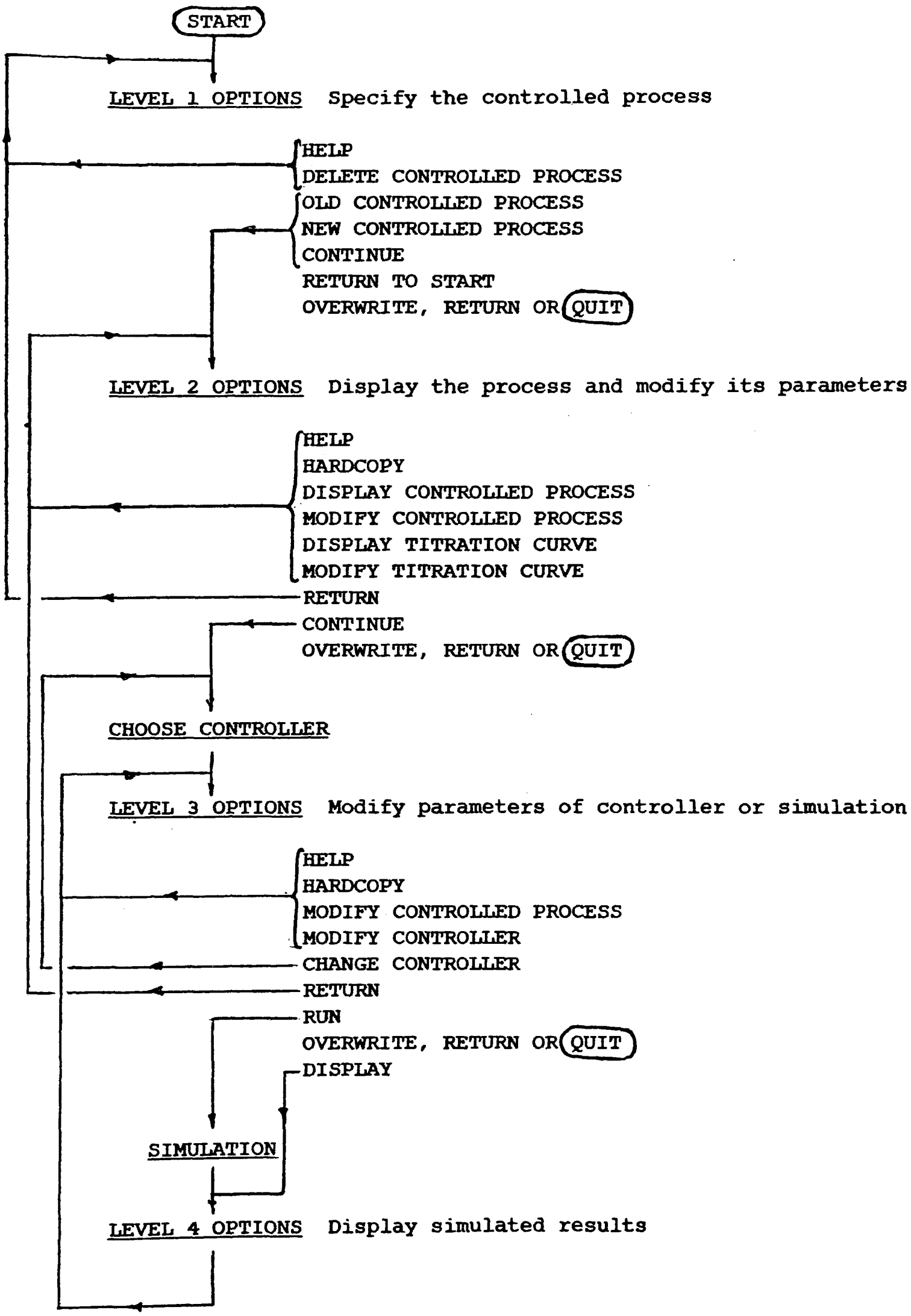


Fig. 2 Interactive options

PLANT 7 USER GUIDE EX.

PH SET POINT	8.000
REACTOR VOL. (M3)	40.000
MAX. TIME DELAY (MIN.)	1.500
DELAY : T. CONST. RATIO	0.100
REACTOR TEMP. (C)	50.00
REAGENT CONC. (N.)	5.200
MAX. REAGENT FLOW (M3/HR.)	0.500
STRONG (0) - BUFF.(1) REAG.	1

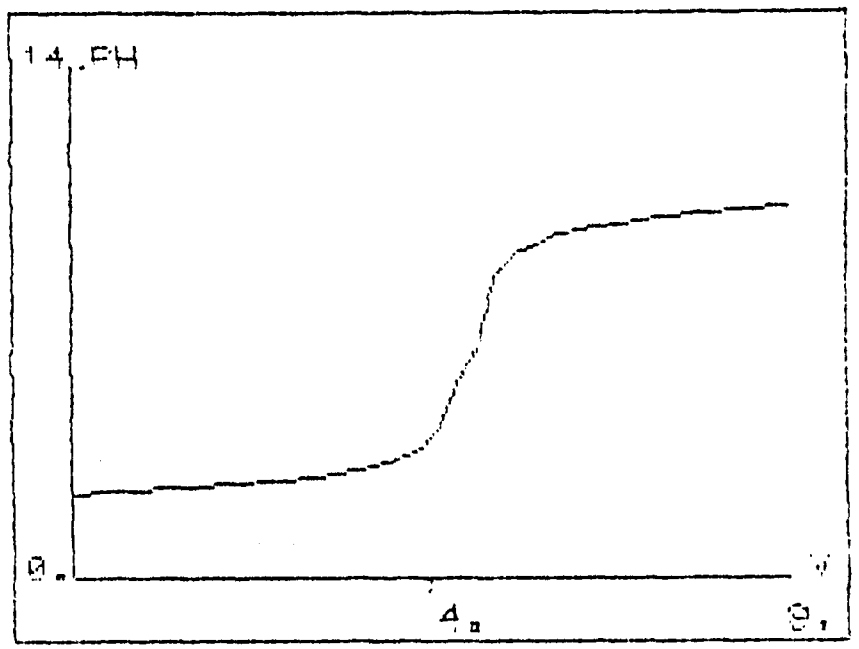


Fig. 3 Parameters of controlled process: option DP

DISTURBANCES : WIENER PROCESSES OR PLANT DATA

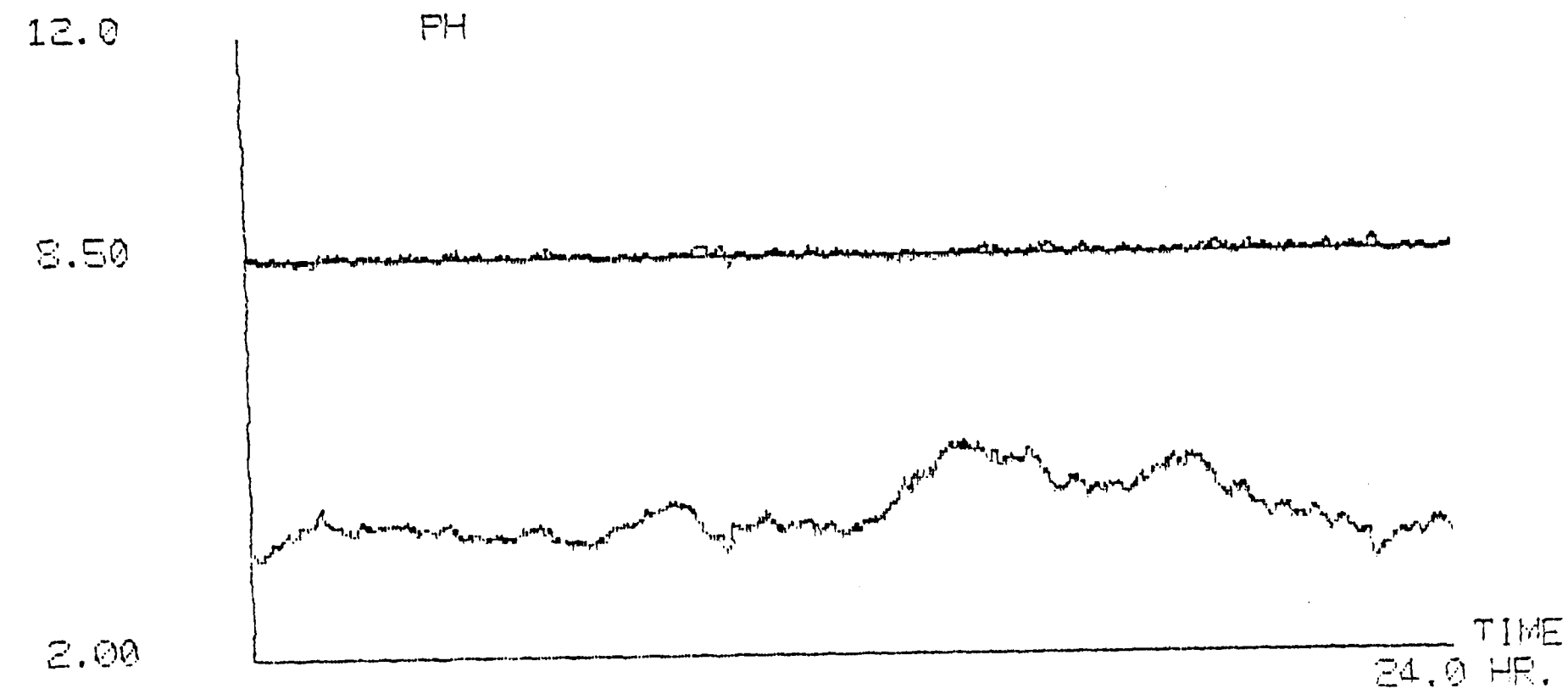
	T. CONST.(MIN.)	MEAN	STAND. DEV.
FLOW (M3/HR.)		*** PLANT DATA ***	
CONC. (N.)	0.120E+03	-0.316E-02	0.500E-03

MEASUREMENTS:

	SD. NOISE	FILTER (MIN.)	PRESENT	BIAS
PH OUT (PH)	0.01	0.10	1	0.00 - 0
FLOW IN (M3/HR)	5.00	3.00	0	
PH IN (PH)	0.01	1.50	0	

SIMULATED pH PROCESS: HE,HC,DP,DT,MP,MT,RE,CO,OO ? HC

PLANT 7 USER GUIDE EX.



ACTUAL PH OUT TOTAL CONTROL ACTION

Fig. 4 Typical time-histories of display options

ST-PID on pH

PERFORMANCE INDICES :	RMSE (pH)	AEA (pH)	ARF (M3/H.)
	5.254E-02	2.122E-02	0.115

PH,Y1-Y3,F1-F3,X1-X3,M1-M3,S1-S3,XZ,MZ,SZ,DZ,TZ,UT,UF,UO,PY,PE,P1-P14
DISPLAY OPTIONS: HE,LE,CY,HC,OO,RE ?

APPENDIX E

STABILITY ANALYSIS OF COUPLED SYSTEMS

In this appendix, a stability analysis of a coupled two-stage configuration, shown in figure E.1, is carried out. This configuration is used in the simulation of a two-stage neutralisation process in the Unilever case study of chapter 8. The analysis is to indicate whether the reagent line to the second stage causes stability problems in the coupled system.

The mixing dynamics of neutralisation in a CSTR can be approximately represented by:

$$V\dot{x}_{out} \simeq F(x_{in} - x_{out}) + x_r u \qquad \text{(E.1)}$$

where V is the tank volume, F is the effluent flowrate, x_{in} & x_{out} are the effluent incoming and outgoing ionic concentrations, x_r is the reagent ionic concentration, and u is the reagent flowrate.

In figure E.1, the feedback pH controller of each stage is assumed, for simplicity, to be a proportional-only controller. Hence, the amount of reagent u in each stage is given by:

$$u_j = K_j(X_j - x_j) \qquad j = 1,2 \qquad \text{(E.2)}$$

where K is the controller gain, X is the controller setpoint in ionic

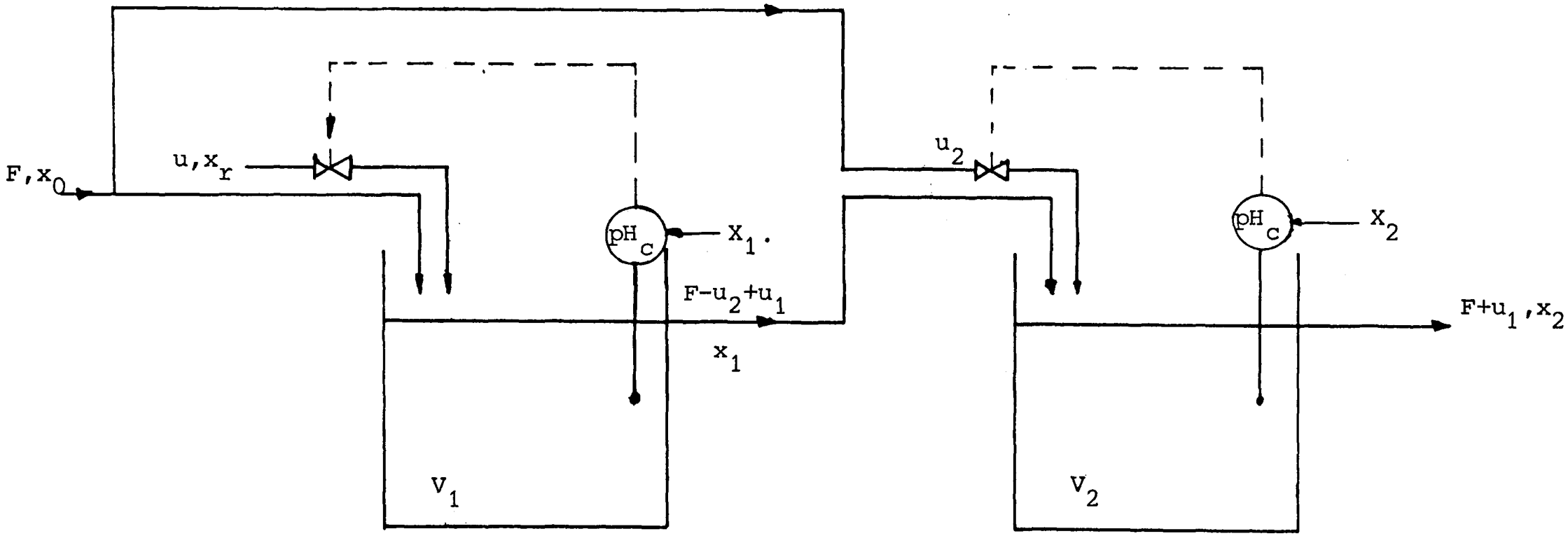


Fig E.1 Two-stage configuration

concentration, and x is the outgoing ionic concentration. Replacing for u in equation E.1 for each stage, we have:

$$V_1\dot{x}_1 = (F - K_2X_2 + K_2x_2)(x_0 - x_1) + x_rK_1(X_1 - x_1) \qquad \text{(E.3a)}$$

$$V_2\dot{x}_2 = (F + K_1X_1 - K_1x_1)(x_1 - x_2) + x_0K_2(X_2 - x_2) \qquad \text{(E.3b)}$$

Rearranging equations E.3:

$$V_1\dot{x}_1 = (-F + K_2X_2 - K_1x_r)x_1 + K_2x_0x_2 \qquad \text{(E.4a)}$$
$$- K_2x_1x_2 + (F - K_2X_2)x_0 + K_1X_1x_r$$

$$V_2\dot{x}_2 = (F + K_1X_1)x_1 + (-F + K_1X_1 - K_1x_0)x_2 \qquad \text{(E.4b)}$$
$$+ K_1x_1x_2 - K_1x_1^2 + K_2X_2x_0$$

Equations E.4 can be written as:

$$\dot{x}_1 = a_{11}x_1 + a_{12}x_2 - K_2x_1x_2/V_1 + (F - K_2X_2)x_0/V_1 + K_1X_1x_r/V_1 \qquad \text{(E.5a)}$$

$$\dot{x}_2 = a_{21}x_1 + a_{22}x_2 + K_1x_1x_2/V_2 - K_1x_1^2/V_2 + K_2X_2x_0/V_2 \qquad \text{(E.5b)}$$

Because the value of the non-linear elements in equations E.5 is small compared to that of the linear ones, the non-linear section maybe disregarded. Hence, the steady-state dynamics of the coupled system is given by a transition matrix A:

$$A \equiv \begin{bmatrix} a_{11} & a_{12} \\ a_{21} & a_{22} \end{bmatrix} = \begin{bmatrix} (-F + K_2X_2 - K_1x_r)/V_1 & K_2x_0/V_1 \\ (F + K_1X_1)/V_2 & (-F + K_1X_1 - K_1x_0)/V_2 \end{bmatrix}$$

A necessary condition for stability is that the eigenvalues of A are negative. This is equivalent to the Routh-Hurwitz criteria:

$$a_{11}a_{22} > a_{12}a_{21} \quad \text{and} \quad a_{11} + a_{22} < 0$$

Both inequalities are satisfied because F/V » KX/V.

REFERENCES

ALSPASCH D and H W SORENSON (1970) 'Approximation of density function by a sum of gaussian for non-linear Bayesian estimation' Symposium on Non-linear Estimation, San Diego.

AOKI M (1967) 'Optimization of stochastic systems' Academic Press, New York.

BASSEVILLE M and A BENVENISTE (1983) 'Design and comparative study of some sequential jump detection algorithms for digital signals' IEEE Trans. On ASSP, Vol. 31, 3, pp 521-535.

BELLETRUTTI J, CHENG R and D M SLOAN (1976) 'Control of industrial acidic waste system subject to large acid influx' ISA Trans., Vol. 15, 3, pp 274-281.

BERGMANN S and K-H LACHMAN (1980) 'Digital parameter adaptive control of a pH process' Proc. JACC 1980 San Francisco, Paper TA2-E.

BEST R (1978) 'The impact of microelectronics on pH' Proc. JACC 1978 Philadelphia, Vol. 1, pp 1-14.

BIERMAN G J (1977) 'Factorization methods for discrete sequential estimation' Academic Press, New York.

BIERMAN G J and C THORNTON (1977) 'Numerical comparisons of Kalman filter algorithms: orbit determination case study' Automatica, Vol. 13, pp 25-35.

BOWN M (1983a) 'Lessons in pH control of industrial effluent' Process Engineering, January 1983, pp 53,55.

BOWN M (1983b) 'Tuning in to dynamics of effluent neutralisation' Process Engineering, February 1983, pp50-51.

BUCHHOLT F and M KUMMEL (1979) 'Selftuning control of pH neutralisation' Automatica, Vol. 15, pp 665-671.

BUCY R S and K D SENNE (1970) 'Realization of optimum discrete time nonlinear estimators' Symposium on Non-linear Estimation, San Diego.

CLARKE D W (1982) 'Model following and pole-placement self-tuners' Optimal Control Applications and Methods, Vol. 3, 4, pp 323-335.

CLARKE D W and R HASTINGS-JAMES (1971) 'Design of digital controllers for randomly disturbed processes' Proc. IEE, Vol. 118, pp1503-1506.

CLARKE D W, HODGSON A J F and P S TUFFS (1983) 'The offset problem and k-incremental predictors in self-tuning control' Proc. IEE, Vol. 130, Part D, pp 217-225.

CONSIDINE D M (1957) 'Process instruments and controls handbook' Mc Graw Hill, New York.

CREASON S (1978) 'Titration curve - The key to pH control' Instrument. and Control System, Vol. 51, 8, pp 45-48.

DUMONT G A and P R BELANGER (1978) 'Control of Titanium dioxide kiln' IEEE Trans. On AC, Vol. 23, 4, pp 521-531.

ERSU E and X MAO (1983) 'Control of pH by use of a self-organizing concept with associative memories' Proc. ACI 1983 Copenhagen.

FIELD W (1959) 'Design of a pH control system by analog simulation' ISA Journal, Vol. 6, 1, pp 42-50.

FINDLEY M (1961) 'Concentration control by electrochemical methods' Industrial & Eng. Chemistry, Vol. 53, 6, pp 471-474.

FRAADE D (1978) 'Using a microprocessor to solve pH control problems' Instrument. Technology, Vol. 25, 11, pp 61-65.

FRIEDLAND B (1969) 'Treatment of bias in recursive filtering' IEEE Trans. On AC, Vol. 14, 4, pp 359-367.

FRIEDLAND B (1978) 'Note on separate bias estimation' IEEE Trans. On AC, Vol. 23, 4, pp 735-738.

FRIEDLAND B and S GRABOUSKY (1982) 'Estimating sudden changes of biases in linear dynamic systems' IEEE Trans. On AC, Vol. 27, 1, pp 237-240.

GALETTI B and P FRIEDMAN (1972) 'Digital dynamic simulation for effective

pH control system design' Analysis Instrum., 10, pp 13-18.

GAUTHIER J P and G BORNARD (1981) 'Observability for any u(t) for a class of non-linear systems' IEEE Trans. On AC, Vol. 26, 4, pp 917-922.

GOODWIN G McINNES B and R LONG (1982) 'Adaptive control algorithms for waste water treatment and pH neutralisation' Optimal Control Applications and Methods, Vol. 3, pp 443-459.

GRASSEL J VON (1974a) 'Investigation of the evaluation of controllability of pH control lines; Part 1' Regelungstechnische Praxis, Vol. 16, 4, pp 100-105.

GRASSEL J VON (1974b) 'Investigation of the evaluation of controllability of pH control lines; Part 2' Regelungstechnische Praxis, Vol. 16, 5, pp 126-129.

GRAY D (1980) 'Characterized pH control' Proc. 1980 Symp. Instrument. in the Petroleum & Chemical Industries, Vol. 16, pp 103-107.

GREER W (1966) 'The measurement and automatic control of pH' Leeds & Northrup Technical Publication D2.1000-766.

GUPTA S and D COUGHANOWR (1974) 'An analog adaptive controller for on-line identification and control of a first order process with time-varying gain' ISA Trans., Vol. 13, 1, pp 59-69,

GUPTA S and D COUGHANOWR (1978) 'On-line identification of flow processes with application to adaptive pH control' AICh.E, Vol. 24, 4, pp 654-664.

HARRIOT P (1964) 'Process control' Mc Graw Hill, New York.

HERMANN R and A J KRENER (1977) 'Non-linear controllability and observability' IEEE Trans. On AC, Vol. 22, 5, pp 728-740.

HEWKIN P (1979) 'The control of pH using modern control algorithms and on-line computers' D. Phil. thesis, University of Oxford.

HOFFMAN F (1979) 'Neutralisation of industrial waste by pH control' Proc. 25th annual ISA, Vol. 17, pp 246-248.

HOYLE D (1975) 'Controlling pH in waste streams' Plant Engineering, January 25th, pp 125-128.

HOYLE D (1976) 'Designing for pH control' Chemical Engineering November 1976, pp 121-126.

ISERMAN R (1981) 'Digital control systems' Springer-Verlag, New York.

IVERSON A and S OCHIAI (1977) 'Controlling effluent pH' Instrument. Technol., Vol. 24, 5, pp 65-68.

JACOBS O L R (1974) 'Introduction to control theory' Oxford University Press, Oxford.

JACOBS O L R (1983) 'Non-linear estimation by on-line computation of Bayesian statistics' OUEL report No 1451/83.

JACOBS O L R and W A BADRAN (1983a) 'CAD of pH control systems' IFAC Congress, Budapest.

JACOBS O L R and W A BADRAN (1983b) 'CAD package for designing pH control systems' Promecon Conference, London.

JACOBS O L R, BADRAN W A and C. G. PROUDFOOT (1984) 'CAD of systems for regulating pH' The Chemical Engineer, March 1984.

JACOBS O L R and M S BRIGGS (1984) 'Monte-Carlo comparisons of estimators for pH non-linearity' to appear in Trans. Inst. Meas. and Control.

JACOBS O L R, HEWKIN P F and C WHILE (1980) 'On-line computer control of pH in an industrial process' Proc. IEE, Vol. 127, Part D, pp 161-168.

JACOBS O L R and J W PATCHELL (1972) 'Caution and probin in stochastic control' Int. J. Control, Vol. 16, pp 189-199.

JAZWINSKI A H (1970) 'Stochastic processes and filtering theory' Academic Press, New York.

JUNGCK P and E WOYTOWICZ (1971) 'Understanding pH control' Instrum. Technol., Vol. 17, 11, pp 43-46.

JUTILA P (1983) 'An application of adaptive pH-control algorithms based on physico-chemical modelling in a chemical waste-water treatment plant' Int. J. Control, Vol. 38, 3, pp 639-655.

JUTILA P and P ORAVA (1981) 'Control and estimation algorithms for physico-chemical models of pH processes in stirred tank reactors' Int. J. Syst. Sci., Vol. 12, 7, pp 855-875.

JUTILA P, ORAVA P and B SALMELIN (1981) 'A physico-chemical model and simulation of pH-process in continuous stirred tank reactors' Math. Comp. in Simul., Vol. 23, 2, pp 99-106.

KAESSER R (1980) 'Adaptive continuous pH control monitored by on-line gain identification' 4th IFAC 1980, Ghent.

KALMAN R E (1963) 'Mathematical description of linear dynamic systems' J. SIAM Control, Series A, Vol. 1, 2 pp 557-562.

KALMAN R E and R S BUCY (1961) 'New results in linear filtering and prediction theory' J. Basic Engineering, Vol. 83D, pp 95-108.

KIRLIN R and W MARSHALL (1975) 'The case for state variables in pH controller design' Control Engineering, Vol. 2, 2, pp 47-49.

KUHN J and E BENDER (1981) 'The formation of models as an aid to the design of pH control in industrial waste water' Regelungstechnische Praxis, Vol. 23, 9, pp 311-314.

LAJOY M (1954) 'Industrial Automatic control' Prentice Hall, London.

LEE R C K (1964) 'Optimal estimation, identification, and control' Res. Monograph N. 28, MIT Press, Cambridge.

LEIGH J (1982) 'Applied control theory' IEE Publications, London.

MARRA R (1974) 'Analysis of a continuous neutralisation; a case study' AICh.E Workshop on Industrial Process Control, Tampa 1974, pp 40-47.

McAVOY T (1972) 'Time optimal and Ziegler-Nichols control' Ind. Eng. Chem. Process Des. Develop., Vol. 11, 1, pp 71-78.

McAVOY T (1974) 'Dynamic modelling of pH in aqeous systems' AICh.E Workshop on Industrial Process Control, Tampa 1974, pp 35-39.

McAVOY T, HSU E and S LOWENTHAL (1972) 'Dynamics of pH in a CSTR' Ind. Eng. Chem. Process Des. Develop., Vol. 11, 1, pp 68-70.

McCORMACK P (1962) 'Theoretical prediction of optimum pH controller

setting' Instrument Practice, September 1962, pp 1089-1096.

MEHRA R K and J PESCHON (1971) 'An innovation approach to fault detectio and diagnosis in dynamic systems' Automatica, Vol. 7, pp 637-640.

MELLICHAMP D, COUGHANOWR D and L KOPPEL (1966) 'Charaterization and gain identification of time varying flow processes' AICh.E, Vol. 12, 1, pp 75-82.

MENDEL J and H WASHBURN (1978) 'Multi-stage estimation of bias states in linear systems' Int. J. Control, Vol. 28, 4, pp 511-524.

MOORE R (1978) 'Neutralisation of waste water by pH control' ISA, New York.

MORRIS A, WRIGHT A, NAZER Y, CHISHOLM K, WOOD R and H LIEUSON (1981) 'Selftuning control of some pilot plant processes' Microprocessors & Microsystems, Vol. 5, 1, pp 3-12.

MYRON T and F SHINSKEY (1974) 'Advanced control systems for waste pH processes' AICh.E Workshop on Industrial Process Control, Tampa 1974, pp 29-34.

NIEMI A (1978) 'Process dynamic Approach' JACC 1978 Philadelphia, Vol. 1, pp 37-42.

NIEMI A and P JUTILA (1977) 'pH control by linear algorithm' IFAC Conf. on Digital Computer Applications to Process Control, The Hague 1977, pp 289-297.

NIEMI A and P JUTILA (1978a) 'Process models and control of acidity' Kemia-Kemi, Vol. 5, 4, pp 123-126.

NIEMI A and P JUTILA (1978b) 'Algorithms for pH control' 2nd Polish English Seminar on Real Time Process Control, Rogow Poland, 1978, Tech. Univ. of Warsaw, Inst. of Control & Indust. Electronics, pp 282-292.

NIHTILA M and P JUTILA (1982) 'Dynamic models and state linear filtering schemes for pH-processes' Symp. on Application of Multivariable Systems Theory, Plymouth.

ORAVA P and A NIEMI (1974) 'State model and stability analysis of a pH control system' Int. J. Control, Vol. 20, 4, pp 557-567.

PAPOULIS A (1965) 'Probability, random variables and stochastic processes' Mc Graw Hill, New York.

PATCHELL J W and O L R JACOBS (1971) 'Separability, neutrality and certainty-equivalence' Int. J. Control, Vol. 13, pp337-342.

PETERS R VON (1970) 'pH regulation' Regelungstechnische Praxis, Vol. 12, 1, pp 10-16.

PLUHAR K (1983) 'Off-the-shelf analyzer offers measurement, alarming, proportional control' Control Engineering, August 1983, pp 76-77.

PROUDFOOT C G (1983) 'Industrial implementation of online computer control of pH' D. Phil. thesis, University of Oxford.

PROUDFOOT C G, GAWTHROP P J and O L R JACOBS (1983) 'Self-tuning PI control of a pH neutralisation process' Proc. IEE, Vol. 130, Part D, pp 267-272.

PROUDFOOT C G and O L R JACOBS (1984) 'Application of an extended Kalman filter to a neutralisation process' IEE/I Chem. E colloqium on Experiences in the use of modern control techniques, 24 May 1984.

PROUDFOOT C G and S McALPINE (1984) 'Conclusions arising from the use of modern control algorithms for the control of pH' ICI internal report.

RANG E (1975) 'Application of Popov criteria to pH neutralisation control' Adv. in Instrument., Vol. 30, 3, pp 764/1-4.

RANG E (1977) 'pH computations in terms of the hyperbolic functions' Computers & Chemistry, Vol. 1, 2, pp 91-92.

RICHTER J, FOURNIER C, ASH R and S MARCIKIC (1974a) 'Feedforward adaptive pH control' AICh.E Workshop on Industrial Process Control, Tampa 1974, pp 48-53.

RICHTER J, FOURNIER C, ASH R and S MARCIKIC (1974b) 'Waste neutralisation control - Digital simulation spots non-linearities' Instrum. Technol., Vol. 21, 4, pp 35-40.

ROBERTS P (1971) 'Non-linear control of a neutralization process' Meas. & Control, Vol. 4, 9, pp T151-157.

ROWTON E (1968) 'Sampled data control of pH' Instrument. Technol.,

Vol. 14, 6, pp 63-65.

SAGE A P and J L MELSA (1971) 'Estimation theory' Mc Graw Hill, New York.

SHINSKEY F (1968) 'Feedforward control of pH' Instrument. Technol., Vol. 14, 6, pp 65-69.

SHINSKEY F (1973) 'pH and pIon control' Wiley, New York.

SHINSKEY F (1974) 'adaptive pH control monitors non-linear process' Control Engineering, Vol. 21, 2, pp 57-59.

SHINSKEY F (1979) 'Process control systems' 2nd Ed., McGraw Hill, New York.

SOLIMAN M A, RAY W A and J SZEKELY (1974) 'application of non-linear filtering to the stainless steel decarbonization process' Int. J. Control, Vol. 20, 4.

SOMMER R (1981) 'The design of a controller for a waste water neutralisation plant' Regelungstechnische Praxis, Vol. 23, 9, pp 315-320.

SORENSON H W (1974) 'On the development of practical non-linear filters' Info. Sci., Vol. 7, pp 253-284.

SORENSON S (1909a) 'Etudes enzymatiques; II. Sur la mesure et l'importance de la concentration des ion hydrogenes dans les reactions enzymatiques' Compt. Rend. Trav. Lab. Carlsberg, Vol. 8, pp 1-60.

SORENSON S (1909b) 'Enzymstudien; II. Uber die messung und die bedung der Wasserstoffionenkonzentration bei enzimatischen Prozessen' Biochem. Z., Vol. 21, pp 131-201.

SORENSON S and K LINDERSTROM-LANG (1924) 'On the determination and value of Π_0 in electrometric measurements of hydrogen ion concentrations' Compt. Rend. Trav. Lab. Carlsberg, Vol. 15, 6.

STANSBURY J, JOHNSON R and J WEBB (1980) 'A good tight pH control' Instrum. & Control System, Vol. 53, 8, pp 31-34.

TREVATHAN V (1972) 'pH control in waste stream' ISA 27th Annual Conference New York 1972, Paper 725.

TREVATHAN V (1974) 'Characteristics of pH control' AICh.E Workshop on Industrial Process Control, Tampa 1974, pp 24-28.

TREVATHAN V (1978) 'Advanced control of pH' Proc. JACC 1978 Philadelphia Vol. 1, pp 43-56.

WALLACE J N and R CLARKE (1983) 'The application of kalman filtering estimation techniques in power station control systems' IEEE Trans. On AC, Vol. 38, 3.

WALTER S and K WILKE (1973) 'A new method for pH regulation' Chemie-Ing. Techn., Vol. 45, 17, pp 1071-1072.

WELLSTEAD P E, EDWARDS J M, PRAGER D and P ZANKER (1979) 'Selftuning pole/zero assignement regulators' Int. J. Control, Vol. 30, 1.

WILLIAMS E (1971) 'Feedforward for pH control' Pollution Engineering, March/April 1971, pp 24-26.

WILLSKY A S and H L JONES (1976) 'A generalized likelihood ratio approach to the detection and estimation of jumps in linear systems' IEEE Trans. On AC, Vol. 21, 1, pp 108-112.

WILSON H and W WYLUPEK (1969) 'Design of pH control systems' Meas. & Control, Vol. 2, 9, pp 336-341.

WOLFENDER E, BEYERLE T and M ALT (1978a) 'Continuous neutralisation of sewage water with the aid of a mini process computer; Part 1' Regelungstechnische Praxis, Vol. 20, 4, pp116-120.

WOLFENDER E, BEYERLE T and M ALT (1978b) 'Continuous neutralisation of sewage water with the aid of a mini process computer; Part 2' Regelungstechnische Praxis, Vol. 20, 5, pp151-154.

ZIEGLER J G and N E NICHOLS (1944) 'Optimum settings for automatic controllers' Trans. On ASME, Vol. 64, pp 759-768.